Alginate Composition
by Solid-State Spectroscopy and Chemometrics

PhD Thesis by Tina Salomonsen

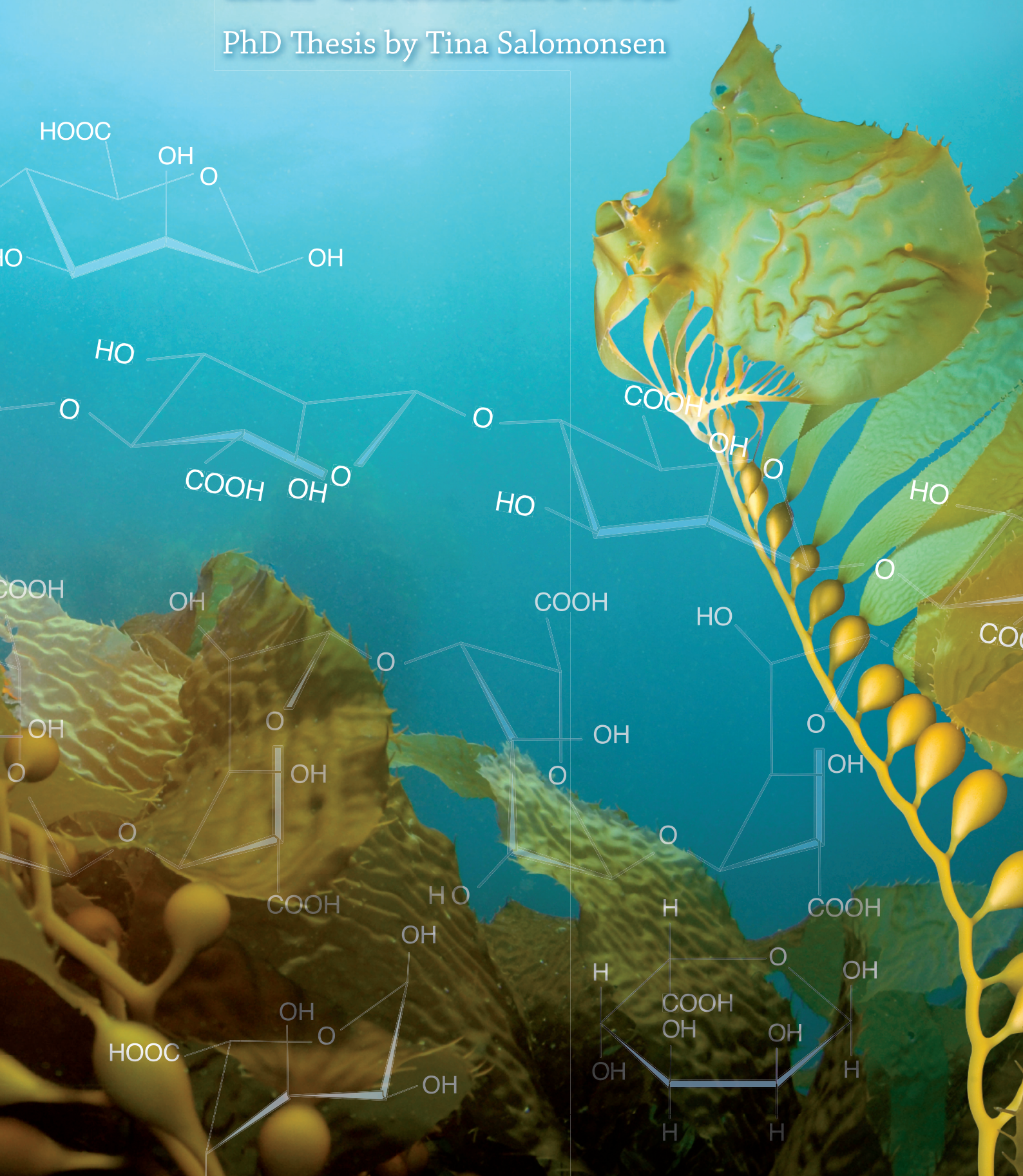

FACULTY OF LIFE SCIENCES
UNIVERSITY OF COPENHAGEN

DANISCO
First you add knowledge...

ALGINATE COMPOSITION BY SOLID-STATE SPECTROSCOPY AND CHEMOMETRICS

Tina Salomonsen
PhD Thesis • 2009

University of Copenhagen · Faculty of Life Sciences
Department of Food Science · Quality and Technology
Rolighedsvej 30 · 1958 Frederiksberg C · Denmark

Danisco A/S
Advanced Analysis
Edwin Rahrs Vej 38 · 8220 Brabrand · Denmark

Title:
Alginate Composition by Solid-State Spectroscopy and Chemometrics

Supervisors:
Professor Søren Balling Engelsen, Quality and Technology, Department of Food Science, Faculty of Life Sciences, University of Copenhagen, Denmark

Associate Professor Flemming Hofmann Larsen, Quality and Technology, Department of Food Science, Faculty of Life Sciences, University of Copenhagen, Denmark

Senior Scientist Henrik Max Jensen, Advanced Analysis, Danisco A/S, Denmark

Senior Scientist Graham Sworn, Danisco A/S, France

Opponents:
Professor Rasmus Bro, Quality and Technology, Department of Food Science, Faculty of Life Sciences, University of Copenhagen, Denmark

Professor Kurt Ingar Draget, Department of Biotechnology, Norwegian Biopolymer Laboratory, Norwegian University of Science and Technology, Norway

Professor Mike Gidley, Centre for Nutrition and Food Sciences, School of Land, Crop and Food Sciences, University of Queensland, Australia

Cover illustration:
Brown seaweed of the species *Macrocystis pyrifera* (also known as 'Giant Kelp'), the building blocks of alginate, mannuronic acid and guluronic acid, as well as chains of α-(1-4)-linked L-guluronic acid and β-(1-4)-linked mannuronic acid. The illustration has been made by Anja Kaltoft.

PhD Thesis · 2009 © Tina Salomonsen
Printed by SL Grafik, Frederiksberg C, Denmark
ISBN: 978-87-7611-294-3

PREFACE

This PhD thesis has been carried out as an industrial PhD project from May 2006 to April 2009 within the Advanced Analysis Department of Danisco A/S and Quality & Technology (Q&T), Department of Food Science, The Faculty of Life Sciences, University of Copenhagen. The project has been sponsored by Danisco A/S and the Ministry of Science, Technology and Innovation, which are greatly appreciated. The project has been supervised by Professor Søren Balling Engelsen and Associate Professor Flemming Hofmann Larsen from University of Copenhagen as well Senior Scientist Henrik Max Jensen and Senior Scientist Graham Sworn from Danisco.

I am particularly grateful to all my supervisors. The combination of your various professional competences and personal qualities has provided me the best possible supervision. You have all inspired me and supported me in different ways and different levels. It has been a pleasure working with you – THANKS!

Special gratitude is shown to Professor Andrew Whittaker and all the people I worked with during my four month stay at Centre for Magnetic Resonance at The University of Queensland (UQ). You all made my stay in Australia an unforgettable experience and provided me with an invaluable knowledge on applied NMR spectroscopy. I also wish to thank Bent Pedersen from Carlsberg Laboratory and Stefan Steunagel from Bruker Biospin for their interest in my project.

I am thankful to all my colleagues at Q&T and Danisco for contributing to a pleasant, welcoming and professionally fruitful working environment. Special thanks to Hanne and Nanna and my two Matlab-helpers Thomas and Karin. Your support and friendship are greatly appreciated. I am also particularly indebted to Dorthe for teaching me about alginate and Bente and Keld for invaluable help with the experimental work.

I am also especially grateful for the sympathy and support from friends and family during this mission. Special thanks to Sanne, Valborg, Anja and Tine for keeping me in touch with every day life during the last three years. Special thanks to Anja for the cover illustration. And Sanne – you are the best proof reader – thank you so much!

Tina Salomonsen
Copenhagen, April 2009

ABSTRACT

Commercial alginates are extracted from brown seaweed (*Phaeophyceae*) and used as thickeners, stabilisers and gelling agents in a range of different applications. Alginates are linear polysaccharides composed of mannuronic acid (M) and guluronic acid (G). The M/G ratios as well as the distribution of M and G along the polymer chains determine the functionality in the applications in which they are used. Various applications and various markets demand different alginates with respect to quality and functionality. Moreover, the costumers expect consistent and fully controlled products, because in some applications it is crucial that the alginate is not deviating from its specifications. Thus, for obvious reasons the alginate industry wishes to control and monitor the alginate composition as close as possible in order to be able to produce standardised alginates or alginates with designed functionalities. Consequently, it is extremely important for alginate manufacturers to have access to methods that can provide reliable estimates of the M/G ratio. Such methods should preferable be rapid and easy-to-use, so that they potentially can be implemented for industrial quality control.

The purpose of this PhD thesis has been to explore the unique potentials of vibrational spectroscopy (i.e. infrared (IR), Raman and near infrared (NIR) spectroscopy) and nuclear magnetic resonance (NMR) for rapid and reliable quantitative analysis of intact alginate powders with respect to the M/G ratio. Different multivariate data analytical techniques (chemometrics) have been employed in order to extract the maximum of relevant information from the recorded spectra. The results have been compared with the results from the traditional ^{1}H solution-state NMR method, which in contrast to solid-state NMR and vibrational spectroscopy requires a time consuming and labour intensive sample preparation.

The impact of water suppression on ^{1}H solution-state NMR spectra of alginates was investigated in PAPER I. The results clearly showed that presaturation of the water signal can introduce undesired and uncontrolled variability to the spectra leading to erroneous quantitative results. Thus, the ^{1}H solution-state NMR spectra in this study were acquired without water suppression.

In PAPER II and III, robust chemometric calibration models based on IR, Raman and NIR spectra for the prediction of alginate M/G ratio were established using ^{1}H solution-state NMR spectroscopy as reference method. The predicted M/G ratio values were determined with higher accuracy from the vibrational spectroscopy spectra than when calculated from the ^{1}H solution-state NMR spectra. In conclusion, there lies a great potential in using vibrational spectroscopy for

industrial quality control of alginates as these methods are rapid, relatively inexpensive and simple to operate.

In PAPER IV and V, the potential of using solid-state NMR spectroscopy for unsupervised determination of alginate M/G ratio was investigated. The ^{1}H high resolution (HR) magic angle spinning (MAS) NMR spectra of semi-solid gel-like alginates provided M/G ratio values comparable to those obtained from ^{1}H solution-state NMR spectra. However, samples with high calcium content were overestimated as in the ^{1}H solution-state NMR method. The M/G ratios could also be extracted from the broad and overlapping ^{13}C cross polarisation (CP)-MAS NMR spectra of solid alginate powders using appropriate chemometric tools. Actually, this non-destructive technique proved to be more reliable in characterising the alginate M/G ratio because of its insensitiveness to calcium ions in the samples.

In conclusion, the research presented in this thesis has demonstrated the unique potentials of using vibrational spectroscopy and solid-state NMR spectroscopy in combination with advanced chemometric techniques for rapid and reliable analysis of alginate powders. The methods are non-destructive, require no sample preparation and may serve as good alternatives to the techniques traditionally used.

RESUMÉ

Kommercielle alginater udvindes fra brune tangplanter (*Phaeophyceae*) og anvendes som fortykningsmidler, stabilisatorer og geleringsmidler i en række forskellige produkter. Alginater er lineære polysakkarider bestående af mannuronsyre (M) og guluronsyre (G). M/G-forholdet samt fodelingen af M og G i polymerkæderne er afgørende for funktionaliteten i de produkter, hvori de anvendes. De forskellige produkter og forskellige markeder kræver forskellige alginater med hensyn til kvalitet og funktionalitet. Derudover forventer kunderne ensartede og fuldt kontrollerede alginater, eftersom det i nogle produkter er af afgørende betydning, at alginaten ikke afviger fra dens specifikationer. Således ønsker alginatindustrien af indlysende årsager at kontrollere og overvåge alginaternes sammensætning så tæt som muligt med henblik på at kunne producere standardiserede alginater eller alginater med designede funktionaliteter. Derfor er det ekstremt vigtigt for alginatproducenter at have adgang til metoder, der kan give pålidelige estimater af M/G-forholdet. Sådanne metoder bør være hurtige og nemme at bruge, så de potentielt kan anvendes til industriel kvalitetskontrol.

Formålet med dette ph.d.-studium har været at udforske de unikke potentialer af kernemagnetisk resonans (NMR) og vibrationsspektroskopi (dvs. infrarød (IR), Raman og nærinfrarød (NIR) spektroskopi) med henblik på hurtig og pålidelig kvantitativ analyse af M/G-forholdet i intakte alginatpulvere. Forskellige multivariate dataanalyseteknikker (kemometri) er blevet anvendt for at ekstrahere den maksimale relevante information fra de målte spektre. Resultaterne er blevet sammenlignet med resultaterne fra den traditionelle ^{1}H væske NMR metode, som i modsætning til fast-stof NMR spektroskopi og vibrationsspektroskopi kræver en tids- og arbejdskrævende prøveforberedelse.

Effekten af vandundertrykkelse på ^{1}H væske NMR spektre af alginater blev undersøgt i ARTIKEL I. Resultaterne viste klart, at undertrykkelse af vandsignalet kan medføre uønsket og ukontrolleret variation i spektrene og dermed fejlagtige kvantitative resultater. Derfor blev ^{1}H væske NMR spektrene i dette studium målt uden vandundertrykkelse.

I ARTIKEL II og III blev der etableret robuste kemometriske kalibreringsmodeller baseret på IR, Raman og NIR spektre til prædiktion af M/G-forholdet i alginater. Referenceværdierne blev bestemt ved hjælp af ^{1}H væske NMR spektroskopi. De prædikterede M/G-forhold blev bestemt med større nøjagtighed fra vibrationsspektroskopi-spektrene, end når de blev beregnet fra ^{1}H væske NMR spektrene. Derfor ligger der et stort potentiale i at anvende de vibrationsspektroskopiske teknikker til industriel kvalitetskontrol af alginater, eftersom disse metoder er hurtige, relativt billige og enkle at betjene.

I ARTIKEL IV og V blev potentialet i at anvende fast-stof NMR spektroskopi til bestemmelse af M/G-forholdet i alginat uden anvendelse af en referencemetode undersøgt. Ud fra ^{1}H højopløste (HR) NMR spektre af halvfaste gel-lignende alginater målt ved rotation i den magiske vinkel (MAS) kunne der opnås M/G-forhold, der var sammenlignelige med værdierne opnået fra ^{1}H væske NMR spektrene. Prøver med højt calciumindhold blev dog overestimeret som i ^{1}H væske NMR metoden. M/G-forholdene kunne også ekstraheres fra de brede og overlappende ^{13}C krydspolariserede (CP)-MAS NMR spektre af faste alginatpulvere ved hjælp af relevante kemometriske værktøjer. Faktisk viste det sig, at denne ikke-destruktive teknik var mere pålidelig til karakterisering af M/G-forholdet i alginater, eftersom den ikke er følsom over for calciumioner i prøverne.

Forskningen præsenteret i denne afhandling har demonstreret de unikke potentialer for at anvende vibrationsspektroskopi og fast-stof NMR spektroskopi i kombination med avancerede kemometriske teknikker til hurtig og pålidelig analyse af alginatpulvere. Metoderne er ikke-destruktive, kræver ingen prøveforberedelse og er gode alternativer til de teknikker, der traditionelt anvendes.

LIST OF PUBLICATIONS

PAPER I
Salomonsen, T., Jensen, H.M., Larsen, F.H. & Engelsen, S.B. (2009). The quantitative impact of water suppression on NMR spectra for compositional analysis of alginates. In M. Guðjónsdóttir, P.S. Belton & G.A. Webb (Eds.), *Magnetic Resonance in Food Science. Challenges in a Changing World*. (pp. 12-19) Cambridge: RSC Publishing.

PAPER II
Salomonsen, T., Jensen, H.M., Stenbæk, D. & Engelsen, S.B. (2008). Chemometric prediction of alginate monomer composition. A comparative spectroscopic study using IR, Raman, NIR and NMR. *Carbohydrate Polymers*, 72, 730-739.

PAPER III
Salomonsen, T., Jensen, H.M., Stenbæk, D. & Engelsen, S.B. (2008). Rapid determination of alginate monomer composition using Raman spectroscopy and chemometrics. In P. A. Williams & G. O. Phillips (Eds.), *Gums and Stabilisers for the Food Industry 14* (pp. 543-551). Cambridge: RSC Publishing.

PAPER IV
Salomonsen, T., Jensen, H.M., Larsen, F.H., Steuernagel, S. & Engelsen, S.B. (2009). Alginate monomer composition studied by solution- and solid-state NMR – a comparative chemometric study. *Food Hydrocolloids*, 23, 1579-1586.

PAPER VI
Salomonsen, T., Jensen, H.M., Larsen, F.H., Steuernagel, S. & Engelsen, S.B. Direct quantification of M/G ratio from ^{13}C CP-MAS NMR spectra of alginate powders by multivariate curve resolution. *Carbohydrate Research, Accepted*

ADDITIONAL PUBLICATIONS

Winning, H., Viereck, N., Salomonsen, T., Larsen, J. & Engelsen, S.B. (2009). Quantification of blockiness in pectins. A comparative study using vibrational spectroscopy and chemometrics. *Carbohydrate Research*, *In Press*

Viereck, N., Salomonsen, T., van den Berg, F. & Engelsen, S.B. (2009). Raman applications in food analysis. In M.S. Amer (Ed.), *Raman Spectroscopy for Soft Matter Application* (pp. 199-223). Hoboken: John Wiley & Sons, Inc.

Salomonsen, T., Sejersen, M.T., Viereck, N., Ipsen, R. & Engelsen, S.B. (2007). Water mobility in acidified milk drinks studied by low-field ^{1}H NMR. *International Dairy Journal*, 17, 294-301.

Sejersen, M.T., Salomonsen, T., Ipsen, R., Clark, R., Rolin, C. & Engelsen, S.B. (2007). Zeta potential of pectin stabilised casein aggregates in acidified milk drinks. *International Dairy Journal*, 17, 302-307.

POPULAR SCIENTIFIC PUBLICATIONS IN DANISH

Salomonsen, T., Engelsen, S.B., Nørgaard, L. & Bro, R. (2009). Det kemometriske rum. Kemometrisk kvalitetskontrol af alginat – et eksempel fra den virkelige verden. *Dansk Kemi*, 90(4), 28-29.

Pedersen, B. & Salomonsen, T. (2007). Kemometri optimerer fødevare-produktionen. *Plus Proces*, 10, 12-15.

Salomonsen, T., Sejersen, M.T., Viereck, N. & Engelsen, S.B. (2006). Stabilitet af drikkeyoghurt med pectin undersøgt ved hjælp af NMR spektroskopi og kemometri. *Mælkeritidende*, 3-4, 55-58, 78-79.

LIST OF ABBREVIATIONS

1D	one dimensional
2D	two dimensional
ALS	alternating least squares
ATR	attenuated total reflectance
COSY	correlation spectroscopy
CP	cross polarisation
CRAMPS	combined rotational and multiple pulse spectroscopy
CSA	chemical shift anisotropy
DP_n	degree of polymerisation
EDTA	ethylenediaminetetraacetic acid
EISC	extended inverse signal correction
EMSC	extended multiplicative signal correction
ESR	electron spin resonance
FID	free induction decay
FT	Fourier transform
G	guluronic acid/guluronate
GDL	glucono-δ-lactone
HR	high resolution
HSQC	heteronuclear single quantum coherence
iPLSR	interval partial least squares regression
IR	infrared
ISC	inverse signal correction
M	mannuronic acid/mannuronate
M/G	ratio of mannuronic acid and guluronic acid
MAS	magic angle spinning
MCR	multivariate curve resolution

MSC	multiplicative signal correction
NIR	near infrared
NMR	nuclear magnetic resonance
PAT	process analytical technology
PC	principal component
PCA	principal component analysis
PLSR	partial least squares regression
r	correlation coefficient
RF	radio frequency
RMSECV	root mean square error of cross validation
RMSEP	root mean square error of prediction
SHMP	sodium hexametaphosphate
SNV	standard normal variate
std	standard deviation
TSP-d_4	3-(trimethylsilyl)propionate-d_4
VIS	visible
WATERGATE	water suppression by gradient tailored excitation

TABLE OF CONTENTS

INTRODUCTION

1

1.1 BACKGROUND

Alginates are the most abundant polysaccharides in brown seaweed (*Phaeophyceae*) in which they act as structural components providing mechanical strength and flexibility for growth in sea. They comprise 2-7% of the wet seaweed and up to 40% of the dry matter (Black 1950). Alginate was discovered in 1881 by the British chemist E.C.C. Stanford (Stanford 1881). Stanford obtained a water-soluble material, which he called soluble algin, by extracting brown seaweed with sodium carbonate, and an insoluble material, which he called insoluble algin, by acidifying a solution of the soluble algin (i.e. precipitation by lowering pH). Later he realised that the insoluble algin was an acid and that the soluble algin was its sodium salt. Today, the term alginate is used as a common name for all salts of alginic acid and sometimes also refers to alginic acid itself and derivatives of alginic acid.

Almost 130 years have passed since alginate was first discovered and today alginates are widely used as thickeners, stabilisers and gelling agents in a range of different applications. Alginates are for example used in foods which need to be stable for longer periods and maintain good structure after freezing and reheating such as fast food and convenience food. Since today's busy lifestyles and growing awareness of the link between diet and health have lead to a rapid rise in the consumption of healthy fast food and convenience food (IFAU 2007), the demand for stabilising food ingredients such as alginate and other water-binding polysaccharides and proteins (hydrocolloids) are increasing. Even though hydrocolloids are often present in concentrations less than 1% (w/w), they can significantly improve the textural and organoleptic properties of food products. These years, the world hydrocolloid market are growing with a rate of 3-5% p.a. and the estimated value of the market is around €2.3 billion p.a. (IMR International 2009; Nørager 2009). An overview of the value of the hydrocolloid market is given in Figure 1.

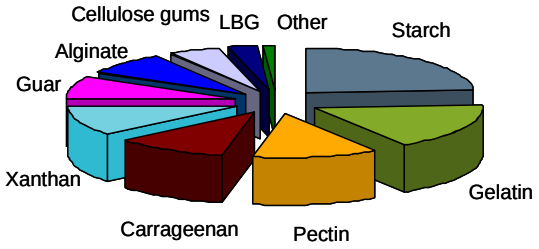

Figure 1 Estimated value of world market for individual hydrocolloids (IMR International 2009; Nørager 2009). LBG = locust bean gum.

The annual industrial production of alginates is about 45,000 metric tonnes (IMR International 2001; Thorøe-Hansen 2009). Despite the fact that alginates account for a relatively small value (8%) of the total value of the hydrocolloid market, their unique ability to form heat stable gels in the presence of calcium ions, make them most interesting molecules to study from an industrial as well as scientific point of view.

In the food industry, alginates are used as thickeners and gelling agents in a range of different food products (e.g. restructured foods, jams and jellies, ice cream and salad dressings). In addition to food uses, alginates are also widely used in the technical industry to control the rheological properties in for example textile print and recently there has been an increasing interest in the use of alginates in biotechnological, biomedical and pharmaceutical applications (Skjåk-Bræk & Espevik 1996), which set new specifications on commercial alginates with respect to purity, mechanical properties and biocompatibility. Thus, various applications and various markets demand different alginates with respect to quality and functionality. Moreover, the costumers expect consistent and fully controlled products, because in some applications it is crucial that the alginate is not deviating from its specifications.

Alginates are linear polymers composed of mannuronic acid (M) and guluronic acid (G). The M/G ratios as well as the distribution of M and G along the polymer chains determine the functionality in the products in which they are used (i.e. viscosity and gel strength). For obvious reasons, the alginate industry wish to control and monitor the alginate composition as close as possible in order to be able to produce standardised alginates or alginates with designed functionalities. It is extremely important for alginate manufacturers and researchers to have access to methods that can provide reliable estimates of the alginate composition. Such methods should preferable be rapid and easy-to-use, so that they can be used for quality control (at- or on-line) and high-throughput screening of large sample sets.

During the past 50 years many efforts have been devoted to measuring the M/G ratio of alginates. The first methods included chemical modifications of the alginates by total hydrolysis and formation of derivatives followed by separation and detection using paper chromatography (Fischer & Dörfel 1955), ion exchange chromatography (Larsen & Haug 1961; Haug & Larsen 1962), colourimetry (Knutson & Jeanes 1968), polarimetry (Siddiqui 1978), high performance liquid chromatography (Annison *et al.* 1983; Krull & Cote 1992) and gas chromatography (Vadas *et al.* 1981). The major disadvantage of these methods is the tedious sample preparation involving numerous steps and chemicals. Moreover, the results are often unreliable due to different degradation rates and reaction activities of the two monomers. Circular dichroism (CD) (Morris *et al.* 1975; Morris *et al.* 1980; Donati *et al.* 2003) has been proposed as a rapid and non-destructive method for determining the monomer composition of intact alginates in solution (Morris *et al.* 1975; Morris *et al.* 1980; Donati *et al.* 2003). However, this method is very sensitive to the presence of divalent ions (e.g. calcium ions), which are often present in commercial alginates.

^{1}H and ^{13}C solution-state nuclear magnetic resonance (NMR) spectroscopy of moderately depolymerised alginates are today the de facto standard methods for structural analysis of alginates (Penman & Sanderson 1972; Grasdalen *et al.* 1977; Grasdalen *et al.* 1979; Grasdalen *et al.* 1981; Grasdalen 1983).

Unfortunately, solution-state NMR spectroscopy is not the most convenient method for routine analysis of large number of samples due to the time-consuming and labour intensive sample preparation required in order to reduce the molecular weight and thereby the viscosity of the alginates to a level suitable for NMR analysis. Thus, development of faster and simpler methods for the characterisation of alginates would be beneficial to the ingredient industry.

The continuous advancement within NMR instrumentation has made it possible to obtain relatively well resolved NMR spectra of semi-solid and solid samples. Moreover, vibrational spectroscopic techniques such as infrared (IR), Raman and near infrared (NIR) spectroscopy, are excellent methods when it comes to rapid measurements of solid samples such as alginate powders. However, the potentials of these spectroscopic methods can only be fully exploited when regressed to a primary method of analysis due to the overlapping nature of the obtained spectra. Therefore, mathematical tools which can handle the multivariate, covariate spectroscopic data is required. In the context of chemical analysis, the multivariate analytical methods are referred to as chemometrics, originating from *chemeia* (Greek, chemistry) and *metros* (Greek, measure).

1.2 AIM OF THE THESIS

The aim of this thesis is to explore the unique potentials of NMR and vibrational spectroscopy for rapid and reliable quantitative analysis of intact alginate powders with respect to molecular composition. Different multivariate data analytical techniques are employed in order to extract the maximum of relevant information from the recorded spectra. The results are compared with the results from the traditional solution-state NMR method based on the analysis of depolymerised alginates.

1.3 THESIS OUTLINE

The thesis consists of an introductory part followed by two conference proceedings (PAPER I and III) and three peer reviewed scientific papers (PAPER II, IV and V). Moreover, two popular scientific publications in Danish are enclosed in a supplement. The introductory part serves to introduce the reader to alginate, the methods used in the study as well as the major results, and are organised as follows:

Chapter 2 presents an initial overview of source and manufacture, composition, sequence and structure, functional properties and industrial applications of alginates.

Chapter 3 serves as an introduction to the spectroscopic techniques used in the study. Sufficient theory is provided for the reader to understand the underlying principles of each technique. Moreover, the results of PAPER I will be summarised in this chapter.

Chapter 4 provides an introduction to the data analytical methods applied in the study. This primarily concern multivariate data analysis in the form of chemometrics. All major chemometric methods used in the study are introduced.

Chapter 5 gives an overview of the major results of PAPER II-V, and the advantages and disadvantages of using spectroscopic analysis for alginate powders as opposed to alginate solutions are discussed. The details regarding materials, methods and results are documented in the annexed papers.

Chapter 6 summarises the conclusions and challenges of the study, and the perspectives for the future use of solid-state spectroscopy for the analysis of alginates are discussed.

ALGINATE

2

2.1 SOURCE AND MANUFACTURE

Alginate is located in the intercellular matrix of brown seaweeds as a gel containing the cations found in seawater. The principal ones are sodium, magnesium and calcium ions (Haug & Smidsrød 1967; Baardseth 1969), which are bound to the alginate in proportions depending on the molecular composition of the alginate (Smidsrød & Haug 1968). In brown seaweed the gel provides the necessary mechanical strength as well as flexibility for growth in the sea, and for those plants exposed to air at low tide alginate also prevents desiccation. The molecular composition of alginates is closely related to the stiffness and elasticity of the seaweed and varies with growth environment and plant productive cycle (season) as well as within different species of seaweed and tissues of the same plant (Black 1950; Haug & Jensen 1956; Grant *et al.* 1973; Haug *et al.* 1974; Stockton *et al.* 1980; Indergaard *et al.* 1990). For example, seaweed species growing in turbulent water must be able to withstand more mechanical stress than species growing in calm water. As a consequence hard alginate gels are obtained from seaweed grown in turbulent water whereas more elastic gels are obtained from seaweed grown in calm water. In both cases the plant regulates the gel strength by changing the molecular composition of alginate.

Alginates are also produced by the bacteria *Azotobacter vinelandii* (Gorin & Spencer 1966) and several species of *Pseudomonas* (Linker & Jones 1966). The biological functions of alginates in bacteria include for example protection of the cells from desiccation, mechanical stress and certain antibodies and participation in the adherence to surfaces (Vela 1974; May & Chakrabarty 1994). The main difference between bacterial and seaweed alginates is the presence of *O*-acetyl groups in some bacterial alginates (Skjåkbræk *et al.* 1986). Production of alginate by fermentation is at present not economically attractive and all commercial alginates are today extracted from seaweed.

All brown seaweeds contain alginate but not all are sufficiently abundant and conveniently located for commercial production. The species most widely used for commercial production are *Laminaria hyperborea, Laminaria digitata*, *Macrocystis pyrifera* and *Ascophyllum nodosum* (Draget *et al.* 2006). The seaweed is collected on the beach or harvested from the sea (mechanically or cut by hand). In countries such as China, Japan and the Republic of Korea, where seaweed makes up a major part of the diet, brown seaweed is cultivated. However, cultivated seaweed is normally too expensive for alginate production and is thus only used in the alginate industry if there is a surplus production (McHugh 2003).

Alginate was exploited commercially for the first time in the 1930s and the current production methods are based on modifications of processes invented by

Green (1936) and Le Gloahec and Herter (1938). An overview of the extraction of alginate from seaweed is schematically illustrated in Figure 2.

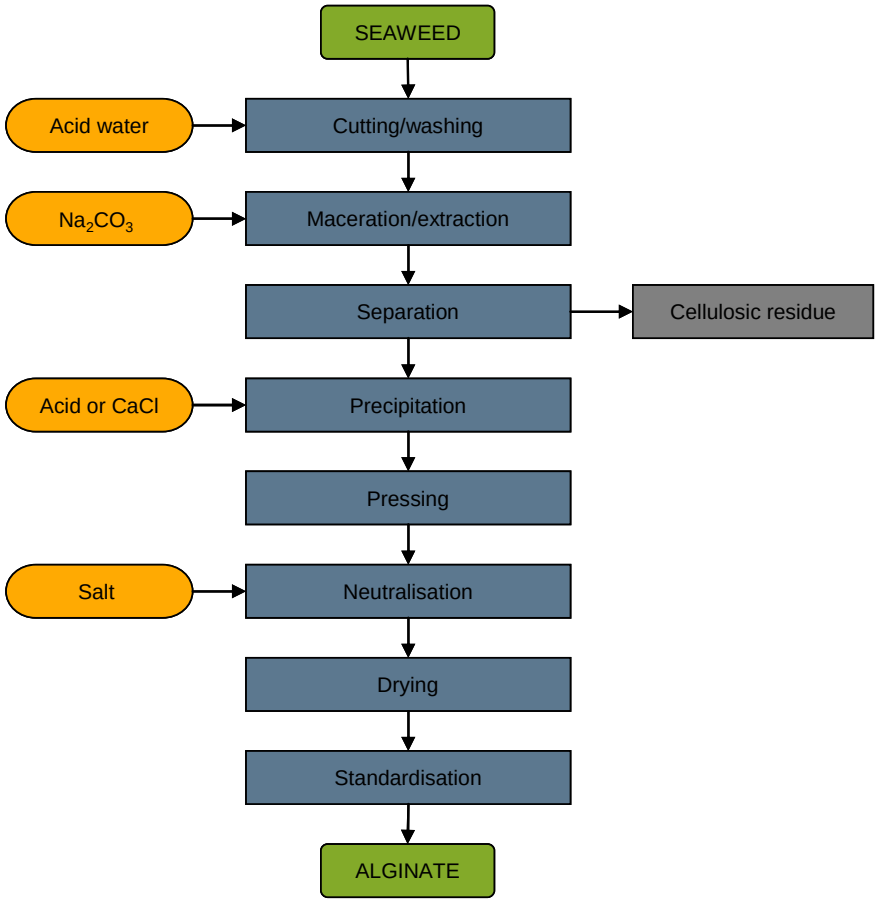

Figure 2 Overview of the extraction of alginate from brown seaweed

The process is generally an ion-exchange process. In the first step, the seaweed is cut into pieces and washed with dilute mineral acid (e.g. hydrochloric or sulphuric acid) in order to convert the water-insoluble calcium and magnesium alginates into alginic acid. The alginic acid is then subsequently extracted with alkali. At the same time, the acid-soluble phenolic compounds are removed. Then the alginic acid is brought into solution by neutralisation with sodium carbonate to form a water-soluble sodium alginate. The dissolved sodium alginate is subsequently separated from the alkali-insoluble seaweed residue, which mainly consists of cellulose. This is done using separation procedures such as sifting, floatation, centrifugation and filtration. Once the solution containing sodium alginate has been separated from the residual seaweed, the sodium alginate is precipitated as alginic acid or its calcium salt by addition of mineral acid or calcium chloride, respectively. Evaporation is not economically feasible because the solution is too dilute. If using calcium chloride for the precipitation, the calcium alginate is afterwards treated with dilute mineral acid (typically hydrochloric acid) to form alginic acid. The alginic acid is pressed and the

resulting paste containing about 75-80% water is used as starting material for preparation of different alginate salts (sodium, potassium, ammonium or calcium) or esterified with propylene oxide to produce propylene glycol alginate (PGA), which are used in other applications than the alginate salts due to its acid solubility and ability to interact with protein (cf. Section 2.4). Sodium alginate is the most commonly used alginate and is therefore produced in higher quantities than the other types. Finally, the alginate is dried to about 10-20% moisture, milled to the desired particle size (mesh grade) and blended with other hydrocolloids or sucrose to meet the costumers' specifications. Alginates from different sources will often be blended together to produce a desired functionality (i.e. gel strength and viscosity). The final product is a white to pale yellowish-brown powder. The colour can be controlled by soaking the seaweed in formalin solution prior to alkali extraction and/or by adding a bleaching agent such as sodium hypochlorite to the filtered alkaline extract or even to the paste at the final conversion stage (McHugh 2003).

Different industries have different requirements with respect to colour and purity of the alginates. The darkest products are typically used in technical applications and are sold for a lower price than the lighter alginates, which are more suitable for food and other applications. Pure alginate powders are colourless and alginates used in certain pharmaceutical products must be ultrapure and low in pyrogens (cf. Section 2.4). Therefore, in the production of these products, the alginate solution is sterilised by filtration (Draget 2001).

2.2 COMPOSITION, SEQUENCE AND CONFORMATION

Alginates were at first thought to be homopolymeric mannuronans, but in 1955 Fisher and Dørfel showed that alginates in addition to D-mannuronic acid (Figure 3a) also contain L-guluronic acid residues (Figure 3b) (Fischer & Dørfel 1955). Alginates are biosynthesised from a linear polymer of β-D-mannuronic acid by enzymatic C-5 inversion of β-D-mannuronic acid (M) to α-L-guluronic acid (G) (Hellebust & Haug 1969; Larsen & Haug 1971; Madgwick *et al.* 1973). Thus, the M/G ratio and sequence are controlled by occurrence and activity of the mannuronan C-5 epimerases, which vary within seaweed species and tissues of the same plant as well as with season and growth conditions (Ishikawa & Nisizawa 1981).

The fact that alginates are true copolymers rather than physical mixtures of mannuronate and guluronate emerged from the work by Haug and co-workers (Haug & Smidsrød 1965; Haug *et al.* 1966; Haug & Larsen 1966; Haug *et al.* 1967a). From their work, based on partial acid hydrolysis and subsequent fractionation, it was concluded that alginates are true block copolymers composed of homopolymeric regions of mannuronate and guluronate, termed M- and G-blocks, respectively, disrupted with regions of alternating mannuronic and guluronic acid residues, termed MG-blocks. Their findings were later confirmed by the use of specific degrading enzymes (Boyd & Turvey 1978) and ^{13}C NMR spectroscopy (Grasdalen *et al.* 1981).

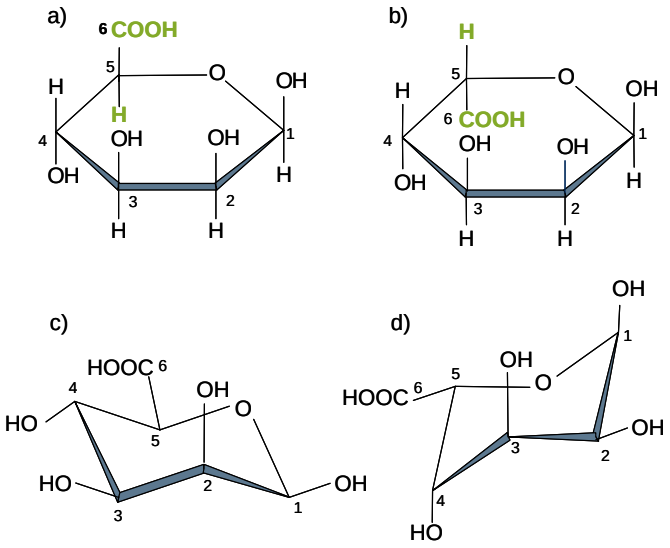

Figure 3 The monomeric units of alginate represented as Harworth projections: (a) mannuronic acid and (b) guluronic acid. The carboxylic group and the hydrogen attached to C-5 are highlighted with green in order to emphasize the difference between the two monomers. (c) Mannuronic acid and (d) guluronic acid is also represented in their preferred chair conformation: $^4C_1$ and $^1C_4$, respectively.

The geometries of the M-, G- and MG-blocks depend on the particular shapes of the monomers and their mode of linkage in the polymer. The two monomers tend to settle into their most energetically favourable conformation and X-ray diffraction studies of mannuronate rich and guluronate rich alginates have showed that the guluronate residues of homopolymeric blocks are in the slightly unusual $^1C_4$ chair conformation (Atkins *et al.* 1970) (Figure 3d), whereas the mannuronate residues are in the $^4C_1$ conformation (Figure 3c). The usual $^4C_1$ conformation of mannuronate refers to the fact that C-4 is above and C-1 is below the plane formed by C-3, C-2, C-5 and O-5 (Rao *et al.* 1998). The M-blocks have an extended ribbon shape and are flexible (Atkins *et al.* 1973a) whereas the G-blocks are buckled and are stiffer (Atkins *et al.* 1973b). The chain conformations of β-(1-4)-linked D-mannuronic acid and α-(1-4)-linked L-guluronic acid are shown in Figure 4. A combination of viscosity experiments and conformational energy calculations has shown that the stiffness of the three types of blocks increased in the order MG-blocks < M-blocks < G-blocks, which indicates that the guluronic acid residue in the alternating sequence had to be set in the $^1C_4$ conformation as well (Smidsrød *et al.* 1973). This was later confirmed by ^{13}C NMR spectroscopy (Grasdalen *et al.* 1977). The molecular geometries of the different blocks are closely related to the gelling of the alginate, which will be described in more details in Section 2.3.3.

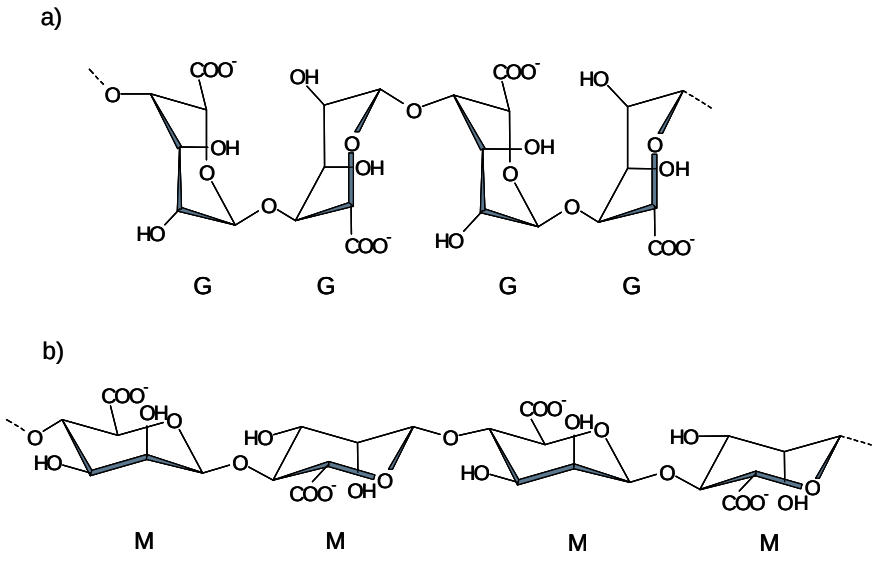

Figure 4 Chain conformation of (a) α-(1-4)-linked L-guluronic acid (G) and (b) β-(1-4)-linked D-mannuronic acid (M)

2.3 FUNCTIONALITY

Functional properties such as solubility, viscosity and gel properties are of primary importance to industrial users of alginate. The functional properties are in turn determined by the composition of the alginate and the counter-ions. For example, the solubility of a specific alginate type is related to the type of salt used as counter-ion, the viscosity is correlated to the molecular weight and the gel strength is associated with the monomer composition and sequence. These relations will be discussed in more details in the following.

2.3.1 Solubility in water and acid

Sodium, potassium and ammonium alginates and PGA are all soluble in cold water. However, care must be taken to avoid lump formation, and therefore homogeneous solutions are best prepared at relatively high stirring rates by sprinkling the powder into the water vortex followed by 10-20 min of stirring at high rate. Calcium alginate and alginic acid are on the other hand insoluble in water and will not form smooth solutions. However, they will swell to form paste-like globules due to absorption of water. PGA is completely soluble in acid and sodium, potassium and ammonium alginates are soluble in weak acids with pH values higher than the pK_a values of the alginate, which depend on the primary structure of the polymer. The pK_a values of M-blocks and G-blocks are 3.5 and 3.7, respectively, and the MG-blocks have the highest acid solubility (pK_a < 3.5). Thus, the acid solubility decreases in the order MG-blocks > M-blocks > G-blocks (Haug *et al.* 1967b).

2.3.2 Viscosity and molecular weight

Alginates are in many applications used as a thickener, which makes viscosity the primary parameter of interest. The viscosity is essentially a measure of a liquid's resistance to flow and it is given in units of Pascals·seconds (Pa·s). In the

industry, the viscosity is typically determined by using a rotational viscometer (e.g. a Brookfield LVT viscometer) and measured in centipoise (cP), which is equal to 0.001 Pa·s. In an alginate solution, viscosity is influenced significantly by the average molecular weight (M_w) as illustrated in Figure 5, which shows average molecular weight as a function of viscosity in 1% (w/w) alginate solutions.

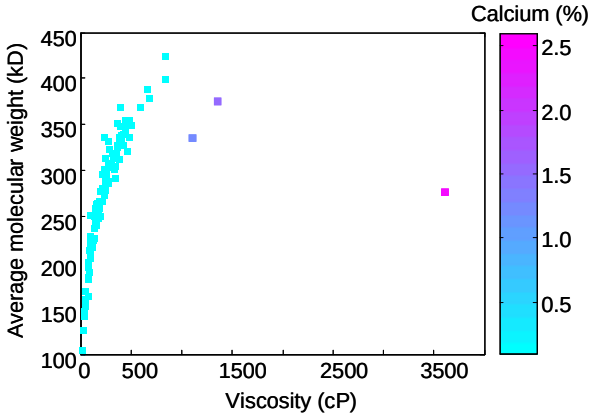

Figure 5 The average molecular weight as a function of the viscosity in 103 alginate solutions (1% (w/w)). The samples are coloured according to the calcium content. The measurements were carried out as described in PAPER IV.

In Figure 5 it can be observed that the viscosity increases exponentially with increasing molecular weight. This is because of increasing entanglement of the long polymer chains as they randomly tumble in solution. Above a certain molecular weight the effect from separate chains entangling into each other becomes more pronounced with resultant higher viscosity dependency. In addition to molecular weight, the viscosity of alginate solutions will also vary with respect to alginate concentration, temperature and presence of ions (especially divalent ions). The latter is also illustrated in Figure 5, where three of the alginates contain significantly higher amounts of residual calcium ions (1.1%, 1.4%, 2.4%) than the other samples (0.01-0.2%) resulting in a significantly higher apparent viscosity due to calcium-alginate cross-linking and thereby formation of a weak gel (cf. Section 2.3.3). Consequently, the measured viscosity of the samples with high calcium content is not correlated to the molecular weight. The effect of the calcium ions can be compensated for by adding a chelating agent (e.g. EDTA or sodium hexametaphosphate).

The average molecular weight and thereby the viscosity is influenced by the processing conditions. Thus, alginates may be prepared in a wide range of average molecular weights to suit the application. The average molecular weights of commercial alginates vary between the different products and typically lie in the range of 50 kD to 425 kD, which corresponds to an average degree of polymerisation (DP_n) in the range of approximately 280 to 3000. However, average molecular weights of laboratory extracted alginates have been reported to be as high as 1640 kD (Draget *et al.* 2006). It is important to keep in mind that the functional properties of alginates, which exhibit relative large variations in DP_n, are not only influenced by their molecular weight but also the molecular

weight distribution. A very broad molecular weight distribution can have implications for the uses of alginates. For example, a very broad molecular weight distribution can lead to leakage of the low molecular weight fragments (Stokke *et al.* 1991), which for example can be a problem when using alginates to encapsulate active drugs or living cells for *in vivo* use.

2.3.3 Gelation

Alginates are especially known for their ability to form heat stable gels (i.e. the gel can be heated without melting). This property is due to the selective binding of certain divalent earth metal ions resulting in the formation of a three-dimensional gel structure. It has been shown that the affinity of alginates for divalent metal ions increases in the order magnesium << calcium < strontium < barium (Smidsrød & Haug 1968; Haug & Smidsrød 1970). However, in food and pharmaceutical applications, calcium ions are the most suitable because of their non-toxicity. The selectivity for binding of calcium ions and thereby the gel-forming properties vary widely with alginate composition (Smidsrød & Haug 1972) and sequence (Smidsrød & Haug 1968; Haug & Smidsrød 1970; Smidsrød 1974). Generally, alginates containing a high amount of guluronate form strong, brittle gels with good heat stability, while alginates containing a high amount of mannuronate form weaker, more elastic gels that are less heat stable but have better freeze-thaw stability. These different properties can be ascribed to the fact that the selective binding of calcium ions and the corresponding gel strength increase in the order MG-blocks $\leq$ M-blocks << G-blocks (Smidsrød 1974).

As described in Section 2.2, the G-blocks adopt a buckled configuration providing a number of electronegative cavities, whose size and geometry appear to be effective binding sites for some cations as illustrated for calcium in Figure 6. The ions interact not only with the carboxyl groups but also with the electronegative oxygen atoms of the hydroxyl groups (Grant *et al.* 1973).

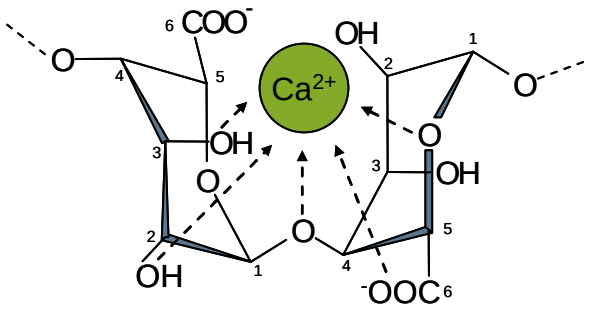

Figure 6 Binding of calcium ions in the G-blocks as suggested by Grant *et al*. (1973). The main attractive interaction is of an electrostatic nature between the calcium ion and the partial negatively charged oxygen atoms is illustrated with arrows.

This specific binding of divalent cations between the long, structurally and sterically regular G-blocks results in the formation of junction zones and a three-dimensional gel network as illustrated in Figure 7. This model has been named 'the egg-box model' (Grant *et al.* 1973) because the arrangement of the calcium ions between the G-blocks is similar to the way in which eggs are packed in boxes. This model is simple and intuitive, and even though other steric arrangements have been suggested (Mackie *et al.* 1983; Steginsky *et al.* 1992), it

still persists as an intuitive working model. However, it has been discussed whether the junction zones consist of only one row of 'eggs' (dimerisation) or more rows of 'eggs' (lateral association) as illustrated in Figure 7b and c, respectively. Grant *et al.* (1973) considered the 'egg-boxes' to be multinuclear aggregates but later it was suggested that the primary mechanism of interchain association is by dimerisation (Smidsrød 1974; Morris *et al.* 1978). However, this simple dimerisation of alginate chains in the egg-box model does not seem to be entirely compatible with new experiments. Data from small angle X-ray scattering on alginate gels suggests lateral association far beyond pure dimerisation with increasing calcium ion content and guluronic acid content of the alginate (Stokke *et al.* 2000). In fact, dimensions corresponding to a pure dimerisation of alginate chains seem to be an exception.

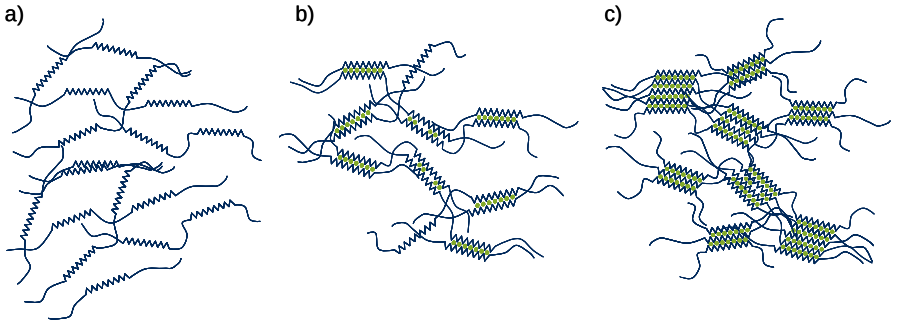

Figure 7 The egg-box model for the alginate network formation (Grant *et al.* 1973). (a) The buckled part of the polymer represents the G-blocks and calcium ions are represented as green circles. (a) Single chains when no calcium ions are present. (b) Dimerisation of alginate chains. (c) Lateral association of multiple alginate chains.

The discovery of alginate epimerases, which can be used to modify alginates with high contents of mannuronate into alginates with long strictly alternating sequences (Ertesvåg & Valla 1996) has provided new insight into the role of MG-blocks in the alginate gel network. Results from a recent study indicate mixed junction zones between G- and MG-blocks (Donati *et al.* 2005). Thus, G-blocks are not the only sequences involved in junction formation.

Methods for gel formation

As described above, alginate gels are most commonly formed by the use of calcium ions. However, the way the calcium ions are introduced into the original sodium alginate solution is important for the quality of the resulting gel. There are essentially two main methods for the preparation of alginate gels, namely the diffusion setting method and the internal setting method. Diffusion setting is when the gel is formed by allowing calcium ions to diffuse into an alginate solution (or paste) from an external bath (or spray) typically containing a calcium chloride solution. This method is normally used to produce small spheres or thin strips, or to provide a thin biofilm coating on the surface of a product. Internal setting, on the other hand, is when, the calcium ions are released slowly from the system. This is done by using an inactive form of the calcium ion, either bound by a sequestering (e.g. phosphate, citrate or EDTA) or as an insoluble salt (e.g. calcium sulphate or calcium carbonate). Calcium ions are then released by lowering the pH, typically by adding a solution of slowly hydrolysing glucono-δ-lactone (GDL). GDL is an ester, which when added to the alginate solution,

hydrolyzes to form gluconic acid (GH), a weak acid, which dissociates over time and thus gradually lowers the pH. Calcium ions are released due to the acidic properties of the sequestering agent and a gel is formed. The time needed for a gel to form can be controlled by the amount and solubility of the calcium source and the GDL as well as the temperature.

Figure 8 shows the gel strength as a function of time after addition of GDL to three solutions based on alginates with different M/G ratios. The pH values of the gels are also plotted.

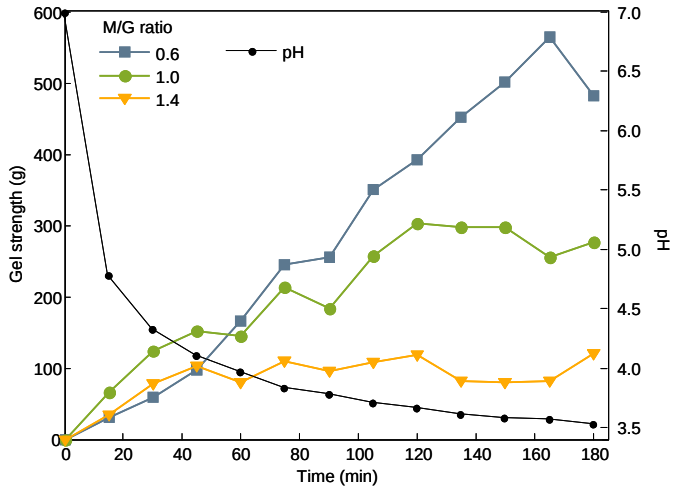

Figure 8 Gel strength measured in grams (g) as a function of time after addition of GDL to solutions of alginates with three different M/G ratios. The pH values of the gels are also plotted and did not decrease further after 180 min. The measurements were carried out as described in PAPER II.

Measurement of gel strength

Gel texture is one of the most important sensory qualities of gelled food products (Renard *et al.* 2006). The gel texture can be evaluated by sensory analysis but instrumental measurements are often preferred. A simple empirical method often used in the food industry for the measurement of gel textures is the penetration method. This method is, as the name suggest, a simple penetration of the gels using a force-deformation instrument. The force required to break the gel is called the 'gel strength' or the 'gel hardness'. However, such results are highly dependent on probe and sample geometry, temperature, recipe and history of the sample and of course the instrument settings (e.g. speed of penetration).

Texture profiles of three gels based on alginates with different M/G ratios are shown in Figure 9. The force used to compress the alginate gels is recorded as a function of time. In the beginning of compression, a build-up of force occurs followed by a fracture of the gel at the point of maximum force. This force is the measure of the gel strength. Compression continues after gel fracture, resulting of accumulation of force until probe retraction.

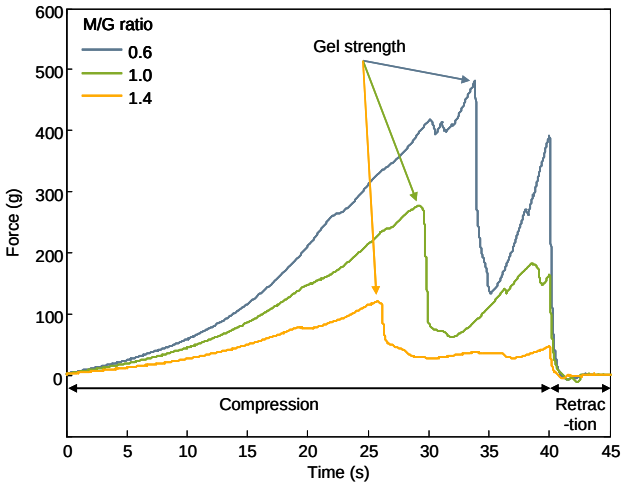

Figure 9 Texture profiles of three alginate gels with different M/G ratios. The point of maximum force of compression is defined as the gel strength in grams (g) units. The measurements were carried out as described in PAPER II.

Another approach for measuring gel texture is the more fundamental rheological characterisation where the gel is studied by the use of small amplitude oscillating shear viscometers. The effect of an oscillating force on the movement of the gel is examined and the amount of energy stored in the system per cycle (dynamic storage modulus, G') and energy lost per cycle (dynamic loss modulus, G''), which are analogous to gel strength and viscosity, respectively, are recorded. Such viscometers are generally more expensive than the more simple texture analysers and are normally more frequently used in research laboratories than in quality control laboratories.

2.4 INDUSTRIAL APPLICATIONS

Alginates are used as thickeners, stabilisers and gelling agents in a wide range of different food, technical, pharmaceutical and cosmetic applications. An overview of the most important alginate markets from a quantitative perspective is shown in Figure 10 and examples on selected applications are given in the following. A more extensive account of the many different applications of alginate can be found in reviews by Sime (1990), Onsøyen (1996), Nussinovitch (1997) and McHugh (2003).

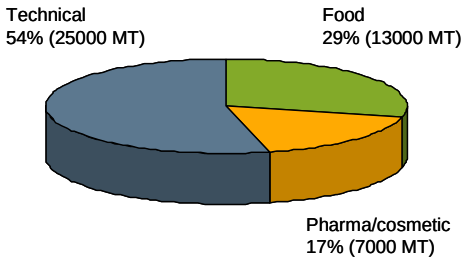

Figure 10 Overview of the quantitative main markets for alginate (IMR International 2001; Thorøe-Hansen 2009).

In the food industry alginate is primarily used as a gelling agent. A steadily growing application of alginate in the food industry is in the production of restructured foods, where flaked, sectioned, chunked or milled food are bound together by alginate to make the food resemble the original. Examples on alginate restructured food products are meat products, onion rings, pimento olive fillings, crabsticks, and cocktail berries. Alginate is also advantageous to use in jams, jellies and fruit-fillings because of its ability to form heat stable gels. This is especially beneficial in the production of bake-off products. In addition, alginates are used as stabiliser and thickener in ice creams, emulsions (e.g. low fat mayonnaise), sauces and salad dressings and beverages resulting in improved texture and prolonged shelf-life. PGA can be used to stabilise acidic products as opposed to the unmodified alginates, which would precipitate at pH values below approximately 3.5 (cf. Section 2.3.1). Moreover, PGA is used to stabilise foams in beer because of its ability to interact with proteins.

As a curiosity is can also be mentioned that alginate has recently been introduced in the field of molecular gastronomy (the scientific investigation of culinary practice (This 2007)) by the three Michelin starred restaurant El Bulli in Catalonia, Spain, which has been judged as the best restaurant in the world in 2002, 2006, 2007, 2008 and 2009 by the British magazine Restaurant (World's 50 best restaurants 2009). El Bulli markets alginate to the public under the name Algin as a part of their product line called Texturas. The target group is chefs and people who like to experiment in the kitchen and El Bulli also provides recipes for the making of mini-spheres, caviar, raviolis, balloons, gnocchi, pellets etc.

For technical applications, alginate is primarily used as a thickener to control the rheological properties. It is used in water-based textile print in order to prevent the paint from running and control levelness of print, colour yield and penetration. Other technical alginate applications are for example treatment of paper and board to improve smoothness and printability, control the rheological properties of compounds used for can sealing and increase the water holding capacity of ceramics resulting in reduced surface cracking and distortion.

In the last decade, there has been an increasing interest in the use of alginates in biotechnological, biomedical and pharmaceutical applications (Skjåk-Bræk & Espevik 1996). In the pharmaceutical industry, alginates are used in different clinical disciplines such as wound healing and treatment of gastroesophageal reflux and as excipients in tablets to control the drug release of the bioactive ingredient. Another new promising area of application is the ultrapure grades of alginates that have a controllable level of pyrogeneicity and thus may be used to encapsulate active drugs or living cells for *in vitro* or *in vivo* use. In addition, alginates are also used in the manufacture of dental impression materials and in cosmetic creams and lotions.

SPECTROSCOPY

3

3.1 INTRODUCTION

Spectroscopy is a general term for the study of interaction between electromagnetic radiation and matter (McNaught & Wilkinson 1997). Electromagnetic radiation interacts with the matter (i.e. atoms and molecules in the sample) in various ways depending on the energy of the radiation and the available excitation states present in the system.

Electromagnetic waves can be described by their wavelength (λ) and frequency (ν), which are inversely correlated. In addition to wave properties, electromagnetic radiation also has particle nature (photons) and the energy of a photon (E) is proportional to its frequency (ν). If a molecule or atom in its lowest energy level (ground state) is exposed to electromagnetic radiation with a specific frequency, it will absorb the energy and be promoted to a higher energy level (excited state). This phenomenon is called resonance and the specific frequency is referred to as the resonant frequency. The allowed states or levels are specific for the interacting molecules or atoms and may also be influenced by their surrounding molecular environment. Consequently, the response from a sample upon radiation at specific wavelengths will provide information of the chemical and physical states of the sample.

Electromagnetic radiation can be classified as gamma rays, X-rays, ultraviolet radiation, visible light, near infrared radiation, infrared radiation, microwaves and radio waves according to wavelength as shown in the electromagnetic spectrum in Figure 11. The electromagnetic spectrum covers wavelengths from less than the size of an atom (gamma rays) to wavelengths of hundreds of meters (radio waves). Consequently, the wavelengths are expressed in different units, e.g. Angström (Å), nanometer (nm), micrometer (μm), etc. However, in the infrared spectral region, the frequencies are often given in units of wavenumber, which is the number of waves per unit length. The most common unit of length is centimetre, in which case wavenumber has units of cm^{-1}.

Spectroscopic methods are grouped according to the type of interaction between the electromagnetic radiation and the matter, which in turn is related to the energy involved during measurement. The spectroscopic methods used in this study are nuclear magnetic resonance (NMR) spectroscopy, where interaction between radio waves and spin states of atomic nuclei in a strong external magnetic field is studied and vibrational spectroscopy, where interaction between infrared radiation and molecular vibrational states is studied. Vibrational spectroscopy includes infrared (IR), near infrared (NIR) and Raman spectroscopy.

The principles of these techniques will be further elaborated on in Section 3.2 and 3.3.

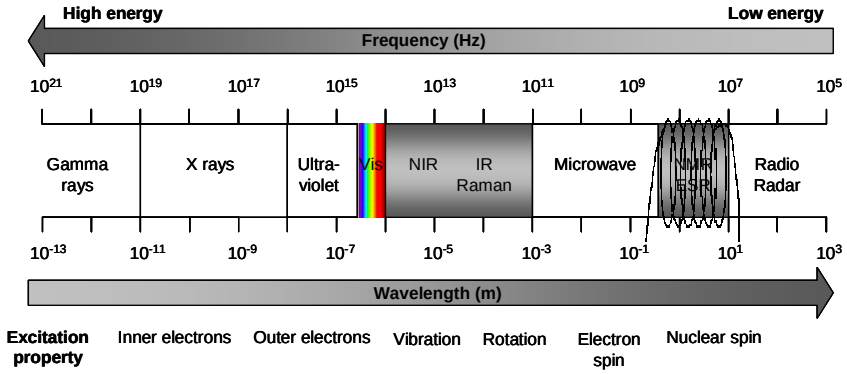

Figure 11 The electromagnetic spectrum showing the range of all possible electromagnetic radiation frequencies classified according to wavelength in gamma rays, X-rays, ultraviolet radiation, visible (VIS) light, near infrared (NIR) radiation, infrared (IR) radiation, microwaves and radio waves. The wavelength ranges of the spectroscopic methods used in this study (nuclear magnetic resonance spectroscopy (NMR), IR, Raman and NIR) are highlighted with grey. The coil is shown to illustrate that an external magnetic field is required for NMR and electron spin resonance (ESR) spectroscopy.

3.2 NMR SPECTROSCOPY

NMR spectroscopy is one of the most powerful tools available for obtaining structural, dynamic and quantitative information on molecules in solution-, semi-solid-, solid- and gaseous-state. The theoretical basis for NMR spectroscopy was early on proposed by Pauli (1924) who suggested that certain nuclei have the properties of spin and magnetic moment, which consequently would lead to a splitting of their energy levels when exposed to a magnetic field. However, it was not until 1946, Bloch (Bloch *et al.* 1946) and Purcell (Purcell *et al.* 1946) performed the first NMR experiments on liquids and solids, for which they shared the Nobel price in physics in 1952. Since that time, applications of NMR have increased steadily in response to the technical developments, which include the general adoption of pulse and Fourier transform methods, the consequent expansion of multinuclear NMR, the introduction of new methods for solid samples and the rapid growth of two-dimensional (2D) NMR, imaging and in vivo spectroscopy. Hence, modern NMR spectroscopy is now a highly developed, but yet still evolving, technique.

In this study, NMR spectroscopy is used for quantitative analysis of the molecular composition of alginates in solution-, semi-solid- and solid-state. Alginate molecules are build from H, C and O atoms and among these ^{1}H and ^{13}C are suitable NMR nuclei in natural abundance, whereas the very low natural abundance of ^{17}O makes this of very little practical relevance. The more specific choice of NMR methodology depends on the physical state of the sample. Standard solution-state NMR methods such as one-dimensional (1D) ^{1}H and ^{13}C spectra as well as 2D homo- or heteronuclear experiments such as ^{1}H-^{1}H COSY or ^{1}H-^{13}C HSQC experiments can be used to study molecules in solution. Similar experiments may be performed on semi-solid samples (e.g. viscous liquids or gels) when these experiments are combined with magic angle spinning (MAS) –

using the so-called high resolution (HR)-MAS approach (cf. Section 3.2.2). In this case line broadening induced by minor anisotropic interactions such as chemical shift anisotropy (CSA) or heteronuclear (^{1}H-^{13}C) dipolar coupling are removed by MAS and line widths comparable to those for solutions are obtained.

Analysis of powders usually employs different experiments. First of all, the very strong homonuclear ^{1}H-^{1}H dipolar couplings make it difficult to acquire ^{1}H NMR spectra with sufficient spectral resolution and therefore ^{13}C is the nucleus of primary interest. Unfortunately, the low natural abundance (1.1 %) of this isotope often results in very time consuming experiments. Therefore, polarisation transfer from the highly abundant ^{1}H is often employed using the cross polarisation (CP) technique (cf. Section 3.2.2). It has to be noted that the cross polarisation technique utilises the ^{1}H-^{13}C dipolar coupling and therefore it is primarily signals from carbons located in the immobile regions of the sample that will be enhanced by CP whereas the CP is less efficient for the mobile regions. The CP technique induces a sensitivity gain of four and in addition the recycle delay depends on the longitudinal relaxation of ^{1}H, which is usually significantly shorter than that for ^{13}C. In order to obtain the best possible spectral resolution CP is combined with MAS and ^{1}H decoupling. Often both ^{13}C single pulse MAS and ^{13}C CP-MAS experiments are acquired in order to compare the signals from all of the carbons with the signals from the immobile regions (cf. Section 3.2.3).

The following includes a short introduction to the basic principles of NMR spectroscopy valid for all NMR experiments (Section 3.2.1). Full accounts on the subject can be found in the many textbooks devoted to the subject by for example Sanders & Hunter (1993), Claridge (1999) and Lambert & Mazzola (2004). In Section 3.2.2, focus is on describing problems related to measuring NMR spectra of semi-solids and solids and how these problems can be partly solved by MAS, high-power decoupling and CP. Finally, the sources of variations, which might be crucial with respect to the quantitative nature of the NMR spectra, are discussed (Section 3.2.3 and 3.2.4).

3.2.1 Basic principles

NMR is a method based on the magnetic properties of certain nuclei. Whether a particular nucleus has magnetic properties or not is given by its spin quantum number (I), which depends on the atomic number and mass of the isotope. When the atomic number and mass are even (e.g. ^{12}C and ^{16}O), the nucleus has no magnetic properties ($I = 0$) and cannot be detected by NMR. However, about two-thirds of all stable nuclei have magnetic properties ($I \neq 0$), and can in principle be detected by NMR. When either the atomic number and/or atomic mass is uneven, the nucleus has magnetic properties ($I \geq ½$). $I = ½$ for nuclei with a spherical shape (e.g. ^{1}H, ^{13}C, ^{15}N and ^{31}P), and $I > ½$ for quadrupolar nuclei, which have a non-spherical shape (e.g. ^{2}H, ^{17}O and ^{23}Na).

Since all nuclei are positively charged, any that have spin will have a circulating current, and thereby an associated magnetism. This magnetic moment (μ) is generated by a spinning, charged nucleus and can be considered as a tiny bar magnet. The strength of the magnetic moment is proportional to the magnetogyric ratio (γ), which varies between the different types of nuclei. The magnetic moments (spins) have vector quantities, which mean that they have both magnitude and direction. Normally, the spins will be randomly distributed in all directions due to thermal motions, and the macroscopic magnetic moment of a sample or material will be zero. However, when placed in an external magnetic

field (B_0), the spins adopt one of a small number of allowed orientations (energy levels). Nuclei with I = ½ (spin-½) has two permitted energy levels. One is parallel with B_0 (α-state) and the other is anti-parallel (β-state). For a system in thermal equilibrium, there will always be a slight excess of nuclei in the lower energy state (α-state), since this is the energetically more favourable state. The population difference between these two orientations is determined by their energy difference as described by the Boltzmann distribution:

Equation 1

$$\frac{N_\beta}{N_\alpha} = \exp\left(-\frac{\Delta E}{k \cdot T}\right)$$

where N_α and N_β is the populations of the lower and upper energy states, respectively, k is Boltzmann's constant, T is the absolute temperature in Kelvin, and ΔE is the energy difference between the spin states.

It is universal practice to define the direction of the static magnetic field (B_0) as being along the z-axis of a set of Cartesian coordinates, so that a spin-½ nucleus will have a component of its magnetic moment along the z-axis (the longitudinal component) and an orthogonal component in the xy-plane (the transverse component). Under the influence of the external magnetic field, the spins will start to precess about the direction of the magnetic field with a nucleus specific frequency called the Larmor frequency (ω_0). The Larmor frequency is proportional to the magnetogyric ratio and the external magnetic field ($\omega_0 = \gamma \cdot B_0$). As a result of the uneven distribution of the spin populations, a weak net magnetisation (M_0) aligned with the z-axis is created (Figure 12a). At equilibrium, the magnetisation vector, aligned with the field (B_0), has no net transverse component. This can be explained by the fact that the individual nuclei are oriented randomly about the direction of field (B_o). If the net magnetisation (M_0) is perturbed by a radio-frequency (RF) with duration precisely long enough to flip the M_0 vector into the xy-plane (a 90° pulse), the largest possible signal in the xy-plane will be generated. Once in the xy-plane, the magnetisation vector will continue to precess about B_0 and thus induce an oscillating signal in the detectors along the x- and y-axes (Figure 12b). As detection cannot be performed in the z-direction this is how the NMR signal is generated.

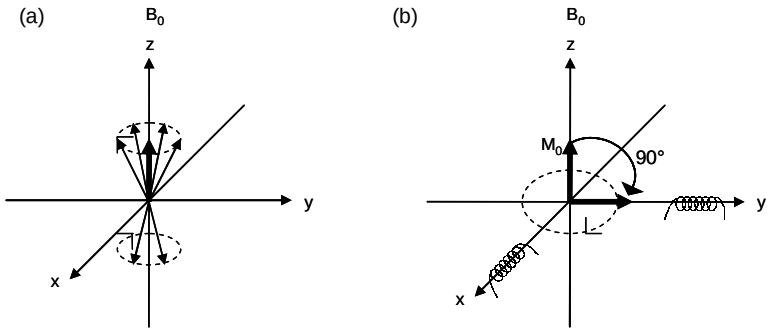

Figure 12 Illustration of the coordinates normally ascribed to the NMR instrument. (a) Individual spins around the external magnetic field (B_0) and the resulting net magnetisation vector (M_0, bold arrow). (b) M_0 can be perturbed by a radio frequency pulse and thereby converts to the xy-plane, where it can be measured as a characteristic frequency in the receiver coil.

With time, the system will loose coherence in the xy-plane, a process known as spin-spin or transverse relaxation described by a time constant called T_2. This process is due to energy exchange between spins as well as inhomogeneities in the magnetic field. Solid materials have shorter T_2 values than liquid materials. Simultaneously with the loss of coherence in the xy-plane, the spins will seek to regain equilibrium along the z-axis due to the influence of the magnetic field. The time it takes for the spins to regain equilibrium distributions between the two energy states depends on the probability of energy exchanges occurring between the spins and their environment (the lattice). The time it takes for the xy-signal to fade out is characterised by a relaxation mechanism referred to as longitudinal or spin-lattice relaxation described by the time constant T_1. When fully returned to equilibrium, the system is ready for a new pulse. Pulses (scans) are typically repeated and the signals are accumulated in order to improve the signal-to-noise ratio in the final spectrum. However, it is very important to allow the system to fully return to equilibrium between pulses, especially if the objective is to obtain quantitative spectra.

The signal obtained from a NMR experiment is collected as a function of time. The decaying signal that follows a pulse is called the free induction decay (FID). An example of a FID from a 90^0 single pulse ^{1}H NMR experiment on depolymerised alginate in solution is shown in Figure 13a. The FID is composed of decaying signals (sinusoids) of all the different protons in the sample. The resonance frequency (i.e. the Larmor frequency) of the protons depends on their chemical environment. The protons in different chemical environments experience different effective magnetic fields due to different shielding effects (i.e. differences in local electron densities) and thus resonate at slightly different frequencies; the so called chemical shifts. The chemical shifts can be derived from the FID by the use of a Fourier transformation, which converts the time domain into the frequency domain. Figure 13b shows the result of a Fourier transformation of the FID in Figure 13a.

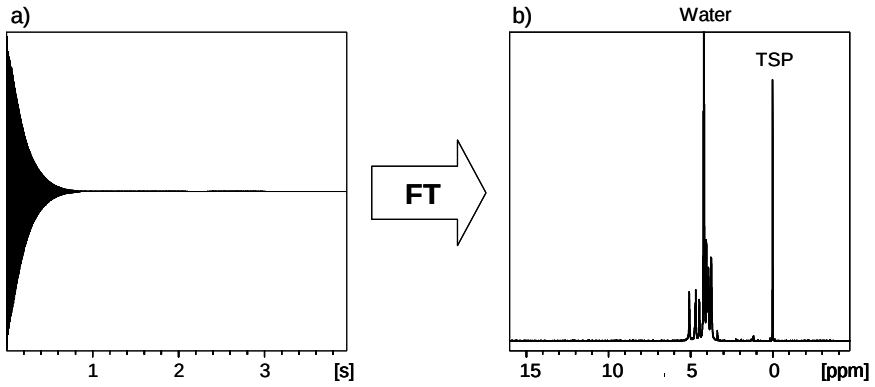

Figure 13 Fourier transformation (FT) of (a) the time domain free induction decay produces the corresponding (b) frequency domain spectra. The data is from a ^{1}H NMR experiment of depolymerised alginate dissolved in D_2O (1% (w/v)) recorded at 90°C on a 400 MHz spectrometer. The recycle delay and acquisition time were 2 and 4 s, respectively, and 16 scans were acquired. The spectra are referenced to TSP-d_4 (δ = 0.0 ppm). The full intensity of the water signal, which was 75 times the intensity of the TSP signal, is not shown in the figure.

The chemical shift is defined in terms of the difference in resonance frequencies between the nucleus of interest and a reference nucleus. The chemical shift is a dimensionless parameter (δ), which is expressed in parts per million (ppm). The definition allows the resonance frequency of a signal to be expressed independent of field strength. The chemical shifts in Figure 13b are referenced with respect to the water-soluble sodium salt of 3-(trimethylsilyl)-propionate (TSP-d_4) (δ = 0.00 ppm).

As explained above, it is the population difference and thereby the energy difference (ΔE) (Equation 1) that is measured by NMR and in turn determines the intensity of the signal. The energy difference is related to the magnetic field strength (B_0) and to the magnetogyric ratio (γ) of the nucleus as described in Equation 2:

Equation 2

$$\Delta E = h \cdot \nu = \frac{h \cdot \gamma \cdot B_0}{2 \cdot \pi}$$

The unit used for the Larmor frequency (ω_0) is radians per second and consequently $\omega_0 = 2\pi\nu$.

From Equation 2, it is obvious that the energy difference and thus the signal-to-noise ratio can be increased by measuring at a higher magnetic field strength, which will increase the energy difference between the two spin populations. For example, the excess proton spins giving rise to the NMR signal when measuring at 25°C on an 800 MHz spectrometer corresponding to a magnetic field strength of 18.8 Tesla is 128 protons out of one million, in contrast to 64 protons out of one million when using a 400 MHz spectrometer. It should be noted that a large total number of protons are required in order to generate an appreciable signal, and it should be obvious why NMR spectroscopy commonly is described as insensitive compared to other spectroscopic methods. Measuring at a higher magnetic field strength also leads to an increased dispersion of the resonances (i.e. resonances with different chemical shifts are further apart). This is illustrated in Figure 14, which shows ^{1}H NMR spectra of alginate in solution measured at a 400 MHz, 600 MHz and 800 MHz spectrometer. More detailed spectra are obtained with increasing field strength due to dispersion of the signals.

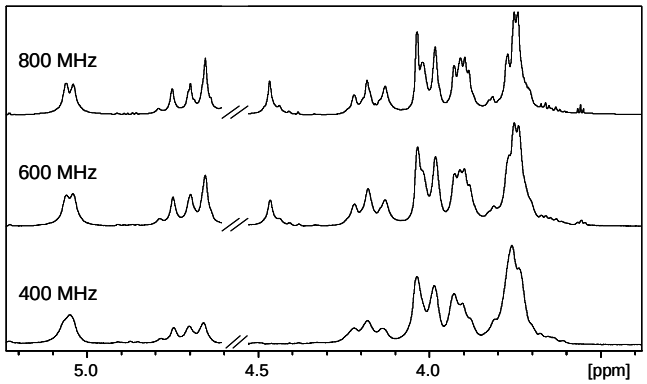

Figure 14 Carbohydrate region of ^{1}H NMR spectra of alginate in solution acquired at 45°C at a 400 MHz, 600 MHz and 850 MHz spectrometer. The water resonance (4.54 ppm) has been removed from the spectra.

Since the magnetogyric ratios vary among nuclei and even among isotopes of a single nucleus, resonance frequencies also vary ($\omega_0 = \gamma \cdot B_0$). The magnetogyric ratio of ^{13}C is for example about four times lower than that of protons and as an example ^{13}C nuclei resonate at 125.7 MHz and protons at 500 MHz at the field strength of 11.74 T. Moreover, since the spin population difference is proportional to the magnetogyric ratio and the natural abundance of ^{13}C is low (1.1%), the NMR signal obtained from a ^{13}C experiment is much lower than the signal from a ^{1}H experiment.

In summary, the relative intensity of a signal depends on three factors: the number of nuclear magnetic moments that make up the magnetisation vector (sample amount and natural abundance), the size of the individual magnetic moments (magnetogyric ratio) and the strength of the magnetic field. Moreover, the temperature (Equation 1) plays a role. For example, at absolute zero (0 K) all spins will be parallel with the magnetic field and a large net magnetisation is produced.

3.2.2 Solid-state NMR spectroscopy

When measuring semi-solid and solid samples by NMR, line broadening effects due to chemical shift anisotropy (CSA) and dipolar interactions with neighbouring nuclei (homonuclear ($^{1}H–^{1}H$) and heteronuclear ($^{1}H–^{13}C$)) become critical problems as opposed to when measuring solutions, where these effects are averaged out. In order to illustrate the consequences of these effects, ^{1}H spectra of depolymerised alginate in solution and the corresponding alginate powder are shown Figure 15. Obviously, the spectrum of alginate powder is dominated by line broadening effects and no detailed information on the alginate molecules can be obtained from this spectrum.

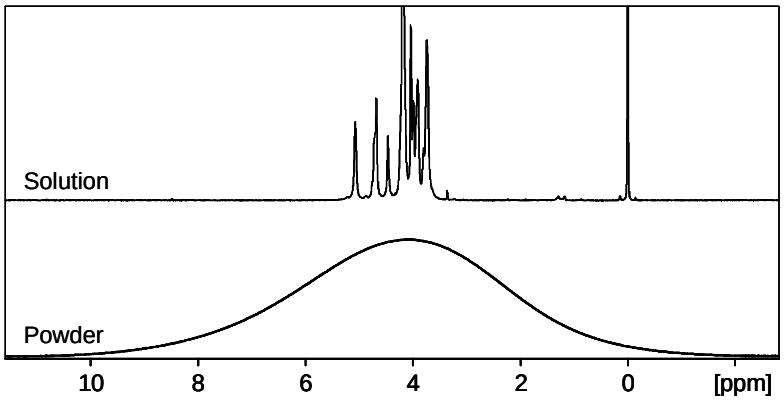

Figure 15 ^{1}H spectra of depolymerised alginate dissolved in D_2O (1% (w/v)) and of alginate powder. The spectra are measured at 90°C in a 400 MHz spectrometer equipped with a 5 mm broad band inverse probe.

The broadening effects can be partly removed by magic angle spinning (MAS) and high-power decoupling. Moreover, cross polarisation (CP) from ^{1}H to ^{13}C is commonly applied in combination with MAS to increase the signal-to-noise ratio in ^{13}C NMR spectra of solid samples. In the following, the mechanisms causing the line broadening (i.e. CSA and dipolar interactions) as well as the techniques commonly applied to minimise the line broadening as well as the CP technique will be described in further detail.

Chemical shift anisotropy
The resonance frequency (chemical shift) of a particular nucleus in a molecule depends, as mentioned in Section 3.2.1, on the electronic environment produced by the surrounding electrons, which shields the nucleus from the external magnetic field. However, it also depends on the orientation of the molecule with respect to the applied magnetic field. The same nucleus experiences small differences in the shielding (i.e. CSA), which result in small differences of the chemical shifts in the NMR spectrum. In solution, the CSA effects are averaged by isotropic tumbling. However, when measuring semi-solids and solids, CSA is a source to line broadening.

Dipolar interactions
The second source of line broadening is dipolar coupling, which arises from interactions between spins of the same type of nuclei (homonuclear coupling) or different types of nuclei (heteronuclear coupling). The dipolar interaction can lead to very broad resonances obscuring any detail in the spectrum such as the chemical shift information. Homonuclear ^{1}H-^{1}H interactions have a strong affect on the broadening of the spectra due to the high abundance of proton nuclei. In contrast, the probability of homonuclear ^{13}C-^{13}C dipolar interactions is low due to the low natural abundance of ^{13}C, and hence negligible in most cases. Thus, ^{13}C are mainly broadened by heteronuclear dipolar interactions with neighbouring proton nuclei. In solution-state NMR spectroscopy, where molecules tumble rapidly, these dipolar interactions are averaged out.

Magic angle spinning
The technique MAS (Andrew *et al.* 1958; Andrew *et al.* 1959) is used to simulate molecular motion in order to average out CSA and dipolar interactions. This is done by fast spinning of the sample around an axis, which makes an angle with the applied magnetic field direction of 54.7º (the so-called magic angle) as illustrated in Figure 16b.

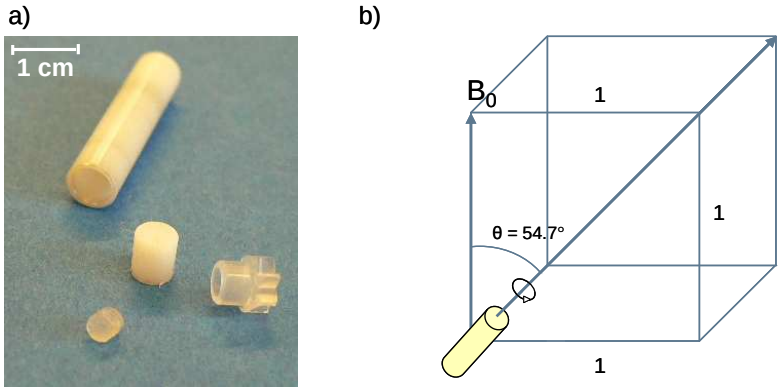

Figure 16 (a) 4 mm ZrO_2 rotor together with insert, screw and cap. Rotors used for HR-MAS NMR spectroscopy are usually with Teflon inserts to define a 50 µl volume in order to increase sensitivity. (b) Illustration of a rotor spinning at the magic angle.

In semi-solid samples, MAS can handle both CSA and dipolar interactions and hence well-resolved ^{1}H and ^{13}C HR-MAS NMR spectra can be obtained. In solid samples, however, the ^{1}H-^{1}H and ^{1}H-^{13}C dipolar couplings are so strong that they

cannot be averaged out by MAS alone at standard spin rates (5-20 kHz). Actually, ^{1}H-^{1}H dipolar couplings are so strong in solids that spin-rates in excess of 40 kHz are required to obtain HR spectra (Samoson *et al.* 2001). Owing to this, when measuring solid samples it is most common to observe the ^{13}C nuclei. Then one does not have to deal with the ^{1}H-^{1}H, and the ^{1}H-^{13}C can be dealt with by high-power decoupling as will be described below. Moreover, ^{13}C has a much larger (isotropic) chemical shift range through which one can more easily discriminate subtle structural differences.

Decoupling
The line broadening in ^{13}C spectra of solids due to heteronuclear dipolar couplings to protons can be removed by irradiation using a strong RF at proton frequency (heteronuclear decoupling) (Hodgkinson 2005). Heteronuclear decoupling is generally applied when recording ^{13}C solution-state NMR spectra. However, in solids the interaction may be of the order of 10's of kHz rather than the 0-200 Hz found in solution. Consequently, the decoupling power must be much higher in solid-state experiments (up to 1 kW) than in solution-state experiments (> 5 W). Homonuclear decoupling is much more technically demanding which is why it is not common to record ^{1}H NMR spectra of solid samples. There are, however, several experiments in use, which can remove the homonuclear dipole-dipole interaction. The combined rotational and multiple pulse spectroscopy (CRAMPS) experiment (Gerstein *et al.* 1977), which also includes MAS to remove CSA, is one of the solutions to obtain ^{1}H NMR spectra of solids with reasonable resolution. However, the proton line widths are still about 1 ppm (Gerstein 1981), which is large considering the 10 ppm chemical shift range in ^{1}H NMR spectroscopy.

Cross polarisation
When measuring solid samples it is normally more advantageous to observe the ^{13}C nuclei and thereby avoid the problems with the strong ^{1}H-^{1}H dipolar couplings. However, the obvious disadvantage of observing the low abundance ^{13}C nucleus is the low signal-to-noise ratio and that the spin-lattice relaxation times (T_1) in general are longer than for ^{1}H. However, by application of cross polarisation (CP) (Pines *et al.* 1972; Pines *et al.* 1973), where magnetisation is transferred from ^{1}H (high magnetogyric ratio) by dipolar coupling to ^{13}C nuclei (low magnetogyric ratio) the intensity of the ^{13}C spectra can be increased. In addition, because relaxation is via the rapid ^{1}H pathway rather than the slower ^{13}C route, experiments can be repeated more rapidly, with consequent increases in signal-to-noise ratio. Thus, combining the techniques CP, MAS and high power decoupling enables one to acquire fairly well-resolved ^{13}C NMR spectra with a good signal-to-noise ratio of solid samples within a reasonable measurement time (30-60 min).

3.2.3 Internal molecular motions in relation to the observed NMR signal
In solution-state NMR, it is a requirement that the molecules under inspection are completely dissolved in order for them to be fully detected (i.e. to be able to rely on that the resonance intensity of a given nucleus is proportional to the concentration). Restricted molecular mobility leads to reduced spin-lattice relaxation times, which is reversely correlated to the resonance line widths. Thus, the less flexible or rigid parts of molecules will result in broad signals (possibly beyond the limit of detection) resulting in wrong quantitative estimations. In relation to alginate, the above described phenomenon is critical if calcium ions are present in the sample. This will lead to the formation of rigid junction zones between the G-blocks (cf. Section 2.3.3) resulting in an underestimation of the

signals originating from guluronic acid (cf. PAPER III, IV and V). This is also a significant problem when studying semi-solids by ^{1}H HR-MAS NMR spectroscopy. Especially when studying complex semi-solid matrices containing macromolecules of different sizes, it is not always possible to make quantitative comparisons between small and large molecules (Seefeldt *et al.* 2008; Winning *et al.* 2009b).

In contrast, when measuring solid samples by ^{13}C CP-MAS NMR spectroscopy, the very mobile molecules or parts of molecules are not observed due to inadequate magnetisation transfer. However, single pulse ^{13}C MAS NMR spectroscopy of solid-samples acquired with high-power heteronuclear decoupling results in spectra showing signals from all carbons in the sample. The disadvantage of this experiment is that many scans must be acquired in order to obtain a good signal-to-noise ratio and long recycle delays must be used because of the slower T_1 relaxation of ^{13}C. Combined, this leads to very long measurement times. Nevertheless, comparative studies of ^{13}C CP-MAS and single pulse ^{13}C MAS spectra are for example very useful in the characterisation of gel network dynamics because the relative proportions of rigid and more flexible domains of the polymer gel network can be evaluated by comparison of spectra obtained from the two different experiments (Gidley 1989; Saito *et al.* 1990; Saito 2005). Moreover, comparative studies of ^{13}C CP-MAS and ^{13}C MAS spectra can provide information on the cross polarisation efficiency. This approach was used in PAPER IV and V, where it was concluded that the relative signal intensities of the anomeric (90-110 ppm) and pyranose (60-90 ppm) carbon signals in the ^{13}C CP-MAS and ^{13}C MAS spectra were identical (Figure 17).

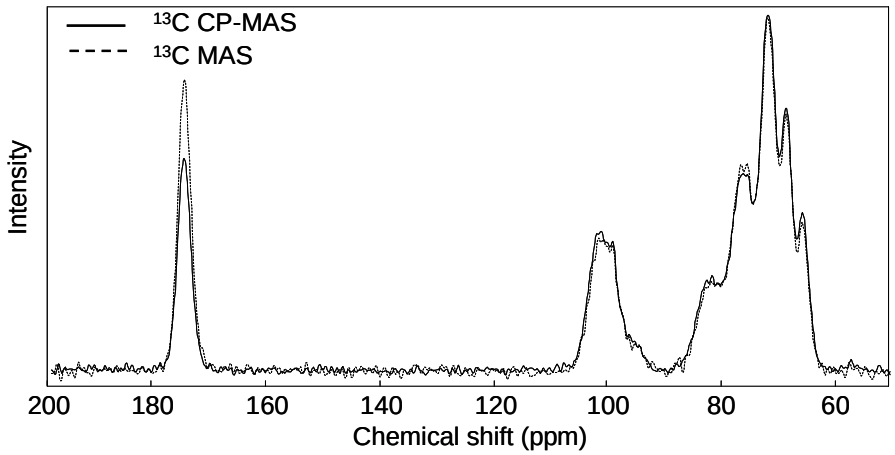

Figure 17 ^{13}C CP-MAS and single pulse ^{13}C MAS NMR spectra recorded with a recycle delay of 2 s and 120 s, respectively, and 1024 and 3328 scans, respectively.

Consequently, the ^{13}C CP-MAS spectral intensities of these signals are not distorted by different cross polarisation dynamics and are thus quantitatively reliable. In contrast, the cross polarisation conditions for the carboxyl carbons (172-180 ppm) with small dipolar proton coupling were not optimal resulting in lower ^{13}C CP-MAS signal intensity.

3.2.4 Sources of variation in NMR spectra

NMR spectroscopy is an extremely versatile technique offering a huge number of experimental methodologies, which provide different information on the sample under investigation. In order to fully exploit the potential of the different experiments, the experimental parameters of the specific experiment must be optimised. In the quantitative analysis of NMR spectra, it is for example, of utmost importance to consider the quantitative nature of the NMR experiment applied. The quantitative nature of NMR spectra can be affected by a variety of distortions related to the sample preparation or imposed by non-optimised experimental parameters. The general requirement for quantitative NMR analysis is that the intensity of a signal is directly proportional to the number of nuclei evoking the signal, analogous to the obedience of Beer's law in optical spectroscopy. Moreover, for bilinear multivariate data analysis (cf. Chapter 4) it is a requirement that the signal from a given site remain stable on the ppm axis and that the intensity between spectra are comparable on an absolute scale. In the following, some of the experimental variables affecting these requirements are described. Some experimental variables are crucial and cannot be corrected for after measurement, whereas others can be compensated for by different spectral post-processing techniques, which will be described in Section 4.5.2. However, such multivariate techniques should never be considered as substitutes for non-optimally tuned instrumental parameters.

Sample preparation

Samples for solution-state NMR and HR-MAS NMR spectroscopy are usually prepared with a deuterated solvent in which a small amount of reference compound has been dissolved. The deuterium signal is monitored during the experiment and used to correct for frequency drifting. This practice is referred to as locking the signal. The preferred choice of locking-solvent for water-soluble molecules such as alginates is usually deuterated water (D_2O). In solution-state NMR spectroscopy it is generally easy to control the concentration of the solute by dissolving a specific amount in the solvent and afterwards transfer it to the NMR tube. Thus, all samples in a series can be prepared relatively consistent and it is typically not necessary to correct for different sample amounts after measurement. In HR-MAS it is more complicated to prepare the samples consistently. Sample for HR-MAS NMR spectroscopy are prepared in small rotors (outer diameter: 4 mm and height: 20 mm) (Figure 16). The sample is placed in the rotor and subsequently filled with deuterated solvent. Thus, it is difficult to control if the sample is homogeneously soaked. Moreover, when measuring powders, the particle size distribution and density also plays a role with respect to how the powders are soaked. Similar problems exist for solid-state NMR samples, which are also prepared in small rotors. Consequently, the intensities of NMR spectra of semi-solids or solids usually have to be normalized before quantitative comparison between samples can be made (cf. Section 4.5.2).

Tuning and matching

NMR probes are designed to give optimum performance over a narrow frequency range in order to achieve maximum sensitivity. Therefore, the probe must be adjusted to the frequency of the nucleus being studied (tuning). Moreover, the probe must be adjusted to make sure that the maximum possible power will be passed from the transmitter to the sample (matching). A poorly tuned and matched probe reflects a lot of power of the pulses (i.e. a 90° pulse will in reality be for example a 50° pulse) resulting in a smaller observed signal. Thus, if all

samples in a sample set are not tuned and matched optimally they do not have the same intensity scale.

Receiver gain
The receiver gain is a parameter related to the dynamic range of the observed signal (i.e. the ratio between the largest and the smallest signal). Thus, the receiver gain is a scaling factor. The receiver gain should be optimised according to the largest signal in order to measure the correct intensity of this signal and avoid severe distortion of the spectrum. Since the receiver gain determines how small a signal can be detected relative to the largest signal in the sample, the presence of very large signals may limit the detection of the smaller signals. This situation is most commonly encountered in ^{1}H NMR experiments where the water resonance usually is much larger than the signals of the molecules under investigation. However, this can be solved by selective reduction of the water signal by different solvent suppression techniques as will be described below. The receiver gain is typically optimised on each sample. However, it should be noted that when the purpose is to compare spectra in between, for example by the use of chemometrics (cf. Chapter 4), one should thrive to measure all samples in the sample set with the same receiver gain due to the non-linear response of the amplifiers, which can lead to non-linear variations which may be larger than the quantitative variations between the samples. As a minimum, the gain factor should be divided out before further data analysis (cf. Section 4.5.2).

Shimming
Shimming is a process in which the homogeneity of the magnetic field is adjusted in order to enhance spectral resolution. It is a way to make sure that every part in the sample experiences exactly the same field strength. The resolution of solution-state spectra is very sensitive to field inhomogeneities. Thus, when measuring solutions it is common practice to 'fine tune' the magnetic field every time a new sample is introduced into the magnet in order to enhance the resolution of the spectra. In modern solution-sate spectrometers, shimming is often performed through automation. When measuring semi-solids by HR-MAS NMR spectroscopy it is still necessary to manually shim the magnetic field. However, when measuring a series of similar samples it is often just necessary to optimise the shim on the first sample. Shimming is not critical in the measurement of solids because the line broadening effect induced by CSA and dipolar coupling overshadows what is gained by shimming.

Recycle delay
For quantitative reliable results, it is critical that all sites are fully relaxed between pulses (scans). The time between scans are typically called recycle delay or relaxation delay and should be minimum five times the spin-lattice relaxation time (T_1) for the slowest relaxing component.

Contact time in ^{13}C CP-MAS NMR experiments
In ^{13}C CP-MAS NMR experiments, the contact time is an important parameter since it influences the efficiency of magnetisation transfer from ^{1}H to ^{13}C. For example, for carbons with a small dipolar proton coupling (e.g. carboxyl carbons) maximum intensity will be obtained for longer contact times than for carbons with a larger dipolar proton coupling (e.g. anomeric and pyranose carbons). Moreover, the overall intensity of a ^{13}C CP-MAS spectrum decreases with increasing contact time due to relaxation of the protons in the spin lock field (i.e. less magnetisation is transferred at long contact times) resulting in overall lower spectral intensity.

Consequently, conducting experiments with long contact times will require longer measurement times. To illustrate the effect of contact time on the relative signal intensities of carboxylic, anomeric and pyranose resonances in ^{13}C CP-MAS spectra of alginate powders, the relative signal intensities from a series of ^{13}C CP-MAS spectra are shown in Figure 18. The relative intensities of the signals in a single pulse ^{13}C MAS spectrum are also shown. It can be observed that the relative intensities of the anomeric and pyranose signals are independent of the contact time in the investigated range, whereas the relative intensity of the carboxylic carbon signal increases with increasing contact time.

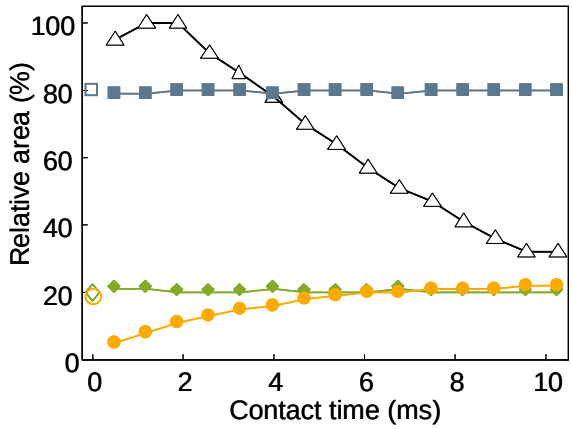

Figure 18 Overall integrated signal intensities (∇) of all signals in the ^{13}C CP-MAS NMR spectra and integrated signal intensities of carboxylic (●), anomeric (♦) and pyranose (■) carbon signals relative to the total intensity of the anomeric and pyranose signals as a function of contact times. The relative integrated intensities of the single pulse ^{13}C MAS NMR carboxylic (○), anomeric (◇) and pyranose (□) carbon signals are indicated for comparison (contact time = 0 ms).

Parameters influencing chemical shift variations

Temperature, pH, solvent and metal binding differences can all give rise to chemical shift variations. Thus, care should be taken when comparing spectra of samples, which vary with respect to these parameters. The water resonance is for example very sensitive to temperature variations as illustrated in Figure 19, which shows the carbohydrate region of ^{1}H NMR spectra of alginate in solution recorded on a 400 MHz spectrometer at 45°C, 55°C, 65°C and 75°C. Thus, if the water resonance interferes with the resonances of interest when acquiring ^{1}H NMR spectra, it can be moved by changing the temperature. The chemical shifts of many of the alginate signals are also sensitive to temperature to different degrees (Figure 19). As in all other analytical instruments, it should be noted that the temperature read by the spectrometer not always reflects the temperature in the sample. This is especially relevant when measuring semi-solid and solid samples, where the high speed spinning produces frictional heating in the sample. A study carried out by Brus (2000) showed that the temperature in lead nitrate increased from 7°C to 65°C as an effect of increasing the spinning speed from 2.5 kHz to 18 kHz. Thus, in order to know the true sample temperature, appropriate calibration must be carried out (van Geet 1970; Raiford *et al.* 1979).

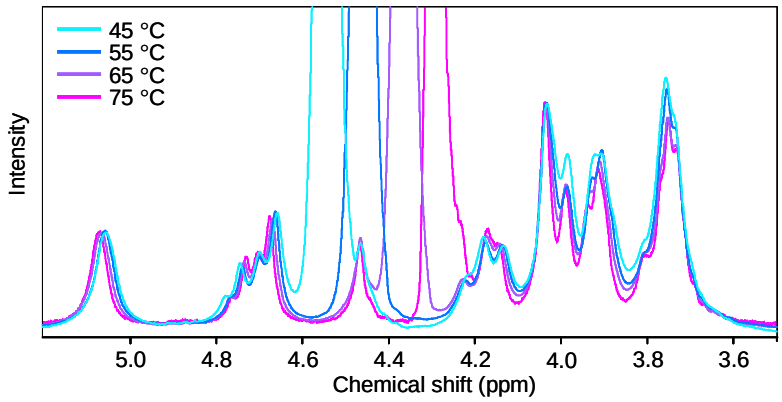

Figure 19 Carbohydrate region of ^{1}H NMR spectra of alginate in solution (1% (w/v)) acquired at 45°C, 55°C, 65°C and 75°C. The spectra are referenced to TSP-d_4 (δ = 0.0 ppm).

Water suppression

In ^{1}H NMR spectra of biological samples the magnitude of the water resonance is normally much stronger than the other signals in the spectra due to residual water in the samples. Thus, it can be an advantage to apply water suppression in order to change the dynamic range of the signals and to recover signals that overlap the broad baseline of the intense water resonance. One of the simplest and most widely used methods is presaturation of the water resonance (Hoult 1976), where the water signal is dephased through a long weak RF pulse, which affects only the spectral region of the water signal. The presaturation is applied in the beginning of a pulse sequence and can thus be implemented into practically any pulse experiment. The method is simple and reasonably effective, but has the disadvantage of other signals close to the water signal are also partly suppressed. More advanced pulse techniques such as WATERGATE (Piotto *et al.* 1992) applying pulsed field gradients for the water suppression are very effective but requires optimisation of several critical parameters.

In a previous ^{1}H NMR study of alginates, water suppression was found to alter the intensities of the signals of interest (Neiss & Cheng 2003) whereas another study concluded that water suppression had no effect on the intensities of the signals near the water resonance (Shinohara *et al.* 1999). In order to clarify this ambiguity, it was in the present study investigated how some of the most common presaturation techniques influence the ^{1}H NMR spectra of alginates in solution and in turn the calculated M/G ratios (PAPER I). From this study, it was concluded that the three different types of presaturation (presaturation followed by a single 90° pulse, presaturation followed by a 90° pulse composite pulse and NOESY-presaturation) applied for water suppression introduced undesired and uncontrolled variability to the spectra leading to erroneous M/G ratio estimations. Figure 20 shows the ^{1}H NMR spectra of an alginate in solution acquired without and with water suppression (simple presaturation). The spectra have been scaled according to the signal at 5.07 ppm (H-1 of guluronate) for a better illustration of the relative differences in the two spectra. This signal was chosen for scaling since it is furthest away from the water resonance and therefore less likely to be influenced by the water suppression.

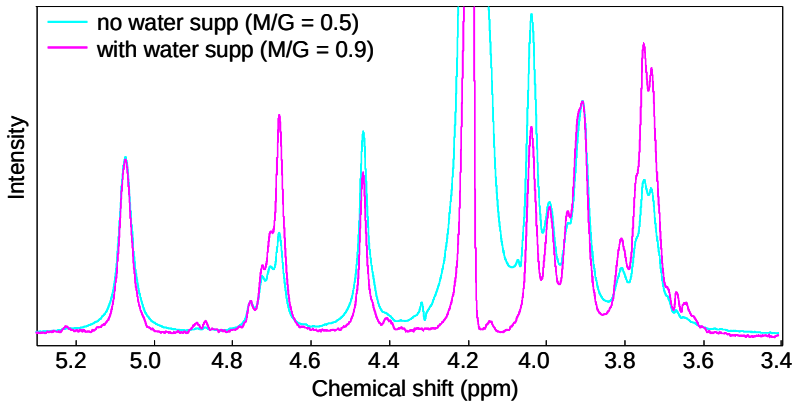

Figure 20 Carbohydrate region of ^{1}H NMR spectra of an alginate in solution (1% (w/v)) recorded without and with water suppression (simple presaturation) at 90°C of the water signal at 4.2 ppm. The M/G ratio calculated from the water suppressed spectra is higher (0.9) than the M/G ratio calculated from the non-water suppressed spectra (0.5). The spectra are scaled according to the signal at 5.07 ppm originating from the anomeric proton in guluronate.

From the comparison of the two spectra it is observed that several signals are affected by the water suppression. The M/G ratio are calculated from the signals in the anomeric region (4.4-5.2 ppm) as described in Section 5.2, and since some of the signals in this region are influenced by the water suppression, the calculated M/G ratios are far from being identical. The M/G ratios calculated from the water-suppressed spectra were for all 42 samples investigated higher than the M/G ratios calculated from the non-water-suppressed spectra. An analysis of the relative difference between the non-water suppressed and the water suppressed spectra of all 42 samples showed that water suppression resulted in a 27-44% decrease of the signals near the water resonance (4.38-4.55 ppm and 3.96-4.07 ppm) and a 2-25% increase of the signals originating from M in the regions 4.68-4.70 ppm and 3.67-3.83 ppm. The signal increase for the M protons was unexpected, since presaturation normally is expected to lead to a signal decrease of the signals near the water resonance. Since the increase is observed only for the protons originating from M residues (and especially H-1 of M positioned next to another M (4.68 ppm)) it is reasonable to assume that the signal increase is related to the molecular geometry and flexibility differences of M- and G-blocks (cf. Section 2.2) A plausible explanation may be that the M-blocks interact with water to a higher extend than the G-blocks due to their more linear structure and higher flexibility. Water suppression can potentially disturb this interaction and therefore induce changes for protons in the M-blocks leading to increased signal intensity.

3.3 VIBRATIONAL SPECTROSCOPY

Vibrational spectroscopy is based on the interaction of infrared (IR) and near infrared (NIR) radiation with vibrating molecular bonds (Griffiths 2002b). The British astronomer and composer F. W. Hershel discovered in 1800 by accident the invisible 'heat' radiation of the sun (Herschel 1800), which we today refer to as NIR radiation. However, it was not until around the mid-1900s that commercial instrumentation appeared, and significant progress in the use of vibrational spectroscopy for routine analysis first occurred during the late 1900s with the

development of computers, Fourier transform (FT) instruments and visible and NIR lasers for Raman spectrometers (McCreery 2000; Sheppard 2002; McClure 2003).

In this project, FT-IR, FT-Raman and NIR spectroscopy has been used for the quantitative analysis of the molecular composition of alginate powders (PAPER II and III). The following sections provide the basic principles of the methods, a description of the quantitative nature of the spectra and finally, a discussion of advantages and disadvantages associated with the various techniques and their use as quality control methods in the industry.

3.3.1 Basic principles

Molecules exhibit oscillating motions called vibrations. Different types of vibrations exist (symmetric stretching, asymmetric stretching, bending, rocking, wagging and twisting) depending on the complexity of the molecule. A simple diatomic molecule has only one mode of vibration (stretching), whereas molecules containing more than two atoms exhibit more complex modes of vibration. For a linear molecule with N atoms, there are 3N-5 vibrational modes and for a non-linear molecule, there are 3N-6 vibrational modes (Griffiths 2002b).

IR spectroscopy

The fundamental vibrational modes correspond in energy to wavenumbers ranging from 4000 to 400 cm^{-1} (corresponding to wavelengths of 2500 nm to 25 µm), often referred to as mid-IR. In IR spectroscopy the IR light is absorbed when its energy matches the frequency of the vibrating bond, resulting in excitation of the vibrational energy state of a molecular bond from the ground state to a discrete higher energy level. However, absorption of IR radiation can occur only if the vibration causes a change in the dipole moment of the molecule. The vibration frequency is determined by the masses of the involved atoms, the type of vibration, other groups attached to the atoms and to a lesser extend temperature and pH. Since different functional groups have different absorption bands (i.e. they absorb different ranges of the IR radiation), the IR spectrum (absorption as a function of wavenumber) provides information about the content of various functional groups in the sample. In this project, FT-IR spectra were obtained using an attenuated total reflectance (ATR) sampling unit, which is a method where the IR beam bounces inside a crystal on which the sample is placed. The sample must have a lower refractive index than the crystal in order for it to obtain internal reflectance and the intensity of the final spectrum will largely depend on the optical contact between the sample and the crystal.

Raman spectroscopy

Raman spectroscopy is based on scattering of light instead of absorption but measures the same molecular vibrations as is measured by mid-IR. Visible or NIR light from a laser source is emitted into the sample and it is then the frequency shifts of the scattered light that are measured. The bands in Raman spectra arise from vibrations associated with a change in the electronic polarisability that occurs during the vibration as opposed to bands in IR spectra, which arise from molecular vibrations associated with a change in the dipole moment of the molecule. Consequently, electron rich symmetric bonds and symmetric vibrations (e.g., C=C and C-C) provide strong Raman signals whereas signals of the polar bonds (e.g., C-H, O-H and C=O) are weak or absent in Raman spectra but strong in the IR spectra. Thus, IR and Raman spectra offer complementary information.

NIR spectroscopy

Overtone and combination bands of the high energy fundamental vibrations (i.e. integer multiples and summations of the fundamental vibrational frequencies) can be observed by NIR spectroscopy in the wavelength range from 780 nm to 2500 nm (corresponding to wavenumbers in the range 12800 to 4000 cm^{-1}). It is primarily the anharmonic vibrations (i.e. bonds including hydrogen atoms such as C-H, O-H, N-H) that are observed in NIR spectroscopy, which makes NIR spectra less distinctive than IR spectra. Nevertheless, the chemical information is present, since the first, second and third overtone in the NIR spectrum contains the same chemical information as the fundamental vibration band. However, due to the broad and overlapping features of NIR spectra chemometric techniques (cf. Chapter 4) are necessary to extract detailed information from the spectra.

Figure 21 shows an example of an IR, Raman and NIR spectrum of alginate. The IR and Raman spectra contain complementary information and provide rather distinct bands compared to the bands in the NIR spectrum. The information found in the NIR spectrum is similar to the information found in the high energy IR spectrum (3600-2800 cm^{-1}), but in the NIR spectrum this information is presented in a more complex way due to overlapping bands from the anharmonic overtone and combination vibrations.

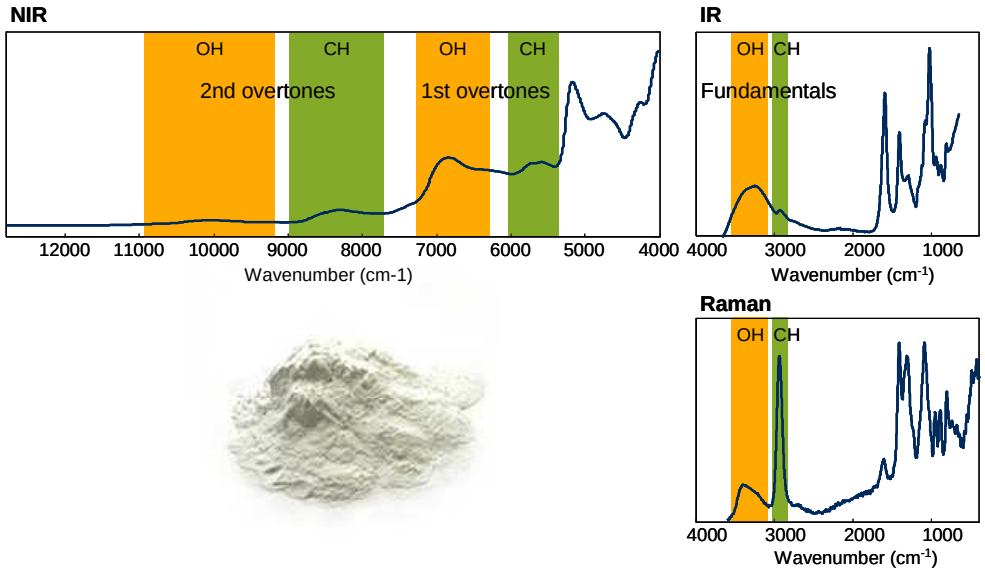

Figure 21 IR, Raman and NIR spectra of alginate powder. The fundamental C-H and O-H stretching bands are highlighted in the IR and Raman spectra, illustrating the different intensities of the bands in the spectra. The fundamental vibrations in the IR region are repeated as first and second overtones in the NIR spectrum. The third overtones are too weak to be observed.

3.3.2 Quantitative analysis of powders by vibrational spectroscopy

IR and NIR spectroscopy of solid materials such as powders are based on the measurement of absorbance (*A*), which is dependent on the molar absorptivity (ε), the (effective) path length (*l*) and the concentration (*c*) of the absorbing analyte as given in Beer's law (Griffiths 2002a):

Equation 3 $$A = \varepsilon \cdot l \cdot c$$

Beer's law does not apply to Raman spectroscopy, as Raman spectroscopy involves scattering, not absorption. However, the intensity of Raman scattering (I_{Raman}) can be expressed by an equation analogous to Beer's law (Pelletier 1999):

Equation 4 $$I_{Raman} = K \cdot I_L \cdot \sigma \cdot \bar{\nu}^4 \cdot P \cdot C$$

where K is a constant that includes the measurement parameters, I_L is the intensity of the incident laser radiation, σ is the absolute Raman scattering cross-section (in cm^2 per molecule), $\bar{\nu}$ is the wavenumber of the incident laser light, P is a pathlength equivalent term and C is the number of scattering centres per unit volume (concentration).

In summary, the intensity of the signals obtained by IR, Raman and NIR spectroscopy are linearly correlated to the concentration of the components in the sample, which is one of the prerequisites for the application of bilinear methods such as chemometrics. Deviations from this linear relationship can be caused by for example differences in physical properties of the samples (e.g. particle size, packing density and fluorescence) and measurement conditions (e.g. changes in size/path length and instrument drift) (Griffiths 2002a). Fortunately, different pre-processing techniques can be applied to compensate for these deviations and restore the linear relationship (cf. Section 4.5.1).

3.3.3 Advantages and disadvantages of vibrational spectroscopy

The major advantages of IR, Raman and NIR spectroscopic techniques are that they are rapid, non-destructive and provide information on the total composition of the sample (i.e. it is possible to determine more than one parameter from a single spectrum). Moreover, the instruments are generally simple to operate and can be operated in nearly any environment. Another main advantage is that the sample can be measured as is with no or very limited sample preparation.

When analysing powders, it is recommendable that the size of the powder particles is in the same range (estimated limit: ± 100 µm). NIR and Raman measurements of powder particles of very different sizes (e.g. 100 µm and 300 µm) will result in different amounts of scatter and when performing IR measurements using ATR sampling it is difficult to obtain reproducible contact to the crystal if the particle sizes differ too much. Moreover, optimal contact to the crystal cannot be obtained if the powder is too coarse (estimated limit: > 300 µm) resulting in very low intensity spectra. Thus, large differences in particle size within a sample set can lead to huge sample-to-sample spectral intensity variations, which complicate the following data analysis. Large-scale heterogeneity in powders is problematic in IR and Raman measurements due to the rather small penetration depth and measurement area in these methods. In NIR measurements, inhomogeneity is not problematic to the same extend due to the longer possible penetration depth and the larger measurement area.

The disadvantage of IR spectroscopy, with respect to quality control, is that IR radiation cannot be transmitted through quartz, which is the material used in optic fibres for remote on-line measurements. Thus, lack of alternative material

for production of optic fibres means that IR spectroscopy cannot be used for remote on-line analysis as opposed to Raman and NIR.

The disadvantages of Raman spectroscopy is the low signal-to-noise ratio (compared to IR and NIR), interference from fluorescence and heating of the sample. The problems with fluorescence are minimised with NIR lasers because longer wavelength excitation reduces the probability of exciting fluorophores. Heating of the sample can be reduced by reducing the laser power and/or the acquisition time at the expense of the signal-to-noise ratio.

DATA ANALYSIS

4

4.1 INTRODUCTION

Spectroscopic measurements may result in data containing several hundreds or thousands of variables for each sample. The individual variables are often strongly correlated and the signals in the spectra may be highly overlapping. Consequently, efficient multivariate data analytical techniques are required for extraction of the relevant information. Chemometric methods decompose complex multivariate data into simpler and potentially interpretable structures which can ease the understanding of the chemical and physical information in the data. Thus, application of chemometric methods is an obvious choice for analysing spectroscopic data of a large array of samples. The data can be analysed with a minimum of *a priori* assumptions by the so-called unsupervised methods. Unsupervised methods are used when the purpose is to explore the data for expected and unexpected trends, grouping and outliers and when no reference values are available. This explorative approach may lead to the development of hypotheses *a posteriori*, which eventually may lead to a better understanding of the system under investigation (Munck *et al.* 1998). In contrast, supervised methods are very useful when the purpose is to relate a set of spectroscopic data to one or several physico-chemical variables (reference values) and thereby construct a regression model which can be used for future predictions.

An introduction to the different data analytical methods used in this study as well as model validation and spectral pre-treatment of data are given in the following sections. This includes unsupervised and supervised chemometric methods as well as spectral deconvolution of individual NMR spectra.

4.2 UNSUPERVISED DATA ANALYSIS

4.2.1 Principal component analysis

Principal component analysis (PCA) (Hotelling 1933) is the fundamental chemometric method for unsupervised data analysis of large bilinear data structures. By PCA, the main variation in a multidimensional data set is found by creating new linear combinations from the underlying latent structures in the raw data. The data matrix (X) representing a number of samples (n) and variables (m) is decomposed into a score matrix (T) (n samples, p principal components) and a loading matrix (P) (m variables, p principal components) by consecutive orthogonal subtraction of the largest variation in the data (principal components) until the variation left is approximately unsystematic. Thus, the score matrix and loading matrix contain the systematic variation with respect to samples and variables, respectively, leaving the unsystematic contribution in the residual

matrix (E) (n samples, m variables). Consequently, the PCA model can be written as:

Equation 5 $$X_c = T \cdot P^T + E$$

where superscript T means transposed and X_c is the original data matrix (X), which has been centred by subtracting the mean of each variable from the original measurement. For spectral data, the loadings (rows in the transposed loading matrix) can be considered as spectral profiles that are common to all the measured spectra and the scores (columns in the score matrix) is the concentrations of the hidden profiles in the individual spectra. The outer products of each score and loading vector are called principal components (PC1, PC2, etc.).

An important feature of PCA is the associated graphical interface. Scatter plots of the scores make it easy to identify outliers as well as trends and groupings of the samples, and line plots of the loadings reveal the importance of the original variables for each PC allowing for identification of the qualitative differences causing the trends and groupings in the data. An example on how the results of a PCA of ^{13}C CP-MAS NMR spectra of 42 alginate powders (data from PAPER IV and V) can be graphically presented is given in Figure 22.

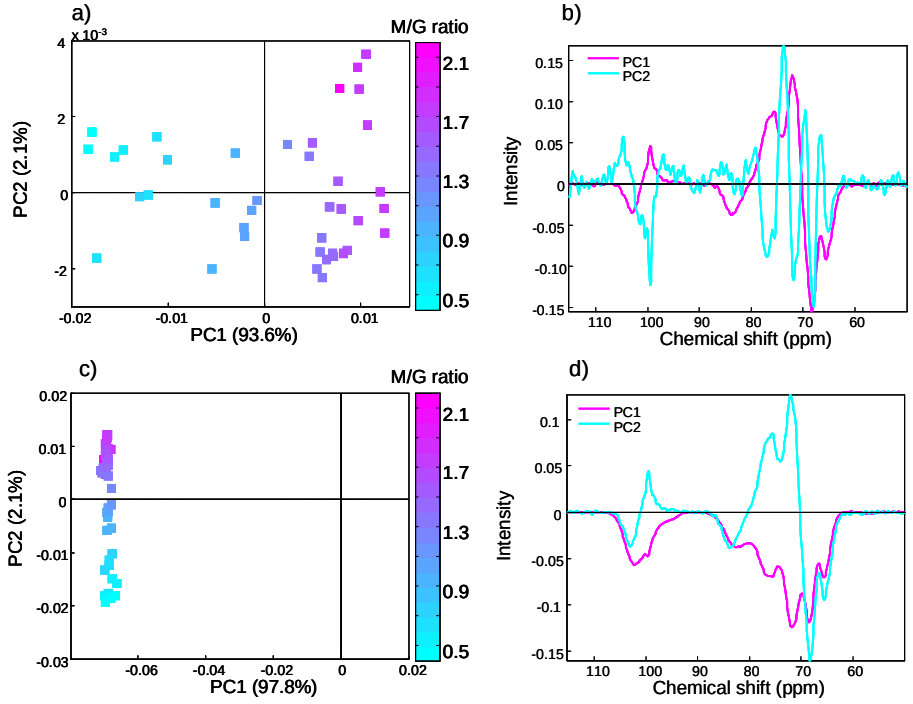

Figure 22 (a) Score plot and (b) loading plot showing the first two principal components from PCA of the centred ^{13}C CP-MAS NMR spectra of 42 alginate powders. (c) The score plot and (d) loading plot from PCA of the non-centred data are also shown. The samples in the score plots are coloured according to the M/G ratios calculated from ^{1}H solution-state NMR spectra. The data is from PAPER IV and V.

The PCA score plot of the first two principal components (Figure 22a) clearly shows that the main variation is related to the M/G ratio (i.e. the samples are

distributed with increasing M/G ratio along PC1, which describes 93.6% of the total spectral variation) and the loading vector of PC1 (Figure 22b) gives an overview of which parts of the spectra that are positively and negatively correlated to the M/G ratio. When comparing the loading profile of PC1 with the spectral assignments of the ^{13}C CP-MAS NMR spectra (cf. PAPER V) it is observed that the positive parts of the loading vector are the part of the spectra containing signals from M and the negative parts of the spectra loadings contain signals from G. Thus, the extracted loading contains both information on M and G. However, due to the orthogonality constraint applied in PCA it is not possible to obtain direct estimates of the pure spectra of M and G as can be done with multivariate curve resolution (cf. Section 4.2.2).

Generally, the original spectral data matrix (*X)* is always centred before performing PCA. This is done in order to focus on the differences between the samples rather than the direction of the overall variance. Figure 22c and d show the score and loading plots, respectively, from a PCA of the non-centred ^{13}C CP-MAS NMR spectra. In this case the model focuses on describing the common features of the spectra instead of the variation between the samples. Consequently, the variance related to the M/G ratio is described in PC2 instead of PC1 and the PC2 loading vector in Figure 22d is similar to the PC1 vector in Figure 22b. When analysing discrete variables measured in different units and thus magnitude (e.g. kg, °C and min), the variables should be scaled to the same unit by dividing each variable by its standard deviation in addition to centring. This pre-transformation is called autoscaling and was applied to the chemical and physical data of the alginates in PAPER II prior to PCA.

In PAPER II, PCA was used to investigate to which extend the different spectroscopic methods (IR, Raman and NIR) allowed for discrimination between alginates with different M/G ratios. The preliminary explorative analysis gave an indication of that it was possible to develop regression models with good prediction performances. Moreover, the PCA was in PAPER II used to obtain an overview of the variance structure in the chemical and physical data. In PAPER IV, PCA was applied to the three sets of NMR data (^{1}H solution-state, ^{1}H HR-MAS and ^{13}C CP-MAS) and PCA score plots revealed that 1) the main variation in all three data sets was related to the M/G ratio, 2) samples with high calcium content were estimated differently in the three methods and 3) the extend to which spectral variation such as line broadening and chemical shift differences contributed to the overall spectral variation increased in the order ^{13}C CP-MAS NMR < ^{1}H HR-MAS NMR < ^{1}H solution-state NMR.

4.2.2 Multivariate curve resolution

Multivariate curve resolution (MCR) (Tauler 1995) is an unsupervised method which generally is similar to PCA. However, as opposed to PCA, MCR does not impose the orthogonality constraint when subtracting components from the raw data. Consequently, it is possible to obtain direct estimates of pure component spectra and concentrations. Analogous to PCA, a data matrix (*X*) (*n* samples, *m* variables) consisting of spectra of the relevant chemical components are decomposed into a concentration matrix (*C*) (*n* samples, *p* pure components), which contains estimated concentrations of the chemical components, a spectra matrix (*S*) (*m* variables, *p* pure components), which contains the estimated pure spectra of the chemical components, and a residual matrix (*E*) (*n* samples, *m* variables), which contains the unsystematic variation not explained in *C* and *S*. Thus, the MCR model can be written as:

Equation 6 $$X = C \cdot S^T + E$$

The model parameters are typically estimated using an alternating least squares (ALS) regression algorithm (Tauler 1995) that iteratively fits the *C* and *S* matrices to the experimental data *X*, and modelling is completed when no further improvements are observed. In contrast to PCA, the MCR solution is not unique and in most cases a number of equally well-fitting solutions can be found. However, this problem can often be dealt with by presuming that the concentrations as well as the spectra are non-negative. The application of non-negativity constraints provide stabilisation of the algorithm and sometimes leads to elimination of the so-called rotational ambiguity and thereby gives the desired uniqueness.

In PAPER V, MCR was applied to the 60-110 ppm region in the ^{13}C CP-MAS NMR spectra of the 43 alginates under investigation. The raw spectra and the estimated pure spectra from a two component MCR analysis, which resemble the real pure spectra, are shown in Figure 23.

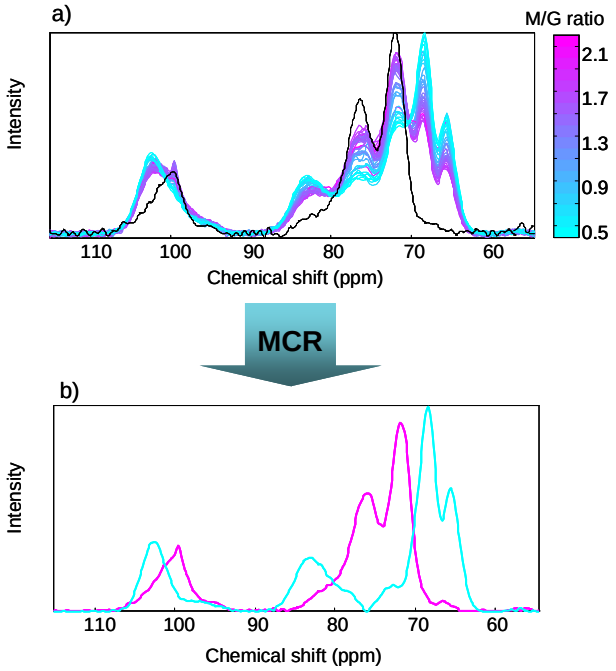

Figure 23 (a) The measured ^{13}C CP-MAS NMR spectra of 42 seaweed alginates and a pure mannuronate isolated from *Pseudomonas fluorescenc* (black) and (b) the estimated pure spectra of mannuronate (pink) and guluronate (blue) from a two component MCR analysis. The data are from PAPER V.

The relatively robust solution was obtained by applying non-negativity constraints on concentrations and spectra in the least squares sense (Bro & de Jong 1997). However, this perfect solution could only be obtained when the spectrum of pure mannuronate was included in the data set. The M/G ratio estimated from the estimated concentrations of M and G correlated very well with the values obtained from ^{1}H solution-state NMR spectra, and MCR has thus proven to be very useful in

the analysis of ^{13}C CP-MAS NMR spectra of alginates. However, when only a single or a few samples are available and/or pure mannuronate is not obtainable it is necessary to use another approach as will be described in Section 4.2.3.

4.2.3 Spectral deconvolution

Spectral deconvolution of signals in NMR spectra by curve fitting of either Gaussian or Lorentzian line shapes, or a combination of both (e.g. Voight) to selected signals in each individual NMR spectra is a well-established approach. The advantage of this approach, as opposed to MCR, is that it can be performed on a single spectrum. Thus, when only a single or a few samples are available and/or the pure components are not obtainable, this rather labile approach can be used but a well defined strategy is required in order to obtain unambiguous fitting results. Application of constraints is one way to navigate the fitting towards a stable and meaningful solution. However, using too many constraints is undesirable due to the risk of overfitting. In PAPER V, the M/G ratios of the studied alginates were attempted quantified by deconvolution of the five signals in the pyranose region (60-90 ppm) of each ^{13}C CP-MAS NMR spectrum. Fairly good estimates were obtained from the fitting of Gaussian line shapes. However, the approach was found inferior compared to the MCR approach. An example from the fitting of Gaussian functions is shown in Figure 24.

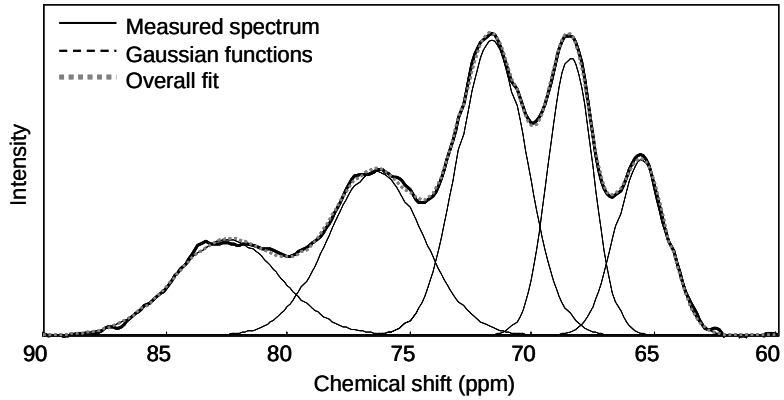

Figure 24 Example of the results obtained from the fitting of Gaussian functions to the pyranose region (60-90 ppm) in a ^{13}C CP-MAS NMR spectrum of alginate (M/G ratio = 1). The five Gaussian functions as well as the overall fit are shown.

4.3 SUPERVISED DATA ANALYSIS

4.3.1 Partial least squares regression

Partial least squares regression (PLSR) (Wold *et al.* 1983) is the fundamental method for supervised data analysis of large bilinear data structures by which two sets of data, *X* (e.g. spectra) and *y* (e.g. physico-chemical parameters), are related by means of regression. The purpose of PLSR is to establish a linear model which enables the prediction of *y* from the measured spectra in *X*. PLSR is based on a similar decomposition of the *X* matrix as known from PCA. However, PLSR is a two-block regression method, which means that the decomposition of *X* is performed under the consideration of *y* in a simultaneous analysis of the two data sets. Thus, the PLSR algorithm actively reduces the influence of *X*-variations not correlated to *y*. The PLSR model can be written as:

Equation 7 $$y_c = X_c \cdot b + e$$

where X_c contains the centred spectra (n samples, m *spectral* variables), b is a vector containing the regressions coefficients (m spectral variables, p reference paramters) determined during the calibration step, y_c contains the centred reference data (n samples, p reference parameters), desired to be predicted from X_c and e contains the y-residuals (n samples, p reference parameters). The PLSR model needs to be calibrated on samples which span the variation in y well and in general are representative of future samples.

PLSR has in this study been successfully applied in the modelling of IR, Raman and NIR spectra for the prediction of alginate M/G ratio (PAPER II and III). This is a valuable achievement, since vibrational spectroscopic techniques have a high industrial potential for at- or on-line quality control as well as screening of large number of samples. In PAPER IV, PLSR was also used to investigate the relation between the three sets of NMR data sets.

Interval partial least squares regression (iPLSR) (Nørgaard *et al.* 2000) is an extension to PLSR, which develops local PLSR models on spectral subintervals of equal width and compares the subinterval models to the model of the full-spectrum region. The advantage of the iPLSR approach is that smaller intervals will contain less interference from other parts of the spectrum and thus result in simpler, more precise and more easily interpretable models. It can be used to provide an overall picture of the relevant information in the different spectral regions. iPLSR has in this study (PAPER II and III) been applied to encircle the significant regions in the IR, Raman and NIR spectra with respect to the M/G ratio and to test the possibility of developing optimised local PLSR models for prediction of the M/G ratio using fewer variables. However, in this case it was concluded that it was not possible to develop models based on local regions with a better prediction performance than the full-spectrum model.

4.4 VALIDATION

Validation of chemometric models is of key importance in order to obtain reliable estimates of the prediction error, to detect outliers and to determine the optimal number of components (principal components and PLSR components) so that overfitting is avoided. Cross validation and test set validation can be applied, depending on the data set. Cross validation is used when the number of samples in the data set is limited and all samples are needed for both calibration and validation. The data matrix (X) is divided into a number of segments containing one (full cross validation) or more (segmented cross validation) samples. One by one the segments are left out and a model is calibrated on the remaining samples and used to predict the samples in the left out segment. Test set validation is used when the data set is large enough to be divided into a calibration set, which is used for calibration of the model, and a validation set, which is used to estimate the prediction error. Since different samples are used for calibration and validation, test-set validation is a stronger test of the model than cross-validation. A commonly used estimation of the prediction error is the root mean square error of prediction (RMSEP), which mimics the standard deviation and is in the same units as the reference values:

Equation 8

$$\mathrm{RMSEP} = \sqrt{\frac{\sum_{i=1}^{n} (y_{i,pred} - y_{i,ref})^2}{n}}$$

where $y_{i,pred}$ is the predicted value, $y_{i,ref}$ is the reference value for sample i and n is the total number of samples. When RMSEP is found by calibration or cross validation it is called RMSEC (root mean square error of calibration) and RMSECV (root mean square error of cross validation), respectively.

The PLSR models in PAPER II and III, were developed using segmented cross-validation on the calibration set consisting of 75 samples and afterwards applied and tested using an independent test set consisting of 25 samples. Cross-validation was used to determine the optimal number of PLSR components to use in the prediction model. For the model based on the EISC-corrected (cf. Section 4.5.1) Raman spectra the optimal number of components was evaluated to be one (Figure 25a). The fact that the RMSECV values continue to decrease with increasing number of PLSR components is in this case a sign of overfitting, which is confirmed when comparing the RMSECV values with the RMSEP values. Thus, a model based on more components would have resulted in overfitting as can be seen when comparing with the RMSEP values. The measured versus predicted plot (Figure 25b) is used to evaluate the model performance. In this case the test sample are predicted with the same precision as the calibration samples, which indicates that the model is very robust when it comes to predicting new samples.

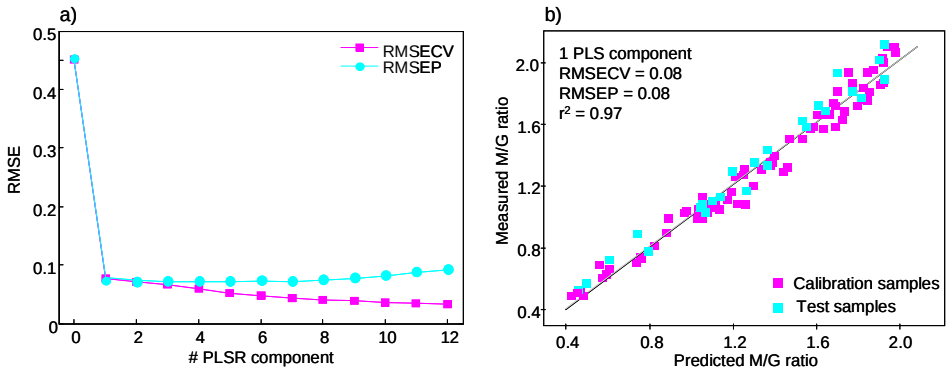

Figure 25 (a) Root mean square error of cross-validation (RMSECV) and prediction (RMSEP) versus number of PLSR components and (b) measured versus predicted M/G ratio from a PLSR model based on EISC-corrected (cf. Section 4.5.1) Raman spectra. The data is from PAPER II and III.

4.5 PRE-TREATMENT OF DATA

4.5.1 Vibrational spectroscopic data

In addition to the chemical or physical information of interest, spectral data obtained by vibrational spectroscopy often contains non-relevant information due to for example scatter effects from particles and/or fluorescence signals, changes in sample size/path length, spectroscopic artefacts/imperfections and other physical phenomena. Such variation complicate the data analysis, and therefore it is an advantage to reduce the impact of this non-relevant spectral information by

the application of spectral pre-processing methods prior to modelling in order to obtain simpler and more robust regression models and better interpretability of the data. In the following paragraph some of the most common pre-processing methods will be presented.

One of the most widely used pre-processing techniques is multiplicative signal correction (MSC) (Geladi *et al.* 1985). Originally, MSC was developed to correct scatter effects and hence MSC was at first an abbreviation of 'multiplicative scatter correction'. However, the method has been found useful for other types of multiplicative problems and for this reason the 'S' in MSC is today an abbreviation of 'signal' instead of 'scatter'. MSC is used to compensate for the additive and multiplicative effects. This is done by calculating the slope (b_0) and intercept (b_{ref}) of the regression between each individual sample spectrum (x_{org}) and a reference spectrum (x_{ref}), which is typically the average spectrum of the calibration set):

Equation 9 $$x_{org} = b_0 + b_{ref} \cdot x_{ref} + e$$

The corrected spectra (x_{corr}) are obtained by subtracting the intercept value (b_0) from each spectrum variable in all the sample spectra (x_{org}) followed by a division with the slope value (b_{ref}). MSC has been further developed to the extended multiplicative signal correction (EMSC) (Martens & Stark 1991), which includes wavelengths dependency and polynomial terms and thereby corrects non-linear behaviour in addition to additive and multiplicative effects. Moreover, inverse versions of both MSC and EMSC exist and are called ISC (Helland *et al.* 1995) and EISC (Pedersen *et al.* 2002; Martens *et al.* 2003), respectively. The main difference between MSC/EMSC and ISC/EISC methods is that when calculating the correction coefficients (slope and intercept) in the ISC/EISC methods, the reference spectrum is regressed on the sample spectrum, while in the MSC/EMSC methods, the sample spectrum is regressed on the reference spectrum. One disadvantage with the above mentioned pre-processing techniques is that the mean spectrum is used in the calculations and therefore the correction will be influenced by outliers and extreme samples and change if the sample set is modified. Thus, sometimes it can be an advantage to use the standard normal variate (SNV) (Barnes *et al.* 1989) pre-processing method, which corrects each individual spectrum independent on the other spectra in the sample set. In the SNV method, the corrected spectrum is obtained by subtracting the average intensity of the spectrum from each spectrum variable followed by a division with the standard deviation of the spectrum. In general, SNV and the original MSC lead to very similar results (both spectrally and regression-wise) (Dhanoa, 1994).

Another approach to eliminate the additive and multiplicative signal effects in the spectra is by calculating the derivatives. The first derivative eliminates the additive effects and the second derivative eliminates both the additive and multiplicative effects (Rinnan *et al.* 2009). The derivative calculations are often performed by running the data through a window-wise symmetric filter in order not to amplify high frequency noise. The most commonly used method for calculating derivatives is the Savitzky-Golay routine (Savitzky & Golay 1964), which fits a polynomial for each individual data point in a pre-defined window size symmetric left and right of the data point of interest. The disadvantage of pre-processing by calculating the derivatives is that the appearance of the spectra changes and thus complicates spectral interpretation. The advantage is that each spectrum is corrected independent of the other spectra in the data set.

Figure 26 shows the effect of some of the above mentioned spectral pre-processing methods on the Raman spectra of alginate powders from PAPER II and III, which are affected by varying levels of fluorescence (Figure 26a). All the pre-processing methods result in a decrease in the offset between the samples, and the data become visibly more linear dependent on the M/G ratio. As can be seen for both the first (Figure 26b) and second (Figure 26c) derivatives the amount of noise, especially in the high frequency end of the spectra has increased. The SNV (Figure 26d), MSC (Figure 26e) and EISC (Figure 26f) spectra look very similar with the SNV and MSC spectra being practically identical.

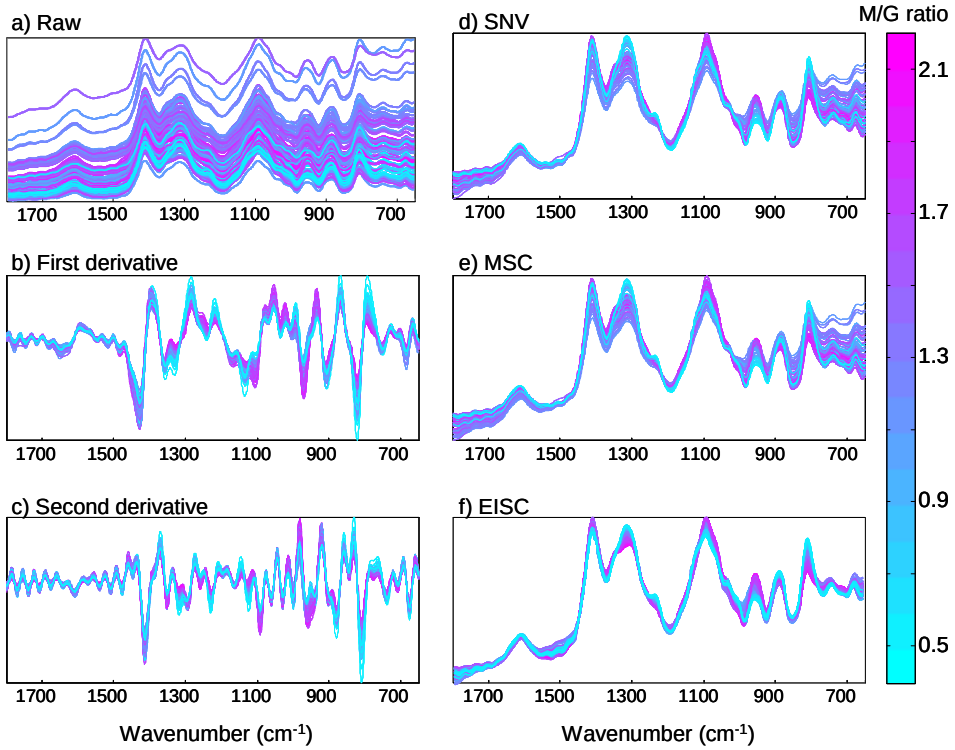

Figure 26 (a) Raw Raman spectra of 75 alginates and the effect of different pre-processing techniques: Savitzky-Golay (b) first and (c) second derivatives calculated by 15-point second-order polynomial smoothing, (d) standard normal variate (SNV), (e) multiplicative signal correction (MSC) and (f) extended inverse signal correction (EISC). The data is from PAPER II and III.

Usually, the optimal pre-processing method is selected based on the performance and number of components required in PLSR modelling (using a trial-and-error approach). To illustrate this, Table 1 lists the results of PLSR models for prediction of the M/G ratio based on the raw and pre-processed spectra from Figure 26. The optimal number of components is determined by cross-validation of the 75 calibration samples and the models are tested using a test set consisting of 25 samples as described in PAPER II and III.

Table 1 Results of PLSR models for prediction of the M/G ratio based on the raw and differently pre-processed Raman spectra shown in Figure 26. The models are validated as described in PAPER II and III.

Pre-processing	# PLS components	r^2	RMSECV	RMSEP
Raw	4	0.93	0.12	0.12
First derivative	1	0.95	0.11	0.11
Second derivative	3	0.94	0.11	0.12
SNV	3	0.97	0.08	0.08
MSC	3	0.96	0.08	0.09
EISC	1	0.97	0.08	0.08

From the results in Table 1 it is clear that pre-processing improves the prediction performance (i.e. fewer components are needed and a lower prediction error is obtained). In this particular case pre-processing by SNV, MSC or EISC result in significantly better models than pre-processing by derivative calculations. This is probably due to the noise observed in the derivative spectra (Figure 26b and c). However, increasing the filter width for noise reduction did not improve the model performance. The SNV and MSC models perform almost identical, as would also be expected due to the similarity of the pre-processed spectra, and the EISC pre-processing results in the simplest model using only one PLSR component.

4.5.2 NMR spectra

NMR data does not contain the same spectral disturbances as vibrational spectroscopy data, and the pre-processing techniques described in the previous section are therefore not relevant for NMR data. However, as discussed in Section 3.2.4, the quantitative nature of NMR spectra can be affected by a variety of distortions related to the sample preparation or imposed by non-optimised experimental parameters. Such data does not meet the prerequisites for bilinear chemometric analysis, however in some cases the distortions can be dealt with by different spectral post-processing techniques. The post-processing techniques relevant for this study will be described below. For a more thorough account on how to prepare NMR data for chemometric analysis it is referred to the reviews by Alam & Alam (2005) and Viereck *et al*. (2006).

Fourier transformation

Prior to Fourier transformation, the time domain data can be apodized and/or zero filled. This will influence the signal-to-noise ratio and the line width and shape in the Fourier transformed spectra. Thus, it is important to treat all spectra in a data set equally if it is to be analysed by chemometrics.

Phasing and baseline correction

After Fourier transformation, the NMR spectra need to be corrected for deviations from a flat horizontal baseline and phase errors. Baseline and phase corrections can normally be performed automatically in the NMR software. However, it is often necessary to perform the phase correction manually due to imperfect correction by the software.

Normalisation

Normalisation of the NMR spectra is mainly used to correct for differences in spectral intensities applied in order to make the data from all samples directly comparable with each other. The spectral sample-to-sample variation may be related to sample preparation (i.e. concentration, powder density), tuning and matching and receiver gain as discussed in Section 3.2.4. Normalisation is an operation, where each data point in the spectrum is divided by a factor such as sample weight, a single data point, the sum of intensities (area) of a specific signal or the area of a spectral region. An example on how variations related to different packing densities of alginate powders can be eliminated by normalising the ^{13}C CP-MAS NMR spectra are shown in Figure 27. The raw ^{13}C CP-MAS NMR spectra of 42 alginate powders are shown in Figure 27a. The spectra are coloured according to the M/G ratio and some systematic variation with respect to the M/G ratio can be observed but a few samples are deviating. This undesired variation can be removed by normalising the spectra by dividing with the total area of the 60-110 ppm region (Figure 27b).

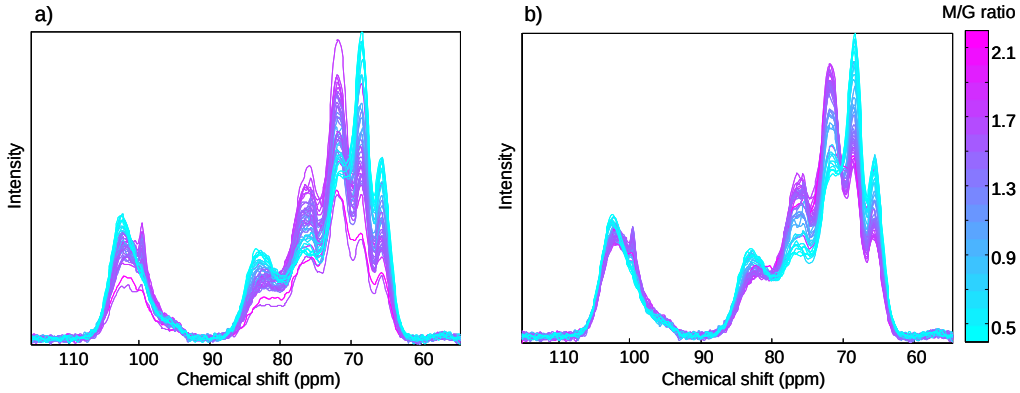

Figure 27 (a) Untreated and (b) normalised ^{13}C CP-MAS NMR spectra of 42 alginate powders

Chemical shift alignment

The major bilinear problem with NMR data is caused by chemical shift variations, which are induced by small instrumental drifts and/or differences in sample-related parameters such as pH, metal binding and temperature. The overall sample-to-sample variations can be compensated for by a rigid shift of the entire spectrum using a reference compound. In the analysis of solutions and semi-solids, the reference compound (presently 3-(trimethylsilyl) propionate-d_4 (TSP-d_4, 0.0 ppm) is used) is typically added to the solvent, whereas in the analysis of solids, the spectra are referenced to an external standard, for example the carbonyl signal of glycine in case of ^{13}C NMR. The chemical shift variability related to the sample-related parameters can of course be interesting from a chemical point of view. However, very often they are undesired. These peak-to-peak chemical shift variations can be removed by smoothing and/or data reduction in the form called binning or bucketing. However, less pragmatic and more elegant methods have been proposed including partial line fit (Vogels *et al.* 1996) and genetic algorithm alignment (Forshed *et al.* 2003). The so-called warping techniques that have been developed for correction of peak shifts in chromatographic data (Bylund *et al.* 2002; Tomasi *et al.* 2004; Skov *et al.* 2006) are also very promising but the solution is interval co-shifting (Larsen *et al.*

2006; Veselkov *et al.* 2009) in which spectral alignment is performed in spectral intervals providing more accurate alignment while still preserving the shape of the peaks.

SPECTROSCOPIC QUALITY CONTROL OF ALGINATE POWDERS

5

5.1 INTRODUCTION

The ratio of mannuronic (M) and guluronic (G) acid (M/G ratio) of alginates is closely related to the functionality in the various applications in which they are used and varies according to season, species and geographic location of the seaweed (cf. Chapter 2). Consequently, it is extremely important for alginate manufacturers and researchers to have access to methods that can provide reliable estimates of the M/G ratio. Such methods should be rapid and easy-to-use, so that they potentially can be implemented for industrial quality control and used for high throughput screening of large sample sets preferable direct on the process line.

Today, ^{1}H and ^{13}C solution-state NMR spectroscopy are the most widely used methods for the analysis of alginate M/G ratio. The disadvantage of using solution-state NMR spectroscopy for the analysis of alginates is due to a relatively time-consuming and labour intensive sample preparation. Moreover, NMR instrumentation is very expensive and demands highly qualified personnel to run the experiments and to maintain the instrument. Consequently, solution-state NMR spectroscopy is not suitable for at- or on-line quality control of alginates, and hence development of faster and simpler methods for characterisation of alginate composition would be beneficial.

The aim of the work presented in this thesis was to explore the unique potentials of vibrational spectroscopy for rapid and reliable quantitative analysis of alginate M/G ratio of intact alginate powders (PAPER II and III). In contrast to solution-state NMR spectroscopy, vibrational spectroscopic techniques such as IR, Raman and NIR spectroscopy require no sample preparation, and the instruments are relatively inexpensive and simple to operate. However, since spectra obtained by vibrational spectroscopy normally only can be fully exploited if regressed to a set of reference values, ^{1}H solution-state NMR spectroscopy is required as a reference method. It has also been investigated if the reference values alternatively could be obtained by ^{1}H HR-MAS NMR and ^{13}C CP-MAS NMR spectroscopy of semi-solid and solid alginates, respectively, in order to avoid the time consuming sample preparation required in the solution-state NMR experiments (PAPER IV and V).

This chapter provides a summary of the major results of PAPER II-V. First, the solution-state NMR reference method is described (Section 5.2), followed by a presentation of the sample sets used in the study (Section 5.3). Then a presentation of the chemometric calibration models based on IR, Raman and NIR spectroscopy is given (Section 5.4). The potential of analysing semi-solid and solid alginates by NMR spectroscopy is discussed in Section 5.5 and finally all the methods are compared in Section 5.6. The details regarding materials, methods and results are documented in the annexed papers.

5.2 THE REFERENCE METHOD: ^{1}H SOLUTION-STATE NMR SPECTROSCOPY

The ^{1}H and ^{13}C solution-state NMR methods, which today are widely used in the structural analysis of alginates (Draget *et al.* 2000; Donati *et al.* 2003; Campa *et al.* 2004; Holtan *et al.* 2006) are based on the work by Penman & Sanderson (1972) and Grasdalen and co-workers (1977; 1979; 1981; 1983). Solution-state NMR spectroscopy of alginates requires that the alginates are partly depolymerised prior to NMR analysis in order to reduce the viscosity to a level suitable for obtaining well resolved NMR spectra. The depolymerisation is carried out by mild acid hydrolysis and is a relatively time consuming and labour intensive procedure. The spectra are typically recorded at 80-90°C in order to reduce the viscosity further and to shift the water resonance away from the anomeric region, which contains the signals of interest for the M/G ratio calculations. In PAPER I-V, the alginate M/G ratios are calculated from ^{1}H solution-state NMR spectra as described in the following paragraphs.

Figure 28 shows the anomeric region of the ^{1}H NMR spectra of two depolymerised alginates in solution. The alginates analysed in this study were depolymerised to approximately 30-40 kDa (DP_n ~ 200) independent of the initial molecular weight which was in the range of 56-424 kDa (DP_n ~ 300-3000). The signals in the anomeric region of the ^{1}H NMR spectra (A (5.07 ppm), B (4.70 ppm) and C (4.46 ppm)) are assigned according to Grasdalen *et al*. (1979; 1983) to the anomeric proton of G (A), the anomeric proton of M and H-5 of G-units adjacent to M (B), and H-5 of G-units adjacent to G (C). Thus, in addition to the anomeric protons, H-5 in G-units also resonates in the anomeric region, because it is less shielded than the other ring protons. Moreover, the deshielding is sequence-dependent and consequently, the H-5 of G-units resonates differently, depending on its neighbour. The integrated intensities of signal A, B and C allow calculations of the fractions of M (F_M) and G (F_G) as well as the fractions of the MM, GG and MG/GM dimers (F_{GG}, F_{MM} and $F_{MG/GM}$), as also shown in Figure 28. The fractions of the GGG, MGM and MGG/GGM trimers can also be calculated using the relative intensities of the individual signals in signal B as described by Grasdalen (1983). ^{13}C solution-state NMR spectroscopy provides even more details on the sequential composition of alginates by allowing computation of the fractions of all eight possible trimers as well as the four fractions of dimers (Grasdalen *et al.* 1981). However, in this study only ^{1}H solution-state NMR spectroscopy is used for the calculations of the M/G ratio and the fractions of dimers as visualised in Figure 28.

In order to obtain comparable values of the M/G ratios between samples, the relative integrals of the three signals were calculated using an in-house built routine where the same integration limits for all the spectra were applied. The limits for signal A, B and C were set to 5.18-4.96 ppm, 4.82-4.57 ppm and 4.55-

4.38 ppm, respectively. The integration limits are indicated with grey boxes in Figure 28. Changing these limits yielded slightly different M/G ratio values, emphasising the importance of using the same limits in all the calculations. The error of quantification of the M/G ratio using the described ^{1}H solution-state NMR method was estimated to be between 0.01 and 0.08 (the standard deviation quantifications of triplicates).

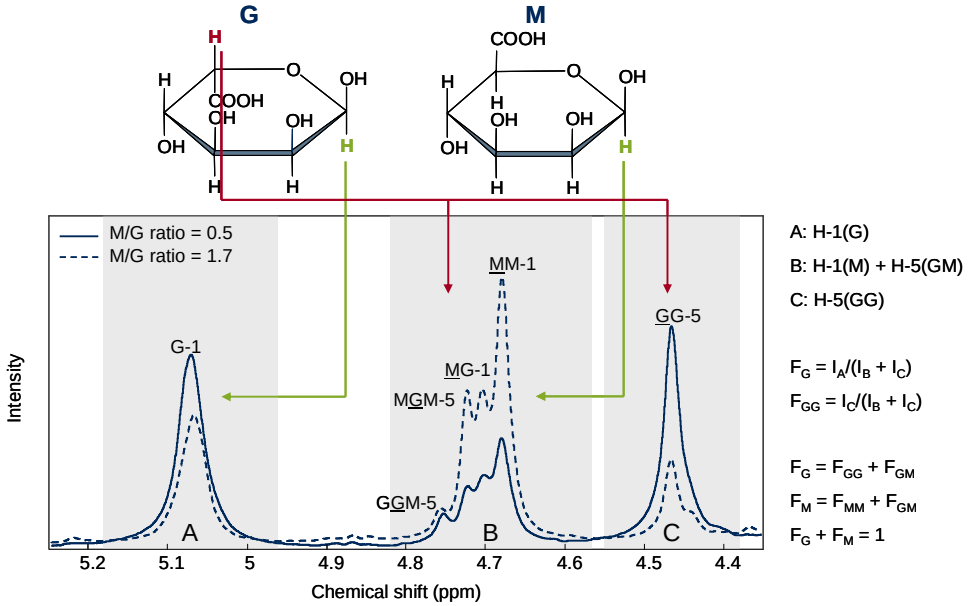

Figure 28 Anomeric region of ^{1}H NMR spectra of two depolymerised alginates in solution (1 % (w/v)). The M/G ratios are calculated from the relative areas of signal A, B and C. The integration limits are indicated by the grey boxes.

When analysing alginates by solution-state NMR spectroscopy, it is important to consider the problems related to the presence of calcium ions in the samples. The formation of rigid junction zones between the G-blocks in the alginate molecules will lead to wrong estimations of the M/G ratios. The effects of increasing calcium content on the signals in the anomeric region of the ^{1}H solution-state NMR spectra of alginate are illustrated in Figure 29. The alginates with different calcium contents were prepared by exchanging some of the sodium ions in the sodium alginate with calcium ions. The same sodium alginate was used as starting material for all samples. It was dissolved in demineralised water and added different amounts of slowly soluble calcium sulphate. The samples were left stirring overnight and afterwards precipitated in alcohol and dried. The resulting alginates, which contained different amounts of calcium, were depolymerised and measured by ^{1}H solution-state NMR spectroscopy. The spectra in Figure 29 clearly show the line broadening effects induced by the calcium ions and the resulting overestimation of the M/G ratio. However, the availability of the calcium ions can be controlled by addition of a chelating agent such as sodium hexametaphosphate (SHMP) to the solution when analysing alginates by solution-state NMR spectroscopy. SHMP binds the calcium ions so that they cannot react with the alginate and hence do not influence the results.

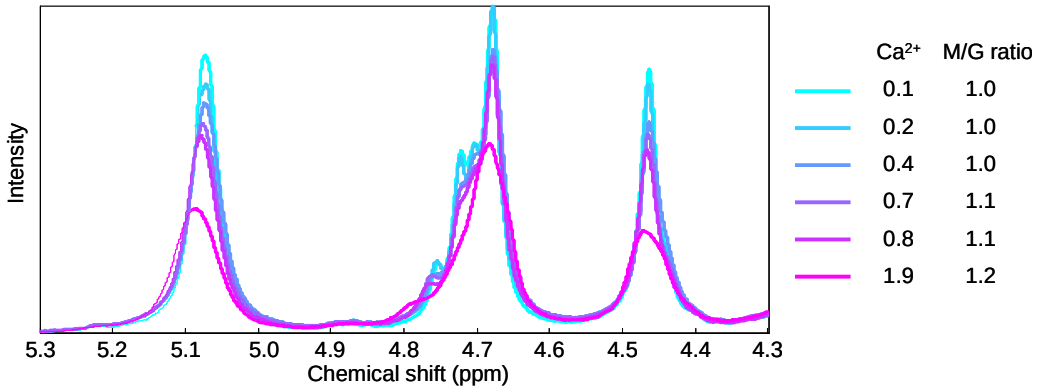

Figure 29 Anomeric region of 400 MHz ^{1}H NMR spectra of depolymerised alginates in solution (1% (w/v)) with varying calcium content. The alginates containing different calcium contents were prepared by ion exchange of the same sodium alginate by addition of different amounts of calcium sulphate.

5.3 THE SAMPLE SETS

5.3.1 Samples for development of calibration models (PAPER II and III)

For the development of the IR, Raman and NIR calibration models (PAPER II and III), a set of 100 different sodium alginate powders were collected. The powders were sieved to ensure that the powder particles were $\leq$ 106 μm in order to prevent too large intensity variations in the IR, Raman and NIR spectra (cf. Section 3.3.3). Different physico-chemical parameters including M/G ratio, fraction of dimers, water content, gel strength, viscosity and molecular weight (M_w) were measured in order to describe the samples. The solution-state NMR measurements were carried out at a 200 MHz spectrometer. The range and average values of the physico-chemical parameters of the 100 different sodium alginates are listed in Table 2.

Table 2 The range, average values and average standard deviations (std) of the physico-chemical properties of the 100 different sodium alginate samples.

Physico-chemical property	Range	Average	Average std
M/G ratio	0.5-2.1	1.3	0.06[a]
GG-dimers (%)	9-44	23	1.0[a]
MM-dimers (%)	10-49	34	1.8[a]
MG/GM-dimers (%)	34-51	43	2.4[a]
Water content (%)	11.0-17.8	14.9	0.18[b]
Gel strength (g)	70-1139	566	15.5[c]
Viscosity (cP)	23-846	269	12.3[d]
M_w (kDa)	104-424	277	8.6[b]

[a] Based on true triplicates of 9 different samples
[b] Based on true replicates of all samples
[c] Based on the results from two gels of all alginates made from the same solution of the respective alginate
[d] Based on measuring the viscosity of the same sample six times

Since the main purpose of the studies presented in PAPER II and III was to find correlations between the M/G ratio and spectra obtained by vibrational spectroscopy, the samples were selected to provide as much variation as possible with respect to the M/G ratio. The samples spanned the M/G ratio range of 0.5-2.1. The relatively large number of samples available allowed for the use of an independent test set for validation of the calibration models. The test set was selected prior to model development by sorting the samples according to the M/G ratio and then selecting every fourth sample. Figure 30a shows the M/G ratio of the 75 calibration samples and 25 test samples sorted according to the M/G ratio. The samples did not only vary with respect to the M/G ratio, but also with respect to the other physico-chemical properties. To investigate the variance structure in the physico-chemical properties, a PCA was performed on the autoscaled physico-chemical data. The PCA score plot in Figure 30b shows that both the calibration samples and the test samples spanned the variation within all the physico-chemical parameters. The PCA loading plot in Figure 30c shows how the different physico-chemical parameters are correlated.

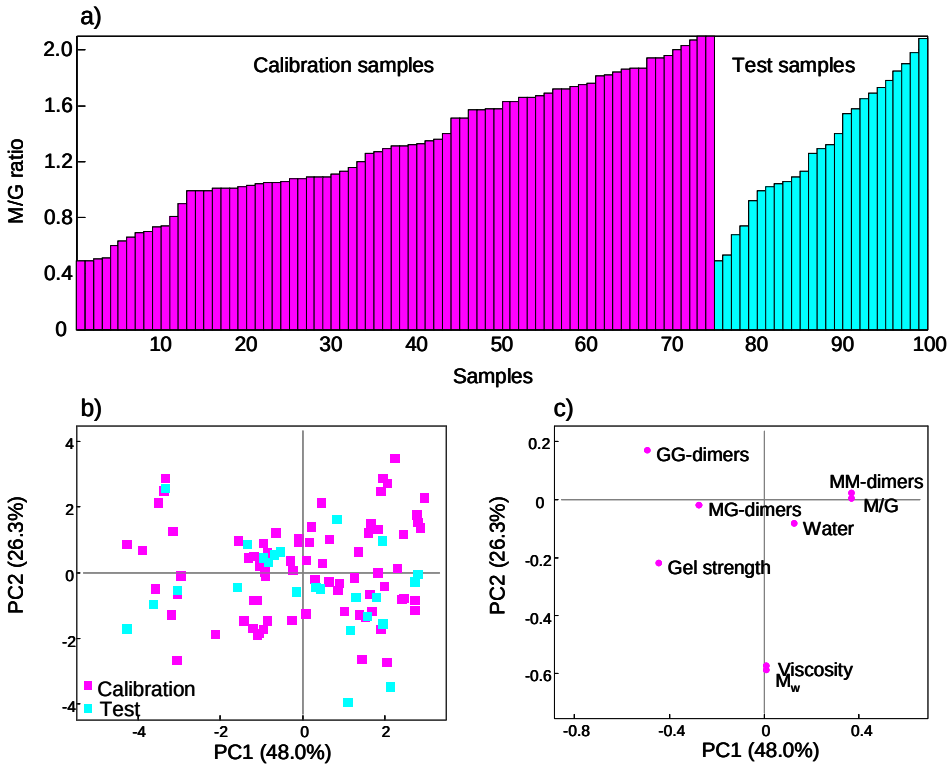

Figure 30 (a) M/G ratio of the 75 samples in the calibration set and the 25 samples in the test set calculated from spectra recorded on a 200 MHz NMR spectrometer. PCA (a) score and (b) loading plot based on the physico-chemical properties of the calibration of test samples showing the first two principal components which explain 74.3% of the variation.

In PAPER III, three additional samples, which contained higher amounts of calcium (1.1%, 1.4% and 2.4%) than the other samples (<0.25%) were added to the sample set. The physico-chemical parameters of these three samples are included in Table 3 (Section 5.3.2). These were not used in the development of

the calibration models, but included to illustrate that Raman spectra are not sensitive to the higher calcium content in contrast to ^{1}H solution-state NMR spectra.

5.3.2 Samples for solid-state NMR spectroscopy (PAPER IV and V)

For the development of a new M/G ratio reference method based on solid-state NMR spectroscopy (PAPER IV and V), a sample set of 42 different sodium alginates were collected. The major part of the samples (38 samples) was from the sample set described above (Section 5.3.1). In addition, the three samples containing a higher calcium content (1.1%, 1.4% and 2.4%) as well as a low molecular weight sample (M_w = 58 kDa) were included in the data set. An overview of the physico-chemical properties of the 42 samples are given in Table 3.

Table 3 Overview of the physico-chemical properties of the 39 different sodium alginate samples and the three samples with higher calcium content.

Physico-chemical property	**Range[a]**	**Samples with high Ca**		
M/G ratio	0.4-1.7	1.8/1.6[b]	1.5/1.3[b]	2.1/1.5[b]
GG-dimers (%)	14-53	16/17[b]	19/22[b]	11/19[b]
MM-dimers (%)	12-44	38/38[b]	43/34[b]	51/39[b]
MG/GM-dimers (%)	24-46	46/47[b]	38/44[b]	38/42[b]
Water content (%)	11.0-17.8	13.3	16.3	16.2
Gel strength (g)	56-1052	507	407	302
Viscosity (cP)	8-846	1142	1414	3619
M_w (kDa)	56-424	332	371	273
Ca (%)	0.01-0.02	1.1	1.4	2.4
Na (%)	6.5-8.7	7.5	6.1	5.1

[a] Samples with calcium content in the range of 0.01-0.20
[b] First and second value are estimated from the ^{1}H solution-state NMR spectrum of sample without and with addition of sodium hexametaphosphate (SHMP), respectively.

The M/G ratio and fractions of dimers of these samples were estimated from ^{1}H solution-state NMR spectra recorded on a 400 MHz spectrometer. This resulted in slightly different M/G ratio values for some of the samples (±0.1), compared to the values estimated from the spectra obtained on the 200 MHz spectrometer. The M/G ratios of the 42 sodium alginates are shown in Figure 31a. The M/G ratios calculated from the solution-state NMR spectra of the three samples containing 1.1%, 1.4% and 2.4% calcium were 1.8, 1.5 and 2.1, respectively. However, the M/G ratios calculated from the spectra obtained after addition of SHMP were lower (1.6, 1.3 and 1.5, respectively). The M/G ratios of the samples with <0.2% calcium were the same when measured with and without SHMP. Obviously, the M/G ratios of the samples with high calcium content are overestimated when SHMP is not added. PCA score and loading plots of the physico-chemical properties of the 42 samples are shown in Figure 31b and c, respectively.

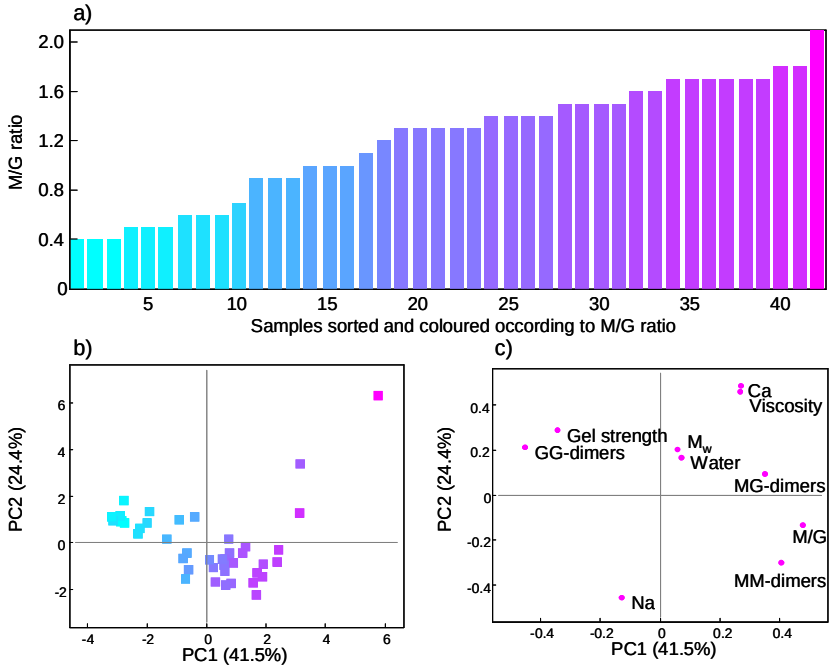

Figure 31 (a) M/G ratio of the 42 sodium alginates calculated from spectra recorded on a 400 MHz spectrometer. PCA (a) score and (b) loading plot based on the physico-chemical properties of the 42 samples showing the first two principal components which explain 65.9% of the variation. The samples are coloured according to the M/G ratio.

5.4 CALIBRATION MODELS BASED ON VIBRATIONAL SPECTROSCOPY

Investigations of other polysaccharides have shown that the combination of vibrational spectroscopy and chemometrics is successful when the aim is to develop rapid, non-destructive and robust methods for monitoring different structural characteristics of polysaccharides (Engelsen & Nørgaard 1996; Dolmatova *et al.* 1998; Dyrby *et al.* 2004; Winning *et al.* 2009a). It has been shown that FT-IR, FT-Raman and NIR can be used for determination of the degree of esterification, amidation (Engelsen & Nørgaard 1996) and distribution of ester groups (Winning *et al.* 2009a) in pectins and for the determination of the content of different types of carrageenan in carrageenan powders (Dyrby *et al.* 2004) using PLSR. Moreover, FT-IR spectra of modified corn starches have been used for classification and recognition of their modifications using artificial neural network processing (Dolmatova *et al.* 1998).

The following paragraphs demonstrate the potential of using FT-IR, FT-Raman and NIR spectroscopy combined with chemometrics for reliable and rapid determination of the M/G ratio in sodium alginate powders. Calibration models were developed using PLSR and ^{1}H solution-state NMR spectroscopy was used as the reference method (PAPER II and III).

5.4.1 IR spectroscopy

The best IR calibration model was obtained using the region of 1800-650 cm^{-1} in the IR spectra, which were pre-processed by the EISC method. Intensity

variations in the raw IR spectra (Figure 32a) due to differences in the contact to the crystal were compensated for by the EISC method (Figure 32b). Four PLS components were needed for an optimal description of the data and a prediction error of 0.08 was obtained. The measured versus predicted plot from the model developed on the 75 calibration samples and tested with the 25 test samples are shown in Figure 32c and the PLSR regression coefficients are shown in Figure 32d. The regression coefficients give an overview of which parts of the spectra that contribute to the prediction of the M/G ratio. It is observed that several bands in the rather crowded fingerprint region are important for the M/G ratio prediction. When comparing the regression coefficients with the EISC-corrected spectra, it can be observed that it is the small shifts in the overlapping spectra rather than distinct bands that give rise to the highest regression coefficients. For further details on which bands giving rise to M/G ratio related intensity differences in the IR spectra it is referred to PAPER II. The overlapping nature of the IR spectra makes it difficult to assign the individual bands, however, it can be concluded that the asymmetric stretching band centred around 1600 cm^{-1}, which originates from the carboxylate ion, does not contribute significantly to the prediction of the M/G ratio.

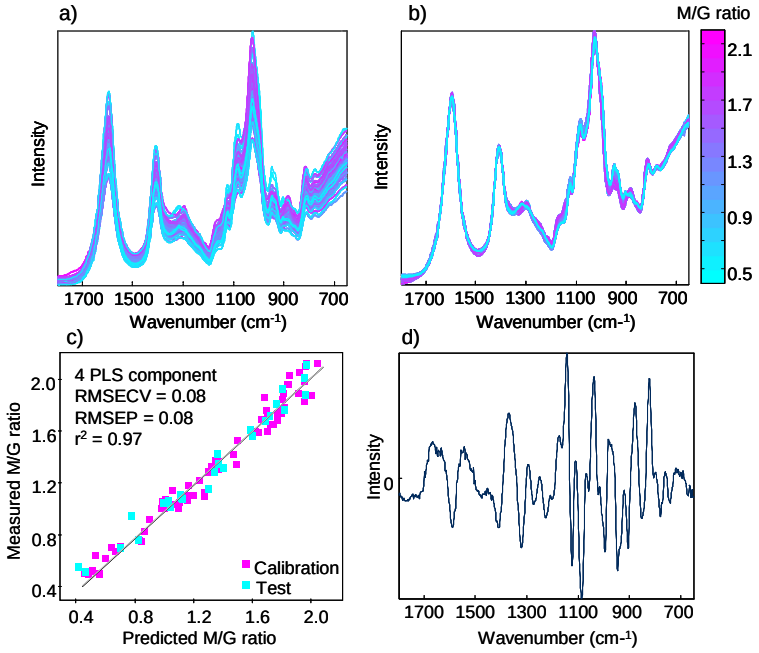

Figure 32 (a) Raw and (b) EISC-corrected IR spectra of the 75 calibration samples. (c) M/G ratio measured by ^{1}H solution-state 200 MHz NMR spectroscopy versus M/G ratio predicted using the PLSR model based on the EISC-corrected IR spectra. (d) The regression coefficients used in the PLSR model.

5.4.2 Raman spectroscopy

The best Raman calibration model was also obtained by pre-processing the spectra by the EISC method. The intensity variations in the raw Raman spectra (Figure 33a) which were eliminated by application of the EISC method (Figure 33b) are primarily due to fluorescence. The model based on the EISC-corrected Raman spectra requires only one PLSR component to predict the M/G ratio and as for the IR model the prediction error is 0.08. The measured versus predicted plot

and the regression coefficients of the PLSR model are shown in Figure 33c and d, respectively. As for the IR model, it can be concluded that it is generally the whole fingerprint region of 1500-800 cm^{-1} that is responsible for the prediction of the M/G ratio. However, especially the bands centred at 955 cm^{-1} and 806 cm^{-1} are contributing to the prediction. The band at 806 cm^{-1} is the most influential spectral band and arises from the α-configuration of the G-units. The second most influential spectral band is centred at 955 cm^{-1} and may be related to the β-configuration of the M-units. Actually, the ratio between the intensities at 955 cm^{-1} (M) and 806 cm^{-1} (G) correlated well (r^2=0.95) to the M/G ratio calculated from the NMR spectra. Moreover, the ratio between the intensities of 1290 cm^{-1} (M) and 1320 cm^{-1} (G) in the EISC-corrected IR spectra correlated very well (r^2=0.96) to the M/G ratio, as also found by Filippov & Kohn (1974). While these bi-variate methods are almost as good as the multivariate calibration methods to estimate the M/G ratio, they are more sensitive to noise and interferences and will thus be less robust for industrial quality control.

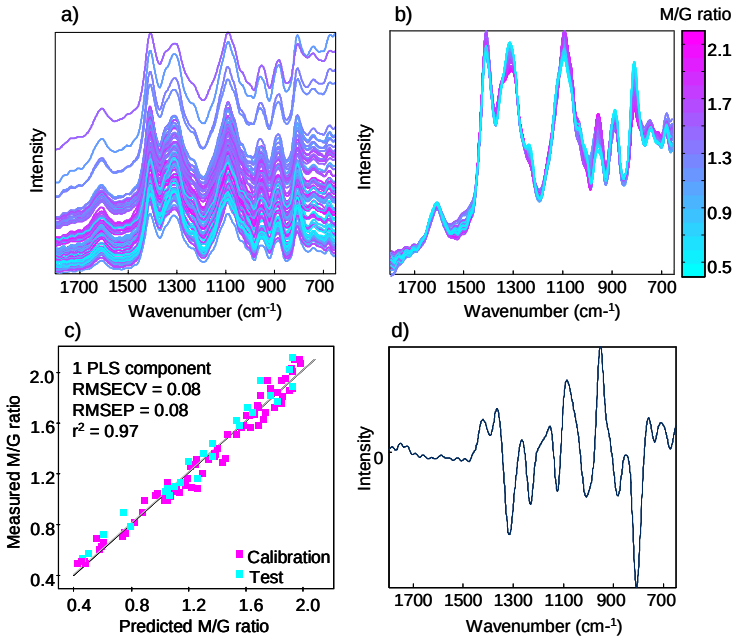

Figure 33 (a) Raw and (b) EISC-corrected Raman spectra of the 75 calibration samples. (c) M/G ratio measured by ^1H solution-state 200 MHz NMR spectroscopy versus M/G ratio predicted using the PLSR model based on the EISC-corrected Raman spectra. (d) The regression coefficients used in the PLSR model.

5.4.3 NIR spectroscopy

The best NIR calibration model was obtained using the second derivative NIR spectra from 1100-2500 nm. The intensity variations in the raw NIR spectra (Figure 34a) are primarily due to scatter effects from particles of different sizes. The second derivative NIR spectra are shown in Figure 34b. The M/G ratio could be predicted from the second derivative NIR spectra using three PLSR components and with a prediction error of 0.08. The measured versus predicted plot and the regression coefficients of the PLSR model are shown in Figure 33c and d, respectively. Since the NIR spectra are even less distinctive than the IR

and Raman spectra assignment of the spectral regions contributing to the calibration is even more difficult. However, the regression coefficients show that the first overtone C-H stretching modes in the 1700-1800 nm region and the combination bands in the 2250-2400 nm region are important for the prediction of the M/G ratio.

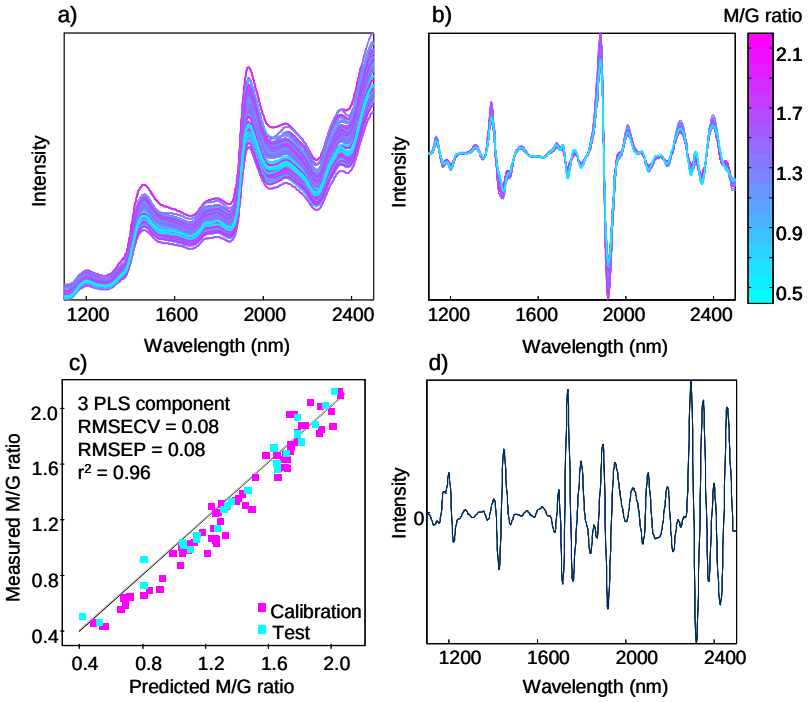

Figure 34 (a) Raw and (b) second derivative NIR spectra of the 75 calibration samples. (c) M/G ratio measured by ^{1}H solution-state 200 MHz NMR spectroscopy versus M/G ratio predicted using the PLSR model based on the second derivative NIR spectra. (d) The regression coefficients used in the PLSR model.

5.4.4 Comparison of the calibration models

An overview of the results of the best IR, Raman and NIR calibration models for the prediction of the M/G ratio of sodium alginate powders are listed in Table 4. Generally, the M/G ratio can be predicted with the same prediction error (0.08), which is comparable to the standard deviation of the NMR reference method (0.01-0.08). The simplest model is obtained using the Raman spectra requiring only one PLSR component to explain the M/G ratio. It should be noted that the calibration error (RMSECV) and the prediction error (RMSEP) values are the same for all models indicating that the models are very robust (i.e. the models can predict new samples that have not been involved in the modelling with high precision).

Table 4 Results of PLSR models based on EISC-corrected IR and Raman spectra and second derivative NIR spectra of sodium alginate powders for prediction of the M/G ratio. The models were developed using the 75 calibration samples and the prediction ability was tested using the 25 test samples.

	Pre-processing	# PLS comp	r^2	RMSECV	RMSEP
IR	EISC	4	0.97	0.08	0.08
Raman	EISC	1	0.97	0.08	0.08
NIR	Second derivative	3	0.96	0.08	0.08

The overall conclusions from PAPER II and III are that rapid, non-destructive and robust quantitative calibration models for measuring the M/G ratio of sodium alginate powders can be developed using vibrational spectroscopy and chemometrics. However, it should be noted that the calibration models are dependent on a reliable reference method for measurement of the M/G ratio. Moreover, the performances of the calibration models depend on the quality of the reference values. In cases where the error of the reference method is high, it may turn out that the predicted values are more accurate than the reference values. In order to investigate if that was the case in this study, PLSR models based on the EISC-corrected IR spectra and second derivative NIR spectra were developed using the M/G ratios predicted from the Raman PLSR model described in Section 5.4.2 as reference values. The measured versus predicted plots from the two PLSR models are shown in Figure 35. It can be observed that the prediction error is reduced by 0.04 when using the M/G ratio values predicted from the Raman spectra as reference values as opposed to when using the M/G ratio values calculated from the ^{1}H solution-state NMR spectra (Table 4). Thus, the M/G ratio values obtained by vibrational spectroscopy are more precise than the values calculated from the ^{1}H solution-state NMR spectra.

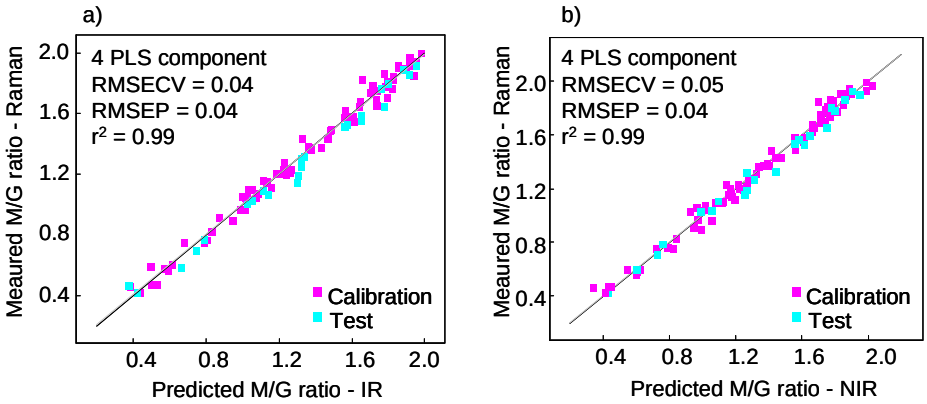

Figure 35 Measured versus predicted plot from PLSR models based on (a) the EISC-corrected IR spectra and (b) the second derivative NIR spectra. The M/G ratios used as reference values are predicted from the Raman spectra (cf. Section 5.4.2).

In addition to prediction of the M/G ratio, it was also investigated if the fractions of GG-, MM- and GM/MG-dimers, water content, gel strength, viscosity and average molecular weight (M_w) could be predicted form the IR, Raman and NIR spectra. The PLSR results are listed in Table 5.

Table 5 Results of PLSR models based on IR, Raman and NIR spectra of sodium alginate powder for prediction of alginate physico-chemical properties.

	IR		Raman		NIR	
	EISC corrected		EISC corrected		Second derivative	
	r^2	RMSEP	r^2	RMSEP	r^2	RMSEP
GG-dimers	0.97	1.3	0.95	1.4	0.97	1.6
MM-dimers	0.96	2.4	0.95	2.6	0.96	2.7
GM/MG-dimers	0.59	2.3	0.44	3.0	0.57	2.4
Water content (%)	0.69	0.6	-	-	0.83	0.7
Gel strength (g)	0.63	137	0.69	140	0.62	140
Viscosity (cP)	-	-	-	-	-	-
Mw (kDa)	-	-	-	-	-	-

The fraction of GG- and MM-dimers could be modelled well using all three spectroscopic data sets. The fraction of GM/MG-dimers could on the other hand not be modelled as well. Thus, the relative good predictions of the fraction of GG- and MM-dimers are most likely due to the indirect correlation to the M/G ratio. The water content could be predicted from the IR spectra and the NIR spectra with prediction errors of 0.6 (r^2=0.69) and 0.7 (r^2=0.83), respectively. The O-H stretching band from water is very weak in Raman spectra due to the weak polarizability of O-H bonds and consequently the water content could not be predicted from the Raman spectra. The gel strength could be predicted with a prediction error of 137-140 g, which is rather high, and the viscosity and M_w could not be predicted at all, which can be explained by the fact that the viscosity and the M_w are mainly related to the alginate chain length and less to the chemical composition.

5.5 SOLID-STATE NMR SPECTROSCOPY AS NEW REFERENCE METHOD

The potential of using ^{1}H HR-MAS NMR spectra of alginates suspended in D_2O or ^{13}C CP-MAS NMR spectra of alginate powders as alternative methods to the traditional ^{1}H solution-state NMR spectroscopy method for the analysis of the M/G ratio was investigated in PAPER IV and V and the main results are summarised in Section 5.5.1 and 5.5.2.

5.5.1 ^{1}H HR-MAS NMR spectroscopy

Figure 36 shows the carbohydrate regions of a ^{1}H solution-state NMR spectrum of an alginate in solution (1% (w/v)) and a ^{1}H HR-MAS NMR spectrum of the same sample in semi-solid state (2 mg powder added 45 µl D_2O resulting in a gel-like texture).

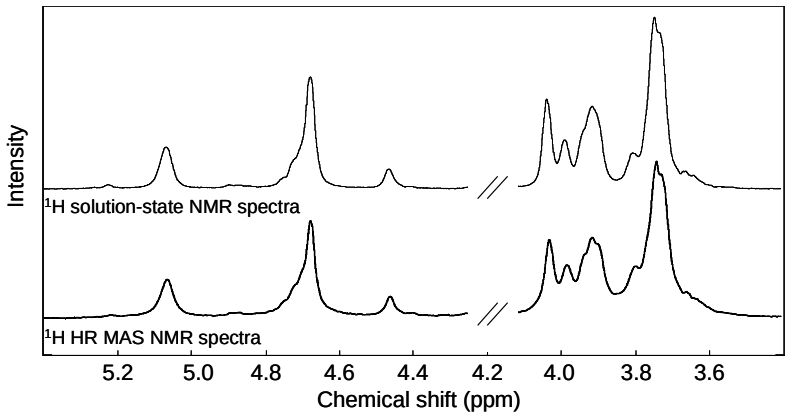

Figure 36 The carbohydrate region of the ^{1}H solution-state NMR spectra of depolymerised alginate and ^{1}H HR-MAS NMR spectra of alginate powder soaked in D_2O recorded at 90ºC. The M/G ratio of the sample shown is 1.3. The water resonance (4.1-4.3 ppm) is removed from the spectra. The resolution of the two spectra is comparable.

The resolution of the ^{1}H HR-MAS NMR spectra of the swollen alginate is comparable to the resolution of the spectra of the dissolved and depolymerised alginate. Thus, it can be concluded that it is possible to obtain fairly well-resolved ^{1}H HR-MAS NMR spectra of intact alginates and thereby avoid the destructive and time-consuming acid hydrolysis generally used for analysis of alginates in solution-state. The M/G ratio values of the 42 samples investigated were calculated from the signals in the anomeric region of the ^{1}H solution-state NMR spectra and the ^{1}H HR-MAS NMR spectra as described in Section 5.2. The M/G ratios from the HR-MAS NMR spectra were compared with the M/G ratios from the solution-state NMR spectra obtained with (Figure 37a) and without (Figure 37b) addition of the chelating agent SHMP. From the comparison, it can be observed that the M/G ratios calculated from the ^{1}H HR-MAS NMR spectra are generally in good agreement with the values calculated from the solution-state NMR method (±0.1). However, the three samples with high calcium content are also overestimated in the HR-MAS NMR spectra due to immobilisation of parts of the alginate molecule when calcium concentrations are high.

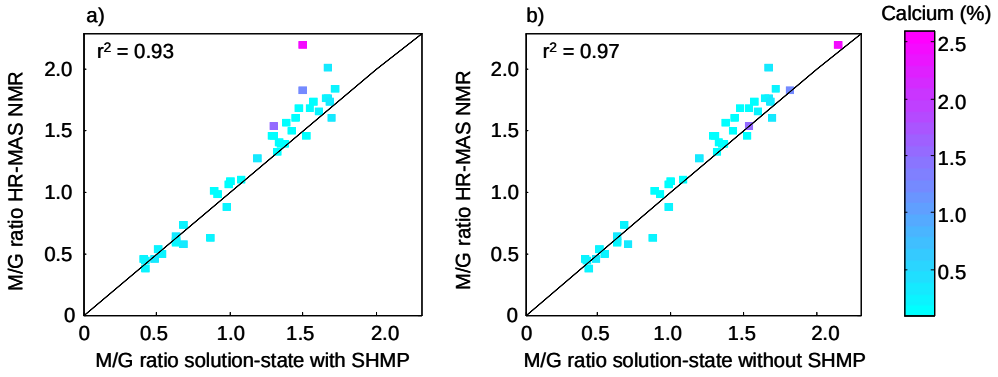

Figure 37 M/G ratios of the 42 sodium alginates calculated from ^{1}H HR-MAS NMR spectra versus the M/G ratios calculated from the ^{1}H solution-state NMR spectra measured (a) with sodium hexametaphosphate (SHMP) and (b) without SHMP.

5.5.2 ^{13}C CP-MAS NMR spectroscopy

In PAPER V, it was demonstrated how the M/G ratio can be quantified directly from the ^{13}C CP-MAS NMR spectra of alginate powders using two different unsupervised data analytical approaches: multivariate curve resolution (MCR) (cf. Section 4.2.2) and spectral deconvolution by the fitting of Gaussian and/or Lorentzian functions (cf. 4.2.3). It was demonstrated that without *a priori* knowledge of the monomer composition, the M/G ratio can be robustly estimated from ^{13}C CP-MAS NMR spectra of alginate powders by MCR. However, it was found necessary to include the spectra of a pure mannuronate isolated from *Pseudomonas fluorescenc* to the sample set in order to obtain meaningful results. MCR of the 60-110 ppm region of the ^{13}C CP-MAS NMR spectra of the 42 alginate powders only (Figure 38a) and the 42 alginate powders plus the pure mannuronate (Figure 38b) resulted in two different solutions. Both solutions included an estimated pure spectrum representing the spectrum of pure guluronate (Figure 38c and d). However, only the MCR analysis of the data set including the rare pure mannuronate resulted in a good resolution of the two pure spectra (Figure 38d).

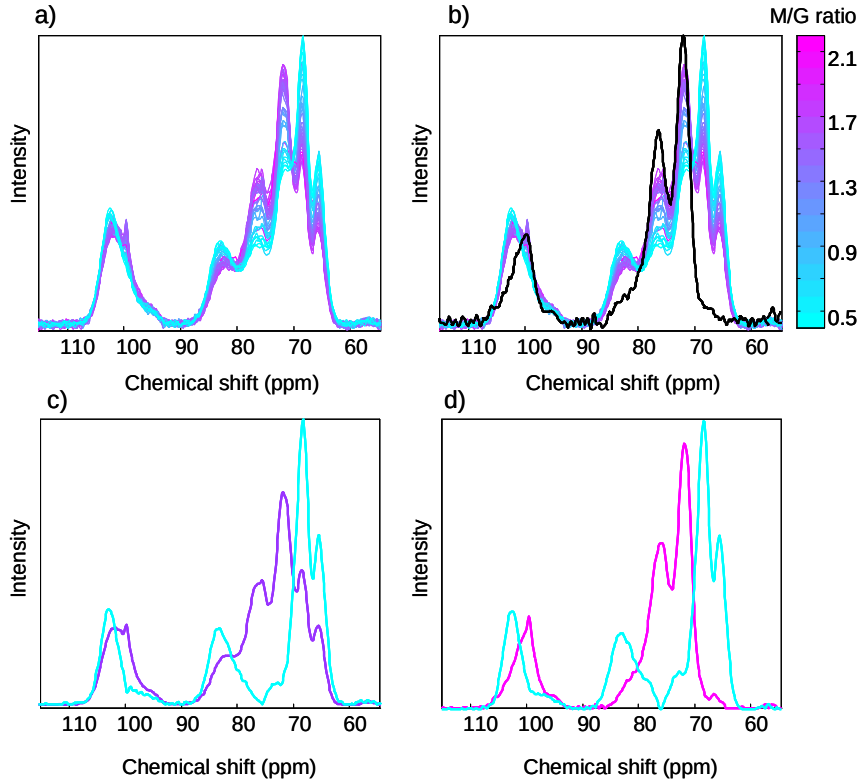

Figure 38 The measured ^{13}C CP-MAS NMR spectra of (a) the 42 sodium alginates and (b) the 42 sodium alginates plus the spectrum of pure mannuronate isolated from *Pseudomonas fluorescenc* (black). (c) The MCR loadings representing the average ^{13}C CP-MAS NMR spectrum of the 42 alginates (purple) and the estimated pure ^{13}C CP-MAS NMR spectrum of guluronate (blue) based on the analysis of the 42 alginates. (d) The MCR loadings representing the estimated pure ^{13}C CP-MAS NMR spectra of mannuronate (pink) and guluronate (blue) based on analysis of the 42 alginates plus the spectrum of pure mannuronate.

From the MCR modelling, each sample has a score (estimated concentration of mannuronate or guluronate) for each of the loadings (estimated pure spectra of mannuronate or guluronate). Thus, the M/G ratio can be estimated from the score values. In Figure 39a, the M/G ratio values estimated from the MCR score values calculated from the ^{13}C CP-MAS NMR spectra are compared with the M/G ratio values calculated from the solution-state NMR spectra of the depolymerised alginates after addition of SHMP. Hence, the calcium ions are not influencing the results. The figure reveals an excellent correlation between the M/G ratio values obtained by the two methods (r^2=0.99). For comparison, the M/G ratios estimated from the MCR score values calculated from the ^{13}C CP-MAS NMR spectra are also compared with the M/G ratio values calculated from the solution-state NMR spectra of the depolymerised alginates without addition of SHMP (Figure 39b). This comparison clearly shows that the M/G ratios obtained from the solution-state NMR spectra of the samples with calcium contents higher (1.1-2.4%) than the other samples (0.01-0.2%) are overestimated. In contrast, the ^{13}C CP-MAS spectra NMR spectra are not influenced by the calcium content differences.

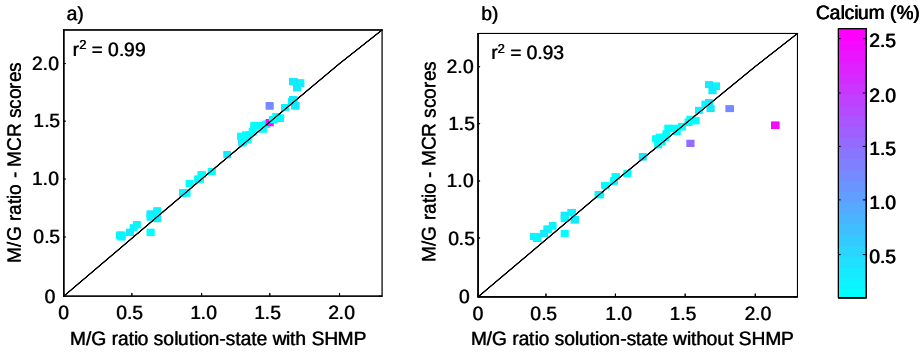

Figure 39 M/G ratios of the 42 sodium alginates calculated from the estimated concentrations of mannuronate and guluronate from the MCR analysis of the ^{13}C CP-MAS NMR spectra versus the M/G ratios calculated from the ^{1}H solution-state 400 MHz NMR spectra measured (a) with and (b) without SHMP.

When only a single or a few samples are available and/or the pure components are not obtainable, the M/G ratio can be relatively accurately estimated from a spectral deconvolution of the five pyranose signals in the region 60-90 ppm of the ^{13}C CP-MAS NMR spectrum using Gaussian line shapes (Figure 40a) as demonstrated in PAPER V. The best correlation between the M/G ratios obtained from ^{1}H solution-state NMR spectroscopy and the M/G ratios estimated from the fitting results of the ^{13}C CP-MAS NMR spectra (integrated intensities or heights of the deconvoluted signals) were obtained by taking the ratio of the heights of the fitted functions at 71.6 ppm and 68.4 ppm (Figure 40b). The signal at 71.6 ppm is assigned to C-2 and C-3 of mannuronate and the signal at 68.4 ppm is assigned to C-3 and C-5 of guluronate. However, when comparing Figure 39a and Figure 40b it is clear that the MCR method is superior to the Gaussian curve fitting approach with respect to M/G ratio estimation.

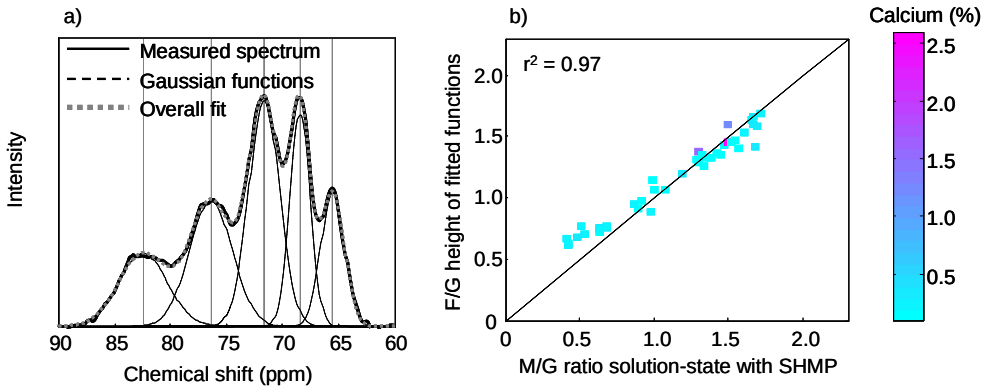

Figure 40 (a) Example of the results obtained from the fitting of Gaussian functions to the pyranose region (60-90 ppm) in a ^{13}C CP-MAS NMR spectrum of alginate. (b) M/G ratios of the 42 alginates estimated from the ratio of the height of the fitted functions of the ^{13}C CP-MAS NMR spectra at 71.6 ppm and 68.4 ppm versus the M/G ratios calculated from the ^{1}H solution-state NMR spectra measured with SHMP.

5.6 COMPARATIVE SPECTROSCOPY

In the previous sections different approaches for estimating M/G ratios of alginates have been demonstrated. The M/G ratio can be calculated from ^{1}H solution-state NMR spectra of depolymerised alginate as has been done extensively since Grasdalen and co-workers first described this method in 1979. In addition, several new methods for M/G ratio estimations of alginates have been presented in this thesis. The M/G ratio can be predicted from IR, Raman and NIR spectra using the M/G ratio values from ^{1}H solution-state as reference values. It has been shown that the M/G ratio can be directly calculated from the ^{1}H H-MAS NMR spectra of alginate powders soaked with D_2O and from ^{13}C CP-MAS NMR spectra of alginate powders. Thus, several alternative methods for M/G ratio determination requiring none or very limited sample preparation have been established. In order to compare the different methods, the M/G ratio values obtained from ^{1}H solution-state NMR, ^{1}H HR MAS NMR, ^{13}C CP-MAS NMR and Raman spectra are plotted against each other in Figure 41. The M/G ratio values of the solution-state NMR spectra used in this comparison are obtained from the spectra of solutions without SHMP in order to highlight to what extend the different methods are sensitive to the presence of calcium ions. The M/G ratio values predicted using the IR and NIR calibration models were similar to the values obtained using the Raman model and are therefore not shown. Generally, it can be observed that the best correlations were obtained between the values obtained from ^{1}H solution-state and ^{1}H HR-MAS NMR spectra (r^2=0.97) and the values obtained from the ^{13}C CP-MAS spectra and Raman spectra (r^2=0.96). Generally, the M/G ratios obtained from ^{1}H solution-state and ^{1}H HR-MAS NMR spectra of depolymerised alginate in solution and swollen intact alginate powder, respectively, were in agreement with the measurements of intact alginate powder by ^{13}C CP-MAS NMR and Raman spectroscopy as long as the content of residual calcium ions was not too high (no severe effects up to 1.1% were observed). However, in particular the estimated M/G ratio of the sample with high calcium ion content (2.4%) when measured in solution, swollen-state and solid-state were not in agreement. Since the solution-state and HR-MAS NMR methods cannot detect immobilised parts of the molecule the value obtained from the CP-MAS

NMR and Raman spectra should reflect the true M/G ratio as these methods measure all molecular fragments in dry alginate powder independent on the internal mobility and thus the calcium ion content.

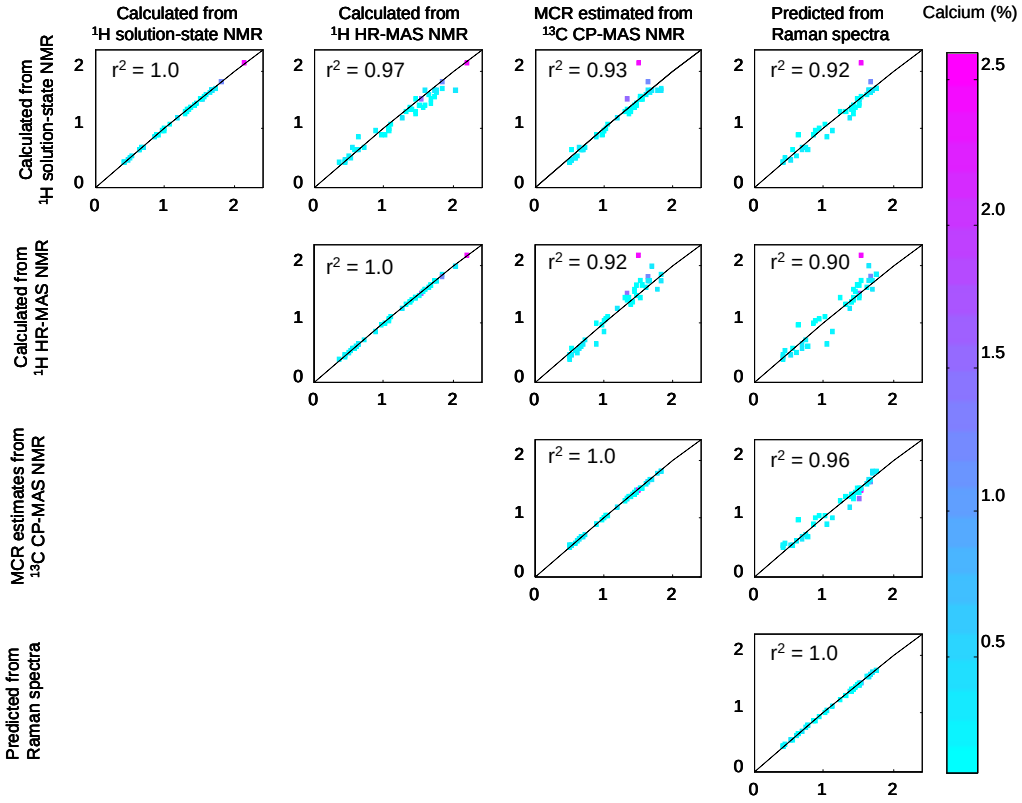

Figure 41 Scatter plots of the M/G ratios of 42 sodium alginates calculated from the ^{1}H solution-state NMR spectra and ^{1}H HR-MAS NMR spectra, estimated by MCR analysis of the ^{13}C CP-MAS NMR spectra and predicted from the Raman spectra using the M/G ratio values calculated from the solution-sate NMR spectra as reference values.

The results above demonstrate that ^{13}C CP-MAS NMR spectroscopy is a reliable, convenient (i.e. no sample preparation is required) and relatively rapid method for M/G ratio determinations of alginates and may serve as a good alternative to the ^{1}H solution-state NMR method. This is illustrated in Figure 42, which shows the measured versus predicted plot from a PLSR model based on the EISC-corrected Raman spectra of the 42 alginate powders using the M/G ratio values estimated from MCR analysis of the ^{13}C CP-MAS NMR spectra of the alginate powders. The cross-validated error (RMSECV) of this model is only 0.04 as opposed to the RMSECV value of 0.08 obtained when using the M/G ratio values calculated from the ^{1}H solution-state NMR spectra. This underlines that the M/G ratio values obtained from the ^{13}C CP-MAS NMR spectra are more precise than the values obtained from the ^{1}H solution-state NMR spectra. The disadvantages of the ^{13}C CP-MAS NMR method are that a relatively large sample set (in this case 42) as well as a pure mannuronate is required for the direct quantification of the M/G ratio by MCR. Alternatively, the M/G ratio can be calculated with lower precision from a single spectrum by fitting Gaussian functions. Moreover, information on

the monomer sequences is not directly obtainable. However, in PAPER V it was described how the positions of the fitted Gaussian functions were related to the monomer composition indicating the presence of unresolved structural information such as underlying resonance shifts due to higher order sequence information. Thus, comparison of these shifts with higher order sequence information obtained by ^{1}H or ^{13}C solution-state NMR spectroscopy as described by Grasdalen *et al*. (Grasdalen *et al.* 1981; Grasdalen 1983) may lead to the discovery of systematic patterns, which may be related to sequence information.

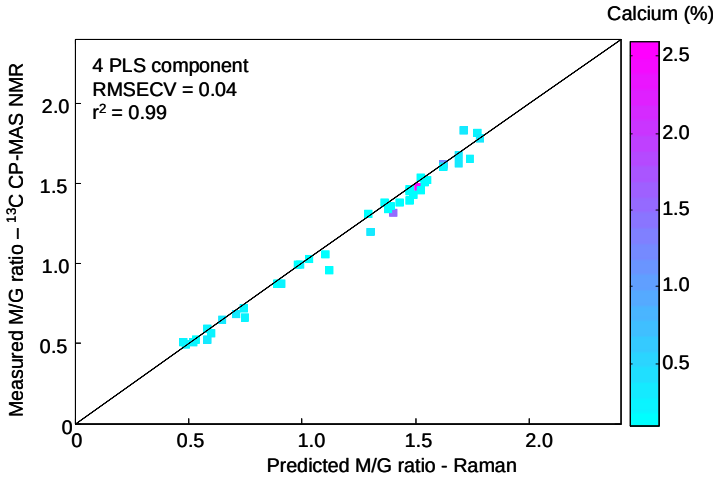

Figure 42 Measured versus predicted plot from a PLSR model based on EISC-corrected Raman spectra and M/G ratio values estimated by MCR analysis of ^{13}C CP-MAS NMR spectra of the 42 alginate powders described in Section 5.3.2.

CONCLUSIONS AND PERSPECTIVES

6

The research presented in this thesis has demonstrated the unique potentials of using vibrational spectroscopy and solid-state NMR spectroscopy in combination with advanced multivariate data analytical techniques for rapid and reliable quantitative compositional analysis of alginate powders. The methods have in common that they are non-destructive, require no sample preparation and may serve as good alternatives to the laborious techniques currently used.

The de facto standard method for measuring the alginate M/G ratio is solution-state NMR, which requires that the alginate is slightly depolymerised and dissolved in water. To perform this analysis under controlled conditions is relatively laborious and gives problems with insoluble rigid alginate regions. The method also gives problems related to water suppression techniques which was investigated in PAPER I. The results clearly showed that presaturation of the water signal can introduce undesired and uncontrolled variability to the spectra leading to erroneous quantitative results. Intensity increases of up to 25% of the signals originating from M-units were unexpectedly observed and consequently lead to an over-estimation of the M/G ratio. Since the increase was observed only for protons originating from mannuronic acid residues it was concluded that the signal increase is related to molecular geometry and flexibility differences of M- and G-blocks.

PAPER II and III demonstrate that it is possible to establish robust chemometric calibration models based on IR, Raman and NIR spectra for the prediction of the alginate M/G ratio. The prediction errors of the models of all three spectral sources investigated were comparable to that of the laborious reference method based on ^{1}H solution-state NMR. In addition, it was demonstrated that the M/G ratio values were determined with higher accuracy from the vibrational spectroscopy spectra than when calculated from the ^{1}H solution-state NMR spectra. Consequently, this study has revealed a great potential for using vibrational spectroscopy for industrial quality control of alginates. The rapid time of analysis makes the spectroscopic approach suitable for at-line and on-line quality control. This aspect is becoming more and more important due to the increasing use of alginates in biotechnological and pharmaceutical applications that demand for tailored high quality alginate products.

The high quality requirements for pharmaceutical products have lead to the recent introduction of a concept called process analytical technology (PAT) within the pharmaceutical industry. Implementation of PAT includes measuring the relevant information in real time during production for process monitoring, control and optimisation. This can involve the incoming raw materials, process streams or parameters, and/or the end product. The objective of PAT is to increase

innovation in process technology and to ensure final product quality control by remote spectroscopic monitoring. The results presented in this thesis show that vibrational spectroscopy has great potential in at- or on-line monitoring of the quality of the finished alginate product. However, when first introduced in the industry, vibrational spectroscopy can also be used to fingerprint compounds related to raw materials or process conditions quickly and non-destructively. Especially, Raman and NIR spectroscopy facilitate the possibility of on-line applications since the radiation used in these methods can be transmitted in optical fibres over long distances with practically no loss. However, the high sensitivity to fluorescence will be a major obstacle for the use of Raman sensors in the alginate industry due to the high content of fluorescent compounds in brown seaweed. For this reason NIR spectroscopy have a great potential for on-line monitoring of the alginate processes.

The potential of using solid-state NMR spectroscopy for replacement of the standard ^{1}H solution-state NMR reference method for determination of alginate M/G ratio was investigated in PAPER IV and V. Like the vibrational spectroscopy, the solid-state NMR methods only require a minimum sample preparation and should preferable be insensitive to residual calcium ions in the samples. Two solid-state NMR methods were investigated: ^{1}H HR-MAS and ^{13}C CP-MAS NMR spectroscopy. The semi-solid method ^{1}H HR-MAS NMR spectroscopy, which measures spectra of alginates soaked in D_2O, provided M/G ratio values comparable to those obtained from ^{1}H solution-state NMR spectra. However, samples with high calcium content were overestimated just like by the ^{1}H solution-state NMR method. The M/G ratios calculated from the true solid-state ^{13}C CP-MAS NMR spectra proved on the other hand insensitive to residual amounts of calcium ions. Despite the fact that the spectral resolution of ^{13}C CP-MAS NMR spectra of alginate powders was lower than ^{1}H NMR spectra of alginate solutions and semi-solids, it was shown that the information on the M/G ratio could be effectively extracted by using the appropriate chemometric tools. Actually, the ^{13}C CP-MAS NMR technique proved to be more reliable in characterising the alginate M/G ratio and consequently, it is concluded that ^{13}C CP-MAS NMR spectroscopy may serve as a good alternative to the ^{1}H solution-state NMR method.

The disadvantage of the broad and overlapping spectra obtained by ^{13}C CP-MAS NMR spectroscopy is that information on how the monomers are distributed along the chain is not immediately accessible as in the baseline separated ^{1}H solution-state NMR spectra. However, in PAPER V, a correlation between the ^{13}C CP-MAS NMR signal positions and the fraction of dimers was observed. It is thus very likely that a comparative ^{1}H and ^{13}C NMR study involving alginates of very different compositional sequence can lead to the discovery of systematic patterns, which may be related to sequence information (block structure of the alginate polymer).

REFERENCES

Alam, T. M. & Alam, M. K. (2005). Chemometric analysis of NMR spectroscopy data: A review. *Annual Reports on NMR Spectroscopy,* 54, 41-80.

Andrew, E. R., Bradbury, A. & Eades, R. G. (1958). Nuclear magnetic resonance spectra from a crystal rotated at high speed. *Nature,* 182, 1659.

Andrew, E. R., Bradbury, A. & Eades, R. G. (1959). Removal of dipolar broadening of nuclear magnetic resonance spectra of solids by specimen rotation. *Nature,* 183, 1802-1803.

Annison, G., Cheetham, N. W. H. & Couperwhite, I. (1983). Determination of the uronic acid composition of alginates by high performance liquid chromatography. *Journal of Chromatography,* 264, 137-143.

Atkins, E. D. T., Mackie, W. & Smolko, E. E. (1970). Crystalline structures of alginic acids. *Nature,* 225, 626-628.

Atkins, E. D. T., Nieduszy, I. A. & Parker, K. D. (1973a). Structural components of alginic acid. I. The crystalline structure of poly-beta-D-mannuronic acid. Results of X-ray diffraction and polarized infrared studies. *Biopolymers,* 12, 1865-1878.

Atkins, E. D. T., Nieduszy, I. A., Parker, K. D. & Smolko, E. E. (1973b). Structural components of alginic acid. II. The crystalline structure of poly-alpha-L-guluronic acid. Results of X-ray diffraction and polarized infrared studies. *Biopolymers,* 12, 1879-1887.

Baardseth, E. (1969). Some aspects of the native extracellular substance in *Fucaceae*. *Proceedings of the International Seaweed Symposium,* 6, 36-37.

Barnes, R. J., Dhanoa, M. S. & Lister, S. J. (1989). Standard normal variate transformation and de-trending of near infrared diffuse reflectance spectra. *Applied Spectroscopy,* 43, 772-777.

Black, W. A. P. (1950). The seasonal variation in weight and chemical composition of the common British *Laminariaceae*. *Journal of the Marine Biological Association of the United Kingdom,* 29, 45-72.

Bloch, F., Hansen, W. W. & Packard, M. (1946). The nuclear induction experiment. *Physical Review,* 70, 474-485.

Boyd, J. & Turvey, J. R. (1978). Structural studies of alginic acid, using a bacterial poly-alpha-L-guluronate lyase. *Carbohydrate Research,* 66, 187-194.

Bro, R. & de Jong, S. (1997). A fast non-negativity-constrained least squares algorithm. *Journal of Chemometrics,* 11, 393-401.

Brus, J. (2000). Heating of samples induced by fast magic-angle spinning. *Solid State Nuclear Magnetic Resonance,* 16, 151-160.

Bylund, D., Danielsson, R., Malmquist, G. & Markides, K. E. (2002). Chromatographic alignment by warping and dynamic programming as a pre-processing tool for PARAFAC modelling of liquid chromatography-mass spectrometry data. *Journal of Chromatography A,* 961, 237-244.

Campa, C., Oust, A., Skjåk-Bræk, G., Paulsen, B. S., Paoletti, S., Christensen, B. E. & Ballance, S. (2004). Determination of average degree of polymerisation and distribution of oligosaccharides in a partially acid-hydrolysed homopolysaccharide: A comparison of four experimental methods applied to mannuronan. *Journal of Chromatography,* 1026, 271-281.

Claridge, T. D. W. (1999). *High-Resolution NMR Techniques in Organic Chemistry*. Oxford: Elsevier Science.

Dolmatova, L., Ruckebusch, C., Dupuy, N., Huvenne, J. P. & Legrand, P. (1998). Identification of modified starches using infrared spectroscopy and artificial neural network processing. *Applied Spectroscopy,* 52, 329-338.

Donati, I., Gamini, A., Skjåk-Bræk, G., Vetere, A., Campa, C., Coslovi, A. & Paoletti, S. (2003). Determination of the diadic composition of alginate by means of circular dichroism: a fast and accurate improved method. *Carbohydrate Research,* 338, 1139-1142.

Donati, I., Holtan, S., Mørch, Y. A., Borgogna, M., Dentini, M. & Skjåk-Bræk, G. (2005). New hypothesis on the role of alternating sequences in calcium-alginate gels. *Biomacromolecules,* 6, 1031-1040.

Draget, K. I. (2001). Alginates. In G. O. Phillips & P. O. Williams (Eds) *Handbook of Hydrocolloids* (pp. 379-395). Cambridge: Woodhead Publishing Limited.

Draget, K. I., Moe, S. T., Skjåk-Bræk, G. & Smidsrød, O. (2006). Alginates. In A. M. Stephen, G. O. Phillips & P. A. Williams (Eds) *Food Polysaccharides and Their Applications* (pp. 289-334). Boca Raton: CRC Press.

Draget, K. I., Strand, B., Hartmann, M., Valla, S., Smidsrød, O. & Skjåk-Bræk, G. (2000). Ionic and acid gel formation of epimerised alginates; the effect of AlgE4. *International Journal of Biological Macromolecules,* 27, 117-122.

Dyrby, M., Petersen, R. V., Larsen, J., Rudolf, B., Nørgaard, L. & Engelsen, S. B. (2004). Towards on-line monitoring of the composition of commercial carrageenan powders. *Carbohydrate Polymers,* 57, 337-348.

Engelsen, S. B. & Nørgaard, L. (1996). Comparative vibrational spectroscopy for determination of quality parameters in amidated pectins as evaluated by chemometrics. *Carbohydrate Polymers,* 30, 9-24.

Ertesvåg, H. & Valla, S. S.-B. G. (1996). Genetics and biosynthesis of alginates. *Carbohydrates in Europe,* 14, 14-18.

Filippov, M. P. & Kohn, R. (1974). Determination of composition of alginates by infrared spectroscopic method. *Chemicke Zvesti,* 28, 817-819.

Fischer, F. G. & Dörfel, H. (1955). Die Papierchromatographische Trennung und Bestimmung der Uronsauren. *Hoppe-Seylers Zeitschrift fur Physiologische Chemie,* 301, 224-234.

Fischer, F. G. & Dørfel, H. (1955). Die Polyuronsauren der Braunalgen - (Kohlenhydrate der Algen-I). *Hoppe-Seylers Zeitschrift fur Physiologische Chemie,* 302, 186-203.

Forshed, J., Schuppe-Koistinen, I. & Jacobsson, S. P. (2003). Peak alignment of NMR signals by means of a genetic algorithm. *Analytica Chimica Acta,* 487, 189-199.

Geladi, P., Macdougall, D. & Martens, H. (1985). Linearization and scatter-correction for near-infrared reflectance spectra of meat. *Applied Spectroscopy,* 39, 491-500.

Gerstein, B. C. (1981). High-resolution NMR in solids with strong homonuclear dipolar broadening . Combined multiple pulse decoupling and magic angle spinning. *Philosophical Transactions of the Royal Society of London Series,* A299, 521-546.

Gerstein, B. C., Pembleton, R. G., Wilson, R. C. & Ryan, L. M. (1977). High-resolution NMR in randomly oriented solids with homonuclear dipolar broadening. Combined multiple pulse NMR and magic angle spinning. *Journal of Chemical Physics,* 66, 361-362.

Gidley, M. J. (1989). Molecular mechanisms underlying amylose aggregation and gelation. *Macromolecules,* 22, 351-358.

Gorin, P. A. J. & Spencer, J. F. T. (1966). Exocellular alginic acid from *Azotobacter vinelandii*. *Canadian Journal of Chemistry,* 44, 993-998.

Grant, G. T., Morris, E. R., Rees, D. A., Smith, P. J. C. & Thom, D. (1973). Biological interactions between polysaccharides and divalent cations: The egg-box model. *FEBS Letters,* 32, 195-198.

Grasdalen, H. (1983). High-field ^{1}H spectroscopy of alginate: sequential structure and linkage conformations. *Carbohydrate Research,* 118, 255-260.

Grasdalen, H., Larsen, B. & Smidsrød, O. (1979). NMR study of the composition and sequence of uronate residues in alginates. *Carbohydrate Research,* 68, 23-31.

Grasdalen, H., Larsen, B. & Smidsrød, O. (1981). ^{13}C NMR studies of monomeric composition and sequence in alginate. *Carbohydrate Research,* 89, 179-191.

Grasdalen, H., Larsen, B. & Smidsrød, O. (1977). ^{13}C NMR studies of alginate. *Carbohydrate Research,* 56, C11-C15.

Green, H. C. (1936). Fibrous alginic acid. *US Patent No.2,036,934*.

Griffiths, P. R. (2002a). Beer's law. In J. M. Chalmers & P. R. Griffiths (Eds) *Handbook of Vibrational Spectroscopy* (pp. 2225-2234). Chichester: John Wiley & Sons Ltd.

Griffiths, P. R. (2002b). Introduction to vibrational spectroscopy. In J. M. Chalmers & P. R. Griffiths (Eds) *Handbook of Vibrational Spectroscopy* (pp. 33-43). Chichester: John Wiley & Sons Ltd.

Haug, A. & Jensen, A. (1956). Seasonal variation in chemical composition of *Laminaria digitata* from different parts of the Norwegian coast. *Proceedings of the International Seaweed Symposium,* 2, 10-15.

Haug, A. & Larsen, B. (1962). Quantitative determination of uronic acid composition of alginates. *Acta Chemica Scandinavica,* 16, 1908-1918.

Haug, A. & Larsen, B. (1966). A study on the constitution of alginic acid by partial acid hydrolysis. *Proceedings of the International Seaweed Symposium,* 5, 271-277.

Haug, A., Larsen, B. & Smidsrød, O. (1966). A study of constitution of alginic acid by partial acid hydrolysis. *Acta Chemica Scandinavica,* 20, 183-199.

Haug, A., Larsen, B. & Smidsrød, O. (1967a). Studies on sequence of uronic acid residues in alginic acid. *Acta Chemica Scandinavica,* 21, 691-704.

Haug, A., Larsen, B. & Smidsrød, O. (1974). Uronic acid sequence in alginate from different sources. *Carbohydrate Research,* 32, 217-225.

Haug, A., Myklesta, S., Larsen, B. & Smidsrød, O. (1967b). Correlation between chemical structure and physical properties of alginates. *Acta Chemica Scandinavica,* 21, 768-778.

Haug, A. & Smidsrød, O. (1965). Fractionation of alginates by precipitation with calcium and magnesium ions. *Acta Chemica Scandinavica,* 19, 1221-1226.

Haug, A. & Smidsrød, O. (1967). Strontium, calcium and magnesium in brown algae. *Nature,* 215, 1167-1168.

Haug, A. & Smidsrød, O. (1970). Selectivity of some anionic polymers for divalent metal ions. *Acta Chemica Scandinavica,* 24, 843-&.

Helland, I. S., Næs, T. & Isaksson, T. (1995). Related versions of the multiplicative scatter correction method for preprocessing spectroscopic data. *Chemometrics and Intelligent Laboratory Systems,* 29, 233-241.

Hellebust, J. A. & Haug, A. (1969). Alginic acid synthesis in *Laminaria digitata* (L.) Lamour. *Proceedings of the International Seaweed Symposium,* 6, 463-471.

Herschel, W. (1800). Investigations of the powers of the prismatic colours to heat and illuminate objects; with remarks, that prove the different refrangibility of radient heat. To which is added, an inquiry into the method of viewing the sun advantageously, with telescopes or large apertures and high magnifying powers. *Phílosophical Transactions of the Royal Society of London,* 90, 255-283.

Hodgkinson, P. (2005). Heteronuclear decoupling in the NMR of solids. *Progress in Nuclear Magnetic Resonance Spectroscopy,* 46, 197-222.

Holtan, S., Zhang, Q., Strand, W. I. & Skjåk-Bræk, G. (2006). Characterization of the hydrolysis mechanism of polyalternating alginate in weak acid and assignment of the resulting MG-oligosaccharides by NMR spectroscopy and ESI-mass spectrometry. *Biomacromolecules,* 7, 2108-2121.

Hotelling, H. (1933). Analysis of complex statistical variables into principal components. *Journal of Educational Psychology,* 24, 417-441.

Hoult, D. I. (1976). Solvent peak saturation with single phase and quadrature Fourier transformation. *Journal of Magnetic Resonance,* 21, 337-347.

IFAU (2007). The Danish Food Service Sector 2007. Trends and developments in the market for quick service foods. *The Institute for Food Studies and Agroindustrial Development*.

IMR International (2001). *Quaterly Review of Food Hydrocolloids*. San Diego: IMR International. The Food Hydrocolloid Information Center.

IMR International (2009). *Quaterly Review of Food Hydrocolloids*. San Diego: IMR International. The Food Hydrocolloid Information Center.

Indergaard, M., Skjåk-Bræk, G. & Jensen, A. (1990). Studies on the influence of nutrients on the composition and structure of alginate in *Laminaria-saccharina* (L) Lamour (Laminariales, Phaeophyceae). *Botanica Marina,* 33, 277-288.

Ishikawa, M. & Nisizawa, K. (1981). Polymannuronic acid C-5 epimerase activities in several brown algae and its location in frond. *Bulletin of the Japanese Society of Scientific Fisheries,* 47, 889-893.

Knutson, C. A. & Jeanes, A. (1968). Determination of composition of uronic acid mixtures. *Analytical Biochemistry,* 24, 482-490.

Krull, L. H. & Cote, G. L. (1992). Determination of gulose and/or guluronic acid by ion chromatography and pulsed amperometric detection. *Carbohydrate Polymers,* 17, 205-207.

Lambert, J. B. & Mazzola, E. P. (2004). *Nuclear Magnetic Resonance Spectroscopy. An Introduction to Principles, Applications, and Experimental methods*. New Jersey: Pearson Education Inc.

Larsen, B. & Haug, A. (1961). Separation of uronic acids on anion exchange columns. *Acta Chemica Scandinavica,* 15, 1397-1398.

Larsen, B. & Haug, A. (1971). Biosynthesis of alginate. Part I. Composition and structure of alginate produced by *Azotobacter vinelandii* (Lipman). *Carbohydrate Research,* 17, 287-296.

Larsen, F. H., van den Berg, F. & Engelsen, S. B. (2006). An exploratory chemometric study of ^{1}H NMR spectra of table wines. *Journal of Chemometrics,* 20, 198-208.

Le Gloahec, V. C. E. & Herter, J. R. (1938). Treating seaweed. *US Patent No.2,138,551*.

Linker, A. & Jones, R. S. (1966). A new polysaccharide resembling alginic acid isolated from *Pseudomonads*. *Journal of Biological Chemistry,* 241, 3845-3851.

Mackie, W., Perez, S., Rizzo, R., Taravel, F. & Vignon, M. (1983). Aspects of the conformation of polyguluronate in the solid-state and in solution. *International Journal of Biological Macromolecules,* 5, 329-341.

Madgwick, J., Haug, A. & Larsen, B. (1973). Polymannuronic acid 5-epimerase from marine alga *Pelvetia canaliculata* (L.) Dcne. et Thur. *Acta Chemica Scandinavica,* 27, 3592-3594.

Martens, H., Nielsen, J. P. & Engelsen, S. B. (2003). Light scattering and light absorbance separated by extended multiplicative signal correction. Application to near-infrared transmission analysis of powder mixtures. *Analytical Chemistry,* 75, 394-404.

Martens, H. & Stark, E. (1991). Extended multiplicative signal correction and spectral interference subtraction: new preprocessing methods for near infrared spectroscopy. *Journal of Pharmaceutical and Biomedical Analysis,* 9, 625-635.

May, T. B. & Chakrabarty, A. M. (1994). *Pseudomonas aeruginosa*: genes and enzymes of alginate synthesis. *Trends in Microbiology,* 2, 151-157.

McClure, W. F. (2003). 204 years of near infrared technology: 1800-2003. *Journal of Near Infrared Spectroscopy,* 11, 487-518.

McCreery, R. L. (2000). *Raman Spectroscopy for Chemical Analysis*. New York: John Wiley & Sons Inc.

McHugh, D. J. (2003). *A guide to the seaweed industry. FAO Fisheries Technical Paper No.441*. Rome: FAO.

McNaught, A. D. & Wilkinson, A. (1997). *UIPAC Compendium of Chemical Terminology. The Gold Book*. Oxford: Blackwell Science.

Morris, E. R., Rees, D. A., Sanderson, G. R. & Thom, D. (1975). Conformation and circular-dichroism of uronic acid residues in glycosides and polysaccharides. *Journal of the Chemical Society,* 1418-1425.

Morris, E. R., Rees, D. A. & Thom, D. (1980). Characterization of alginate composition and block-structure by circular dichroism. *Carbohydrate Research,* 81, 305-314.

Morris, E. R., Rees, D. A., Thom, D. & Boyd, J. (1978). Chiroptical and stoichiometric evidence of a specific, primary dimerization process in alginate gelation. *Carbohydrate Research,* 66, 145-154.

Munck, L., Nørgaard, L., Engelsen, S. B., Bro, R. & Andersson, C. (1998). Chemometrics in food science - a demonstration of the feasibility of a highly exploratory, inductive evaluation strategy of fundamental scientific significance. *Chemometrics and Intelligent Laboratory Systems,* 44, 31-60.

Neiss, T. G. & Cheng, H. N. (2003). Coupled SEC-NMR analysis of alginates. *ACS Symposium Series,* 834, 382-395.

Nørager, A. C. G. (2009). *Business Development Manager, Gums & Systems, Danisco A/S. Personal communication*.

Nørgaard, L., Saudland, A., Wagner, J., Nielsen, J. P., Munck, L. & Engelsen, S. B. (2000). Interval partial least-squares regression (iPLS): A comparative chemometric study with an example from near-infrared spectroscopy. *Applied Spectroscopy,* 54, 413-419.

Nussinovitch, A. (1997). Alginates. In A. Nussinovitch (Ed) *Hydrocolloid Applications. Gum Technology in the Food and other Industries* (pp. 19-39). London: Blackie Academic and Professionals.

Onsøyen, E. (1996). Commercial applications of alginates. *Carbohydrates in Europe,* 14, 26-31.

Pauli, W. (1924). The question of the theoretical meaning of the satellite of some spectralline and their impact on the magnetic fields. *Naturwissenschaften,* 12, 741-743.

Pedersen, D. K., Martens, H., Nielsen, J. P. & Engelsen, S. B. (2002). Near infrared absorption and scattering separated by extended inverted signal correction (EISC): Analysis of near-infrared transmittance spectra of single wheat seeds. *Applied Spectroscopy,* 56, 1206-1214.

Pelletier, M. J. (1999). *Analytical Applications of Raman Spectroscopy*. Oxford: Blackwell Science Ltd.

Penman, A. & Sanderson, G. R. (1972). Method for determination of uronic acid sequence in alginates. *Carbohydrate Research,* 25, 273-282.

Pines, A., Gibby, M. G. & Waugh, J. S. (1973). Proton-enhanced NMR of dilute spins in solids. *Journal of Chemical Physics,* 59, 569-590.

Pines, A., Waugh, J. S. & Gibby, M. G. (1972). Proton-enhanced nuclear induction spectroscopy - method for high-resolution NMR of dilute spins in solids. *Journal of Chemical Physics,* 56, 1776-1777.

Piotto, M., Saudek, V. & Sklenar, V. (1992). Gradient-tailored excitation for single-quantum NMR spectroscopy of aqueous solutions. *Journal of Biomolecular Nmr,* 2, 661-665.

Purcell, E. M., Torrey, H. C. & Pound, R. V. (1946). Resonance absorption by nuclear magnetic moments in a solid. *Physical Review,* 69, 37-38.

Raiford, D. S., Fisk, C. L. & Becker, E. D. (1979). Calibration of methanol and ethylene glycol nuclear magnetic resonance thermometers. *Analytical Chemistry,* 51, 2050-2051.

Rao, V. S. R., Qasba, P. K., Balaji, P. V. & Chandrasekaran, R. (1998). *Conformation of Carbohydrates*. Amsterdam: Harwood Academic Publishers.

Renard, D., van de Velde, F. & Visschers, R. W. (2006). The gap between food gel structure, texture and perception. *Food Hydrocolloids,* 20, 423-431.

Rinnan, Å., Nørgaard, L., van den Berg, F., Thygesen, J., Bro, R. & Engelsen, S. B. (2009). Data pre-processing. In D. W. Sun (Ed) *Infrared Spectroscopy for Food Quality Analysis and Control* (pp. 29-50). New York: Academic Press.

Saito, H., Yoshioka, Y., Yokoi, M. & Yamada, J. (1990). Distinct gelation mechanism between linear and branched (1-3)-β-D-Glucans as revealed by high-resolution solid-state ^{13}C NMR. *Biopolymers,* 29, 1689-1698.

Saito, H. (2005). Conformational and dynamics aspects of polysaccharide gels by high-resolution solid-state NMR. In S. Dumitriu (Ed) *Polysaccharides. Structural diversity and functional versatility* (pp. 253-266). New York: Marcel Dekker.

Samoson, A., Tuherm, T. & Gan, Z. (2001). High-field high-speed MAS resolution enhancement in ^{1}H NMR spectroscopy of solids. *Solid State Nuclear Magnetic Resonance,* 20, 130-136.

Sanders, J. K. M. & Hunter, B. K. (1993). *Modern NMR Spectroscopy. A Guide for Chemists*. New York: Oxford University Press Inc.

Savitzky, A. & Golay, M. J. E. (1964). Smoothing and differentiation of data by simplified least squares procedures. *Analytical Chemistry,* 36, 1627-1639.

Seefeldt, H. F., Larsen, F. H., Viereck, N., Wollenweber, B. & Engelsen, S. B. (2008). Bulk carbohydrate grain filling of barley β-glucan mutants studied by ^{1}H HR MAS NMR. *Cereal Chemistry,* 85, 571-577.

Sheppard, S. J. (2002). The historical development of experimental techniques in vibrational spectroscopy. In J. M. Chalmers & P. R. Griffiths (Eds) *Handbook of Vibrational Spectroscopy* (pp. 1-32). Chichester: Wiley & Sons Ltd.

Shinohara, M., Kamono, H., Aoyama, T., Bando, H. & Nishizawa, M. (1999). Relationships between guluronate contents in alginates determined by ^{1}H-NMR spectroscopy and their average molecular weights. *Fisheries Science,* 65, 909-913.

Siddiqui, I. R. (1978). Polarimetric procedure for determining mannuronic acid guluronic acid ratios in alginates. *Carbohydrate Research,* 67, 289-293.

Sime, W. J. (1990). Alginates. In P. Harris (Ed) *Food Gels* (pp. 53-78). New York: Elsevier Science Publishers Ltd.

Skjåk-Bræk, G. & Espevik, T. (1996). Application of alginate gels in biotechnology and medicine. *Carbohydrates in Europe,* 14, 19-25.

Skjåkbræk, G., Grasdalen, H. & Larsen, B. (1986). Monomer sequence and acetylation pattern in some bacterial alginates. *Carbohydrate Research,* 154, 239-250.

Skov, T., van den Berg, F., Tomasi, G. & Bro, R. (2006). Automated alignment of chromatographic data. *Journal of Chemometrics,* 20, 484-497.

Smidsrød, O. (1974). Molecular basis for some physical properties of alginates in the gel state. *Faraday Discussions of the Chemical Society,* 57, 263-274.

Smidsrød, O., Glover, R. M. & Whittington, S. G. (1973). The relative extension of alginates having different chemical composition. *Carbohydrate Research,* 27, 107-118.

Smidsrød, O. & Haug, A. (1968). Dependence upon uronic acid composition of some ion-exchange properties of alginates. *Acta Chemica Scandinavica,* 22, 1989-1997.

Smidsrød, O. & Haug, A. (1972). Dependence upon gel-sol state of ion-exchange properties of alginates. *Acta Chemica Scandinavica,* 26, 2063-2074.

Stanford, E. C. C. (1881). Manufacture of useful products from seaweeds. *British patent no.142*.

Steginsky, C. A., Beale, J. M., Floss, H. G. & Mayer, R. M. (1992). Structural determination of alginic acid and the effects of calcium-binding as determined by high-field NMR. *Carbohydrate Research,* 225, 11-26.

Stockton, B., Evans, L. V., Morris, E. R., Powell, D. A. & Rees, D. A. (1980). Alginate block structure in *Laminaria digitata:* Implications for holdfast attachment. *Botanica Marina,* 23, 563-567.

Stokke, B. T., Draget, K. I., Smidsrød, O., Yuguchi, Y., Urakawa, H. & Kajiwara, K. (2000). Small-angle X-ray scattering and rheological characterization of alginate gels. 1. Ca-alginate gels. *Macromolecules,* 33, 1853-1863.

Stokke, B. T., Smidsrød, O., Bruheim, P. & Skjåk-Bræk, G. (1991). Distribution of uronate residues in alginate chains in relation to alginate gelling properties. *Macromolecules,* 24, 4637-4645.

Tauler, R. (1995). Multivariate curve resolution applied to second order data. *Chemometrics and Intelligent Laboratory Systems,* 30, 133-146.

This, H. (2007). *Kitchen mysteries - revealing the science of cooking*. New York: Columbia University Press.

Thorøe-Hansen, K. (2009). *Vice President, Commercial Gums & Systems, Danisco A/S. Personal communication*.

Tomasi, G., van den Berg, F. & Andersson, C. (2004). Correlation optimized warping and dynamic time warping as preprocessing methods for chromatographic data. *Journal of Chemometrics,* 18, 231-241.

Vadas, L., Prihar, H. S., Pugashetti, B. K. & Feingold, D. S. (1981). A gas chromatographic method for the quantitative determination of hexuronic acids in alginic acid. *Analytical Biochemistry,* 114, 294-298.

van Geet, A. L. (1970). Calibration of methanol nuclear magnetic resonance thermometer at low temperature. *Analytical Chemistry,* 42, 679-680.

Vela, G. R. (1974). Survival of *Azotobacter* in dry soil. *Applied Microbiology,* 28, 77-79.

Veselkov, K. A., Lindon, J. C., Ebbels, T. M. D., Crockford, D., Volynkin, V. V., Holmes, E., Davies, D. B. & Nicholson, J. K. (2009). Recursive segment-wise peak alignment of biological ^{1}H NMR spectra for improved metabolic biomarker recovery. *Analytical Chemistry,* 81, 56-66.

Viereck, N., Nørgaard, L., Bro, R. & Engelsen, S. B. (2006). Chemometric analysis of NMR data. In G. A. Webb (Ed) *Modern Magnetic resonance* (pp. 1811-1821). Berlin: Springer.

Vogels, J. T. W. E., Tas, A. C., Venekamp, J. & Van der Greef, J. (1996). Partial linear fit: A new NMR spectroscopy preprocessing tool for pattern recognition applications. *Journal of Chemometrics,* 10, 425-438.

Winning, H., Viereck, N., Salomonsen, T., Larsen, J. & Engelsen, S. B. (2009a). Quantification of blockiness in pectins - A comparative study using vibrational spectroscopy and chemometrics. *Carbohydrate Research,* In press.

Winning, H., Viereck, N., Wollenweber, B., Larsen, F. H., Jacobsen, S., Søndergaard, I. & Engelsen, S. B. (2009b). Exploring abiotic stress on asynchronous protein metabolism in single kernels of wheat studied by NMR spectroscopy and chemometrics. *Journal of Experimental Botany,* 60, 291-300.

Wold, S., Martens, H. & Wold, H. (1983). The multivariate calibration problem in chemistry solved by the PLS method. *Lecture Notes in Mathematics,* 973, 286-293.

World's 50 best restaurants (2009). http://www.theworlds50best.com. *Retrieved on 22 April 2009*.

PAPER I

The quantitative impact of water suppression on NMR spectra for compositional analysis of alginates

T. Salomonsen, H.M. Jensen, F.H. Larsen & S.B. Engelsen

Magnetic Resonance in Food Science. Challenges in a Changing World

Cambridge, RSC Publishing, (2009), pp. 12-19

Eds. M. Guðjónsdóttir, P.S. Belton & G.A. Webb

Magnetic Resonance in Food Science
Challenges in a Changing World

Edited by

María Guðjónsdóttir
Matvælarannsóknir Íslands, Reykjavík, Iceland

Peter Belton
School of Chemical Sciences and Pharmacy, University of East Anglia, Norwich, UK

Graham Webb
c/o Royal Society of Chemistry, Burlington House , Piccadilly, London, UK

RSC Publishing

The proceedings of the 9th International Conference on the Applications of Magnetic Resonance in Food Science: Challenges in a Changing World held in Reykjavik, Iceland on 15-17 September 2008.

Special Publication No. 319

ISBN: 978-0-85404-117-6

A catalogue record for this book is available from the British Library

Published by The Royal Society of Chemistry,
Thomas Graham House, Science Park, Milton Road,
Cambridge CB4 0WF, UK

Registered Charity Number 207890

For further information see our web site at www.rsc.org

THE QUANTITATIVE IMPACT OF WATER SUPPRESSION ON NMR SPECTRA FOR COMPOSITIONAL ANALYSIS OF ALGINATES

T. Salomonsen[1,2], H.M. Jensen[1], F.H. Larsen[2] and S.B. Engelsen[2]

[1] Danisco A/S, Edwin Rahrs Vej 38, 8220 Brabrand, Denmark
[2] Department of Food Science, Faculty of Life Sciences, University of Copenhagen, Rolighedsvej 30, 1958 Frederiksberg C, Denmark

1 INTRODUCTION

Solution-state ^{1}H nuclear magnetic resonance (NMR) spectroscopy is an effective tool in the compositional analysis of alginates,[1,2] which are binary copolymers of (1-4) linked β-D-mannuronic acid (M) and α-L-guluronic acid (G) extracted from brown seaweeds. The M/G ratio, which can be determined by NMR, varies according to season, age of population, species and geographic location[3-5] and is closely related to the application of the alginates as thickeners, stabilisers and gelling agents in the food and pharmaceutical industries.[6-8]

Solutions of alginates, in the concentrations required for a good signal-to-noise in the ^{1}H NMR spectra, are generally too viscous to give well-resolved spectra. Therefore, the viscosity is typically reduced by lowering the molecular weight prior to the NMR analysis. In addition, the spectra are recorded at 80-90 ºC in order to reduce the viscosity further and to shift the water resonance away from the anomeric region, which contains the signals used in the calculations of the M/G ratio.

The magnitude of the water resonance is normally several orders of magnitude higher than the other signals in the spectra due to residual water in the alginates. Thus, it can be an advantage to apply water suppression, which allows one to recover signals that overlap the broad baseline of the intense water resonance. However, water suppression can possibly affect the intensity of other signals in the spectra, which may lead to significant errors in the quantitative analysis.

In a previous NMR study of alginates, water suppression was found to alter the intensities of the signals of interest[9] whereas other studies concluded that water suppression had no effect on the intensities of the signals near the water resonance.[10] In this study we set out to investigate how some of the common water suppression techniques influence the ^{1}H NMR spectra of alginates in solutions and thereby the calculated M/G ratios.

2 MATERIALS AND METHODS

2.1 The Samples

A total of 40 different commercial sodium alginates were kindly provided by Danisco A/S (Brabrand, Denmark). The average molecular weights (M_w) of the alginates were reduced from ~300 kDa to ~30 kDa by partial acid hydrolysis[1] in order to reduce the viscosity of the alginate solutions for the NMR analysis. The samples were prepared for NMR analysis by dissolving the hydrolysed alginates in D_2O (1% (w/v)) followed by neutralisation (pH 7). 3-(trimethylsilyl)propionic acid-d_4 sodium salt (TSP-d4) was added as chemical shift reference. The solutions (550 µl) were filtrated through Whatman 13 mm syringe filters (pore size 0.45 µm) into 5 mm NMR tubes.

2.2 NMR Data Acquisition

^{1}H NMR spectra of the samples were collected on a Bruker Avance^{TM} 400 spectrometer (Bruker Biospin Gmbh, Rheinstetten, Germany) operating at 400.13 MHz for protons and equipped with a 5 mm broad band inverse probe. Four unique NMR spectra of each sample were acquired using the pulse sequences schematically depicted in Figure 1. Spectra without water suppression were recorded with a single 90º pulse (Figure 1a) and spectra with water suppression were recorded using three different water suppression techniques: conventional presaturation (Figure 1b), presaturation followed by a 90º composite pulse (Figure 1c) and NOESY-presaturation (Figure 1d). The experiments will be denoted *zg*, *zgpr*, *zgcppr* and *noesypr1d* (Bruker notation), respectively. In the *noesypr1d* experiment, saturation was also employed during the NOESY mixing period, which was set to 150 ms.

All spectra were acquired using a relaxation delay of 2 s, a spectral width of 8278 Hz, an acquisition time of 3.96 s and a sample temperature of 90 °C. All acquisitions were initiated with two dummy scans followed by 16 scans. All *zg* spectra were recorded with one receiver gain and all water-suppressed spectra with another (4.5 times higher).

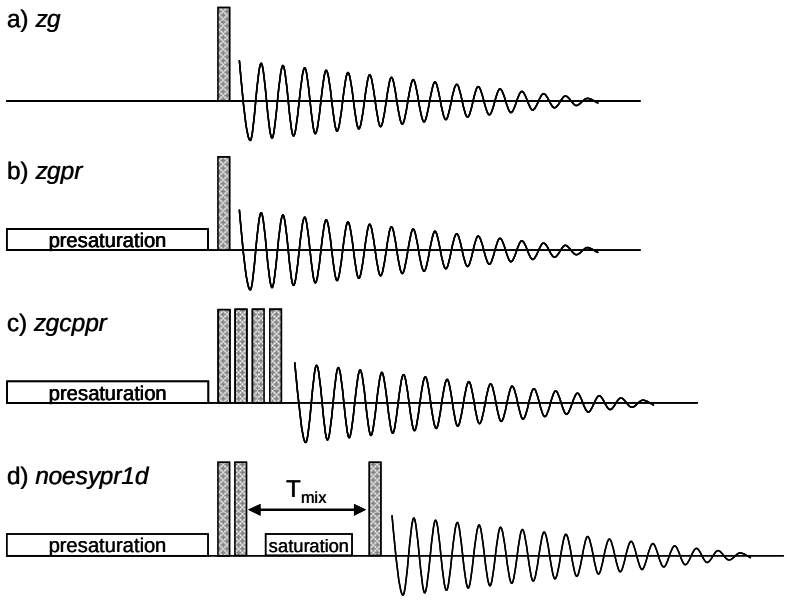

Figure 1 *Schematic drawing of the four different pulse sequences used in the study*

The FIDs were zero filled to 64K data points and apodized by a 1.0 Hz exponential line broadening before Fourier transformation. The resulting spectra were individually phased and baseline corrected using the Bruker TOPSPIN 1.3 software (Bruker Biospin Gmbh, Rheinstetten, Germany). All spectra were referenced to TSP-d4 at 0.000 ppm.

2.3 FT-Raman Spectroscopy

Raman spectra were collected on a Perkin Elmer System NIR FT-Raman interferometer (Perkin Elmer Instruments, Waltham, Massachusetts, USA) using 1064 nm laser excitation with a power of 200 mW as described by Salomonsen *et al.*[11] The range 650-1800 cm^{-1} was used in the data analysis.

2.4 M/G Ratio Calculations

The M/G ratio was calculated using the relative areas of the signals in the anomeric region as described by Grasdalen *et al.*[1,2] The integration limits applied in the calculations of the areas of the signals denoted A, B and C in the anomeric region (Figure 2) were 4.96-5.18 ppm (H-1 of G at 5.07 ppm), 4.57-4.82 ppm (H-5 of G at 4.76 and 4.72 ppm, H-1 of M at 4.70 and 4.68) and 4.38-4.55 ppm (H-5 of G at 4.46 ppm), respectively. Assignments were made according to Grasdalen *et al.*[2]

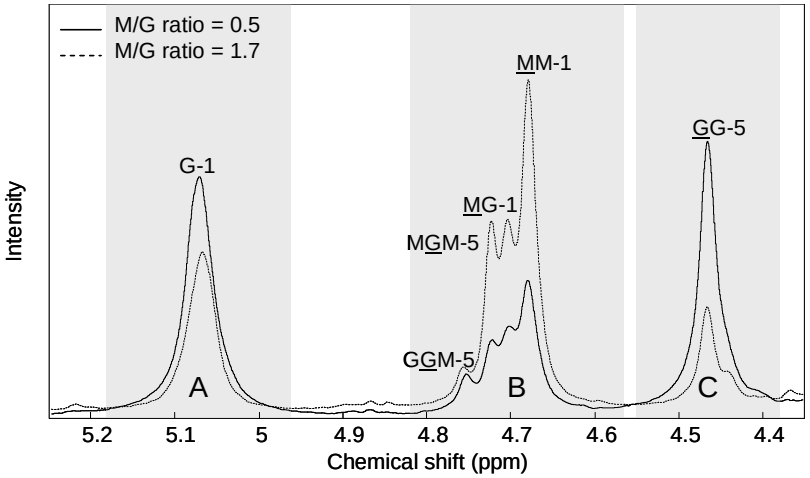

Figure 2 *^{1}H NMR spectra of two hydrolysed alginates in solution (1 % (w/v)). The M/G ratios are calculated from the relative areas of signal A, B and C. The integration limits are indicated by the grey boxes.*

2.5 Partial Least Squares Regression

Linear models between the multivariate Raman spectra and the M/G ratio values calculated from the four sets of NMR spectra were established using partial least squares regression (PLSR)[12]. The Raman spectra were transformed with extended inverted scatter correction (EISC)[13,14] and mean centred prior to PLSR model development. The PLSR models were validated using segmented cross-validation (6 segments). The PLSR analyses were performed using LatentiX version 2.0 (Latent5, Copenhagen, Denmark, http://www.latentix.com), whereas EISC pre-processing was performed in MatLab 7.4 (Mathworks, Natick, Massachusetts, USA) using the command line EMSC/EISC toolbox (http://www.models.life.ku.dk).

3 RESULTS AND DISCUSSION

The M/G ratio of alginate is traditionally determined from the relative intensities of the signals in the anomeric region in the ^{1}H NMR spectra of mildly hydrolysed alginate in solution. It is therefore highly relevant to establish if water suppression influence the quantitative analysis. We have evaluated the impact of three commonly used water suppression techniques, namely conventional presaturation (*zgpr*), presaturation followed by a composite pulse (*zgcppr*) and NOESY-presaturation (*noesypr1d*). The carbohydrate region (3.4-5.3 ppm) of the spectra of an alginate sample acquired without water suppression (*zg*) and with the three different water suppression techniques is shown in Figure 3. The relative areas of the three signals in the anomeric region as well as the M/G ratio calculated from these are indicated at each spectrum.

The intensity of the water signals (4.18 ppm) in all three water suppression experiments is reduced significantly compared to the intensity of the signal in the *zg* experiment. A 98% reduction is observed in the *zgpr* and *zgcppr* experiment and an almost 100% reduction is observed in the *noesypr1d* experiment. Thus, the *noesypr1d* experiment gives the most efficient suppression. The residual water signal in the *zgcppr* spectra was slightly narrower than in the *zgpr* spectra. This is due the composite 90^o pulse, which results in a more accurate 90^o pulse by compensating for inhomogeneities in the applied B_1 field.

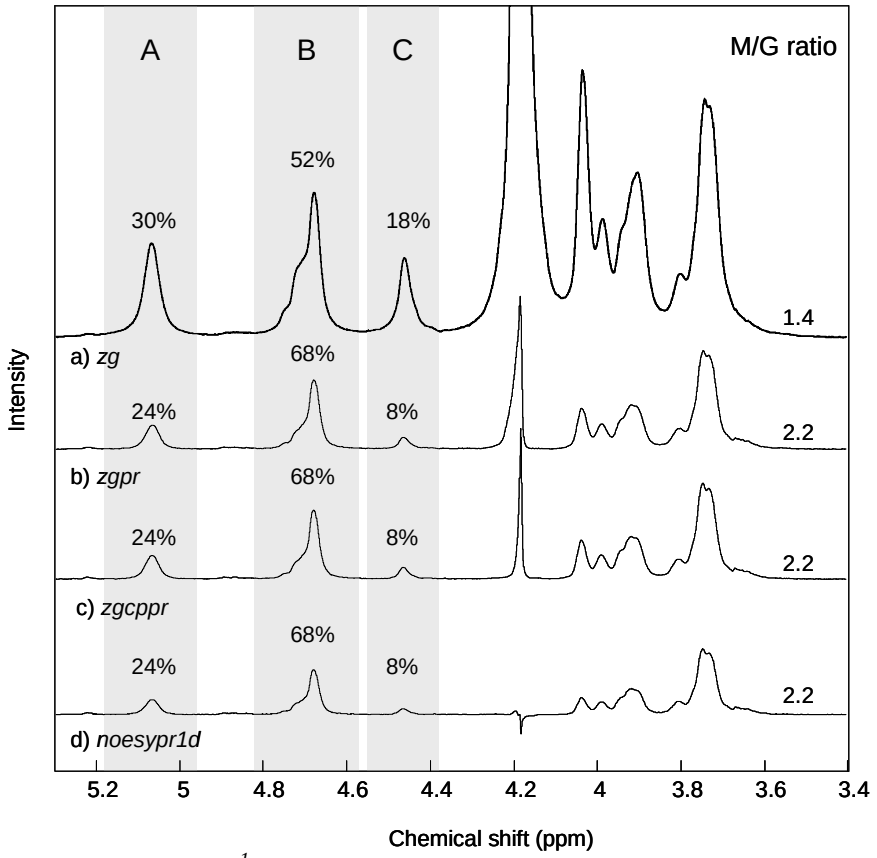

Figure 3 *Stack plot of the ^{1}H NMR spectra (carbohydrate region) of an alginate sample acquired without (a) and with water suppression (b, c and d). The zg spectrum is vertically scaled by a factor of 4.5 (receiver gain adjustment). The relative areas of the signals in the anomeric region (A, B and C) and the M/G ratios calculated from these are indicated at each spectrum.*

The four spectra presented in Figure 3 were vertically scaled such that the intensities of the TSP-d4 signals in the four spectra were equal. In reality this only required vertical scaling of the *zg* spectrum by a factor of 4.5 to compensate for the lower receiver gain used when compared to the water-suppressed spectra. The intensities of the carbohydrate signals, however, were generally higher in the *zg* spectra than in the water-suppressed spectra. On the other hand, when comparing the intensities of the carbohydrate signals in the water-suppressed spectra, the *zgpr* and *zgcppr* spectra were found to match perfectly when superimposed, whereas the intensities of most of the carbohydrate signals in the *noesypr1d* spectrum were 1.6 times lower than in the *zgpr* and *zgcppr* spectra. This effect is most likely due to relaxation during the mixing time. In the *noesypr1d* spectra the signals close to the water resonance were 2.0-2.3 times lower than the same signals in the *zgpr* and *zgcppr* experiments. This indicates that the *noesypr1d* pulse sequence affects the signals near the water resonance to a higher extend than the *zgpr* and *zgcppr* experiments.

The relative intensities of the signals in the anomeric region (A, B and C) and thereby also the calculated M/G ratios are clearly affected by the water suppression. The M/G ratios calculated from the water-suppressed spectra were all higher (2.2) than the M/G ratios calculated from the non-water-suppressed spectra (1.4). The same trend was observed for all other samples. However, the relative difference was not the same for all samples. The area of signal A, B and C in percent of the total area of the three peaks were 30%, 52% and 18% (1.7:2.9:1.0), respectively, in the *zg* spectra and 24%, 68% and 8% (3.0:8.5:1.0), respectively, in the three water-suppressed spectra. Obviously, the relative intensities of the three signals are affected in the same way by the different water suppression techniques. Generally, the assumption would be that signals closest to the water signal were subjected to the greatest influence from the water suppression, but in this case signal B is significantly enhanced relative to the other signals.

In order to investigate if the receiver gain influenced the relative intensities of the signals in the anomeric region, we recorded a *zgpr* spectrum with a receiver gain optimised for the *zg* experiment. This resulted in overall lower signal intensities, but the relative intensities and thereby the calculated M/G ratio remained the same as with the optimised receiver gain. Moreover, it was observed that the relaxation time and thereby the presaturation time had no significant impact on the results. Comparing spectra acquired with relaxation times of 2 and 20 s, resulted in spectra with equal intensities.

For a better demonstration of the differences observed between spectra with and without water suppression, the *zg* and *zgpr* spectra of two different alginates are shown in Figure 4. The intensities of signal A (H-1 of G) in the *zgpr* spectra have been scaled up to match the intensity of the same signal in the *zg* spectra to reveal the relative differences. Signal A was chosen for scaling since it is furthest away from the water resonance and therefore less likely to be influenced by the water suppression. The spectra in Figure 4 shows that when keeping the intensity of signal A constant an increase in signal B and a decrease in signal C is observed. Moreover, the intensity of the signals just upfield the water resonance decreases, whereas an increase of the signals around 3.7-3.8 ppm, which have been assigned to H-3, H-4 and H-5 of M,[7] is observed. Investigating the relative difference between the *zg* and *zgpr* spectra of all samples showed that water suppression resulted in a 27-44% decrease of the signals near the water resonance (4.38-4.55 ppm and 3.96-4.07 ppm) and a 2-25% increase of the signals originating from M (4.68-4.70 ppm and 3.67-3.83 ppm). All changes are given relative to the H-1 resonance of G. The signal increase for the M protons was unexpected and we are currently investigating this phenomenon in greater detail to understand the underlying mechanisms.

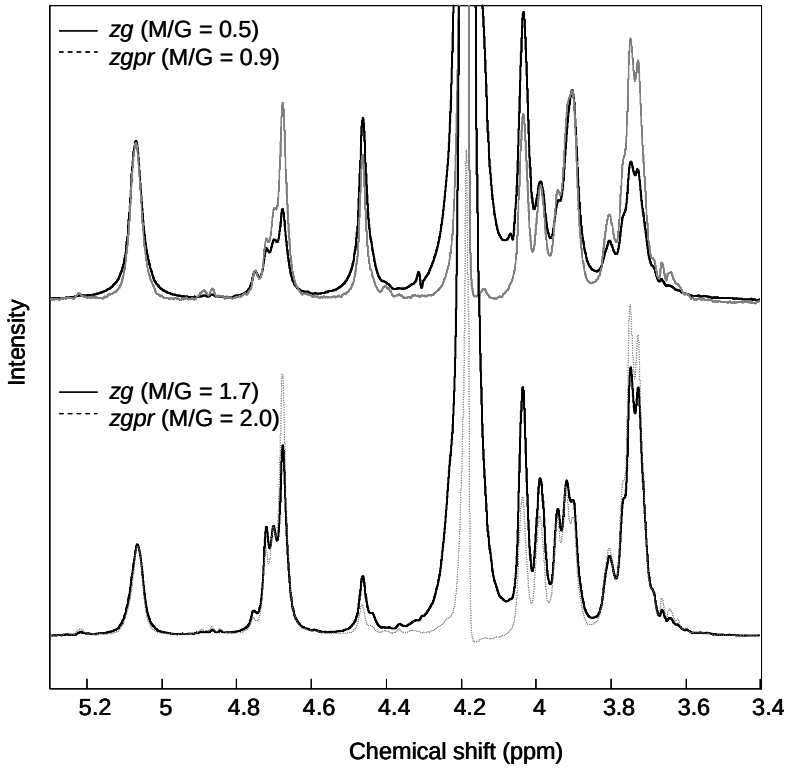

Figure 4 *^{1}H NMR spectra (carbohydrate region) of two alginate samples with high and low M/G ratio recorded without (zg) and with (zgpr) water suppression. Higher M/G ratios are obtained from the zgpr spectra than from the zg spectra.*

Since the increase is observed only for the protons originating from M (and especially H-1 of M sitting next to another M (4.68 ppm)) it is reasonable to assume that the signal increase is related to the molecular geometry and flexibility differences of M- and G-blocks. M and G are distributed along the linear alginate polymer in either blocks of M, blocks of G or as alternating MG units.[15] The geometries of the M-, G- and MG-blocks are related to the particular shapes of the monomers and their mode of linkage in the polymer. The M-blocks have an extended ribbon shape and are flexible,[16] the G-blocks are buckled and stiff[17] and the MG-block regions are of intermediate stiffness. Thus, a plausible explanation for the observed signal increase, may be that the M-blocks interact with water to a higher extend than the G-blocks due to their more linear structure and higher flexibility. Water suppression can potentially disturb this interaction and therefore induce changes for protons in the M-blocks.

Figure 5 shows the M/G ratios of the 40 alginates calculated form the four sets of NMR spectra plotted against each other in order to illustrate how they correlate. The best correlation was found between the M/G ratios calculated from the *zgpr* and *zgcppr* spectra (Figure 5d). This was expected since these spectra were practically identical when comparing within each sample. The M/G ratios calculated from the *noesypr1d* correlate fairly well with the values from the *zgpr* and *zgcppr* experiments with exception of one outlying sample (Figure 5e and f). The correlation coefficients between the M/G ratios calculated from the *zg* spectra and the *zgpr*/*zgcppr* and *noesypr1d* spectra were 0.90 (Figure 5a and b) and 0.88 (Figure 5c), respectively. It should be noted that samples with high M/G ratio deviate more from the target line than samples with low M/G ratio, indicating that samples with high content of M are influenced more by the water suppression than samples with low content of M.

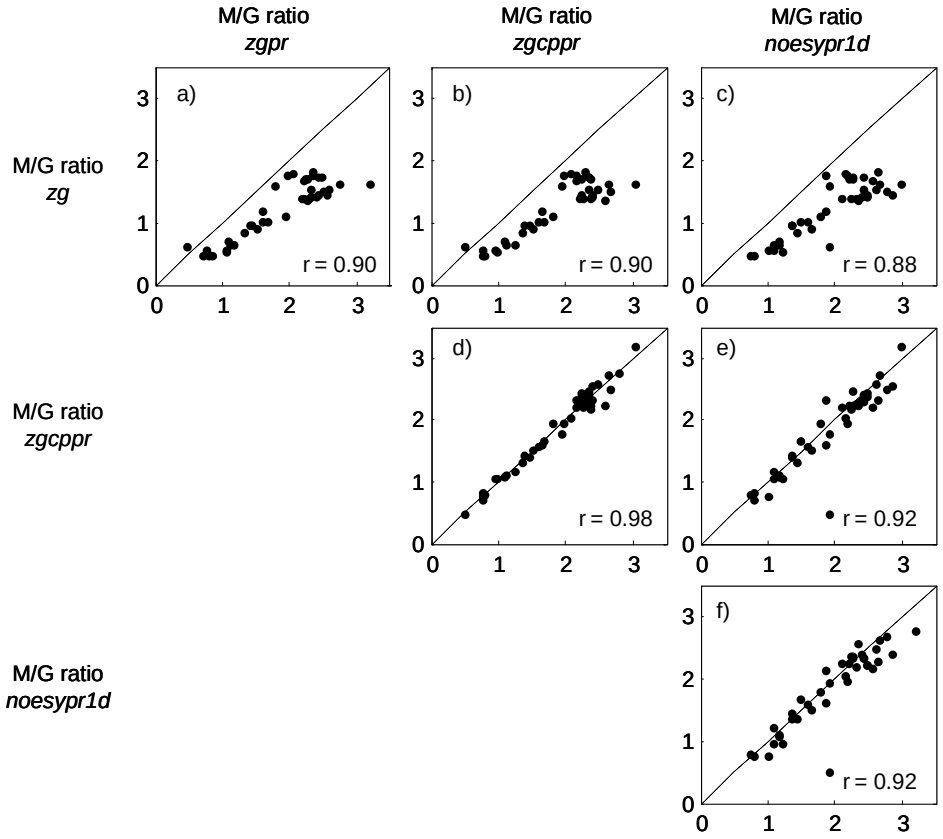

Figure 5 *Scatter plots of M/G ratios calculated from the four different sets of NMR spectra. The correlation coefficients are given in each plot.*

In a previous study[11] we have shown that the M/G ratio of alginates can be determined from Raman spectra of intact alginate powders using PLSR regression and M/G ratios from ^{1}H NMR spectra as response values. In order to elucidate if the M/G ratio values obtained by the non-water-suppressed spectra result in more reliable and consistent M/G ratio values than the values obtained from the water-suppressed spectra, PLSR models between Raman spectra and the M/G ratios calculated from the four sets of data were established. It is assumed that the solid-state Raman spectra, which are measured on a much faster time scale than the NMR spectra, are independent of water interferences and of biopolymer dynamics and therefore will provide a good measure of the validity of the M/G ratios established from the different solution-state NMR experiments. The M/G ratios calculated from the *zg* and *zgpr* spectra versus the M/G ratio predicted from the Raman spectra (using the *zg* and *zgpr* values as reference values, respectively) are shown in Figure 6a and b, respectively. As evident from Figure 6, the model established between the M/G ratios calculated from the *zg* spectra and the Raman spectra significantly improved compared to the model based on the M/G ratios calculated from the *zgpr* spectra. The correlation coefficient was improved from 0.82 to 0.97 (r =0.97) for the non-water-suppressed NMR measurements and the prediction error was reduced from RMSECV= 0.28 to RMSECV=0.08. The same tendency was observed in the models based on the M/G ratios from the *zgcppr* and *noesypr1d* spectra.

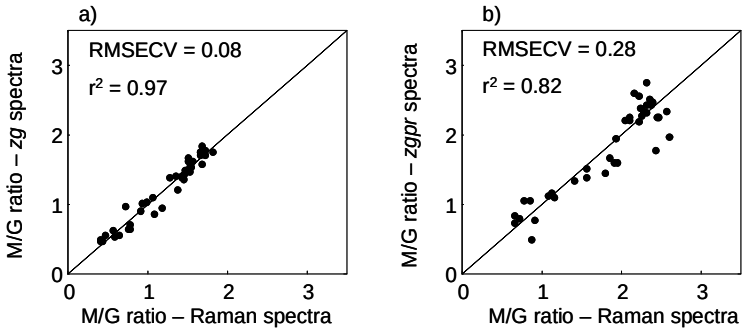

Figure 6 *Measured versus predicted plots from the PLSR analyses. M/G ratio measured by NMR without (a) and with (b) water suppression (zgpr) versus the M/G ratio predicted from the Raman spectra. RMSECV = root mean square error of cross validation. Both models are based on two PLS components.*

4 CONCLUSIONS

From this work, it is clear that the application of water suppression techniques in the NMR analysis of alginates can introduce undesired and uncontrolled variability to the spectra leading to erroneous quantitative results. Our results indicate that it was mainly resonances originating from M-units that were prone to intensity changes. This effect may be due to a closer water association in the M-blocks than the G-blocks.

References

1 H. Grasdalen, B. Larsen and O. Smidsrød, *Carbohydr. Res.*, 1979, **68**, 23.
2 H. Grasdalen, *Carbohydrate Research*, 1983, **118**, 255.
3 A. Haug, B. Larsen and O. Smidsrød, *Carbohydr. Res.*, 1974, **32**, 217.
4 M. Indergaard, G. Skjåk-Bræk and A. Jensen, *Botanica Marina*, 1990, **33**, 277.
5 B. Stockton, L.V. Evans, E.R. Morris, D.A. Powell and D.A. Rees, *Botanica Marina*, 1980, **23**, 563.
6 A. Haug, S. Myklesta, B. Larsen and O. Smidsrød, *Acta Chem. Scand.*, 1967, **21**, 768.
7 C.A. Steginsky, J.M. Beale, H.G. Floss and R.M. Mayer, *Carbohydr. Res.*, 1992, **225**, 11.
8 B.T. Stokke, O. Smidsrød, P. Bruheim and G. Skjåk-Bræk, *Macromolecules*, 1991, **24**, 4637.
9 T.G. Neiss and H.N. Cheng, *ACS Symposium Series*, 2003, **834**, 382.
10 M. Shinohara, H. Kamono, T. Aoyama, H. Bando and M. Nishizawa, *Fisheries Science*, 1999, **65**, 909.
11 T. Salomonsen, H.M. Jensen, D. Stenbæk and S.B. Engelsen, *Carbohydr. Polym.*, 2008, **72**, 730.
12 S. Wold, H. Martens and H. Wold, *Lect. Notes Math.*, 1983, **973**, 286.
13 H. Martens, J.P. Nielsen and S.B. Engelsen, *Anal. Chem.*, 2003, **75**, 394.
14 D.K. Pedersen, H. Martens, J.P. Nielsen and S.B. Engelsen, *Appl. Spectrosc.*, 2002, **56**, 1206.
15 A. Haug, B. Larsen and O. Smidsrød, *Acta Chem. Scand.*, 1966, **20**, 183.
16 E.D.T. Atkins, I.A. Nieduszy and K.D. Parker, *Biopolymers*, 1973, **12**, 1865.
17 E.D.T. Atkins, I.A. Nieduszy, K.D. Parker and E.E. Smolko, *Biopolymers*, 1973, **12**, 1879.

PAPER II

Chemometric prediction of alginate monomer composition. A comparative spectroscopic study using IR, Raman, NIR and NMR

T. Salomonsen, H.M. Jensen, D. Stenbæk & S.B. Engelsen

Carbohydrate Polymers, 72, (2008), 730-739

Available online at www.sciencedirect.com
ScienceDirect
Carbohydrate Polymers 72 (2008) 730–739
Carbohydrate Polymers
www.elsevier.com/locate/carbpol

Chemometric prediction of alginate monomer composition: A comparative spectroscopic study using IR, Raman, NIR and NMR

Tina Salomonsen [a,b,*], Henrik Max Jensen [b], Dorthe Stenbæk [b], Søren Balling Engelsen [a]

[a] *University of Copenhagen, Faculty of Life Sciences, Department of Food Science, Quality & Technology, Rolighedsvej 30, 1958 Frederiksberg C, Denmark*
[b] *Danisco A/S, Edwin Rahrs Vej 38, 8220 Brabrand, Denmark*

Received 14 August 2007; received in revised form 23 October 2007; accepted 25 October 2007
Available online 7 November 2007

Abstract

The potential of using infrared (IR), Raman and near infrared (NIR) spectroscopy combined with chemometrics for reliable and rapid determination of the ratio of mannuronic and guluronic acid (M/G ratio) in commercial sodium alginate powders has been investigated. The reference method for quantification of the M/G ratio was solution-state ^{1}H nuclear magnetic resonance (NMR) spectroscopy. For a set of 100 commercial alginate powders with a M/G ratio range of 0.5–2.1 quantitative calibrations using partial least squares regression (PLSR) were developed and compared for the three spectroscopic methods. All three spectroscopic methods yielded models with prediction errors (RMSEP) of 0.08 and correlation coefficients between 0.96 and 0.97. However, the model based on extended inverted signal corrected (EISC) Raman spectra stood out by only using one PLS component for the prediction. The results are comparable to that of the experimental error of the reference method estimated to be between 0.01 and 0.08.

Keywords: Alginate; Spectroscopy; Chemometrics; NMR; IR; Raman; NIR

1. Introduction

Commercial alginates are extracted from brown seaweed (*Phaeophyceae*) and used as thickeners, stabilisers and gelling agents in the food and pharmaceutical industries. Chemically, they are a family of binary copolymers of (1–4) linked β-D-mannuronic acid (M) and its C-5 epimer α-L-guluronic acid (G). Alginates are typically described by their M/G ratio, distribution of M- and G-units along the chain and average molecular weight, since these parameters are closely related to the functionality of the alginates, i.e. solubility, interaction with metals, gel properties and viscosity (Haug, Myklesta, Larsen, & Smidsrød, 1967; Steginsky, Beale, Floss, & Mayer, 1992; Stokke, Smidsrød, Bruheim, & Skjåk-Bræk, 1991). The composition and sequential structure and thereby also the functionality of alginates vary according to season, age of population, species and geographic location (Haug, Larsen, & Smidsrød, 1974; Indergaard, Skjåk-Bræk, & Jensen, 1990; Stockton, Evans, Morris, Powell, & Rees, 1980). Because of these variations within the different alginate types, it is of great importance for the alginate industry to obtain detailed knowledge about the composition of its products in order to design the functionality of the final product.

Solution-state nuclear magnetic resonance (NMR) spectroscopy is a highly effective tool in compositional and structural analysis of alginates (Grasdalen, 1983; Grasdalen, Larsen, & Smidsrød, 1977, 1979, 1981; Penman & Sanderson, 1972). However, at the concentrations required for a good signal-to-noise ratio in the NMR analysis, alginate solutions are too viscous to give well-resolved spectra even

* Corresponding author. Address: University of Copenhagen, Faculty of Life Sciences, Department of Food Science, Quality & Technology, Rolighedsvej 30, 1958 Frederiksberg C, Denmark. Tel.: +45 8943 5285/+45 3533 3510; fax: +45 8925 1077.
E-mail addresses: tina.salomonsen@danisco.com, tisa@life.ku.dk (T. Salomonsen).

0144-8617/$ - see front matter © 2007 Elsevier Ltd. All rights reserved.
doi:10.1016/j.carbpol.2007.10.022

at elevated temperatures (up to 90 °C). To reduce the viscosity, it is necessary to partially degrade the alginate chain by a mild acid hydrolysis prior to NMR analysis. This hydrolysis is relatively time-consuming and labour intensive. Hence, solution-state NMR of alginates is rather elaborate and time-consuming and certainly not suitable for at- or on-line monitoring of alginate composition. Thus, development of a faster and simpler method for characterisation of the alginate composition would be beneficial.

Vibrational spectroscopy, e.g. infrared (IR), Raman and near infrared (NIR) spectroscopy are, in combination with multivariate data analysis (chemometrics), useful analytical tools that can reveal detailed information concerning the composition and properties of material at a molecular level. Some of the advantages of these techniques compared to solution-state NMR are that they are rapid, non-destructive, easy to operate and in most cases require no sample preparation. Because of these qualities all three vibrational spectroscopic techniques are applicable for at-line analysis. However, only Raman and NIR spectroscopy can be implemented directly on the production line using optical quartz fibres for on-line analysis.

IR spectroscopy has proven useful for quantitative estimation of the M/G ratio of alginates (Filippov & Kohn, 1974; Mackie, 1971; Sakugawa, Ikeda, Takemura, & Ono, 2004). In these studies, it was found that the ratio of absorption band intensities at 1290 and 1320 cm^{-1} (Filippov & Kohn, 1974), 808 and 787 cm^{-1} (Mackie, 1971) and 1030 and 1080 cm^{-1} (Sakugawa et al., 2004) in the IR spectra of KBr tablets or films containing alginate gives a fairly good estimation of the M/G ratio. IR spectroscopy has also been used for determination of alginate concentration in solution (Bociek & Welti, 1975) and for identification of the type of polysaccharide (alginate, carrageenan or agar) derived from different seaweeds (Pereira, Sousa, Coelho, Amado, & Ribeiro-Claro, 2003). The literature concerning the analysis of alginate using Raman and NIR spectroscopy is sparse. Pereira et al. (2003) showed that Raman spectroscopy can be used to differentiate alginate from other seaweed polysaccharides (agar and carrageenan) and Horn, Moen, and Østgaard (1999) reported on the use of NIR spectroscopy to determine the alginate content of *Laminaria hyperborea* stipe during biodegradation. To the best of our knowledge, determination of the M/G ratio by Raman and NIR spectroscopy has not been carried out before.

Investigations of other polysaccharides have shown that the combination of vibrational spectroscopy and chemometrics is successful when the aim is to develop rapid, non-destructive and robust methods for monitoring different structural characteristics of polysaccharides (Dolmatova, Ruckebusch, Dupuy, Huvenne, & Legrand, 1998; Dyrby et al., 2004; Engelsen & Nørgaard, 1996). It has been shown that FT-IR, FT-Raman and NIR can be used for determination of the degree of esterification and amidation in pectins (Engelsen & Nørgaard, 1996) and of the content of different types of carrageenan in carrageenan powders (Dyrby et al., 2004) using partial least squares regression (PLSR). Moreover, FT-IR spectra of modified corn starches have been used for classification and recognition of their modifications using artificial neural network (ANN) processing (Dolmatova et al., 1998).

The purpose of this work was to develop a rapid quantitative method for measuring the M/G ratio of sodium alginate powder samples using vibrational spectroscopy and chemometrics. The method was developed using solution-state ^{1}H NMR spectroscopy on hydrolysed samples as the reference method.

2. Materials and methods

2.1. The samples

For this spectroscopic investigation, 100 different commercial sodium alginate samples were kindly provided by Danisco A/S (Brabrand, Denmark) as powders with a particle size of <106 μm. Chemical and physical properties of the samples were obtained from the analyses described below.

2.2. NMR spectroscopy

^{1}H NMR spectra were acquired on a Varian Mercury VX 200 MHz spectrometer (Varian, Inc., Palo Alto, California, USA). The average molecular weights of the alginates were reduced by partial acid hydrolysis (Grasdalen et al., 1979). The hydrolysed alginate was dissolved in D_2O (3.5% (w/v)), neutralised (pH 7) and filtered through a Whatman 13 mm syringe filter (pore size 0.45 μm) into a 5-mm NMR tube. 256 scans were acquired and averaged with a 5 s acquisition time after a 2 s relaxation delay and a 90° pulse. During acquisition the sample temperature was 90 °C. A pulse experiment with water suppression was used. The raw data were multiplied with a 1.0 Hz exponential line broadening function before Fourier transformation. Peak assignments and calculations of M/G ratio and the fractions of diad sequences (MM, GG and GM/MG) were performed as described by Grasdalen et al. (1979).

2.3. Water content

The water content of the alginate powders was determined as percent evaporated water after 2 h at 130 °C. Each sample was measured as true duplicates, and the average values were used in the data analysis.

2.4. Gel strength

For gel strength measurements (i.e. the force required to break the gel), homogeneous alginate gels were prepared by dissolving alginate (0.7% (w/w)) in demineralised water at room temperature. $CaHPO_4$ (0.15% (w/w)) was added as an inactivated form of calcium followed by addition of

the slowly hydrolysing D-glucono-δ-lactone (1.4% (w/w)), resulting in an *in situ* release of calcium cations from $CaHPO_4$. Subsequently, the solutions were filled into two 100 ml glass beakers and left at room temperature for 2 h. The gel strength of the alginate gels was measured using a Texture Analyser TX-XT2i (Stable Microsystems, Surrey, UK) mounted with a half inch cylindrical probe which penetrated 20 mm into the gel. A force–time curve was obtained at a crosshead speed of 0.5 mm/s. The gel strength was evaluated as the maximum resistance to the probe, i.e. the height of the force peak.

2.5. Viscosity

The apparent viscosity of alginate solutions (1% (w/w)) was measured using a Brookfield LVT viscosimeter (Brookfield, Essex, UK). The solutions were prepared with demineralised water and left to equilibrate for 2 h at 20 °C before measurement. The viscosity was read after 30 s at 60 rpm. LV1, LV2 and LV3 spindles were used for samples with a viscosity of <100, 100–500 and >500 cP, respectively.

2.6. Molecular weight

The average molecular weight (M_w) of the alginate samples was determined by size exclusion chromatography with multi-angle light scattering (SEC-MALS) using two columns (PSS SUPREMA-LUX 3000 Å and PSS SUPREMA-LUX 1000 Å, Polymer Standard Service GmbH, Mainz, Germany) in series as well as a DAWN EOS multiangle light scattering photometer and an Optilab rEX differential refractive index detector (both Wyatt Technology Corp., Santa Barbara, California, USA). The columns and the detectors were thermostated at 40 °C. The mobile phase was 0.05 M $LiNO_3$/200 ppm NaN_3 at a flow rate of 0.8 ml/min. Alginate was dissolved in the mobile phase (0.2% (w/v)) and 100 μl of this solution was injected into the columns. Data were analysed using Astra V software (Wyatt Technology Corp., Santa Barbara, California, USA). The refractive increment value (dn/dc) for alginate was set to 0.154 ml/g (Mackie, Noy, & Sellen, 1980). Each sample was measured as a true duplicates, and the average values were used in the data analysis.

2.7. FT-IR spectroscopy

IR spectra were collected on a Perkin Elmer Spectrum One FT-IR spectrometer (Perkin Elmer Instruments, Waltham, Massachusetts, USA). Spectra were acquired using an attenuated total reflectance (ATR) device equipped with a single-bounce diamond crystal. A total of 16 scans were averaged for each sample and the resolution was 4 cm^{-1}. The spectra were ratioed against a single-beam spectrum of the clean ATR crystal and converted into absorbance units. Data were collected in the range 4000–650 cm^{-1}. Each sample was measured three duplicates times and the average values were used in the data analysis.

2.8. FT-Raman spectroscopy

Raman spectra were collected on a Perkin Elmer System NIR FT-Raman interferometer (Perkin Elmer Instruments, Waltham, Massachusetts, USA) equipped with a Nd:YAG laser emitting at 1064 nm with a laser power of 200 mW. Data were collected using an InGaAs detector and stored as Raman shifts in the range 3600–200 cm^{-1}. A 180° back-scattering arrangement was used and no correction for the spectral response was applied. A total of 32 scans were averaged for each sample and the resolution was 32 cm^{-1}. Each sample was measured in two re-packed replicates, and the average values were used in the data analysis.

2.9. NIR spectroscopy

NIR spectra were collected using a NIR systems spectrometer model 6500 (Foss NIRSystem, Silver Springs, USA) in reflectance mode. The samples were packed in a small ring cup (internal diameter, 3.9 cm; depth, 1 cm) with a quartz window and measured using a spinning sample module. The range 1100–2498 nm was acquired using a lead sulphide detector. The angle of incident light was 180° and reflectance was measured at an angle of 45°. The number of scans was 32 and the interval between spectra data points was 2 nm. The NIR reflectance spectra were converted to $\log(1/R)$ units prior to data analysis using an internal ceramic reference. Each sample was measured in two re-packed replicates and the average values were used in the data analysis.

2.10. Multivariate data analysis

The results were evaluated by multivariate data analysis using principal component analysis (PCA) and partial least squares regression (PLSR).

PCA (Hotelling, 1933) is the primary tool for investigation of large bilinear data structures for the study of trends, groupings and outliers. By means of PCA it is possible to find the main variation in a multidimensional data set by creating new linear combinations from the underlying latent structures in the raw data. The two-dimensional data matrix (samples × variables) is decomposed into systematic variation and noise. The systematic variation is described by the principal components (PC1, PC2, etc.), each representing the outer product of scores and loadings. The scores contain information about the samples while the loadings contain information about the variables.

PLSR (Wold, Martens, & Wold, 1983) is a multivariate calibration method by which two sets of data, X (e.g. spectra) and y (e.g. M/G ratio), are related by means of regression. The purpose of PLSR is to establish a linear model which enables the prediction of y from the measured spec-

trum X. PLSR is a two-block regression method, where the decomposition of X is performed under the consideration of y in a simultaneous analysis of the two data sets. Three different IR, Raman and NIR data sets were created prior to calibration: (1) raw spectra, (2) second derivative spectra (Savitzky–Golay with 15 point gap size) (Savitzky & Golay, 1964) and (3) spectra treated with extended inverted signal correction (EISC) (Martens, Nielsen, & Engelsen, 2003; Pedersen, Martens, Nielsen, & Engelsen, 2002). All data sets were mean centred (i.e. the mean of each variable was subtracted from the original measurement) prior to model development. In order to determine the important regions in the spectra with respect to prediction of the M/G ratio and to test the possibility of developing optimised local PLSR models using fewer variables, interval partial least squares regression (iPLSR) (Nørgaard et al., 2000) models were developed. iPLSR is an extension of PLSR, which develops PLSR models on equidistant subintervals of the full-spectrum region.

The relatively high number of samples available allowed for true test set validation. The calibration models were validated using a test set consisting of every fourth sample which were selected prior to development of the calibration model, but after the samples were sorted according to M/G ratio. Models were thus developed using internally segmented cross-validation (10 segments) on the calibration set (75 samples) and afterwards applied and tested using the independent test set (25 samples). The PLSR results are presented as number of PLSR components (# PC), squared correlation coefficients (r^2), root mean square error of cross-validation (RMSECV) and root mean square error of prediction (RMSEP) (test set validations).

The PCA and PLSR analyses were performed using LatentiX version 1.0 (Latent5, Copenhagen, Denmark, http://www.latentix.com), whereas EISC pre-processing and iPLSR regression were performed in MatLab 7.4 (Mathworks, Natick, Massachusetts, USA) using the command line EMSC/EISC toolbox (http://www.models.life.ku.dk) and the PLS-Toolbox 4.02 (Eigenvector Research, Manson, Washington, USA), respectively.

3. Results and discussion

3.1. The samples

The range and average values of the chemical and physical properties of the 100 different sodium alginates are listed in Table 1. Since the main purpose of this work was to find correlations between the M/G ratio and spectra obtained by vibrational spectroscopy, the samples were selected so that they varied as much as possible with respect to the M/G ratio. The samples spanned a M/G ratio range between 0.5 and 2.1. As described in Section 2, the relatively high number of samples available allowed for true test set validation of the calibration models. Fig. 1 shows the M/G ratio of the 75 calibration samples and 25 test samples ordered according to the M/G ratio. The samples

Table 1
The range, average values and average standard deviations (std.) of the chemical and physical properties of the 100 different sodium alginate samples

Chemical/physical property	Range	Average	Average std.
M/G ratio	0.5–2.1	1.3	0.06[a]
Fraction of GG (%)	9–44	23	1.0[a]
Fraction of MM (%)	10–49	34	1.8[a]
Fraction of MG/GM (%)	34–51	43	2.4[a]
Water content (%)	11.0–17.8	14.9	0.18[b]
Gel strength (g)	70–1139	566	15.5[c]
Viscosity (cP)	23–846	269	12.3[d]
M_w (kDa)	104–424	277	8.6[b]

[a] Based on true triplicates of nine different samples.
[b] Based on true duplicates of all samples.
[c] Based on the results from two gels of all alginates made from the same solution of the respective alginate.
[d] Based on measuring the viscosity of the same sample six times.

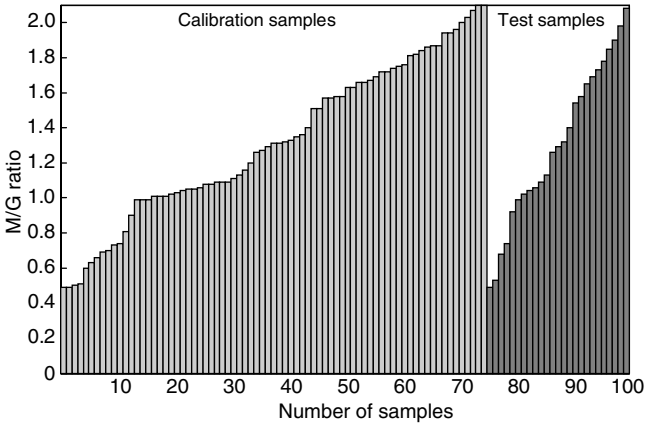

Fig. 1. M/G ratio of the 75 samples in the calibration set and the 25 samples in the test set.

did not only vary with respect to the M/G ratio, but also with respect to the other chemical and physical properties, indicating that we are dealing with a realistic data set representing the many variations found in commercial alginate samples. To investigate the variance structure in the chemical and physical data, a PCA was performed on the autoscaled data (mean centred + dividing each variable by its standard deviation) (Fig. 2). The PCA loading plot in Fig. 2a shows how the different chemical and physical parameters are correlated. The PCA score plot in Fig. 2b shows that the samples in both the calibration sample set and the test sample set spanned the variation within all the chemical and physical parameters.

3.2. The NMR reference method

Solution-state ^{1}H NMR was used as reference method for determination of the M/G ratio. The signals in the anomeric region of the ^{1}H NMR spectra (A (5.07 ppm), B (4.70 ppm) and C (4.46 ppm) in Fig. 3) contain specific information about the alginate composition and were assigned to the anomeric proton of G (A), the anomeric

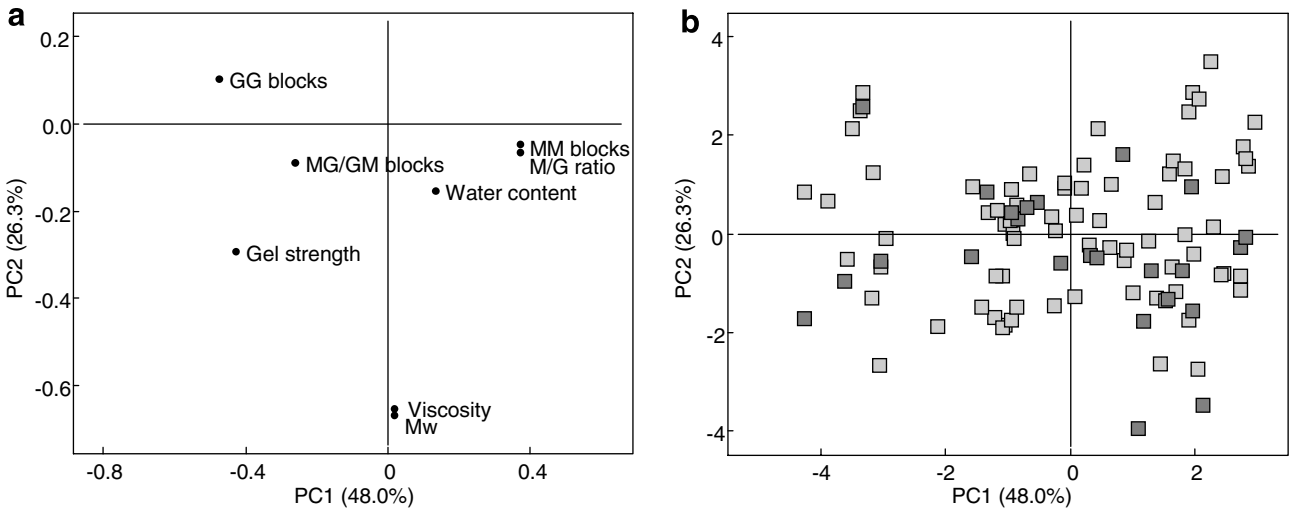

Fig. 2. PCA loading (a) and score (b) plot based on the chemical and physical properties of the 75 calibration (□) and 25 test (■) samples showing the first two principal components which explain 74.3% of the data variation.

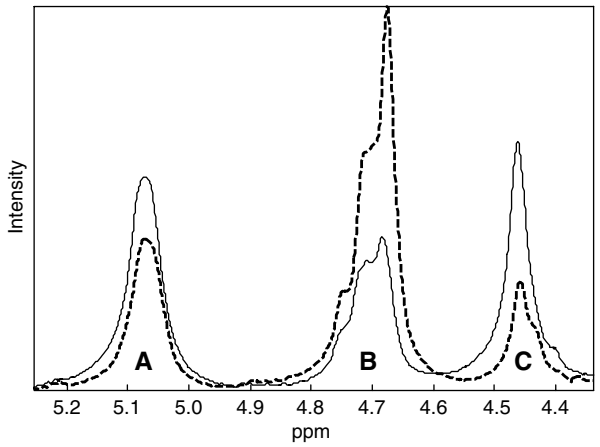

Fig. 3. ^{1}H NMR spectra of 3.5% (w/v) solutions of two hydrolysed sodium alginate samples with M/G ratio of 0.5 (—) and 2.1 (- -).

proton of M and H-5 of G-units adjacent to M (B), and H-5 of G-units adjacent to G (C) (Grasdalen, 1983; Grasdalen et al., 1979; Penman & Sanderson, 1972). Thus, from the relative areas of the three signals in this region the M/G ratio can be calculated, as described by Grasdalen et al. (1979). Furthermore, the fraction of the diad sequences (GG, MM and MG/GM) can be determined (Grasdalen et al., 1979), and if using a NMR spectrometer operating at 400 MHz or above, the fraction of triad frequencies can also be calculated due to the better peak separation at higher frequencies (Grasdalen, 1983).

In order to obtain comparable values of the M/G ratio, the relative integrals of the three signals were calculated using an in-house built routine where the same integration limits for all the spectra were applied. The limits for signal A, B and C (Fig. 3) were set to 5.18–4.96, 4.82–4.57 and 4.55–4.38 ppm, respectively. Changing these limits yielded slightly different M/G ratio values, emphasising the importance of using the same limits in all the calculations. For noise reduction, the spectra were smoothed using a Savitzky–Golay filter (15 point gap size) (Savitzky & Golay, 1964), resulting in more accurate signal integrations. Thus, using this routine, the ^{1}H spectra gave comparable results for the quantification of the M/G ratio, and hence the compositions of the calibration and validation samples used for PLSR models are based on the quantifications from the ^{1}H spectra.

The error of the quantification of the M/G ratio using the described ^{1}H NMR method was estimated to be between 0.01 and 0.08 (the standard deviation of quantifications of triplicates). The degradation of the alginate chain by acid hydrolysis to reduce the viscosity prior to NMR measurement may possibly contribute to this error, since the rate at which the different linkages are cleaved increases in the order: G–G < M–M < M–G < G–M (Grasdalen et al., 1979; Holme, Lindmo, Kristiansen, & Smidsrød, 2003; Smidsrød, Larsen, Painter, & Haug, 1969). Consequently, G-units and M-units will occur at higher frequencies than expected at the reducing and non-reducing ends, respectively, and the homopolymeric G-blocks will be less degraded than the others. Also, it has been shown that different hydrolysis procedures may result in different M/G ratio values (Penman & Sanderson, 1972; Shinohara et al., 2000). Another issue that must be considered when discussing error sources using solution-state NMR for the analysis of alginates is the possible selective micro-aggregation when divalent cations (e.g. calcium ions) are present. It is well known that calcium ions preferentially bind to G-blocks, resulting in gel formation (Draget et al., 2000; Grant, Morris, Rees, Smith, & Thom, 1973). Thus, the restricted motion of the G-blocks as by increase in viscosity reduces the relaxation times, giving rise to a broadening of the NMR lines beyond the level of detection. However, in this study the samples are expected to contain only small amounts of calcium (<0.25%), which will have a very limited influence on the NMR spectra.

3.3. Exploratory analysis

The raw IR, Raman and NIR spectra of the 75 calibration samples are shown in Fig. 4a, b and c, respectively. The spectra show some additive and multiplicative effects which can be explained by differences in physical properties of the samples (e.g. particle size, packing density and water content) and measurement conditions. The IR spectra were recorded using an attenuated total reflectance device where the alginate powder is pressed manually against a diamond. Thus, the intensity of the spectra depends on the contact to the diamond. In the Raman spectra, scatter effects are observed due to different particle sizes and fluorescence. The scatter effects observed in the NIR spectra are due to different particle sizes as well as differences in the water content of the samples. Conclusively, these differences in the spectra are a result of physical differences between the samples, which are not interesting with respect to the purpose of this work where the chemical composition of the alginates is in focus. Therefore, it is preferable to filter away these effects, so that they do not disturb the analysis. Different pre-processing techniques can be used for this purpose. The results of pre-processing the IR, Raman and NIR spectra with the EISC technique are shown in Fig. 4d, e and f, respectively. The spectra are coloured according to the M/G ratio and from a visual inspection of the EISC-corrected IR and Raman spectra it is clear that there are several bands in the spectra that contain information about the M/G ratio. Even though both IR and Raman spectroscopy are based on measurements of the fundamental molecular vibrations, they do not provide exactly the same information. While IR spectroscopy detects vibrations during which the electrical dipole moment changes, Raman spectroscopy is based on the detection of vibrations during which the electrical polarisability changes. Thus, as a rule of thumb IR is more sensitive to side group vibrations and Raman is more sensitive to skeleton vibrations. Therefore, changes in the M/G ratio will manifest differently. In the IR spectra the intensity of the bands at 1290, 1166, 882 and 814 cm^{-1} increase with increasing M/G ratio and the intensity of the bands at 1320, 1123, 1083, 950 and 899 cm^{-1} decrease with increasing M/G ratio. Filippov and Kohn (1974) also found that the bands at 1290 and 1320 cm^{-1} correlated with the M and G content, respectively. In the Raman spectra the intensity of the bands at 1412, 1090, 955 and 708 cm^{-1} increase with increasing M/G ratio and the intensity of the bands at 1313, 1232, 884 and 806 cm^{-1} decrease with

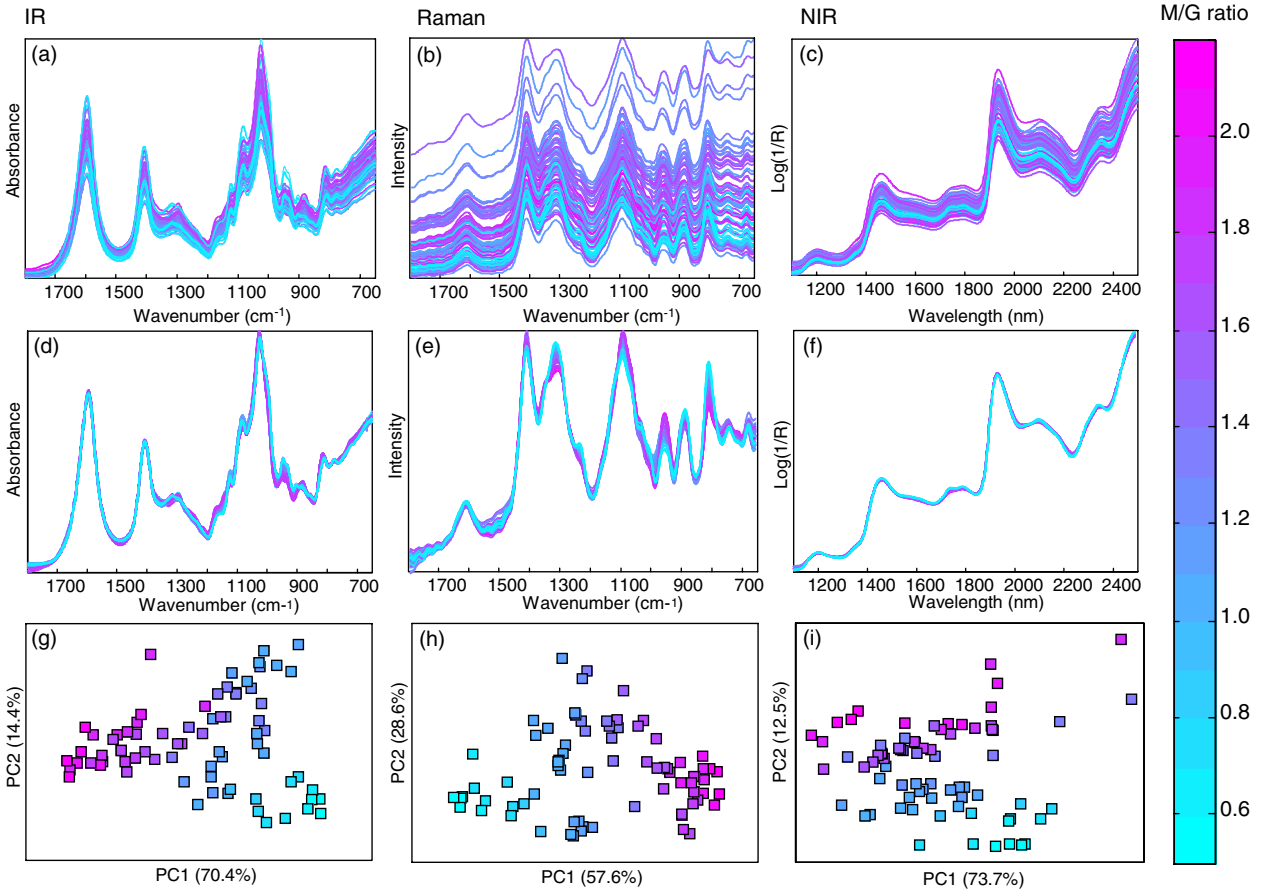

Fig. 4. Raw IR (a), Raman (b) and NIR (c) spectra as well as EISC-corrected IR (d), Raman (e) and NIR (f) spectra of the 75 calibration samples. PCA score plot of the EISC-corrected IR (g), Raman (h) and NIR (i) spectra showing the first two principal components (PCs) which explain 84.8%, 86.2% and 86.2%, respectively, of the data variation. The spectra and the scores are coloured according to the M/G ratio.

increasing M/G ratio. Thus, in the IR and Raman spectra the bands related to the concentration of M and G are all found in the fingerprint region, whereas the asymmetric stretching band from the carboxylate ion centred around 1600 cm^{-1} is not related to the M/G ratio.

In contrast to IR and Raman, NIR spectroscopy measures over- and combination-tones predominantly of the fundamental vibrations that involve hydrogens. Thus, when the variations amongst the samples do not involve hydrogens, the NIR spectra appear almost similar. This explains why the curvature of all the NIR spectra is so alike. However, a slight intensity increase in the 1700–1800 nm region (first overtone C–H stretching modes) and at 2250 nm (combination bands) for samples with low and high M/G ratio, respectively, can be observed in the EISC-corrected spectra (Fig. 4f). Since the spectra are so alike, multivariate data analysis techniques are required to release these highly overlapped and almost similar spectral features related to the M/G ratio.

To obtain an overview of the variation in the multivariate spectra before the development of calibration models, PCA was used to investigate the extent to which the spectroscopic methods allowed for differentiation between alginates with different M/G ratios. The PCA score plot based on the EISC-corrected IR, Raman and NIR spectra of the 75 calibration samples are shown in Fig. 4g, h and i, respectively. The samples are coloured according to the M/G ratio, clearly showing that the main variation in the EISC-corrected IR (Fig. 4g) and Raman (Fig. 4h) spectra are correlated with differences in the M/G ratio of the alginate samples, whereas the main variation of the NIR spectra cannot be explained by the variation in M/G ratio. NIR absorbance is strongly influenced by the different contents of water (Table 1) in the samples. Thus, PC1 from the PCA of the EISC-corrected NIR spectra is modelling the water content (Fig. 4i). However, the variations in M/G ratio are explained along PC2, indicating that there is information about the M/G ratio in the NIR spectra.

In conclusion, the spectra obtained by the three different vibrational techniques all contain information about the M/G ratio. Thus, this preliminary exploratory analysis indicates that it is possible to develop PLSR models with a good prediction performance.

3.4. Calibration models

Calibration models for prediction of the M/G ratio from the raw, second derivative and EISC-corrected IR, Raman and NIR spectra of the alginate powders were developed using PLSR. The models were developed using the 75 calibration samples and tested using the 25 test set samples. For IR and Raman data only the range 1800–650 cm^{-1} was used in the calibrations in order to avoid the noisy low energy range below 650 cm^{-1} and the strong O–H stretching modes in the IR spectra centred around 3300 cm^{-1}. For NIR the whole recorded spectral range 1100–2498 nm was used.

The PLSR models obtained using the three different spectroscopic techniques and different pre-processing techniques are listed in Table 2. Using the raw spectra, the models performed relatively well compared to the upper limit of the experimental error of the M/G ratio measurements, which was 0.08. However, relatively many PLSR components (4–6) were needed in order to deal with the additive and multiplicative effects of the spectra due to the different factors described in the previous section. Using instead the second derivative or EISC-corrected spectra in order to remove these effects and only model the chemical information in the spectra, simpler models with lower number of PLSR components and lower prediction errors were obtained. The models based on the EISC-corrected IR and Raman spectra and the second derivative NIR spectra all resulted in a prediction error of 0.08. However, it is noteworthy that the model based on EISC-corrected Raman spectra only needs one PLSR component to explain the M/G ratio, whereas the best IR and NIR models need four and three, respectively. It is worth noting that the calibration error (RMSECV) and the prediction error (RMSEP) are the same for the best model of all the spectroscopic techniques. This indicates that the models are very robust, i.e. the model can predict new samples that have not been involved in the modelling with high precision. Since it is possible to develop a model with a prediction error comparable to the experimental error of the reference method using all three vibrational spectroscopic techniques, it can be concluded that IR, Raman and NIR are suitable methods for a rapid determination of the M/G ratio of commercial alginate samples. However, it should be noted that the model based on the EISC-corrected Raman spectra is the simplest and therefore probably also more robust when it comes to predicting new samples.

Fig. 5a shows the measured versus predicted plot from the model based on the EISC-corrected Raman spectra ($r^2 = 0.97$). The model is based on only one PLSR component and the prediction error is 0.08. The regression coeffi-

Table 2
Results of PLSR models based on raw, second derivative and EISC-corrected IR, Raman and NIR spectra of sodium alginate powder for prediction of the M/G ratio

	Pre-processing	#PC	r^2	RMSECV	RMSEP
IR	Raw	5	0.95	0.10	0.09
	Second derivative	3	0.95	0.10	0.10
	EISC	4	0.97	0.08	0.08
Raman	Raw	4	0.93	0.12	0.12
	Second derivative	3	0.94	0.11	0.12
	EISC	1	0.97	0.08	0.08
NIR	Raw	6	0.96	0.09	0.11
	Second derivative	3	0.96	0.08	0.08
	EISC	3	0.95	0.10	0.13

The models were developed using the 75 calibration samples and the prediction ability was tested using the 25 test samples. The results are presented as number of PLSR components (#PC), squared correlation coefficients (r^2), root mean square error of cross-validation (RMSECV) and root mean square error of prediction (RMSEP) (test-set validations).

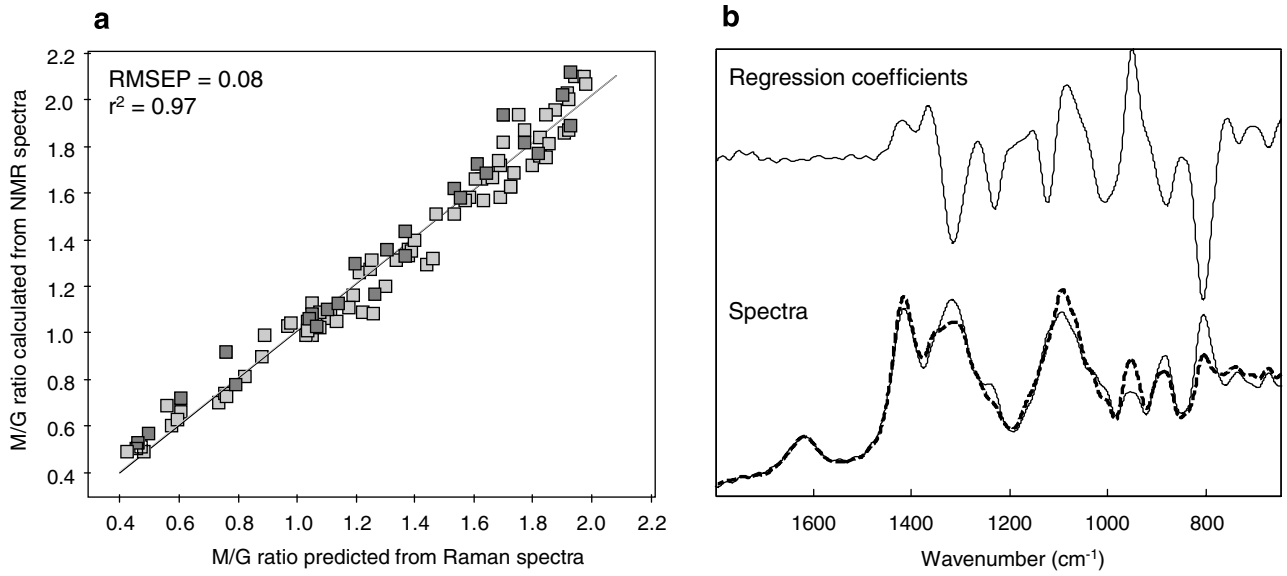

Fig. 5. (a) M/G ratio measured by NMR versus M/G ratio predicted from the EISC-corrected Raman spectra of the 75 calibration (□) and 25 test (■) samples using one PLSR component. (b) The regression coefficients are plotted together with the spectra of two alginates with M/G ratios of 0.5 (—) and 2.1 (- -).

cients shown together with the spectra of a sample with low (0.5) and high (2.1) M/G ratio tell which parts of the spectra that are important for the prediction of the M/G ratio (Fig. 5b). As expected from the visual inspection of the EISC-corrected spectra (Fig. 4e), the carbonyl stretching region at 1607 cm^{-1} does not contribute to the prediction. The most influential spectral band is the band at 806 cm^{-1}, which most likely arises from the α-configuration of the G-units. The second most influential spectral band is centred at 955 cm^{-1}. Actually, the ratio between the intensities 955 cm^{-1} (M) and 806 cm^{-1} (G) correlated well ($r^2 = 0.95$) to the M/G ratio calculated from the NMR spectra. Moreover, the ratio between the intensities of 1290 cm^{-1} (M) and 1320 cm^{-1} (G) in the EISC-corrected IR spectra correlated very well ($r^2 = 0.96$) to the M/G ratio, as also found by Filippov and Kohn (1974). While these bi-variate methods are almost as good as the multivariate calibration methods, they are more sensitive to noise and interferences and will thus be less robust for industrial quality control.

3.5. Variable selection using interval PLSR (iPLSR)

Variable selection by interval PLSR (iPLSR) was applied to encircle the significant regions in the Raman spectra with respect to the M/G ratio and to test the possibility of developing optimised local PLSR models for prediction of the M/G ratio using fewer variables. The iPLSR algorithm is designed to develop local PLSR models on spectral subintervals of equal width of the full-spectrum region. The advantage of the iPLSR approach is that smaller intervals will contain less interference and thus result in simpler, more precise and more easily interpretable models (Nørgaard et al., 2000).

The iPLSR approach was applied to the EISC-corrected IR and Raman spectra and second derivative NIR spectra due to the good performance of the full-spectrum models based on these data sets. Different numbers of variables in the spectral intervals were tested (5, 10, 25 and 50) and the number of components in the local models was restricted to be equal to or less than the optimal number of components in the global model (Table 2). The results of iPLSR of the EISC-corrected IR and Raman of the 75 calibration samples with 50 variables in each interval (23 intervals) are presented in Fig. 6a and b, respectively, together with the spectra of two samples with extreme M/G ratio values. The models were validated with segmental cross-validation using 10 segments. The calibration errors (RMSECV) for each of the 23 intervals are presented as bars and the calibration error of the global model is presented as a horizontal dotted line. All IR models were calculated using four PLSR components with exception of the model based on the spectral region 1150–1100 cm^{-1} (C–O–C pyranose skeleton modes), which is based on only three PLSR components. Thus, the model based on the IR spectral region 1150–1100 cm^{-1} is simpler and has approximately the same calibration error (RMSECV) as the full-spectrum model. Also, the models based on the spectral region 1350–1300 cm^{-1} yield a quantitative performance equal to the full-spectrum model. However, this model uses four PLSR components as the full-spectrum model. All Raman models were calculated using one PLSR component and only one spectral region (850–800 cm^{-1}) containing the band due to the α-configuration of the G-units, resulted in a calibration error equal to the error of the full-spectrum model. This region was also identified as the most influential spectral band in the inspection of the regression coefficients (Fig. 5b) and could be identified by visual inspection of the spectra (Fig. 4e) as an important region for differentiating between alginates with high and low M/G ratio. From iPLSR of the second derivative

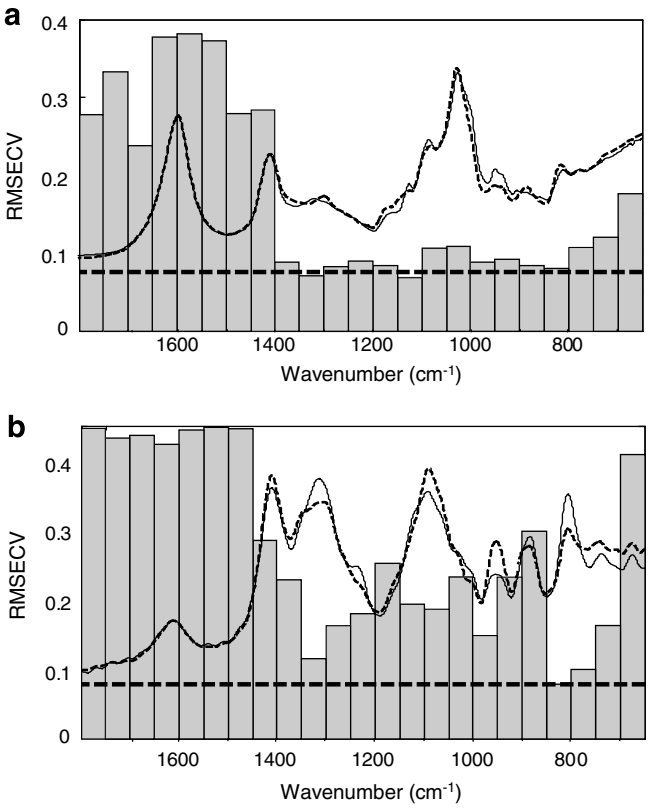

Fig. 6. Interval PLSR results. Cross-validated prediction performance (RMSECV) for 23 PLSR interval models (bars) and for the full-spectrum model (- -) based on the EISC-corrected IR (a) and Raman (b) spectra of the 75 calibration samples plotted together with the spectra of two alginates with M/G ratios of 0.5 (—) and 2.1 (- -). All IR models use four PLSR components with exception of the model based on the spectral region 1150–1100 cm^{-1} using three PLSR components. All Raman models are based on one PLSR component.

NIR spectra the regions 1750–1800 nm performed the same as the full-spectrum model using the same number of PLS components.

The regions in the IR, Raman and NIR spectra identified above using intervals containing 50 variables were also identified as the most important regions using intervals with 5, 10 and 25 variables. However, when testing the prediction performance of the models based on the smaller intervals using the 25 test samples, it resulted in higher prediction errors (0.09–0.11) compared to the full-spectrum model (0.08). Only the model based on the IR spectral region 1150–1100 cm^{-1} using three PLSR components resulted in a prediction error lower than the full-spectrum model when tested (0.08).

In summary, iPLS has been used to show and confirm the relevant areas of the spectra. However, it was not possible to develop models based on fewer variables with a better prediction performance than the full-spectrum model.

4. Conclusion

The present investigation has shown that it is possible to develop a rapid, non-destructive and robust quantitative method for measuring the monomer composition (M/G ratio) of commercial alginate powders using vibrational spectroscopy (IR, Raman and NIR) and chemometrics. The M/G ratio can be predicted from spectra of all three spectral sources investigated with an error comparable to that of the solution-state ^{1}H NMR reference method. This is a valuable achievement, since vibrational spectroscopic techniques have a high industrial potential for at- or on-line quality control as well as screening of large numbers of samples.

Spectral pre-processing was applied in order to remove the additive and multiplicative effects not related to the chemical composition of the samples. This generally improved the predictive capabilities of the three spectroscopic methods IR, Raman and NIR. Especially the Raman results were improved when pre-processing the spectra using the EISC method. This resulted in a very simple model using only one PLSR component and with a prediction error (RMSEP) of 0.08 and a correlation of 0.97, which is comparable to the standard deviation of the NMR reference method (0.01–0.08).

For an even better fit between the measured and predicted values, the error from the reference method must be lowered, since it is not possible to predict values with better accuracy than that of the reference method. We believe that a reduction in the error from the reference method deserves further attention. Therefore, we are currently looking into the possibility of using the NMR techniques ^{1}H high resolution magic angle spinning (HR MAS) NMR and solid-state ^{13}C cross-polarisation (CP) MAS NMR for determination of the M/G ratio. By using these techniques the destructive and time-consuming hydrolysis procedure necessary for solution-state NMR can be avoided.

Acknowledgements

The authors thank the Ministry of Science, Technology and Innovation for partly sponsoring the Industrial PhD project conducted by Tina Salomonsen in co-operation with Danisco A/S and Quality & Technology, Department of Food Science, Faculty of Life Sciences (LIFE) at the University of Copenhagen. At Danisco, many colleagues have contributed to this work. Special credit is given to Bente Høj Andersen, Keld Hartwig and Anita Beck-Rasmussen. Mette Mortensen and Gilda Kischinovsky from LIFE are also acknowledged for help with parts of the experimental work and for proofreading the manuscript, respectively.

References

Bociek, S. M., & Welti, D. (1975). Quantitative analysis of uronic acid polymers by infrared spectroscopy. *Carbohydrate Research, 42*, 217–226.

Dolmatova, L., Ruckebusch, C., Dupuy, N., Huvenne, J. P., & Legrand, P. (1998). Identification of modified starches using infrared spectroscopy and artificial neural network processing. *Applied Spectroscopy, 52*, 329–338.

Draget, K. I., Strand, B., Hartmann, M., Valla, S., Smidsrød, O., & Skjåk-Bræk, G. (2000). Ionic and acid gel formation of epimerised alginates; the effect of AlgE4. *International Journal of Biological Macromolecules, 27*, 117–122.

Dyrby, M., Petersen, R. V., Larsen, J., Rudolf, B., Nørgaard, L., & Engelsen, S. B. (2004). Towards on-line monitoring of the composition of commercial carrageenan powders. *Carbohydrate Polymers, 57*, 337–348.

Engelsen, S. B., & Nørgaard, L. (1996). Comparative vibrational spectroscopy for determination of quality parameters in amidated pectins as evaluated by chemometrics. *Carbohydrate Polymers, 30*, 9–24.

Filippov, M. P., & Kohn, R. (1974). Determination of composition of alginates by infrared spectroscopic method. *Chemicke Zvesti, 28*, 817–819.

Grant, G. T., Morris, E. R., Rees, D. A., Smith, P. J. C., & Thom, D. (1973). Biological interactions between polysaccharides and divalent cations: The egg-box model. *FEBS Letters, 32*, 195–198.

Grasdalen, H. (1983). High-field ^{1}H spectroscopy of alginate: Sequential structure and linkage conformations. *Carbohydrate Research, 118*, 255–260.

Grasdalen, H., Larsen, B., & Smidsrød, O. (1977). ^{13}C NMR studies of alginate. *Carbohydrate Research, 56*, C11–C15.

Grasdalen, H., Larsen, B., & Smidsrød, O. (1979). NMR study of the composition and sequence of uronate residues in alginates. *Carbohydrate Research, 68*, 23–31.

Grasdalen, H., Larsen, B., & Smidsrød, O. (1981). ^{13}C NMR studies of monomeric composition and sequence in alginate. *Carbohydrate Research, 89*, 179–191.

Haug, A., Larsen, B., & Smidsrød, O. (1974). Uronic acid sequence in alginate from different sources. *Carbohydrate Research, 32*, 217–225.

Haug, A., Myklesta, S., Larsen, B., & Smidsrød, O. (1967). Correlation between chemical structure and physical properties of alginates. *Acta Chemica Scandinavica, 21*, 768–778.

Holme, H. K., Lindmo, K., Kristiansen, A., & Smidsrød, O. (2003). Thermal depolymerization of alginate in the solid state. *Carbohydrate Polymers, 54*, 431–438.

Horn, S. J., Moen, E., & Østgaard, K. (1999). Direct determination of alginate content in brown algae by near infra-red (NIR) spectroscopy. *Journal of Applied Phycology, 11*, 9–13.

Hotelling, H. (1933). Analysis of complex statistical variables into principal components. *Journal of Educational Psychology, 24*, 417–441.

Indergaard, M., Skjåk-Bræk, G., & Jensen, A. (1990). Studies on the influence of nutrients on the composition and structure of alginate in *Laminaria saccharina* (L) Lamour (Laminariales, Phaeophyceae). *Botanica Marina, 33*, 277–288.

Mackie, W. (1971). Semi-quantitative estimation of composition of alginates by infra-red spectroscopy. *Carbohydrate Research, 20*, 413–415.

Mackie, W., Noy, R., & Sellen, D. B. (1980). Solution properties of sodium alginate. *Biopolymers, 19*, 1839–1860.

Martens, H., Nielsen, J. P., & Engelsen, S. B. (2003). Light scattering and light absorbance separated by extended multiplicative signal correction. Application to near-infrared transmission analysis of powder mixtures. *Analytical Chemistry, 75*, 394–404.

Nørgaard, L., Saudland, A., Wagner, J., Nielsen, J. P., Munck, L., & Engelsen, S. B. (2000). Interval partial least-squares regression (iPLS): A comparative chemometric study with an example from near-infrared spectroscopy. *Applied Spectroscopy, 54*, 413–419.

Pedersen, D. K., Martens, H., Nielsen, J. P., & Engelsen, S. B. (2002). Near-infrared absorption and scattering separated by extended inverted signal correction (EISC): Analysis of near-infrared transmittance spectra of single wheat seeds. *Applied Spectroscopy, 56*, 1206–1214.

Penman, A., & Sanderson, G. R. (1972). Method for determination of uronic acid sequence in alginates. *Carbohydrate Research, 25*, 273–282.

Pereira, L., Sousa, A., Coelho, H., Amado, A. M., & Ribeiro-Claro, P. J. A. (2003). Use of FTIR, FT-Raman and ^{13}C NMR spectroscopy for identification of some seaweed phycocolloids. *Biomolecular Engineering, 20*, 223–228.

Sakugawa, K., Ikeda, A., Takemura, A., & Ono, H. (2004). Simplified method for estimation of composition of alginates by FTIR. *Journal of Applied Polymer Science, 93*, 1372–1377.

Savitzky, A., & Golay, M. J. E. (1964). Smoothing and differentiation of data by simplified least squares procedures. *Analytical Chemistry, 36*, 1627–1639.

Shinohara, M., Nishida, R., Aoyama, T., Kamono, H., Bando, H., & Nishizawa, M. (2000). Comparison of guluronate contents of alginates determined by different methods. *Fisheries Science, 66*, 616–617.

Smidsrød, O., Larsen, B., Painter, T., & Haug, A. (1969). The role of intramolecular autocatalysis in acid hydrolysis of polysaccharides containing 1,4-linked hexuronic acid. *Acta Chemica Scandinavica, 23*, 1573–1580.

Steginsky, C. A., Beale, J. M., Floss, H. G., & Mayer, R. M. (1992). Structural determination of alginic acid and the effects of calcium-binding as determined by high-field NMR. *Carbohydrate Research, 225*, 11–26.

Stockton, B., Evans, L. V., Morris, E. R., Powell, D. A., & Rees, D. A. (1980). Alginate block structure in Laminaria digitata: Implications for holdfast attachment. *Botanica Marina, 23*, 563–567.

Stokke, B. T., Smidsrød, O., Bruheim, P., & Skjåk-Bræk, G. (1991). Distribution of uronate residues in alginate chains in relation to alginate gelling properties. *Macromolecules, 24*, 4637–4645.

Wold, S., Martens, H., & Wold, H. (1983). The multivariate calibration problem in chemistry solved by the PLS method. *Lecture Notes in Mathematics, 973*, 286–293.

Rapid determination of alginate monomer composition using Raman spectroscopy and chemometrics

T. Salomonsen, H.M. Jensen, F.H. Larsen & S.B. Engelsen

Gums and Stabilisers for the Food Industry 14

Cambridge, RSC Publishing, (2008), pp. 543-551

Eds. P. A. Williams & G. O. Phillips

PAPER III

Gums and Stabilisers for the Food Industry 14

Edited by

Peter A. Williams
Centre for Water Soluble Polymers, North East Wales Institute, Wrexham, UK

Glyn O. Phillips
Phillips Hydrocolloids Research Ltd, London, UK

RSC Publishing

The proceedings of the 14th Gums and Stabilisers for the Food Industry Conference held on 18-22 June 2007 at NEWI, Wrexham, UK.

Special Publication No. 316

ISBN: 978-0-85404-461-0

A catalogue record for this book is available from the British Library

Published by The Royal Society of Chemistry,
Thomas Graham House, Science Park, Milton Road,
Cambridge CB4 0WF, UK

Registered Charity Number 207890

For further information see our web site at www.rsc.org

RAPID DETERMINATION OF ALGINATE MONOMER COMPOSITION USING RAMAN SPECTROSCOPY AND CHEMOMETRICS

T. Salomonsen[1,2], H.M. Jensen[1], D. Stenbæk[1] and S.B. Engelsen[2]

[1] Danisco A/S, Edwin Rahrs Vej 38, 8220 Brabrand, Denmark
[2] Department of Food Science, Faculty of Life Sciences, University of Copenhagen, Rolighedsvej 30, 1958 Frederiksberg C, Denmark

1 INTRODUCTION

Commercial sodium alginates are extracted from brown seaweed (*Phaeophyceae*) and used as thickeners, stabilisers and gelling agents in the food and pharmaceutical industries. Chemically, they are a family of binary copolymers of (1-4) linked β-D-mannuronic acid (M) and its C-5 epimer α-L-guluronic acid (G). Alginates are typically described by their M/G ratio, distribution of M- and G-units along the chain and average molecular weight, since these parameters are closely related to the functionality of the alginates, i.e. solubility, interaction with metals, gel properties and viscosity.[1-3] The composition and sequential structure and thereby also the functionality of alginates vary according to season, age of population, species and geographic location.[4-6] Because of these variations within the different alginate types, it is of great importance for the alginate industry to obtain detailed knowledge about the composition of its products in order to design the functionality of the final product.

Solution-state nuclear magnetic resonance (NMR) spectroscopy is a highly effective tool in compositional and structural analysis of alginates.[7-11] However, at the concentrations required for NMR analysis for a good signal-to-noise ratio, alginate solutions are too viscous to give well-resolved spectra even at elevated temperatures (up to 90ºC). To reduce the viscosity it is necessary to partially degrade the alginate chain by a mild acid hydrolysis prior to NMR analysis. This hydrolysis is relatively time-consuming and labour intensive. Hence, solution-state NMR of alginates is rather elaborate and time-consuming and certainly not suitable for at- or on-line monitoring of alginate composition. Thus, development of a faster and simpler method for characterisation of alginate composition would be beneficial.

Investigations of other hydrocolloids (starch, carrageenan and pectin) have shown that the combination of vibrational spectroscopy (infrared (IR), Raman and near infrared (NIR) spectroscopy) and chemometrics is successful when the aim is to develop rapid, non-destructive and robust methods for monitoring different structural characteristics of hydrocolloids.[12-14] Regarding alginate, IR spectroscopy has proven useful for quantitative estimation of the M/G ratio of alginates by comparing the intensities at two wavelengths correlated to the M and G concentration, respectively.[15-17] However, to the best of our

knowledge, determination of the M/G ratio of alginates using vibrational spectroscopy and chemometrics has not been carried out before.

The work presented in this chapter is a part of a larger investigation where the purpose was to investigate and compare the potential of using IR, Raman and NIR for rapid and non-destructive determination of the M/G ratio in commercial sodium alginate powders.[18] In this chapter the results of the most promising method, Raman spectroscopy, will be presented.

2 MATERIALS AND METHODS

2.1 The Samples

For this chemometric investigation 100 different commercial sodium alginate samples were kindly provided by Danisco A/S (Brabrand, Denmark) as powders with a particle size of $\leq$ 106 μm.

2.2 Nuclear magnetic resonance (NMR)

^{1}H NMR spectra were acquired on a Varian Mercury VX 200 MHz spectrometer (Varian, Inc., Palo Alto, California, USA). The average molecular weights of the alginates were reduced by a partial acid hydrolysis.[7] The hydrolysed alginate was dissolved in D_2O (3.5% (w/v), neutralised (pH 7) and filtered through a Whatman 13 mm syringe filter (pore size 0.45 μm) into a 5 mm NMR tube. 256 scans were acquired and averaged with a 5 s acquisition time after a 2 s relaxation delay and a 90° pulse. During acquisition the sample temperature was 90°C. A pulse experiment with water suppression was used. The raw data were multiplied with a 1.0 Hz exponential line broadening function before Fourier transformation. Peak assignments and calculations of M/G ratio were performed as described by Grasdalen et al.[7]

2.3 FT-Raman Spectroscopy

Raman spectra were collected on a Perkin Elmer System NIR FT-Raman interferometer (Perkin Elmer Instruments, Waltham, Massachusetts, USA) equipped with a Nd:YAG laser emitting at 1064 nm with a laser power of 200 mW. Data were collected using an InGaAs detector and stored as Raman shifts in the range 3600-200 cm^{-1}. However, only the range 1800-650 cm^{-1} was used in the data analysis. A 180º back-scattering arrangement was used and no correction for the spectral response was applied. A total of 32 scans were averaged for each sample and the resolution was 32 cm^{-1}. Each sample was measured in two re-packed replicates, and the average values were used in the data analysis. The analysis time of one spectrum was 50 s.

2.4 Viscosity

The apparent viscosity of alginate solutions (1% (w/w)) was measured using a Brookfield LVT viscosimeter (Brookfield, Essex, UK). The solutions were prepared with demineralised water and left to equilibrate for 2 h at 20°C before measurement. The viscosity was read after 30 sec at 60 rpm. LV1, LV2 and LV3 spindles were used for samples with a viscosity of < 100 cP, 100-500 cP and > 500 cP, respectively.

2.5 Average molecular weight (M_w)

The average molecular weight (M_w) in the alginate samples was determined by size exclusion chromatography with multi-angle light scattering (SEC-MALS) using two columns (PSS SUPREMA-LUX 3000 Å and PSS SUPREMA-LUX 1000 Å, Polymer Standard Service GmbH, Mainz, Germany) in series as well as a DAWN EOS multiangle light scattering photometer and an Optilab rEX differential refractive index detector (both Wyatt Technology Corp., Santa Barbara, California, USA). The columns and the detectors were thermostated to 40 ºC. The mobile phase was 0.05 M $LiNO_3$/200 ppm NaN_3 at a flow rate of 0.8 mL/min. Alginate was dissolved in the mobile phase (0.2 % (w/v)) and 100 µL of this solution was injected into the columns. Data were analysed using Astra V software (Wyatt Technology Corp., Santa Barbara, California, USA). The refractive increment value (dn/dc) for alginate was set to 0.154 mL/g.[19] Each sample was measured as a true replicate, and the average values were used in the data analysis.

2.6 Data Analysis

The calibration models were developed using partial least squares regression (PLSR)[20], which is a multivariate calibration method by which two sets of data, *X* (e.g. spectra) and *y* (e.g. M/G ratio), are related by means of regression. The purpose of PLSR is to establish a linear model which enables the prediction of *y* from the measured spectrum *X*. PLSR is a two-block regression method where the decomposition of *X* is performed under the consideration of *y* in a simultaneous analysis of the two data sets.

Two different Raman data sets were created prior to calibration: (1) raw spectra and (2) spectra treated with extended inverted scatter correction (EISC).[21,22] Both data sets were mean centred (i.e. the mean of each variable was subtracted from the original measurement) prior to model development. In order to determine the important regions in the spectra with respect to prediction of the M/G ratio and to test the possibility of developing optimised local PLSR models using fewer variables, interval partial least squares regression (iPLSR)[23] models were developed. iPLSR is an extension of PLSR which develops PLSR models on equidistant subintervals of the full-spectrum region.

The PLSR analyses were performed using LatentiX version 1.0 (Latent5, Copenhagen, Denmark, http://www.latentix.com), whereas EISC pre-processing and iPLSR regression were performed in MatLab 7.4 (Mathworks, Natick, Massachusetts, USA) using the command line EMSC/EISC toolbox (http://www.models.life.ku.dk) and the PLS-Toolbox 4.02 (Eigenvector Research, Manson, Washington, USA), respectively.

3 RESULTS AND DISCUSSION

3.1 The NMR reference method

The samples were selected in order to vary as much as possible with respect to the M/G ratio (0.5-2.1). Solution-state ^{1}H NMR was used as reference method for determination of the M/G ratio. The signals in the anomeric region of the ^{1}H NMR spectra (A, B and C in Figure 1) contain specific information about the alginate composition.[7,9,11] The signal at 5.07 ppm (A) is assigned to the anomeric proton of G, the signal at 4.70 ppm is assigned to the anomeric proton of M and H-5 of G-units adjacent to M, and the signal at 4.46 ppm is assigned to H-5 of G-units adjacent to G.[7] Thus, from the relative areas of the three signals in this region the M/G ratio can be calculated as described by Grasdalen et al.[7]

In order to obtain comparable values of the M/G ratio, the relative integrals of the three signals were calculated using an in-house built routine where the same integration limits for all spectra were applied. The limits for signal A, B and C (Figure 1) were set to 5.18-4.96 ppm, 4.82-4.57 ppm and 4.55-4.38 ppm, respectively. Changing these limits yielded slightly different M/G ratio values emphasising the importance of using the same limits in all the calculations. For noise reduction the spectra were smoothed using a Savitzky-Golay filter (15 point gap size),[24] resulting in more accurate signal integrations. Thus, using this routine the ^{1}H spectra gave comparable results for the quantification of the M/G ratio, and hence the compositions of the calibration and validation samples used for PLSR models are based on the quantifications from the ^{1}H spectra.

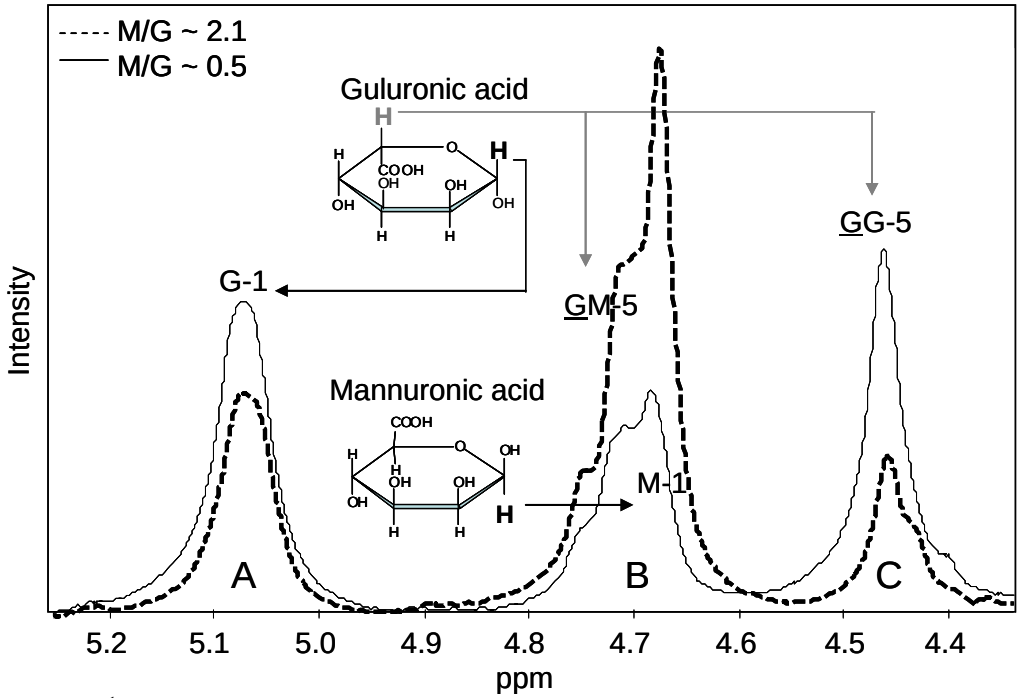

Figure 1 *^{1}H NMR spectra of 3.5% (w/v) solutions of two hydrolysed sodium alginate samples with M/G ratio of 0.5 and 2.1*

The error of the quantification of the M/G ratio using the described ^{1}H NMR method was estimated to be between 0.01 and 0.08 (the standard deviation of quantifications of triplicates). The degradation of the alginate chain by acid hydrolysis to reduce the viscosity prior to NMR measurement may possibly contribute to this error, since the rate at which the different linkages are cleaved increases in the order: G-G < M-M < M-G < G-M.[7,25,26] Consequently, G-units and M-units will occur at higher frequencies than expected at the reducing and non-reducing ends, respectively, and the homopolymeric G-blocks will be less degraded than the others. Also, it has been shown that different hydrolysis procedures may result in different M/G ratio values.[11,27] Another issue that must be considered when discussing error sources using solution-state NMR for the analysis of alginates is the possible selective micro-aggregation when divalent cations (e.g. calcium ions) are present. This issue will be discussed further in Section 3.3.

3.2 Calibration models

Calibration models for prediction of the M/G ratio from the raw and EISC-corrected Raman spectra of the alginate powders were developed using PLSR. The relatively high number of samples available allowed for true test-set validation. Therefore, the calibration models were validated using a test-set consisting of every fourth sample which were selected prior to development of the calibration model, but after the samples were sorted according to M/G ratio. Figure 2 shows the M/G ratio of the 75 calibration samples and 25 test samples ordered according to the M/G ratio. Also, three additional samples with a higher calcium ion content (1.1-2.4%) than the other samples are shown. These samples are not used in the development of the calibration models, but for illustration of the effect of higher calcium content in the samples (Section 3.3). Models were thus developed using internally segmented cross-validation (10 segments) on the calibration set (75 samples) and afterwards applied and tested using the independent test-set (25 samples).

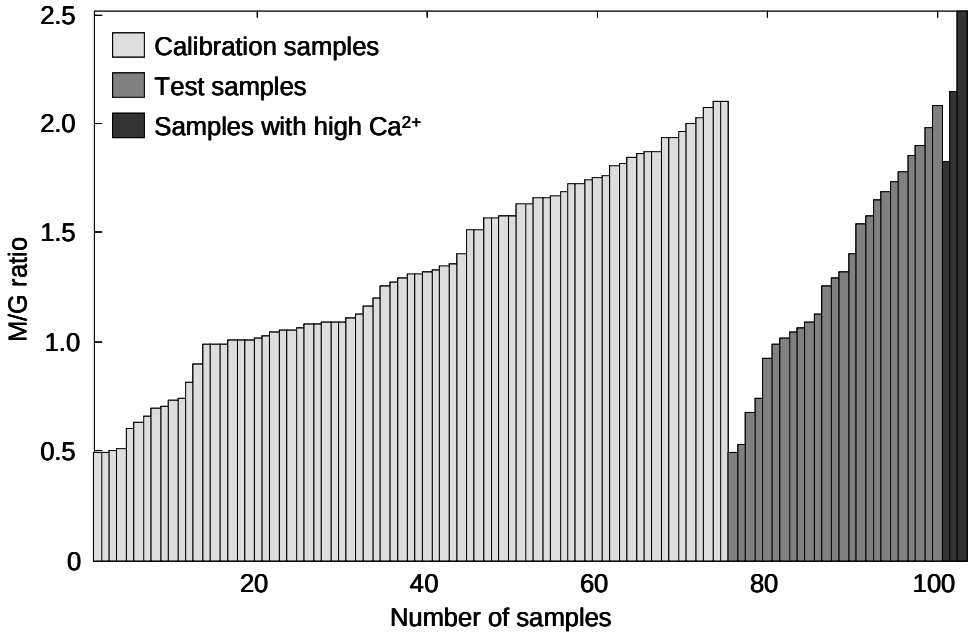

Figure 2 *M/G ratio of the 75 calibration samples, the 25 test samples and three samples with a higher calcium ion content than the other samples*

The raw Raman spectra of the 75 calibration samples are shown in Figure 3a. The spectra show some additive and multiplicative effects due to differences in, for example, particle size, packing density and fluorescence. These differences in the spectra are a result of physical differences between the samples, which are not interesting with respect to the purpose of this work where the chemical composition of the alginates is in focus. Therefore, it is preferable to filter away these effects so that they do not disturb the analysis. Different pre-processing techniques can be used for this purpose. The result of pre-processing the Raman spectra with the EISC technique is shown in Figure 3b. The spectra are coloured according to the M/G ratio and from a visual inspection of the EISC-corrected Raman spectra it is clear that there are several bands in the spectra that contain information about the M/G ratio. The intensity of the bands at 1412, 1090, 955 and 708 cm^{-1} increases with increasing M/G ratio and the intensity of the bands at 1313, 1232, 884 and 806 cm^{-1} decreases with increasing M/G ratio.

Figure 3c shows the measured versus predicted plot from the model based on the raw Raman spectra. The prediction error (RMSEP) of the model was 0.12 and relatively many PLS components (4) were needed in order to deal with the additive and multiplicative effects of the spectra. Using instead the EISC-corrected spectra only containing the chemical information of the spectra, a simpler model with only one PLS component and a lower prediction error was obtained (Figure 3d). The model based on the EISC-corrected Raman spectra resulted in a prediction error of 0.08, which is comparable to the upper limit of the experimental error of the M/G ratio measurements, which also was 0.08.

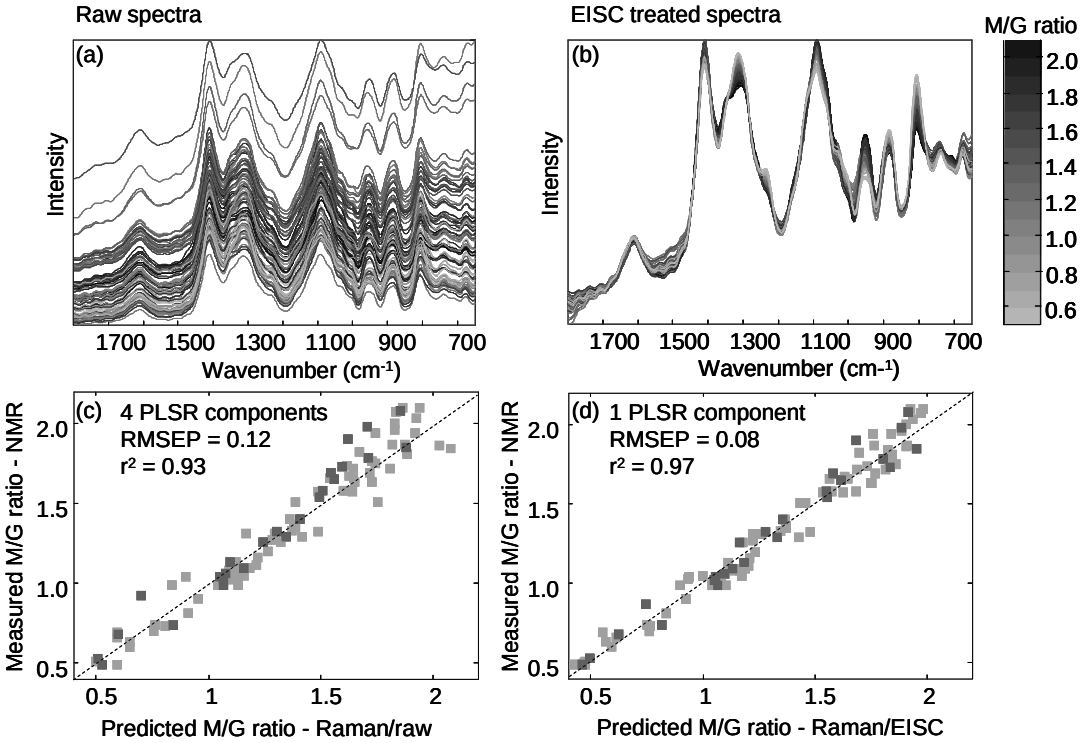

Figure 3 *Raw (a) and EISC-corrected (b) Raman spectra of the 75 calibration samples. M/G ratio measured by NMR versus M/G ratio predicted from the raw (c) and EISC-corrected (d) Raman spectra of the 75 calibration (■) and 25 test (■) samples.*

Variable selection by interval PLSR (iPLSR) was applied to encircle the significant regions in the Raman spectra with respect to the M/G ratio and to test the possibility of developing optimised local PLSR models for prediction of the M/G ratio using fewer variables. The iPLSR approach was applied to the EISC-corrected Raman spectra and different numbers of variables (5, 10, 25 and 50) in the spectral intervals were tested. The results of iPLSR of the EISC-corrected Raman spectra of the 75 calibration samples with 50 variables in each interval (23 intervals) are presented together with the spectra of two samples with extreme M/G ratio values in Figure 4. The models were validated with segmental cross-validation using 10 segments. The cross-validated prediction errors (RMSECV) for each of the 23 intervals are presented as bars and the prediction error of the global model is presented as a horizontal dotted line. The correlation coefficient (r^2) of each sub-model is also shown (connected dots). All models were calculated using one PLSR component and only one spectral region (850-800 cm^{-1}) containing the band due to

the α-configuration of the G-units resulted in a calibration error equal to the error of the full-spectrum model. This region was also identified by visual inspection as the most influential spectral band (Figure 3b) for differentiating between alginates with high and low M/G ratio. When using intervals with 5, 10 and 25 variables, this region was also identified as the most important region for prediction of the M/G ratio. However, when testing the prediction performance (RMSEP) of the models based on this interval only using the 25 test samples, it resulted in higher prediction errors (0.10) than for the full-spectrum model (0.08).

In summary, iPLSR has been used to show and confirm the relevant areas of the spectra. However, it was not possible to develop models based on fewer variables with a better prediction performance than the full-spectrum model.

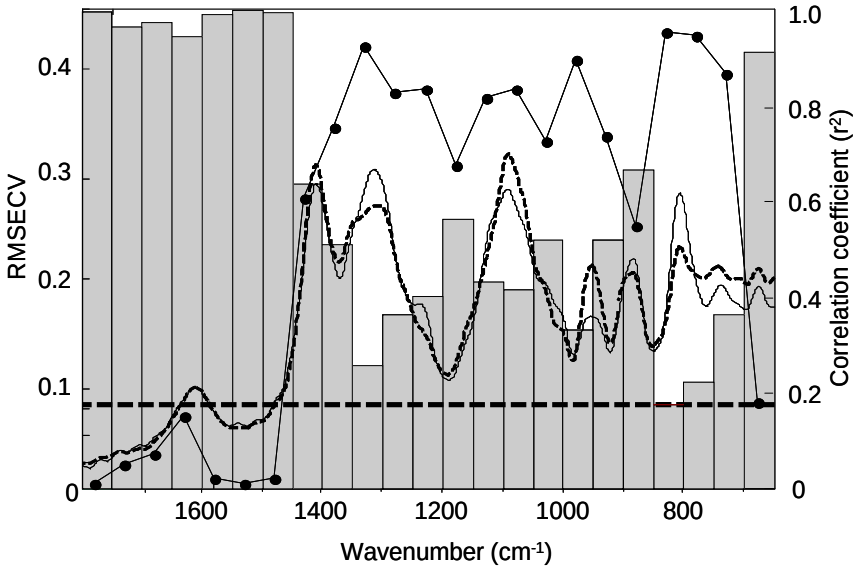

Figure 4 *Interval PLSR results. Cross-validated prediction performance (RMSECV) for 23 PLSR interval models (bars) and for the full-spectrum model (- -) based on the EISC-corrected Raman spectra of the 75 calibration samples plotted together with the correlation coefficients (•) and spectra of two alginates with M/G ratios of 0.5 (—) and 2.1 (- -). All models are based on one PLSR component.*

3.3 Alginate with high calcium ion content

It is well known that calcium ions preferentially bind to G-blocks, resulting in gel formation.[28,29] Consequently, the apparent viscosity of alginates with a certain amount of residual calcium ions will be higher than expected and thus not correlated to the molecular weight, as is usually seen (Figure 5a). The spectra obtained by solution-state NMR will also be affected by higher calcium ion content because of the restricted motion of the G-blocks, as increase in viscosity reduces the relaxation times, giving rise to a broadening of the NMR lines beyond the level of detection. This will result in an underestimation of the G content and thereby overestimation of the M/G ratio. Figure 5b shows the M/G ratio measured by NMR versus the M/G ratio predicted using the model based on the EISC-corrected Raman spectra of three samples with higher calcium ion content (1.1%, 1.4% and 2.4%) than the samples used in the model development (< 0.25%). It is clear that the M/G

ratio measured by NMR is higher than the predicted M/G ratio. Thus, the developed Raman model acts as a kind of evidence that the M/G ratio estimated from the NMR measurements are not correct. This emphasises the need for development of a M/G ratio reference method that will not be affected by the presence of different amounts of counter ions. A potential candidate for this, which we intend to investigate in the future, could be solid-state ^{13}C cross-polarisation (CP) MAS NMR, where the destructive and time-consuming hydrolysis procedure necessary for solution-state NMR can be avoided.

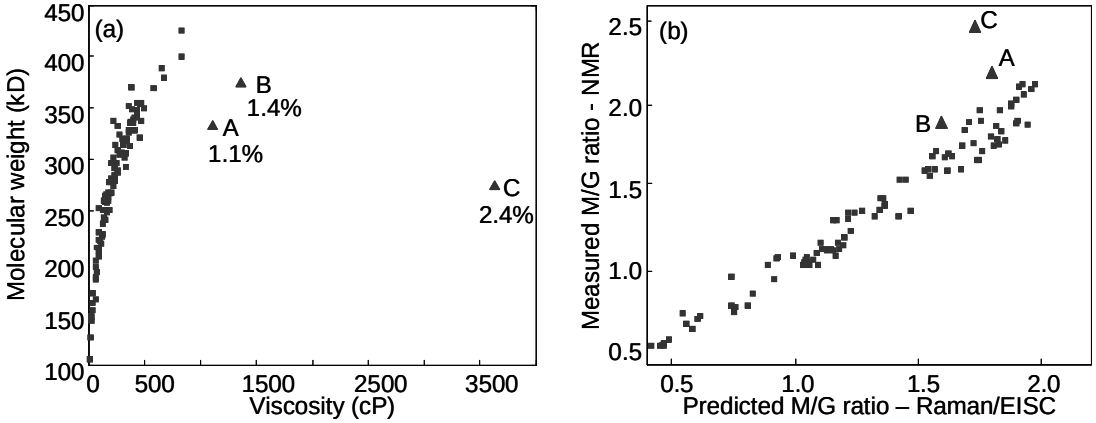

Figure 5 *Comparison of viscosity and molecular weight (a) and M/G ratio measured by NMR with the M/G ratio predicted using the model based on the EISC-corrected Raman spectra (b) of samples with higher calcium ion content*

4 CONCLUSIONS

The present investigation has shown that it is possible to develop a rapid, non-destructive and robust quantitative method for measuring the monomer composition (M/G ratio) of commercial alginate powders using Raman spectroscopy and chemometrics. Spectral pre-processing was applied in order to remove the spectral features not related to the chemical composition of the samples, resulting in a very simple model using only one PLSR component and with a prediction error (RMSEP) of 0.08 and a correlation coefficient of 0.97, which is comparable to the standard deviation of the NMR reference method (0.01-0.08). This is a valuable achievement, since Raman spectroscopy in contrast to IR spectroscopy can be implemented directly at the production lines using optical quartz fibres, thus enabling fast monitoring of the alginate M/G ratio of industrial production batches. Moreover, the Raman method gives more reliable results than the reference method for samples with high calcium content.

4 ACKNOWLEDGEMENTS

The authors wish to thank the Ministry of Science, Technology and Innovation for partly sponsoring the Industrial PhD project conducted by Tina Salomonsen in co-operation with Danisco A/S and Quality & Technology, Department of Food Science, Faculty of Life Sciences (LIFE) at the University of Copenhagen. Gilda Kischinovsky is acknowledged for proofreading the manuscript.

References

1 A. Haug, S. Myklesta, B. Larsen and O. Smidsrød, *Acta Chem. Scand.*, 1967, **21**, 768.
2 C.A. Steginsky, J.M. Beale, H.G. Floss and R.M. Mayer, *Carbohydr. Res.*, 1992, **225**, 11.
3 B.T. Stokke, O. Smidsrød, P. Bruheim and G. Skjåk-Bræk, *Macromolecules*, 1991, **24**, 4637.
4 A. Haug, B. Larsen and O. Smidsrød, *Carbohydr. Res.*, 1974, **32**, 217.
5 M. Indergaard, G. Skjåk-Bræk and A. Jensen, *Botanica Marina*, 1990, **33**, 277.
6 B. Stockton, L.V. Evans, E.R. Morris, D.A. Powell and D.A. Rees, *Botanica Marina*, 1980, **23**, 563.
7 H. Grasdalen, B. Larsen and O. Smidsrød, *Carbohydr. Res.*, 1979, **68**, 23.
8 H. Grasdalen, B. Larsen and O. Smidsrød, *Carbohydr. Res.*, 1981, **89**, 179.
9 H. Grasdalen, *Carbohydr. Res.*, 1983, **118**, 255.
10 H. Grasdalen, B. Larsen and O. Smidsrød, *Carbohydr. Res.*, 1977, **56**, C11.
11 A. Penman and G.R. Sanderson, *Carbohydr. Res.*, 1972, **25**, 273.
12 L. Dolmatova, C. Ruckebusch, N. Dupuy, J.P. Huvenne and P. Legrand, *Applied Spectroscopy*, 1998, **52**, 329.
13 M. Dyrby, R.V. Petersen, J. Larsen, B. Rudolf, L. Nørgaard and S.B. Engelsen, *Carbohydr. Polym.*, 2004, **57**, 337.
14 S.B. Engelsen and L. Nørgaard, *Carbohydr. Polym.*, 1996, **30**, 9.
15 M.P. Filippov and R. Kohn, *Chemicke Zvesti*, 1974, **28**, 817.
16 W. Mackie, *Carbohydr. Res.*, 1971, **20**, 413.
17 K. Sakugawa, A. Ikeda, A. Takemura and H. Ono, *Journal of Applied Polymer Science*, 2004, **93**, 1372.
18 T. Salomonsen, H.M. Jensen, D. Stenbæk and S.B. Engelsen, *Carbohydrate Polymers*, 2007 submitted.
19 W. Mackie, R. Noy and D.B. Sellen, *Biopolymers*, 1980, **19**, 1839.
20 S. Wold, H. Martens and H. Wold, *Lecture Notes in Mathematics*, 1983, **973**, 286.
21 H. Martens, J.P. Nielsen and S.B. Engelsen, *Analytical Chemistry*, 2003, **75**, 394.
22 D.K. Pedersen, H. Martens, J.P. Nielsen and S.B. Engelsen, *Applied Spectroscopy*, 2002, **56**, 1206.
23 L. Nørgaard, A. Saudland, J. Wagner, J.P. Nielsen, L. Munck and S.B. Engelsen, *Applied Spectroscopy*, 2000, **54**, 413.
24 A. Savitzky and M.J.E. Golay, *Analytical Chemistry*, 1964, **36**, 1627.
25 H.K. Holme, K. Lindmo, A. Kristiansen and O. Smidsrød, *Carbohydr. Polym.*, 2003, **54**, 431.
26 O. Smidsrød, B. Larsen, T. Painter and A. Haug, *Acta Chem. Scand.*, 1969, **23**, 1573.
27 M. Shinohara, R. Nishida, T. Aoyama, H. Kamono, H. Bando and M. Nishizawa, *Fisheries Science*, 2000, **66**, 616.
28 K.I. Draget, B. Strand, M. Hartmann, S. Valla, O. Smidsrød and G. Skjåk-Bræk, *Int. J. Biol. Macromol.*, 2000, **27**, 117.
29 G.T. Grant, E.R. Morris, D.A. Rees, P.J.C. Smith and D. Thom, *FEBS Lett.*, 1973, **32**, 195.

Alginate monomer composition studied by solution- and solid-state NMR – a comparative chemometric study

T. Salomonsen, H.M. Jensen, F.H. Larsen, S. Steuernagel & S.B. Engelsen

Food Hydrocolloids, 23, (2009) 1579-1586.

PAPER IV

Food Hydrocolloids 23 (2009) 1579–1586

Contents lists available at ScienceDirect

Food Hydrocolloids

journal homepage: www.elsevier.com/locate/foodhyd

Alginate monomer composition studied by solution- and solid-state NMR – A comparative chemometric study

Tina Salomonsen [a,b,*], Henrik Max Jensen [b], Flemming Hofmann Larsen [a], Stefan Steuernagel [c], Søren Balling Engelsen [a]

[a] University of Copenhagen, Faculty of Life Sciences, Department of Food Science, Quality & Technology, Rolighedsvej 30, 1958 Frederiksberg C, Denmark
[b] Danisco A/S, Advanced Analysis, Edwin Rahrs Vej 38, 8220 Brabrand, Denmark
[c] Bruker-Biospin GMBH, 76287 Rheinstetten, Germany

ARTICLE INFO

Article history:
Received 31 August 2008
Accepted 12 November 2008

Keywords:
Alginate
Calcium
Nuclear magnetic resonance
CP-MAS NMR
HR-MAS NMR
Chemometrics

ABSTRACT

The potential of using ^{1}H high-resolution (HR) magic angle spinning (MAS) nuclear magnetic resonance (NMR) of alginates suspended in D_2O or ^{13}C cross-polarisation (CP) MAS NMR of alginate powders as an alternative method to the traditional ^{1}H solution-state NMR method for the analysis of the alginate monomer composition (mannuronate (M)/guluronate (G) ratio) has been investigated. The MAS NMR experiments can be performed directly on the intact alginate powders and thereby avoiding the relatively time-consuming and labour intensive sample preparation required for the traditional solution-state experiment. A total of 42 different sodium alginate samples were analysed and it was found that the M/G ratio derived from the HR-MAS NMR spectra were comparable to the M/G ratio calculated from the solution-state NMR spectra. However, both these methods overestimated the M/G ratio of samples with high calcium content. In contrast, the ^{13}C CP-MAS NMR spectra were not affected by residual calcium in the samples and thus provided more consistent measurements independent on physico-chemical phenomena such as partial solubility, viscosity and interactions with ions. It is concluded that ^{13}C CP-MAS NMR is a most suitable candidate for accurate analysis of the M/G ratio of intact alginate powders.

1. Introduction

Alginates are commercially extracted from brown seaweed (*Phaeophyceae*) and utilised in the food and pharmaceutical industries because of their gelling, viscosifying and stabilising properties (Draget, Moe, Skjåk-Bræk, & Smidsrød, 2006). From a structural point of view, alginates are linear polysaccharides composed of (1–4) linked β-D-mannuronic acid (M) and α-L-guluronic acid (G) arranged in a blockwise pattern along the chain as homopolymeric (MM or GG) or heteropolymeric (MG) regions. The M/G ratio and blockwise pattern vary according to season, age of population, species and geographic location (Haug, Larsen, & Smidsrød, 1974; Indergaard, Skjåk-Bræk, & Jensen, 1990; Stockton, Evans, Morris, Powell, & Rees, 1980) and are correlated to the functional properties of the alginates, i.e. solubility, interaction with metal ions, gel properties and viscosity (Haug, Myklesta, Larsen, & Smidsrød, 1967; Steginsky, Beale, Floss, & Mayer, 1992; Stokke, Smidsrød, Bruheim, & Skjåk-Bræk, 1991). Therefore, access to reliable methods for compositional analysis of alginates is essential, and for screening of large sample sets and quality control, rapid analytical methods requiring limited sample preparation are of great importance.

^{1}H nuclear magnetic resonance (NMR) spectroscopy has proven to be highly effective in the characterisation of alginates in solution (Grasdalen, 1983; Grasdalen, Larsen, & Smidsrød, 1979; Penman & Sanderson, 1972). However, at the concentrations suitable for an acceptable signal-to-noise ratio, alginate solutions are too viscous to give well-resolved spectra. Thus, the viscosity must be lowered by partial acid hydrolysis of the alginate chain, which is a relatively time-consuming and labour intensive procedure and perhaps more important the hydrolysis will alter the sample significantly compared to the intact sample. Another issue related to the analysis of alginates in solution is the possible selective micro-aggregation when divalent cations (e.g. calcium ions) are present. Calcium ions preferentially bind to the G-blocks (Draget et al., 2000; Grant, Morris, Rees, Smith, & Thom, 1973), resulting in G-block association and the formation of a gel network. This can give rise to a broadening of the ^{1}H NMR resonances originating from the G-units beyond the level of detection (Grasdalen, Larsen, & Smidsrød, 1981), resulting in an overestimation of the M/G ratio.

* Corresponding author. University of Copenhagen, Faculty of Life Sciences, Department of Food Science, Quality & Technology, Rolighedsvej 30, 1958 Frederiksberg C, Denmark. Tel.: +45 8943 5285, +45 3533 3510; fax: +45 8925 1077.
E-mail addresses: tina.salomonsen@danisco.com, tisa@life.ku.dk (T. Salomonsen).

0268-005X/$ – see front matter © 2008 Elsevier Ltd. All rights reserved.
doi:10.1016/j.foodhyd.2008.11.009

In a recent study we showed that vibrational spectroscopy (infrared, Raman and near infrared) can be used for rapid prediction of the M/G ratio (Salomonsen, Jensen, Stenbæk, & Engelsen, 2008a). A calibration model between the M/G ratio calculated from solution-state NMR spectra and the respective vibrational spectra of the alginate powder could be established, allowing for future predictions of the M/G ratios with practically no sample preparation requirements. Thus, the time of analysis was reduced from days to minutes. However, the new spectroscopic method is dependent on a reliable reference method for measurement of the M/G ratio, since the performance of the calibration model is dependent on the quality of the reference values. In the course of the development of the calibration models inconsistencies between the M/G ratios calculated from the solution-state NMR spectra and the values predicted from the vibrational spectra were found for samples with high residual amounts of calcium ions (Salomonsen, Jensen, Stenbæk, & Engelsen, 2008b). In the present study, the possibility of measuring the M/G ratio of intact alginates in semi-solid- (swollen polymer) and solid-state (powder) by NMR, while maintaining the structural integrity of the sample, is investigated.

When measuring semi-solid and solid samples by NMR, line broadening effects due to chemical shift anisotropy (CSA) and dipolar broadening (homonuclear (^{1}H–^{1}H) and heteronuclear (^{1}H–^{13}C)) are dominant features in the spectra as opposed to liquid samples, where these effects are averaged out to zero. However, it is possible to obtain well-resolved ^{1}H NMR spectra of semi-solid samples by using magic angle spinning (MAS) (Andrew, Bradbury, & Eades, 1958, 1959), where the sample is spun fast around an axis tilted by 54.7° (the so-called magic angle) relative to the static magnetic field. Hereby, minor CSA and dipolar interactions will be averaged to zero, resulting in a well-resolved spectrum. In solids, the ^{1}H nuclei exhibit very strong homonuclear dipolar couplings, which demands for MAS spin-rates in excess of 40 kHz (Samoson, Tuherm, & Gan, 2001). At standard spin-rates (below 20 kHz) the homonuclear dipolar coupling will only be partly averaged by spinning, resulting in severe broadening of resonances in the spectra. Thus, when measuring solids it is more advantageous to observe the ^{13}C nuclei, as the homonuclear dipolar couplings between natural abundance ^{13}C nuclei are unobservable and the heteronuclear ^{1}H–^{13}C couplings can be removed by high power ^{1}H decoupling. The disadvantages of observing the rare ^{13}C nucleus is the lower sensitivity and longer T_1 relaxation times. However, these can be overcome by transferring magnetisation from ^{1}H to ^{13}C nuclei using the cross-polarisation (CP) technique (Pines, Gibby, & Waugh, 1973; Pines, Waugh, & Gibby, 1972). Thus, using CP-MAS and high power decoupling enables one to acquire fairly well-resolved ^{13}C NMR spectra of solid samples.

The potential of using ^{13}C CP-MAS NMR in the study of polysaccharides has been demonstrated for the analysis of powders and gels of carrageenan (Gordon-Mills, 1990; Hoffmann, Gidley, Cooke, & Frith, 1995; Rochas & Lahaye, 1989; Saito, Yokoi, & Yamada, 1990), agarose (Gordon-Mills, 1990; Rochas & Lahaye, 1989; Saito et al., 1990), pectin (Jarvis & Apperley, 1995; Sinitsya, Copikova, & Brus, 2003; Sinitsya, Copikova, & Pavlikova, 1998), starch (Baianu & Förster, 1980; Colquhoun, Parker, Ring, Sun, & Tang, 1995; Kulik & Haverkamp, 1997) and cellulose (Hoffmann et al., 1995; Larsson, Hult, Wickholm, Pettersson, & Iversen, 1999). Also, a ^{13}C CP-MAS study on alginate has been perfomed in which two different alginates were examined (Llanes, Sauriol, Morin, & Perlin, 1997). Although the spectra consisted of broad strongly overlapping peaks, the M/G ratio could be calculated from the spectra by curve fitting. However, for one of the samples, the calculated M/G ratio of 1.2 deviated significantly from the value of 2.5 obtained from the ^{1}H solution-state NMR spectra of the corresponding acid hydrolysed sample. A clear indication that at least one of the methods suffers from being strongly influenced by artefacts related to the sample preparation procedure or the data interpretation.

The purpose of this study was to investigate the potential of using ^{1}H high-resolution (HR) magic angle spinning (MAS) NMR of alginates suspended in D_2O or ^{13}C CP-MAS NMR of powders as an alternative method for the determination of the M/G ratio in alginates. The spectra were explored by different chemometric techniques and compared with the results from ^{1}H solution-state NMR.

2. Materials and methods

2.1. The samples

42 different commercial sodium alginate samples were kindly provided by Danisco A/S (Brabrand, Denmark) as powders with a particle size of $\leq$106 μm. The samples were selected so that they varied as much as possible within the M/G ratio range of 0.4–2.1 (determined by ^{1}H solution-state NMR).

2.2. NMR spectroscopy

2.2.1. ^{1}H solution-state NMR

The ^{1}H NMR spectra of alginate in solution were recorded on a Bruker Avance™ 400 spectrometer (Bruker Biospin Gmbh, Rheinstetten, Germany) operating at 400.13 MHz for ^{1}H using a 5 mm broadband inverse probe head. Prior to analysis, the average molecular weight of the alginate was reduced by a mild partial acid hydrolysis performed in two steps. 0.5 g alginate moistened with 5 ml ethanol (96%) was dissolved in 50 ml HCl (pH 1.5). The pH was adjusted to 5.0 by addition of NaOH and hydrolysed at 100 °C under reflux for 10 min. After cooling to room temperature, the pH was adjusted to 3.0 by addition of HCl and heated at 100 °C under reflux for 20 min. After cooling, the solution was neutralised (pH 7) by addition of NaOH and precipitated in ethanol (96%). The precipitate was left for drying over night at 70 °C. The hydrolysed alginate was dissolved in D_2O (1.0% (w/v)), neutralised (pH 7) and 550 μl of the solution was filtered through a Whatman 13 mm syringe filter (pore size 0.45 μm) into a 5 mm NMR tube. The spectra were recorded with a 30° pulse angle and a sweep width of 8278 Hz. The acquisition time and recycle delay were both 4 s. 32 scans were acquired and the spectra were recorded with the same receiver gain. During acquisition, the sample temperature was 90 °C. 3-(trimethylsilyl)propionic acid-d_4 sodium salt (TSP-d4) was used as chemical shift reference compound ($\delta = 0.0$ ppm). The raw data were apodized by 1.0 Hz of exponential line broadening prior to Fourier transformation. No zero filling was applied.

2.2.2. ^{1}H HR-MAS NMR

The ^{1}H HR-MAS NMR spectra of swollen alginate were recorded on a Bruker Avance™ 400 spectrometer (Bruker Biospin Gmbh, Rheinstetten, Germany) operating at 400.13 MHz for ^{1}H using a 4 mm HR-MAS probe head. 45 μl D_2O was added to the alginate powder (2 mg) in a 4 mm ZrO_2 rotor. To optimise the sensitivity of the probe, the rotor was fitted with Teflon inserts to define a 50 μl volume. The samples were spun at 6 kHz and the spectra were recorded with a 30° pulse angle and a sweep width of 10,482 Hz. The acquisition time and recycle delay were 1.6 s and 4 s, respectively. 16 scans were acquired and the spectra were recorded with the same receiver gain. During acquisition, the sample temperature was 90 °C. 3-(trimethylsilyl)propionic acid-d_4 sodium salt (TSP-d4) was used as chemical shift reference compound ($\delta = 0.0$ ppm). The raw data were zero filled to 64 K data points and apodized by 1.0 Hz of exponential line broadening prior to Fourier transformation.

2.2.3. ^{13}C CP-MAS NMR

^{13}C CP-MAS NMR spectra of alginate powder were recorded on a Bruker Avance™ III 500 spectrometer (Bruker Biospin Gmbh, Rheinstetten, Germany) operating at 125.77 MHz for ^{13}C and 500.12 MHz for ^{1}H using a 4 mm CP-MAS probe head. Alginate powder (approximately 40 mg) was packed in a Zirconia rotor and spun at 15 kHz. The spectra were recorded with a sweep width of 62.5 kHz. The acquisition time, recycle delay and contact time were 10 ms, 2 s and 2 ms, respectively. 1024 scans were acquired and the spectra were recorded with the same receiver gain. All spectra were externally referenced to the carbonyl peak of glycine at 176.03 ppm. The raw data were zero filled to 4 K data points prior to Fourier transformation. No line broadening was applied.

2.3. Viscosity

The apparent viscosity of the intact alginates in solution (1% (w/w)) was measured using a Brookfield LVT viscosimeter (Brookfield, Essex, UK). The solutions were prepared with demineralised water and left to equilibrate for 2 h at 20 °C before measurement. The viscosity was read after 30 s at 60 rpm. LV1, LV2 and LV3 spindles were used for samples with a viscosity of <100 cP, 100–500 cP and >500 cP, respectively.

2.4. Molecular weight

The average molecular weight (M_w) in the intact alginates was determined by size exclusion chromatography with multiangle light scattering (SEC-MALS) using two columns (PSS SUPREMA-LUX 3000 Å and PSS SUPREMA-LUX 1000 Å, Polymer Standard Service GmbH, Mainz, Germany) in series as well as a DAWN EOS multi-angle light scattering photometer and an Optilab rEX differential refractive index detector (both Wyatt Technology Corp., Santa Barbara, California, USA). The columns and the detectors were thermostated to 40 °C. The mobile phase was 0.05 M $LiNO_3$/200 ppm NaN_3 at a flow rate of 0.8 ml/min. Alginate was dissolved in the mobile phase (0.2 % (w/v)) and 100 μl of this solution was injected into the columns. Data were analysed using Astra V software (Wyatt Technology Corp., Santa Barbara, California, USA). The refractive increment value (dn/dc) for alginate was set to 0.154 ml/g (Mackie, Noy, & Sellen, 1980). Each sample was measured as a true replicate, and the average values were used in the data analysis.

2.5. Determination of Na and Ca

The contents of Na and Ca in the sodium alginate powders were determined by inductively coupled plasma optical emission spectrometry (ICP-OES) using a Varian Vista-MPX ICP-OES instrument (Varian, Inc., Palo Alto, California, USA). The sodium alginate powders (2 mg) were calcinated for 4 h at 550 °C and thereafter dissolved in 3 ml concentrated HNO_3 and diluted with 23 ml Milli-Q water. The calibration standards were prepared from single-elemental standard solutions (1000 mg/l, Merck, Darmstadt; Germany) in the range of 0.1–10 mg/l. The wavelengths used for measurement of Na and Ca were 589.592 nm and 393.366 nm, respectively. The instrumental operating conditions are listed in Table 1.

Table 1
Instrumental conditions employed in the ICP-OES analysis.

Parameter	Value
RF power (kW)	1.20
Plasma flow (l/min)	15
Nebuliser flow (l/min)	0.80
Pump rate (rpm)	15
Rinse time (s) 10	10
Auxiliary flow (l/min)	1.5
Replicates	3
Replicate read time (s)	5
Instrument stabilisation (s)	15
Sample uptake delay (s)	30

2.6. Chemometric analysis

Principal component analysis (PCA) (Hotelling, 1933) was used for unsupervised analysis of the NMR spectra. PCA is the primary tool for investigation of large bilinear data structures for the study of trends, groupings and outliers. By means of PCA it is possible to find the main variation in a multidimensional data set by creating new linear combinations from the underlying latent structures in the raw data. The two-dimensional data matrix (samples × variables) is decomposed into systematic variation and noise. The systematic variation is described by the principal components (PC1, PC2 etc.), each representing the outer product of scores and loadings. The scores contain information about the samples, and the loadings contain information about the variables.

Partial least squares regression (PLSR) (Wold, Martens, & Wold, 1983) was used for supervised analysis of the NMR spectra. PLSR is a multivariate calibration method by which two sets of data, X (e.g. spectra) and y (e.g. M/G ratio), are related by means of regression. The purpose of PLSR is to establish a linear model which enables the prediction of y from the measured spectrum X. PLSR is a two-block regression method, where the decomposition of X is performed under the consideration of y in a simultaneous analysis of the two data sets. All data sets were mean centred (i.e. the mean of each variable was subtracted from the original measurement) prior to model development. The PLSR models were validated using segmented cross-validation (6 segments) on the 42 samples and compared on the basis of the validation parameters: root mean square error of cross-validation (RMSECV), squared correlation coefficient (r^2) and the optimal number of PLS components (#PLS comp). The PCA and PLSR analyses were performed using LatentiX version 2.0 (Latent5, Copenhagen, Denmark, http://www.latentix.com).

3. Results and discussion

3.1. Physico-chemical properties of the alginates

The 42 sodium alginates analysed in this study had an average molecular weight (M_w) in the range of 56–424 kDa and an apparent viscosity in the range of 8–846 cP for samples with low (<0.02 calcium content) and 1142–3619 cP for samples with high calcium content (1.1–2.4%). A scatter plot of the viscosity and M_w of the intact alginates is shown in Fig. 1. The samples are coloured according to the calcium content in the samples. Three samples were found to contain considerably higher amounts of calcium (1.1%, 1.4% and 2.4%) than the rest of the samples (0.01–0.2%). The content of sodium were found to be in the range of 5.0–8.1% and in the samples with calcium contents of 1.1%, 1.4% and 2.4% the sodium content was 7.5%, 6.1% and 5.0%, respectively. The presence of calcium ions will promote gel formation (Draget et al., 2000; Grant et al., 1973) and increase the viscosity. Consequently, the measured viscosity of the samples with high calcium content were higher than expected and thus not correlated to the molecular weight as samples with low calcium content (Fig. 1).

3.2. ^{1}H NMR spectra of alginate in solution- and swollen-state

Acquisition of a ^{1}H NMR spectrum of a semi-solid sample such as swollen alginate using a conventional solution-state NMR probe will result in a spectrum with broad overlapping lines due to

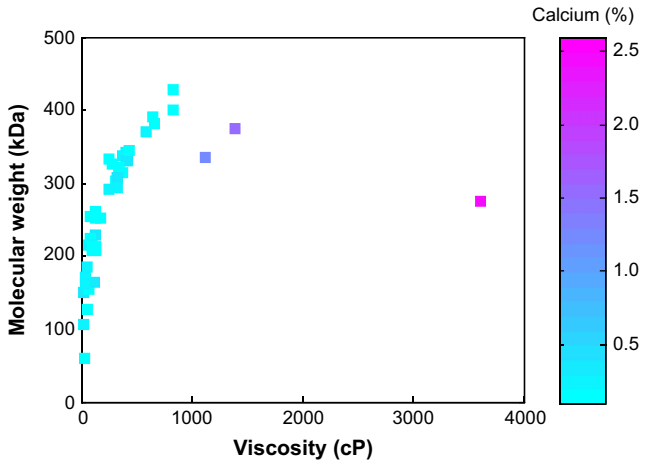

Fig. 1. Scatter plot of viscosity and molecular weight of the 42 sodium alginates. The samples are coloured according to calcium content.

chemical shift anisotropy (CSA) and homonuclear dipolar interactions caused by the restricted mobility in the sample. However, using MAS to average out minor CSA and dipolar interactions will result in a well-resolved ^{1}H spectrum. This effect is illustrated in Fig. 2, where the carbohydrate regions of the ^{1}H NMR spectra of an alginate sample in solution- and in swollen-state are presented. The resolution of the HR-MAS spectra of the swollen alginate is comparable to the resolution of the spectra of the dissolved hydrolysed alginate. Thus, it can be concluded that it is possible to obtain fairly well-resolved ^{1}H HR-MAS NMR spectra of intact alginates and thereby avoid the destructive and time-consuming acid hydrolysis generally used for analysis of alginates in solution-state.

The anomeric regions of the ^{1}H NMR spectra of the 42 alginate samples in solution- and in swollen-state are presented in Fig. 3a and b, respectively. Assignments of the signals in the anomeric region are well documented (Grasdalen, 1983; Grasdalen et al., 1979; Holtan, Zhang, Strand, & Skjåk-Bræk, 2006). Three distinct signals are observed at 5.07 ppm (A), 4.70 ppm (B) and 4.46 ppm (C) and are assigned to the anomeric proton of G (A), the anomeric proton of M and H-5 of G-units adjacent to M (B), and H-5 of G-units adjacent to G (C), respectively. Thus, in addition to the

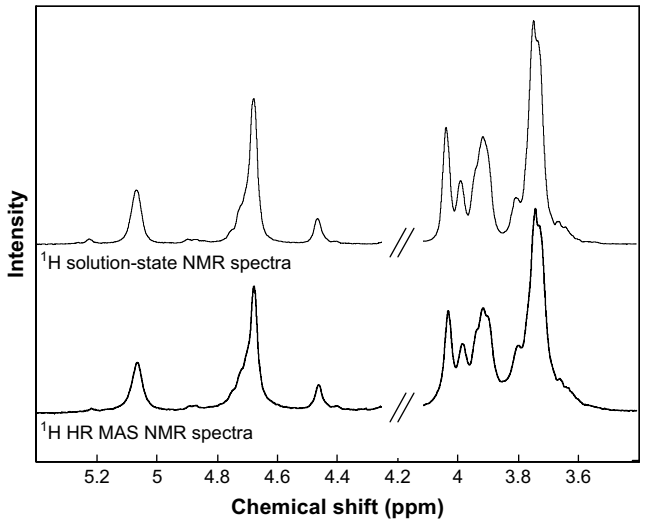

Fig. 2. The carbohydrate region of the ^{1}H solution-state NMR spectra of hydrolysed sodium alginate and ^{1}H HR-MAS NMR spectra of alginate powder soaked in D_2O recorded at 90 °C. The M/G ratio of the sample shown is 1.3. The water resonance (4.3–4.1 ppm) is removed from the spectra.

anomeric protons, the H-5 of G-units also resonates in the anomeric region, because they are less shielded than the other ring protons. Moreover, the deshielding is sequence-dependent and consequently the H-5 of G-units resonates differently, depending on its neighbour. The M/G ratio was calculated from the relative areas in the anomeric region, as described by Grasdalen et al. (1979). The integration limits applied in the calculations of the area of signal A, B and C (Fig. 3a, b) were set to 4.96–5.18 ppm, 4.57–4.82 ppm and 4.38–4.55 ppm, respectively. The M/G ratios calculated from the solution-state spectra of the 42 sodium alginates are shown in Fig. 4. The samples are ordered according to the calculated M/G ratio showing that the samples are almost evenly distributed over the M/G ratio range spanning from 0.4 to 2.1.

As previously mentioned, high calcium ion contents in the samples will in solution-state NMR result in line broadening and shift of proton signals to higher resonance frequencies due to increased viscosity and deshielding of the protons, respectively (Steginsky et al., 1992). These effects are resulting from calcium ion complexation with the hydroxyl and carboxylate groups of the G-blocks and are illustrated in Fig. 3c, where four solution-state spectra with different calcium contents are plotted. Generally, the spectral features of the samples analysed in this study were similar. However, the proton resonances of the three samples with higher calcium content than the rest of the samples were slightly less shielded (0.01–0.03 ppm) as illustrated in Fig. 3c. The M/G ratios calculated from the solution-state spectra of the three different samples with 1.1%, 1.4% and 2.4% calcium were 1.8, 1.5 and 2.1, respectively. However, the M/G ratios calculated from the spectra obtained after addition of sodium hexametaphosphate (chelating agent) were lower (1.6, 1.3 and 1.5, respectively). The M/G ratio of the sample with 0.1% calcium was the same when measured with and without chelator. Obviously, the M/G ratios of the samples with high calcium content are overestimated when not adding a chelator. However, in this comparative study we want to verify if the MAS NMR spectra are also sensitive to residual calcium ions in the samples. Thus, we will use the solution-state M/G ratio values obtained without addition of a chelator when comparing the results.

The resonances in the HR-MAS spectra are not affected to the same extend as the solution-state spectra with respect to the deshielding of the protons with increased calcium content (Fig. 3d). Nevertheless, the M/G ratio of the sample with the high calcium content was estimated to 2.2. Also the other M/G ratios calculated from the ^{1}H HR-MAS spectra were generally in good agreement with the values calculated from the solution-state NMR method (±0.1).

3.3. ^{13}C NMR spectra of alginate powder

The spectral region 50–115 ppm of the ^{13}C CP-MAS NMR spectra of the 42 sodium alginates is presented in Fig. 5, showing the anomeric carbons centred at 101 ppm and the ring carbons in the range of 60–90 ppm. The spectra are coloured according to the M/G ratio, indicating which resonances that are related to M and G. It should be noted that while ^{13}C CP-MAS signals are not internally quantitative, since the efficiency of magnetisation transfer depends on the strength of the dipolar interactions between ^{1}H and ^{13}C, which can be different throughout the molecule, they remain quantitative between samples. Moreover, in alginate molecules the anomeric and ring carbons are so similar in their interaction to protons that the CP dynamics most likely are the same.

Assignment of the observed peaks in Fig. 5 is rather complex due to the broad overlapping peaks. However, supported by assignments of ^{13}C CP-MAS NMR and ^{13}C solution-state NMR spectra made by Llanes et al. (1997) and Grasdalen et al. (1981), Grasdalen, Larsen, and Smidsrød (1977), respectively, together with the

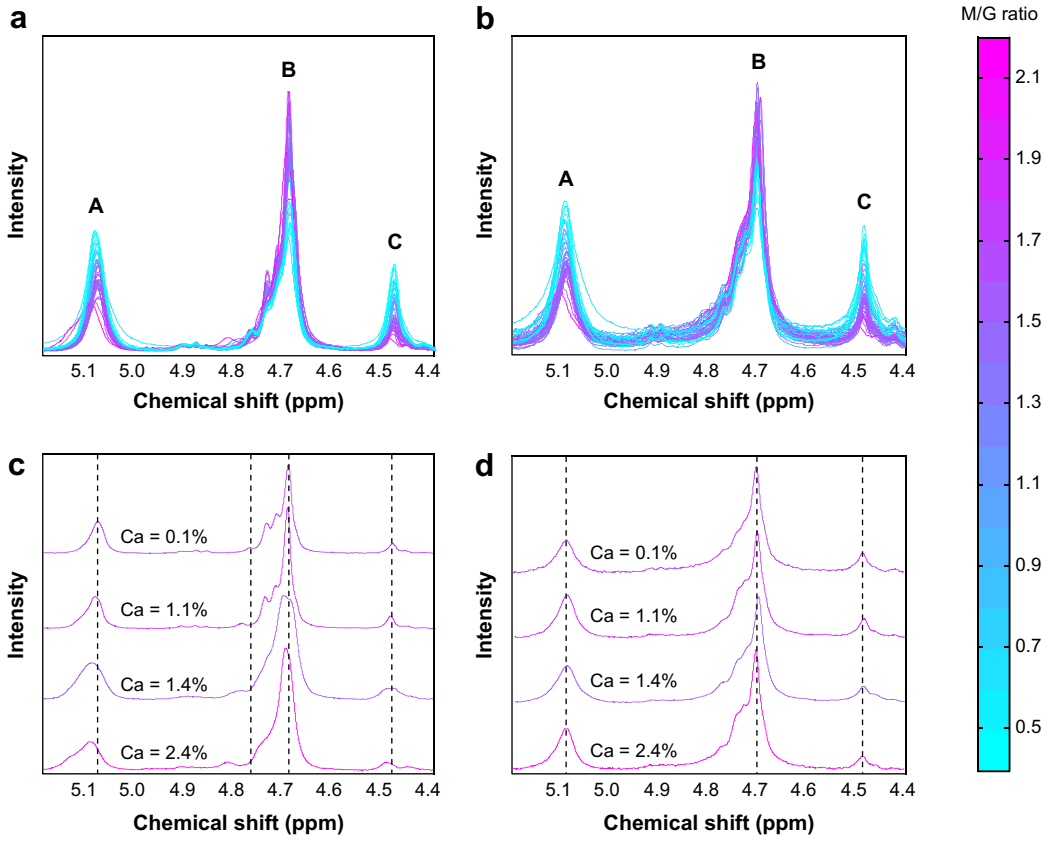

Fig. 3. The anomeric region of the ^{1}H solution-state NMR spectra of the 42 hydrolysed sodium alginates (a) and ^{1}H HR-MAS NMR spectra of the sodium alginate powders soaked in D_2O (b). Spectra of four samples with different calcium contents obtained by solution-state (c) and HR-MAS (d) NMR are shown to illustrate chemical shift differences. The spectra are coloured according to M/G ratio calculated from the ^{1}H solution-state NMR spectra.

variation in the spectra related to the M/G ratio calculated from the solution-state spectra, the resonances were assigned as listed in Table 2. In solution-state NMR, it has been shown that especially the chemical shifts of the anomeric carbons are influenced by the neighbouring residues (Grasdalen et al., 1981). For example, the anomeric carbon of M in mixed sequence (MG) is less shielded than M in the pure sequence (MM) and actually resonates at a higher frequency than the anomeric carbon of G next to a G. Thus, the signal from the anomeric carbon of G next to a G is located between the anomeric carbon M in a MG and MM sequence. However, these effects of neighbouring residues on the chemical shift cannot be observed in the ^{13}C CP-MAS spectra due to the lack of resolution. Thus, the rather sharp signal at 99.5 ppm related to a high M/G ratio is very likely to be the anomeric carbon of M next to another M residue due to its chemical shift and since this sequence becomes more likely to appear when the M/G ratio is high.

3.4. Unsupervised data exploration by PCA

A priori it is known that the main variation in the data is related to the M/G ratio. However, spectral variation such as line broadening and chemical shift differences is also contributing to the spectral variation as previously illustrated. Variations related to the sampling can largely be eliminated by normalising the spectra. Due to different packing densities of the alginate powders it was necessary to normalise the ^{1}H HR-MAS and ^{13}C CP-MAS spectra in order to prepare the data for chemometric analysis. Since the signals in the spectra reflect the amount of the sample actually measured, the ^{1}H HR-MAS NMR and the ^{13}C CP-MAS NMR spectra were normalised by dividing each variable in the spectrum by the total area of the anomeric region (HR-MAS) and the anomeric and ring carbon region (CP-MAS), respectively. This resulted in spectra with the same intensity scale (Figs. 3b and 5).

PCA was applied in order to obtain an overview of the variation in the three sets of NMR data. PCA score plots based on the ^{1}H solution-state, ^{1}H HR-MAS and ^{13}C CP-MAS NMR spectra are shown in Fig. 6a–c, respectively. The samples are coloured according to the M/G ratio calculated by the solution-state NMR method, clearly showing that the main variation in the data are related to the M/G ratio (i.e. the samples are distributed along PC1 that describe

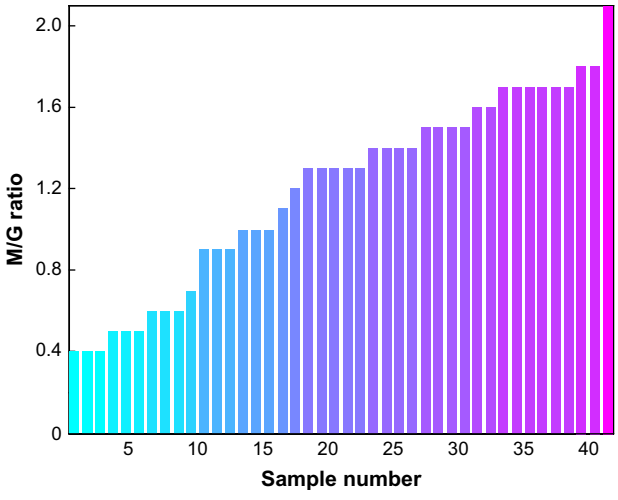

Fig. 4. M/G ratio calculated from the solution-state NMR spectra of the 42 hydrolysed sodium alginates.

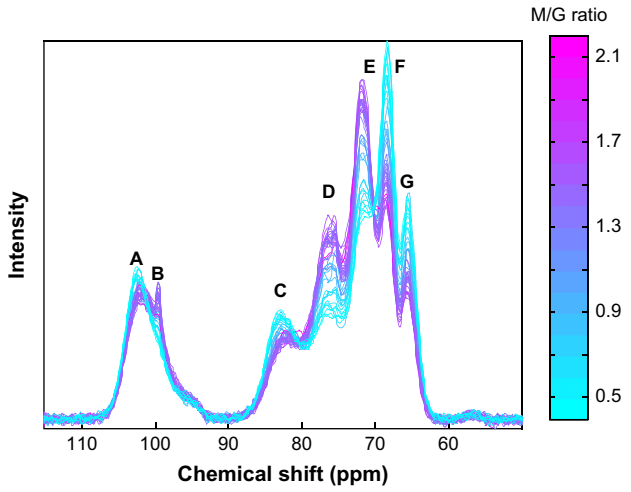

Fig. 5. ^{13}C CP-MAS spectra of the 42 sodium alginate powders. The spectra are coloured according to M/G ratio calculated from the ^{1}H solution-state NMR spectra.

74.9–93.6 % of the total spectral variation with increasing M/G ratio). The variation related to the M/G ratio in the ^{1}H solution-state, ^{1}H HR-MAS and ^{13}C CP-MAS NMR spectra are 74.9%, 86.4% and 93.6%, respectively, and thus the variation not related to the M/G ratio is 25.1%, 13.6% and 6.4%, respectively. Consequently, it can be concluded that the solution-state spectra are influenced more by other factors than the HR-MAS and CP-MAS spectra.

The sample with the highest calcium content (marked with an arrow) is an extreme sample in the score plots based on the solution-state (Fig. 6a) and the HR-MAS spectra (Fig. 6b). The sample was estimated to have the highest M/G ratio from these spectra, which is reflected in the score plots by being the furthest to the right along PC1. In contrast, the same sample is placed together with the samples with M/G ratios of 1.5–1.6 in the score plot based on the CP-MAS spectra. Thus, the M/G ratio value of the sample with a calcium content of 2.4% obtained from the CP-MAS spectra is comparable to the value of 1.5 calculated from the solution-state spectra of the hydrolysed sample when a chelating agent is added. Obviously, the CP-MAS spectra are not affected by residual calcium ions in the samples and thus provide more consistent measurements.

3.5. Supervised data exploration by PLSR

In order to investigate the relation between the M/G ratio calculated from the solution-state NMR spectra (used as reference) and the three sets of multivariate NMR data, calibration models for prediction of the M/G ratio were developed using PLSR. The results

Table 2
Assignments of the ^{13}C CP-MAS NMR resonances of β-D-mannuronic acid (M) and α-L-guluronic acid (G) in Fig. 5.

	Resonance						
	A	B	C	D	E	F	G
Chemical shift (ppm)	102.2	99.5	82.8	76.4	71.6	68.4	65.5
Assignment	G1	M1	G4	M4/M5	M3/M2	G3/G5	G2

from the PLSR models based on the ^{1}H solution-state, ^{1}H HR-MAS and ^{13}C CP-MAS NMR are shown in Fig. 7a–c, respectively. All the calibration models developed are based on only one PLSR component. Since the M/G ratio used as response variable were directly calculated from the solution-state spectra it is not surprising that a very good multivariate calibration model from the solution-state spectra were obtained (RMSECV = 0.05, $r^2 = 0.99$). However, when calibrating the HR-MAS and CP-MAS spectra to the M/G ratio higher prediction errors (RMSECV = 0.13) and lower correlations ($r^2 = 0.92$) were observed. The RMSECV value is the average cross-validated calibration error, composed of large and small errors all together. The measured versus predicted plot of the model based on the HR-MAS spectra (Fig. 7b) shows that many of the samples are deviating from the target line. In the model based on the CP-MAS spectra, on the other hand, most of the samples but one is close to the target line. The one sample that is far from the target line, and thus mainly responsible for the high prediction error, is the sample with the high calcium ion content.

In order to further investigate the assumption that it is the solid-state measurements that gives the correct M/G ratio estimation, a new set of reference M/G ratios for the 42 sodium alginate samples were introduced. These new reference values were calculated from the Raman spectra of the alginate powder using the calibration model described in a previous study (Salomonsen et al., 2008a). Thus, as for the solid-state NMR measurements, these values were obtained from the intact alginate powder in solid-state as opposed to solution-state NMR reference values calculated from the hydrolysed alginate in solution. The results from the PLSR models based on the ^{1}H solution-state, ^{1}H HR-MAS and ^{13}C CP-MAS NMR using the M/G ratios calculated from the Raman spectra as reference values are shown in Fig. 7d–f, respectively. In this case the overall picture is reversed. An excellent correlation ($r^2 = 0.99$) between the CP-MAS spectra and the reference values are observed whereas the models based on the solution-state and HR-MAS spectra are not as good.

Summing up, the M/G ratios obtained from NMR spectra of hydrolysed alginate in solution and swollen intact alginate powder are in agreement with the measurements of intact alginate powder as long as the content of residual calcium ions is not too high (no severe effects up to 1.1% were observed). However, in particular the

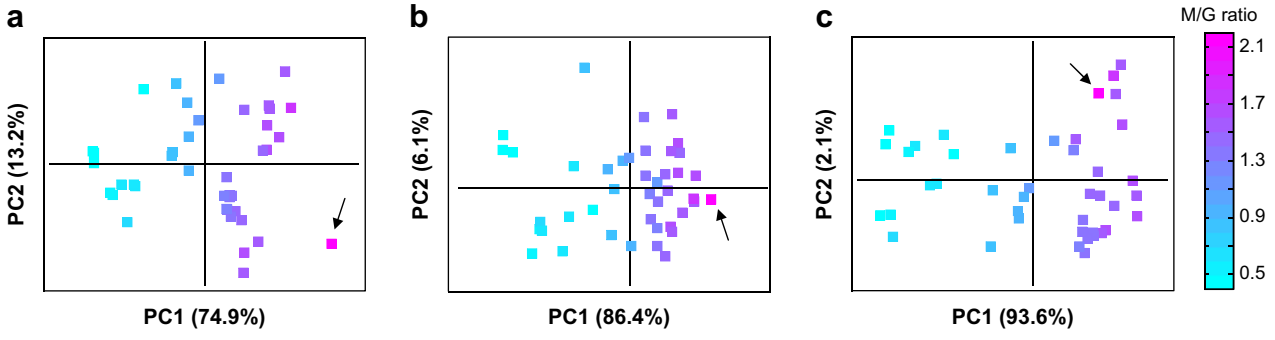

Fig. 6. PCA score plots of the ^{1}H solution-state NMR spectra (a), ^{1}H HR-MAS NMR spectra (b) and ^{13}C CP-MAS NMR spectra (c) showing the first two principal components, which explain 88.1%, 92.5% and 95.7%, respectively, of the data variation. The scores are coloured according to M/G ratio calculated from the ^{1}H solution-state NMR spectra. The sample with the highest calcium content is in each plot marked with an arrow.

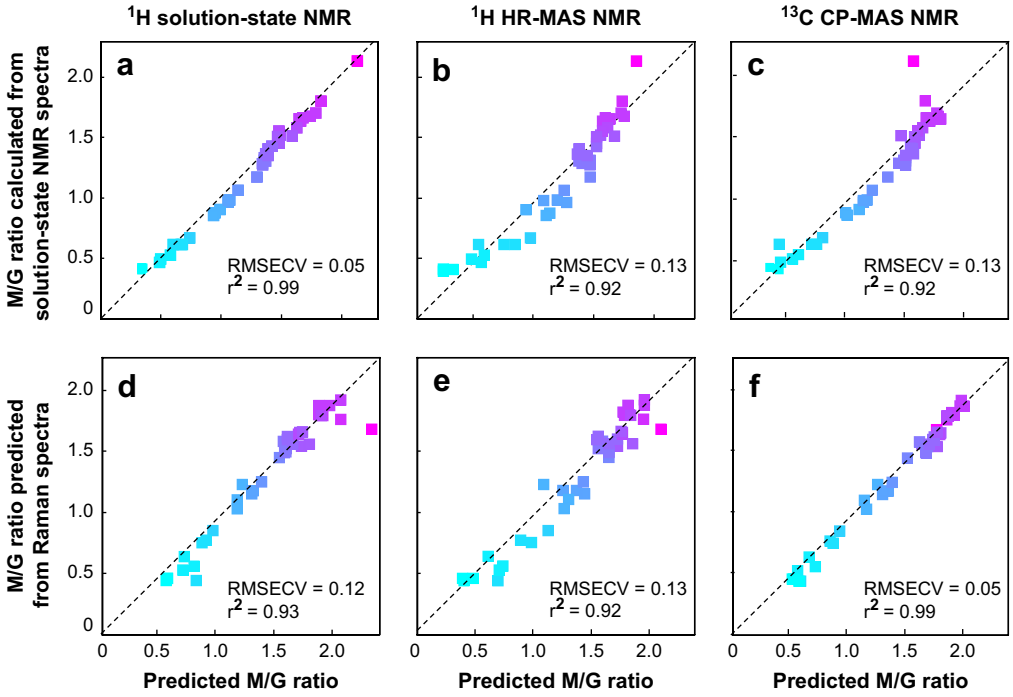

Fig. 7. PLSR model results. M/G ratio measured by ^{1}H solution-state NMR and Raman spectroscopy versus M/G ratio predicted from ^{1}H solution-state NMR (a, d), ^{1}H HR-MAS NMR (b, e) and ^{13}C CP-MAS NMR (c, f) spectra. All models are based on one PLSR component. The samples are coloured according to the M/G ratio calculated from the ^{1}H solution-state NMR spectra. RMSECV = root mean square error of cross validation.

estimated M/G ratio of the sample with high calcium ion content (2.4%) obtained by solution-state, swollen-state and solid-state were not in agreement. Since the solution-state and HR-MAS method cannot detect immobilised parts of the molecule the value obtained from the CP-MAS spectra should reflect the true M/G ratio as the calcium ion content does not effect the ^{13}C CP-MAS spectra. This was further supported by the comparison with the values obtained from the Raman spectra of dry alginate powder which measures all molecular fragments independent on the internal mobility.

4. Conclusion

The present investigation has shown that when analysing alginates with high residual amount of calcium ions in solution- and swollen-state by ^{1}H solution-state and ^{1}H HR-MAS NMR, respectively, the M/G ratio is overestimated. In contrast, the predicted M/G ratio from ^{13}C CP-MAS spectra of the alginate powder is not affected by the calcium ion content. Although the spectral resolution of ^{13}C CP-MAS NMR spectra of alginate powder is lower than ^{1}H spectra of solutions and gels, this non-destructive technique is more reliable in charactering the alginate monomer composition of the intact alginate powder and thus in predicting the alginate functionality. The next step is to investigate if the M/G ratio can be robustly extracted from the solid-state spectra by curve resolution techniques without *a priori* knowledge of the M/G ratio. If successful, this will promote ^{13}C CP-MAS as the preferred choice for non-destructive analysis of the alginate monomer composition.

When the calcium ion content is low, the ^{1}H HR-MAS approach using swollen alginates represents an attractive alternative to the traditional ^{1}H solution-state NMR method as the acid hydrolysis is avoided and similar M/G ratios obtained.

Acknowledgements

The authors wish to thank the Ministry of Science, Technology and Innovation for partly sponsoring the Industrial PhD project conducted by Tina Salomonsen in co-operation with Danisco A/S and Quality & Technology, Department of Food Science, Faculty of Life Sciences (LIFE) at the University of Copenhagen. Bente Høj Andersen and the hydrocolloid analysis group at Danisco A/S are thanked for help with parts of the experimental work and Gilda Kischinovsky, LIFE is acknowledged for proofreading the manuscript.

References

Andrew, E. R., Bradbury, A., & Eades, R. G. (1958). Nuclear magnetic resonance spectra from a crystal rotated at high speed. *Nature, 182*, 1659.
Andrew, E. R., Bradbury, A., & Eades, R. G. (1959). Removal of dipolar broadening of nuclear magnetic resonance spectra of solids by specimen rotation. *Nature, 183*, 1802–1803.
Baianu, I. C., & Förster, H. (1980). Cross-polarization, high-field carbon-13 NMR techniques for studying physocochemical properties of wheat grain, flour, starch, gluten, and wheat protein powders. *Journal of Applied Biochemistry, 2*, 347–354.
Colquhoun, I. J., Parker, R., Ring, S. G., Sun, L., & Tang, H. R. (1995). An NMR spectroscopic characterization of the enzyme-resistant residue from alpha-amylolysis of an amylose gel. *Carbohydrate Polymers, 27*, 255–259.
Draget, K. I., Moe, S. T., Skjåk-Bræk, G., & Smidsrød, O. (2006). Alginates. In A. M. Stephen, G. O. Phillips, & P. A. Williams (Eds.), *Food polysaccharides and their applications* (pp. 289–334). Boca Raton: CRC Press.
Draget, K. I., Strand, B., Hartmann, M., Valla, S., Smidsrød, O., & Skjåk-Bræk, G. (2000). Ionic and acid gel formation of epimerised alginates; the effect of AlgE4. *International Journal of Biological Macromolecules, 27*, 117–122.
Gordon-Mills, E. (1990). Polysaccharides from Australian marine red algae: new methods for characterizing new sources. *Australian Journal of Biotechnology, 4*, 275–278.
Grant, G. T., Morris, E. R., Rees, D. A., Smith, P. J. C., & Thom, D. (1973). Biological interactions between polysaccharides and divalent cations: the egg-box model. *FEBS Letters, 32*, 195–198.
Grasdalen, H. (1983). High-field ^{1}H spectroscopy of alginate: squential structure and linkage conformations. *Carbohydrate Research, 118*, 255–260.
Grasdalen, H., Larsen, B., & Smidsrød, O. (1979). NMR study of the composition and sequence of uronate residues in alginates. *Carbohydrate Research, 68*, 23–31.
Grasdalen, H., Larsen, B., & Smidsrød, O. (1981). ^{13}C NMR studies of monomeric composition and sequence in alginate. *Carbohydrate Research, 89*, 179–191.
Grasdalen, H., Larsen, B., & Smidsrød, O. (1977). ^{13}C NMR studies of alginate. *Carbohydrate Research, 56*, C11–C15.
Haug, A., Larsen, B., & Smidsrød, O. (1974). Uronic acid sequence in alginate from different sources. *Carbohydrate Research, 32*, 217–225.

Haug, A., Myklesta, S., Larsen, B., & Smidsrød, O. (1967). Correlation between chemical structure and physical properties of alginates. *Acta Chemica Scandinavica, 21*, 768–778.

Hoffmann, R. A., Gidley, M. J., Cooke, D., & Frith, W. J. (1995). Effect of isolation procedures on the molecular composition and physical properties of *Eucheuma cottonii* carrageenan. *Food Hydrocolloids, 9*, 281–289.

Holtan, S., Zhang, Q., Strand, W. I., & Skjåk-Bræk, G. (2006). Characterization of the hydrolysis mechanism of polyalternating alginate in weak acid and assignment of the resulting MG-oligosaccharides by NMR spectroscopy and ESI-mass spectrometry. *Biomacromolecules, 7*, 2108–2121.

Hotelling, H. (1933). Analysis of complex statistical variables into principal components. *Journal of Educational Psychology, 24*, 417–441.

Indergaard, M., Skjåk-Bræk, G., & Jensen, A. (1990). Studies on the influence of nutrients on the composition and structure of alginate in *Laminaria-saccharina* (L) Lamour (Laminariales, Phaeophyceae). *Botanica Marina, 33*, 277–288.

Jarvis, M. C., & Apperley, D. C. (1995). Chain conformation in concentrated pectic gels: evidence from ^{13}C NMR. *Carbohydrate Research, 275*, 131–145.

Kulik, A. S., & Haverkamp, J. (1997). Molecular mobility of polysaccharide chains in starch investigated by two-dimensional solid-state NMR spectroscopy. *Carbohydrate Polymers, 34*, 49–54.

Larsson, P. T., Hult, E. L., Wickholm, K., Pettersson, E., & Iversen, T. (1999). CP/MAS ^{13}C NMR spectroscopy applied to structure and interaction studies on cellulose I. *Solid State Nuclear Magnetic Resonance, 15*, 31–40.

Llanes, F., Sauriol, F., Morin, F. G., & Perlin, A. S. (1997). An examination of sodium alginate from *Sargassum* by NMR spectroscopy. *Canadian Journal of Chemistry, 75*, 585–590.

Mackie, W., Noy, R., & Sellen, D. B. (1980). Solution properties of sodium alginate. *Biopolymers, 19*, 1839–1860.

Penman, A., & Sanderson, G. R. (1972). Method for determination of uronic acid sequence in alginates. *Carbohydrate Research, 25*, 273–282.

Pines, A., Gibby, M. G., & Waugh, J. S. (1973). Proton-enhanced NMR of dilute spins in solids. *Journal of Chemical Physics, 59*, 569–590.

Pines, A., Waugh, J. S., & Gibby, M. G. (1972). Proton-enhanced nuclear induction spectroscopy–method for high-resolution NMR of dilute spins in solids. *Journal of Chemical Physics, 56*, 1776–1777.

Rochas, C., & Lahaye, M. (1989). Solid-state ^{13}C NMR spectroscopy of red seaweeds, agars and carrageenans. *Carbohydrate Polymers, 10*, 189–204.

Saito, H., Yokoi, M., & Yamada, J. (1990). Hydration-dehydration-induced conformational-changes of agarose, and kappa-carrageenans and iota-carrageenans as studied by high-resolution solid-state ^{13}C nuclear magnetic resonance spectroscopy. *Carbohydrate Research, 199*, 1–10.

Salomonsen, T., Jensen, H. M., Stenbæk, D., & Engelsen, S. B. (2008a). Chemometric prediction of alginate monomer composition. A comparative spectroscopic study using IR, Raman, NIR and NMR. *Carbohydrate Polymers, 72*, 730–739.

Salomonsen, T., Jensen, H. M., Stenbæk, D., & Engelsen, S. B. (2008b). Rapid determination of alginate monomer composition using Raman spectroscopy and chemometrics. In P. A. Williams, & G. O. Phillips (Eds.), *Gums and stabilisers for the food industry 14* (pp. 543–551). Cambridge: RSC Publishing.

Samoson, A., Tuherm, T., & Gan, Z. (2001). High-field high-speed MAS resolution enhancement in ^{1}H NMR spectroscopy of solids. *Solid State Nuclear Magnetic Resonance, 20*, 130–136.

Sinitsya, A., Copikova, J., & Brus, J. (2003). ^{13}C CP/MAS NMR spectra of pectins: a peak-fitting analysis in the C-6 region. *Czech Journal of Food Science, 21*, 1–12.

Sinitsya, A., Copikova, J., & Pavlikova, H. (1998). ^{13}C CP/MAS NMR spectroscopy in the analysis of pectins. *Journal of Carbohydrate Chemistry, 17*, 279–292.

Steginsky, C. A., Beale, J. M., Floss, H. G., & Mayer, R. M. (1992). Structural determination of alginic acid and the effects of calcium-binding as determined by high-field NMR. *Carbohydrate Research, 225*, 11–26.

Stockton, B., Evans, L. V., Morris, E. R., Powell, D. A., & Rees, D. A. (1980). Alginate block structure in *Laminaria digitata*: implications for holdfast attachment. *Botanica Marina, 23*, 563–567.

Stokke, B. T., Smidsrød, O., Bruheim, P., & Skjåk-Bræk, G. (1991). Distribution of uronate residues in alginate chains in relation to alginate gelling properties. *Macromolecules, 24*, 4637–4645.

Wold, S., Martens, H., & Wold, H. (1983). The multivariate calibration problem in chemistry solved by the PLS method. *Lecture Notes in Mathematics, 973*, 286–293.

Direct quantification of M/G ratio from ^{13}C CP-MAS NMR spectra of alginate powders by multivariate curve resolution

T. Salomonsen, H.M. Jensen, F.H. Larsen, S. Steuernagel & S.B. Engelsen

Carbohydrate Research, Submitted

PAPER V

Direct quantification of M/G ratio from ^{13}C CP-MAS NMR spectra of alginate powders by multivariate curve resolution

Tina Salomonsen[a,b*], Henrik Max Jensen[b], Flemming Hofmann Larsen[a], Stefan Steuernagel[c], Søren Balling Engelsen[a]

[a]*University of Copenhagen, Faculty of Life Sciences, Department of Food Science, Quality & Technology, Rolighedsvej 30, 1958 Frederiksberg C, Denmark*
[b]*Danisco A/S, Advanced Analysis, Edwin Rahrs Vej 38, 8220 Brabrand, Denmark*
[c]*Bruker-Biospin GMBH, 76287 Rheinstetten, Germany*

[*]Corresponding author: Tina Salomonsen, fax: +45 3533 3245, e-mail: tisa@life.ku.dk

Abstract

Multivariate curve resolution (MCR) was applied to ^{13}C cross-polarisation (CP) magic angle spinning (MAS) nuclear magnetic resonance (NMR) spectra of 42 intact seaweed alginate powders plus a pure mannuronate sample isolated from *Psedomonas fluorescenc* for estimation of the mannuronic acid:guluronic acid ratio (M/G ratio). In order to obtain meaningful quantitative results it was necessary to include the pure mannuronate in the sample set. An excellent correlation (r^2=0.99) was established between the MCR-estimated M/G ratios and the M/G ratios obtained from the traditional ^{1}H solution-state NMR method. It was concluded that ^{13}C CP-MAS NMR in combination with multivariate curve resolution is a reliable, convenient (no sample preparation is required) and relatively rapid method for M/G ratio determinations of alginates and it may serve as a good alternative to the chemical techniques traditionally used.

Keywords: Alginate, CP-MAS NMR, Deconvolution, Multivariate curve resolution

1. Introduction

Alginates are a family of linear co-polymers of (1-4) linked β-D-mannuronic acid (M) and α-L-guluronic acid (G)[1,2] of widely varying composition and sequential structure.[3] Alginates occur in nature as structural components in brown seaweed and are produced by the bacteria *Azotobacter vinelandii*[4] and several species of *Pseudomonas*.[5] Commercial alginates are extracted from seaweed and utilised in different industries (e.g. food, pharmaceutical, cosmetic, textile and paper) because of their thickening, stabilising and gelling properties.[6] Among their industrial applications, their ability to form gels in the presence of calcium ions is of particular interest, and since the gelling properties are closely related to the alginate monomer composition, considerably effort has been devoted to determining the M/G ratio of alginates.

Some of the first analytical methods applied to obtain the M/G ratio included chemical modifications of the alginates by total hydrolysis and formation of derivatives followed by separation and detection using paper chromatography,[7] ion exchange chromatography,[8,9] colourimetry,[10] polarimetry,[11] high performance liquid chromatography[12,13] and gas chromatography.[14] The major disadvantage of these methods is the tedious sample preparation involving numerous steps and chemicals. Moreover, the results are often unreliable due to different degradation rates and reaction activities of the two monomers.

Circular dichroism (CD)[15-17] has been proposed as a rapid and non-destructive method for determining the monomer composition of alginates in solution.[15-17] However, this method is very sensitive to the presence of divalent ions (e.g. calcium ions) which are often present in commercial alginates. Infrared (IR), Raman and near infrared (NIR) spectroscopy can also be used for rapid and non-destructive analysis of alginates.[18] With these methods, the M/G ratio of intact alginate powders can be determined in less than a minute using a multivariate calibration model based on the IR, Raman or NIR spectra of the alginates and the corresponding M/G ratios determined by a reference method. Thus, these methods are very powerful for routine analysis of alginates (e.g. quality control). However, they are dependent on a reliable reference method.

^{1}H and ^{13}C solution-state nuclear magnetic resonance (NMR) of moderately depolymerised alginates is today by far the most common methods for structural analysis of alginates.[19-23] Unfortunately, solution-state NMR is not the most convenient method for routine analysis of large numbers of samples due to the time-consuming and labour-intensive sample preparation required in order to the reduce the molecular weight and thereby the viscosity of the alginates to a level suitable for solution-state NMR analysis. Therefore, we have previously[24] investigated the potential of using ^{1}H high-resolution (HR) magic angle spinning (MAS) NMR and

^{13}C cross-polarisation (CP) MAS NMR for the analysis of the intact alginate powders (Little or no sample preparation is required). Both MAS methods proved to be attractive alternatives to the solution-state NMR method.

In the present work, we will show how alginate M/G ratios can be calculated from the ^{13}C CP-MAS NMR spectra of alginate powders using multivariate curve resolution by alternating least squares regression (MCR-ALS)[25] and by spectral deconvolution of each individual spectrum using Gaussian and/or Lorentzian line shapes. The results are compared with the M/G ratios obtained by ^{1}H solution-state NMR. This study aims to be a thorough evaluation of ^{13}C CP-MAS NMR as a rapid, non-destructive and reliable method for quantitative measurements of the monosaccharide components of alginate.

2. Results and discussion

2.1. The samples

The M/G ratios calculated from the ^{1}H solution-state NMR spectra of the 42 hydrolysed sodium alginates ranged from 0.4 to 1.7 (Fig. 1a) and the average molecular weights (M_w) of the intact alginates were measured to be in the range of 56 to 424 kDa (Fig. 1b).

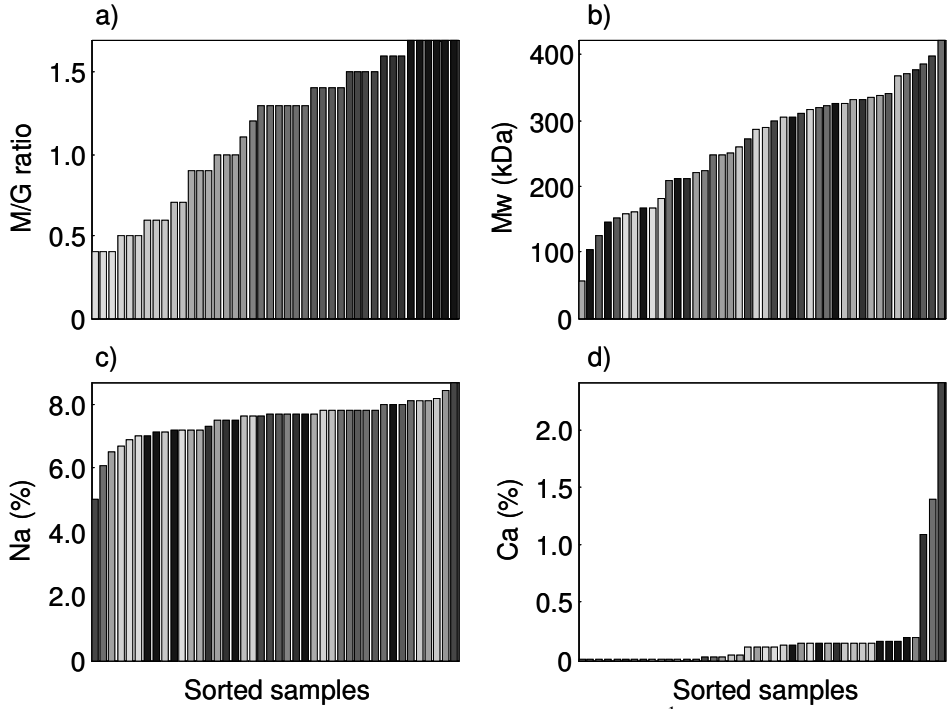

Figure 1. Histograms of (a) the M/G ratios calculated from the ^{1}H solution-state NMR spectra of the 42 hydrolysed seaweed sodium alginates as well as (b) the average molecular weights (Mw), (c) sodium and (d) calcium contents of the intact alginates. The samples are sorted according to the measured values and coloured according to the M/G ratios calculated from the solution-state NMR spectra (from light grey to dark grey with increasing M/G ratio).

The M_w of selected hydrolysed samples were also measured and determined to be in the range of 30-40 kDa independent of the initial M_w value. The M_w of the bacterial mannuronate was 290 kDa. The sodium and calcium contents of the 42 sodium alginates were measured to be in the range 5.0-8.1% (w/w) (Fig. 1c) and 0.01-2.4% (w/w), respectively (Fig. 1d). Three samples in the sample set contained considerably more calcium (1.1%, 1.4% and 2.4%) than the other samples (0.01-0.2%). Calcium ions preferentially bind to guluronate,[26,27] resulting in restricted motion of the G-blocks, which will give rise to a broadening of the solution-state NMR signals. Thus, in order to prevent the guluronate signals from being underestimated, solution-state NMR spectra of the three samples with high calcium contents were also measured after addition of a chelator, which binds calcium and thereby prevents the calcium ions from interacting with the alginate. The M/G ratio values of the samples with 1.1%, 1.4% and 2.4% calcium were found to be 1.6, 1.3 and 1.5, respectively, when calculated from the spectra measured with a chelator, and 1.8, 1.5 and 2.1, respectively, when measured without addition of a chelator. Thus, the M/G ratios of these samples are clearly overestimated from solution-state NMR when no chelator is added.

2.2 Spectral assignments of the ^{13}C CP-MAS NMR spectra

The ^{13}C CP-MAS NMR spectra of three sodium alginate powders containing 35%, 65% and 100% mannuronate, respectively, are shown in Fig. 2.

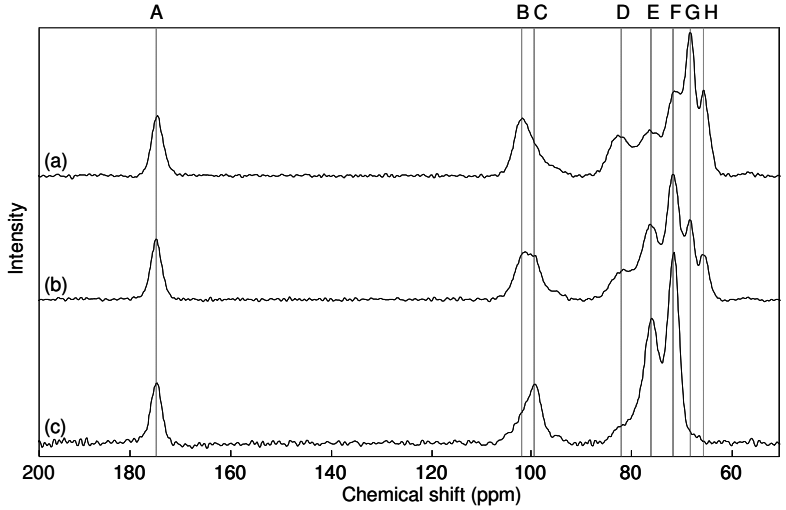

Figure 2. ^{13}C CP-MAS NMR spectra of sodium alginate powders containing (a) 35%, (b) 65% and (c) 100% mannuronate. The capital letters refer to the resonance assignments listed in Table 1.

The carbon spectra can generally be divided into three major regions consisting of the pyranose (60-90 ppm), the anomeric (90-110 ppm) and the carboxyl (172-180 ppm) carbon signals. The signals in the spectra were assigned as previously described[24] and the assignments are verified in this study by comparison with the bacterial alginate containing 100% mannuronate (Fig. 2c). The assignments are listed in Table 1 together with ^{13}C NMR chemical shift values of hydrolysed alginate in solution obtained by Grasdalen et al.[20]

Table 1
Assignments of the resonances in the ^{13}C CP-MAS NMR spectrum of alginate (Fig. 2). The chemical shifts are compared with the ^{13}C resonances obtained from solution-state NMR as reported by Grasdalen et al.[20]

	^{13}C resonances												
	Carboxyl		Anomeric		Pyranose								
Notation in Fig. 2	A		B	C	D	E		F		G			H
Assignment of X*	G6	M6	G1	M1	G4	M4	M5	M3	M2	G3	G5		G2
Chemical shift (ppm)**	176.2		102.2	99.5	82.8	76.4		71.6		68.4			65.5
Chemical shifts according to Grasdalen et al. [20] (ppm)***													
GXG	177.3	177.7	103.3	103.8	82.6	80.7	78.8	74.3	73.3	71.8	69.9		67.8
MXM	177.6	177.1	102.2	102.8	82.6	80.3	78.9	74.1	72.2	72.1	70.2		67.4

* X refers to mannuronate (M) or guluronate (G) and the number refers to the position, i.e. G1 is the C1 carbon atom of the guluronate unit.
** The carboxyl resonance of glycine at 176.03 ppm was used as external reference.
*** The resonances given are of the intermediate residue in the triade sequences (GGG, GMG, MMM and MGM).

It should be noted that the very broad lines in the CP-MAS spectra make it impossible to assign the different carbons with the same accuracy as can be done in the solution-state spectra. Several signals in the CP-MAS spectra consist of contributions from more than one carbon site within each mannuronic and guluronic acid residue (e.g. signals E, F and G in Fig. 2) due to chemical shift distributions. However, by comparison with the solution-state ^{13}C chemical shifts it is observed that the carbons in the CP-MAS spectra generally resonate at a lower frequency (0.6-4.3 ppm) than in the solution-state spectra, as was also observed in another CP-MAS study of alginate.[28] These differences are believed to be due to the different degrees of hydration of the alginate in solution and in the solid state. Chemical shift differences due to different structural modifications induced by hydration have also been observed for other polysaccharides such as pectin,[29] carrageenan,[30] starch[31] and cellulose.[32] The fact that the signals from C1 and C4 in guluronate (G1 and G4, respectively) are shifted significantly less than C1 and C4 in mannuronate (M1 and M4, respectively) could indicate more significant structural changes around M1 and M4 than around G1 and G4 when going from solution to solid-state. This suggests that the mannuronate glycosidic linkage carbons are more exposed to water and thereby more prone to hydration effects, which agrees well with the fact that mannuronate has an extended ribbon shape and is more flexible[33] than guluronate, which is buckled and stiff.[34] Moreover, the signals containing the C1 and C4 resonances of both monomers (signal B, C, D and E) are broader than the other signals. The chemical shifts of glycosidic linkage carbons are more sensitive to the neighbouring residues and thus exhibit a broader range of chemical shifts. In ^{13}C

solution-state NMR spectra of alginate these chemical shifts are separated and information on block structure can be obtained,[20] but in the ^{13}C CP-MAS spectra the signals seem to be too broad and overlapping to obtain direct information on block structure.

2.3 Evaluation of the quantitative quality of the ^{13}C CP-MAS NMR spectra

To ensure that the intensities of the signals in the ^{13}C CP-MAS NMR spectra are quantitatively correct, the ^{13}C CP-MAS NMR spectrum of a sample was compared with the corresponding single pulse ^{13}C MAS NMR spectrum (Fig. 3a). The signal intensities of the anomeric and pyranose signals are roughly identical in both spectra, whereas the intensity of the carboxyl signal is lower in the CP-MAS spectrum than in the single pulse spectrum. This is due to different cross polarisation dynamics for the carboxylic carbons compared to the other carbons. A series of ^{13}C CP-MAS spectra with contact times starting at 500 µs and incremented by 700 µs up to 10.3 ms was acquired in order to investigate how the contact time (i.e. cross polarisation) influences the signal intensities. The integrated intensities of the carboxyl, anomeric and pyranose signals relative to the integrated intensity of the anomeric and pyranose signals as a function of contact time are shown in Fig. 3b. In addition, the relative intensities of the signals in a single pulse ^{13}C MAS spectrum are shown (open symbols). The relative intensities of the anomeric and pyranose signals are independent of the contact time, whereas the relative intensity of the carboxylic carbon signal increases with increasing contact time. For carbons with a small dipolar proton coupling (e.g. carboxyl carbons) maximum intensity will be obtained for longer contact times than for carbons with a larger dipolar proton coupling. Thus, for the evaluation of the carboxylic carbons to be quantitatively correct, the contact time should be approximately 6 ms or longer, which is the point at which the relative intensity of the carboxylic carbon signal in the ^{13}C CP-MAS spectra equals the relative intensity of the carboxylic carbon signal in the single pulse ^{13}C MAS spectra. However, the overall intensity of a ^{13}C CP-MAS spectrum decreases with increasing contact time due to relaxation of the protons in the spin lock field, i.e. less magnetisation is transferred at long contact times, resulting in overall lower spectral intensity (Fig. 3b). Consequently, conducting experiments with long contact times will require longer measurement times. Therefore, the focus in this study will be on the anomeric and pyranose signals which can be evaluated quantitatively under the instrumental conditions chosen (Section 4.3). Thus, we can utilise the significant sensitivity advantages of the ^{13}C CP-MAS experiment over the ^{13}C single pulse MAS experiment due to ^{1}H-to-^{13}C polarisation transfer and shorter recycle delays (T_1 for ^{1}H is much shorter than for ^{13}C).

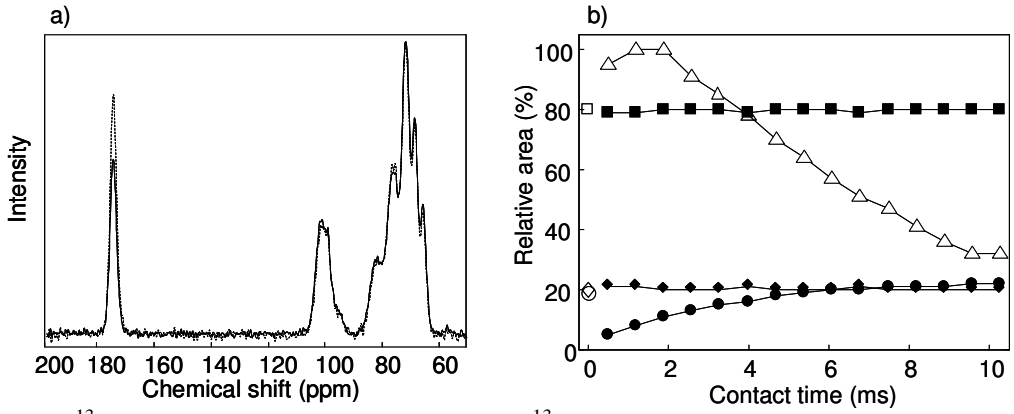

Figure 3. (a) ^{13}C CP-MAS (—) and single pulse ^{13}C MAS (-----) NMR spectra recorded with a recycle delay of 2 s and 120 s, respectively, and 1024 and 3328 number of scans, respectively. (b) Overall integrated signal intensities (∇) of all signals in the ^{13}C CP-MAS NMR spectra and integrated signal intensities of carboxylic (●), anomeric (♦) and pyranose (■) carbon signals relative to the total intensity of the anomeric and pyranose signals as a function of contact times. The relative integrated intensities of the single pulse ^{13}C MAS NMR carboxylic (○), anomeric (◊) and pyranose (□) carbon signals are indicated for comparison (contact time = 0 ms).

2.4 Estimation of M/G ratios from the ^{13}C CP-MAS spectra

In a first attempt to calculate the M/G ratio of alginate directly from its ^{13}C CP-MAS NMR spectra, different combinations of the relative spectral intensities of the signals' resonances denoted as D, E, F, G and H in Fig. 4a were compared. The best correlation (r^2=0.99) was found when comparing the ratio between the spectral intensity (height) of signal F, which mainly contains signal contributions from M3 and M2, and signal G, which mainly contains signal contributions from G3 and G5, with the M/G ratio calculated from the ^{1}H solution-state NMR spectra (Fig. 4b). However, as can be observed in Fig. 4b, the low M/G ratio samples are slightly overestimated and the high M/G ratio samples are underestimated compared to the M/G ratios from solution-state NMR. This is most likely due the highly overlapping nature of the CP-MAS resonances resulting in contributions from other carbons than the ones assigned in Table 1. Signals F and G probably also contain signal contributions from guluronate and mannuronate carbons, respectively, which will influence the height of the signals and thereby the estimation of the M/G ratio.

Another applicable approach for the quantitative evaluation of NMR spectra is to use the integrated intensities of the signals. Presently, the broad and overlapping signals in the alginate ^{13}C CP-MAS NMR spectra call for spectral deconvolution by Gaussian and/or Lorentzian functions. However, fitting of signals in CP-MAS spectra is demanding from a computational point of view, because the complexity of the overlapping signals is often unknown and the fitting is labile and prone to noise and initial guesses. Thus, it requires a well defined strategy to obtain unambiguous fitting results. Application of constraints is one way to navigate the fitting towards a stable and meaningful solution. However, using too many constraints is undesirable due to the risk of overfitting.

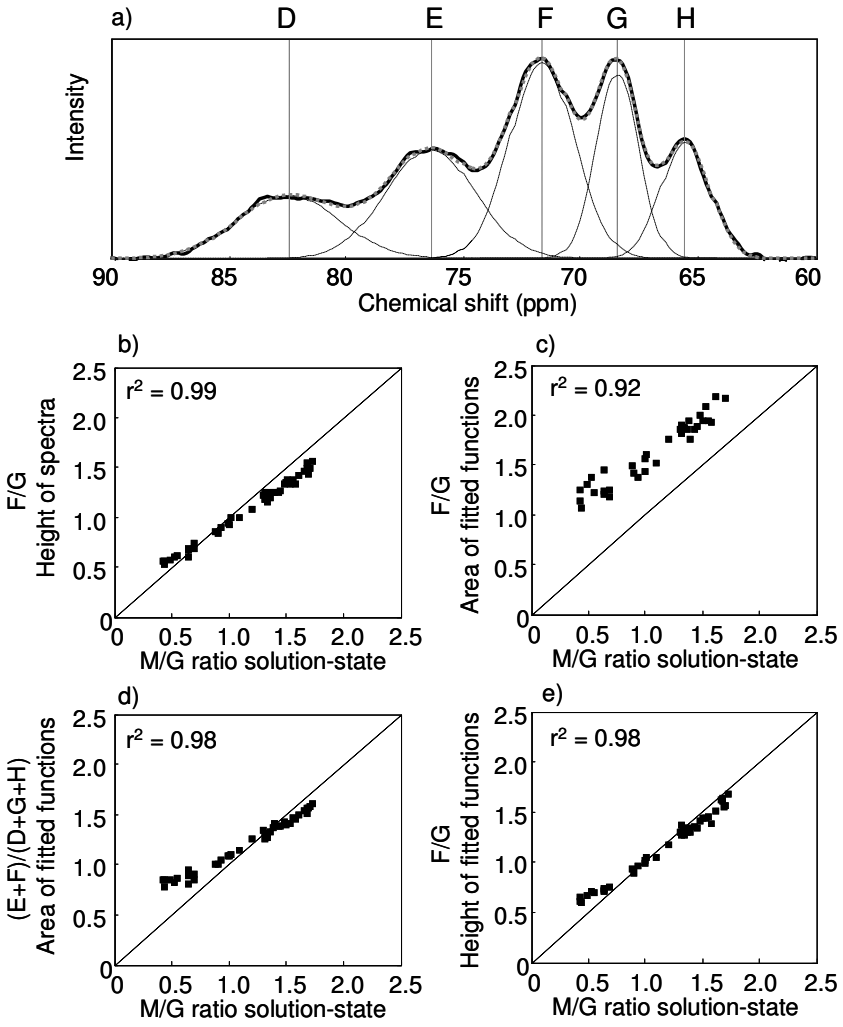

Figure 4. (a) Example of the results obtained from the fitting of Gaussian functions to the pyranose region (60-90 ppm) in a ^{13}C CP-MAS NMR spectrum (——) of alginate (M/G ratio = 1). The five Gaussian functions (-----) as well as the overall fit (▪▪▪▪▪) are depicted. M/G ratios of the 42 seaweed alginates estimated from the ratio of (b) the spectral height of signals F and G, (c) the area of the fitted Gaussian functions of signals F and G, (d) the area of the fitted Gaussian functions of signals D, E, F, G and H and (e) the height of the fitted Gaussian functions of signals F and G.

In the alginate case, it is known that the pyranose region of the ^{13}C CP-MAS NMR spectrum contains signals from at least eight different carbons (four from each monomer) and their chemical shifts depend on the neighbouring residues. However, these signals are not well separated and an attempt to deconvolute the spectra into eight different functions resulted in very ambiguous results. However, the five well separated resonance maxima in the region of 60-90 ppm (signal D, E, F, G and H in Fig. 2) could successfully be resolved into five individual Gaussian or Lorentzian line shapes. Gaussian line shapes resulted in the best fit and only random noise was left in the residuals. No constraints with respect to centre position, width and intensity of the fitted functions were applied. An example from deconvolution using Gaussian line

shapes is shown in Fig. 4a and a comparative overview of centre positions and line widths is given in Table 2. The fitted positions of the narrower signals (G and H) varied to a lesser extent than for the broader signals (D, E and F). Therefore, it was tested whether the fitted positions were related to the content of mannuronate and guluronate. The highest correlation (r^2=0.81) was found between fitted positions of signal F and the contents of mannuronate. The fitted positions of signal F in spectra of alginate with a high content of mannuronate were higher than in spectra with a high content of guluronate. This indicates the presence of unresolved structural information such as underlying resonance shifts due to higher-order sequence information. The fitted positions of signals D and E were weakly correlated (r^2=0.62 and 0.59, respectively) to the content of guluronate (i.e. the higher the content of guluronate, the higher ppm value). No systematic change with respect to the content of guluronate and mannuronate of the fitted positions of the narrow signals G and H was observed.

The highest correlations between the M/G ratios from solution-state NMR and the M/G ratios estimated from the fitting results (integrated intensities or height of the deconvoluted signals) were found by deconvolution using Gaussian line shapes. The ratios between integrated intensities of signals F and G are compared with the M/G ratios from solution-state NMR in Fig. 4c. The values are relatively well correlated (r^2=0.92), but the M/G ratios are systematically overestimated. Thus, the integrated intensity of signal F is probably overestimated due to contributions from other carbons to this signal. In a previous study by Llanes et al.[28] the M/G ratios of two alginates were calculated from the area of the five distinct resonances in the pyranose region of their ^{13}C CP-MAS spectra. The content of mannuronate was estimated from signals E and F, and the content of guluronate from signals D, G and H. Thus, the M/G ratio was estimated to be equal to the integrated intensities of (E+F)/(D+G+H). Fig. 4d shows the M/G ratios estimated as described by Llanes et al.[28] versus the M/G ratios obtained from solution-state ^{1}H NMR. This resulted in a higher correlation (r^2=0.98) than when only using the ratio between integrated intensities of signals F and G to estimate the M/G ratio. Moreover, the difference between the estimated and the solution-state values is smaller. However, the smallest difference between the estimated values and the solution-state values together with a high correlation (r^2=0.98) was found when using the ratio of the height of the functions fitted to signal F and G (Fig. 4e). In summary, estimating the M/G ratio from ^{13}C CP-MAS spectra of alginates is not straightforward due to the highly overlapping signals in the spectra. However, a fairly good estimate can be obtained from the height of the Gaussian deconvoluted signals F and G.

Table 2
Comparative overview of centre positions and widths of the Gaussian functions fitted to the five pyranose signals in the ^{13}C CP-MAS NMR spectra of the 42 alginates investigated in this study. Average values, standard deviation (std.) and range are given.

		^{13}C resonances*				
		D	E	F	G	H
Position (ppm)	Average ± std.	82.8 ± 0.30	76.4 ± 0.15	71.6 ± 0.15	68.4 ± 0.05	65.5 ± 0.06
	Range	81.9-83.1	76.0-76.7	71.2-71.7	68.3-68.5	65.4-65.9
Width (Hz)**	Average ± std.	327 ± 21	302 ± 31	214 ± 21	138 ± 4	164 ± 7
	Range	277-365	215-415	189-252	126-151	151-189

* The letters refer to the notations used in Fig. 1 and Table 1
** a_2 in Equation 1

An alternative method for the estimation of the alginate M/G ratios from the highly overlapping ^{13}C CP-MAS NMR spectra is the multivariate curve resolution method: MCR-ALS.[25] The goal of MCR-ALS is to decompose the spectra into a set of loadings representing the spectra of the pure chemical components and a set of scores representing the estimated concentrations of the chemical components. In this case we wish to decompose the spectra into the pure spectra of mannuronate and guluronate rather than decomposing into individual carbon signals and then calculate the M/G ratio from the estimated concentrations of the two monomers in each sample.

MCR-ALS was applied to the ^{13}C CP-MAS NMR spectra of the 42 seaweed alginates (Fig. 5a) and the resulting estimated pure spectra from a two component MCR-ALS model are shown in Fig. 5c. One of the estimated spectra resembles the spectrum of pure guluronate when comparing the spectral profile with the chemical shift values from the assignment of the real ^{13}C CP-MAS NMR spectra (Fig. 2 and Table 1). However, the other estimated pure spectrum does not resemble the pure spectrum of pure mannuronate (Fig. 5e). Thus, it can be concluded that the pure spectrum of mannuronate cannot be estimated with the spectra of the 42 alginates having an M/G ratio in the range of 0.4-1.7. Better results can usually be obtained if spectra of the pure chemical components are included in the data set used in the modelling. This will add selectivity to the data set, which is one of the key conditions for approaching uniqueness in MCR-ALS. A pure spectrum of bacterial mannuronate was therefore added to the data set (the pure spectra of guluronate was not available). The spectra of the 42 seaweed alginates plus the bacterial mannuronate are shown in Fig. 5b and the estimated spectra from a two-component MCR model are shown in Fig. 5d. The model explained 99.9% of the variance in the data set. The estimated and the real spectra of pure mannuronate are almost identical (Fig. 5f) and the signals related to a high content of guluronate (low M/G ratio) in the spectra in Fig. 5b resemble the

estimated spectrum of pure guluronate (Fig. 5d). It is thus possible to predict the spectrum of pure guluronate.

The principal disadvantage of MCR-ALS is that the obtained solution is not always unique due to rotational ambiguity.[35] In this case, the application of non-negativity constraints on both scores and loadings proved sufficient to provide a robust solution. In order to assess the uniqueness of the model based on the spectra of the 42 seaweed alginates plus the spectrum of the pure mannuronate, the estimation of the MCR-ALS model was restarted several times using the mean spectrum of the 43 spectra in the data set for initialisation and random spectra for the following iterations. When repeating the modelling 1000 times, 98.3% of the solutions resembled the solution in Fig 5d and 1.7% of the solutions resembled another solution which was spectrally incorrect.

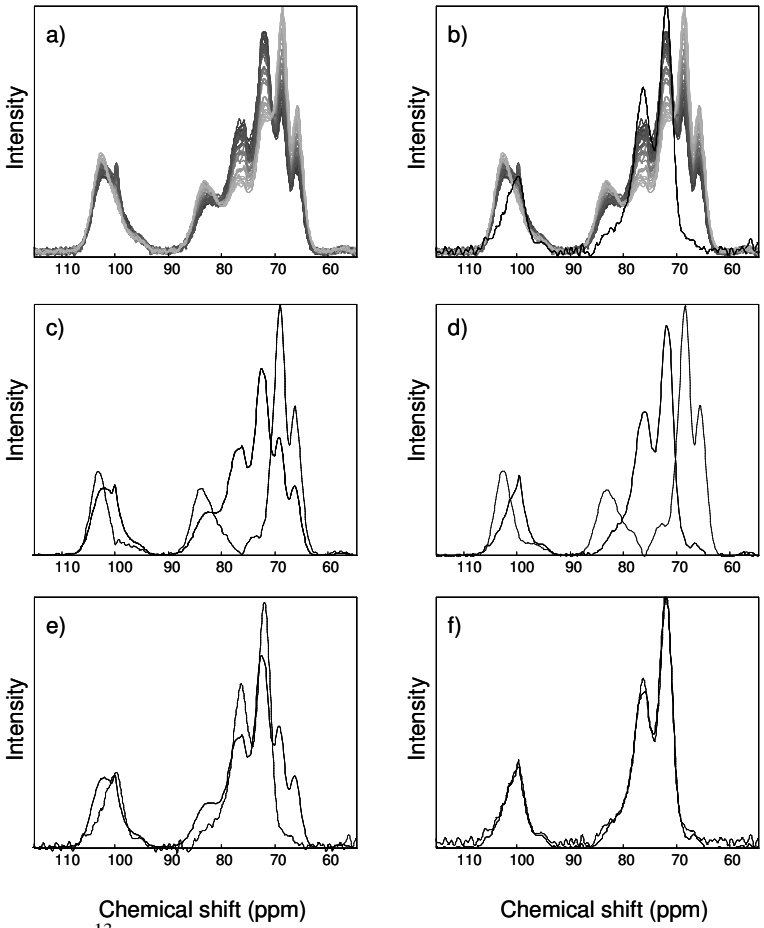

Figure 5. The measured ^{13}C CP-MAS NMR spectra coloured according to the M/G ratio (cf. Fig. 1a) of (a) the 42 seaweed alginates and (b) the 42 seaweed alginates plus the spectrum of pure mannuronate isolated from *Pseudomonas fluorescenc*. MCR-ALS estimated ^{13}C CP-MAS NMR spectra of mannuronate (——) and guluronate (-----) based on the analysis of the spectra of (c) the 42 seaweed alginates and (d) the 42 seaweed alginates plus the spectrum of pure mannuronate. The measured spectrum of pure mannuronate (-----) and the MCR estimated ^{13}C CP-MAS NMR spectrum of mannuronate (——) based on the analysis of (e) the 42 seaweed alginates and (f) the 42 seaweed alginates plus the measured spectrum of the pure mannuronate.

From the MCR modelling, each sample has a score (estimated concentration of mannuronate or guluronate) for each of the loadings (estimated pure spectra of mannuronate or guluronate). Thus, the M/G ratio can be estimated from the score values. In Fig. 6a, the M/G ratio estimated from the MCR score values are compared with the M/G ratio values calculated from the solution-state NMR spectra of the hydrolysed alginates after addition of a chelating agent (i.e. calcium ions are not influencing the results). The figure reveals an excellent correlation between the M/G ratio values obtained by the two methods is obtained (r^2=0.99). For comparison, the M/G ratios estimated from the MCR score values are also compared with M/G ratio values calculated from the solution-state NMR spectra of the hydrolysed alginates without addition of a chelating agent (Fig. 6b). This comparison clearly shows that the M/G ratios obtained from the solution-state NMR spectra of the samples with calcium contents higher (1.1-2.4%) than the other samples (0.01-0.2%) are overestimated by solution-state NMR. Accordingly, the solid-state NMR spectra are, in contrast to the solution-state NMR spectra, not influenced by the calcium content differences.

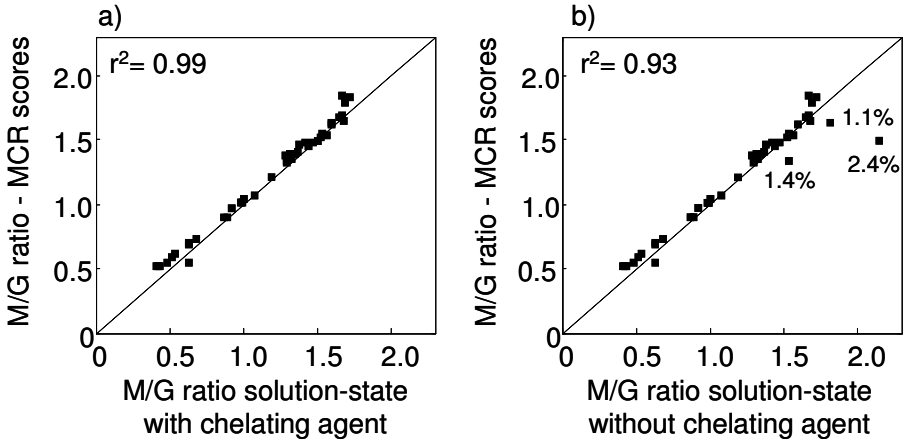

Figure 6. M/G ratios of the 42 seaweed alginates calculated from the MCR estimated concentrations of mannuronate and guluronate versus the M/G ratios calculated from the ^{1}H solution-state NMR spectra measured (a) with a chelator and (b) without a chelator. Three samples contained considerably more calcium (1.1%, 1.4% and 2.4%) than the rest of the samples (0.01-0.2%).

3. Conclusions

It has been demonstrated that without *a priori* knowledge of the monomer composition the M/G ratio can be robustly estimated from ^{13}C CP-MAS NMR spectra of alginate powders by multivariate curve resolution. However, it was found necessary to include the spectra of pure mannuronate to the sample set in order to obtain meaningful results. Furthermore, this method allows for successful determination of the M/G ratio independent of the calcium content (at least up to 2.4%, which was the upper limit in this study). When only a single or a few samples are available and/or the pure components are not obtainable, the M/G ratio can be relatively accurately estimated from a spectral deconvolution of the five pyranose

signals in the region 60-90 ppm of the CP-MAS spectrum using Gaussian line shapes. However, this approach is inferior compared to the multivariate approach. From the present study it can be concluded that ^{13}C CP-MAS NMR in combination with multivariate curve resolution is a reliable, convenient and relatively rapid method for M/G ratio determinations of alginates and serves as a good alternative to the techniques traditionally used.

4. Experimental

4.1. The samples

42 different seaweed sodium alginates were provided by Danisco A/S (Brabrand, Denmark). A high molecular mass mannuronan isolated from the fermentation broth of an epimerase negative strain of *Pseudomonas fluorescenc* was kindly donated by Professor Kurt I. Draget (Department of Biotechnology, Norwegian University of Science and Technology, Trondheim, Norway). Purification and deacetylation were carried out as described by Gimmestad and co-workers.[36]

4.2. Chemical analyses

The average molecular weight (M_w) of the intact alginates was determined by size exclusion chromatography with multi-angle light scattering (SEC-MALS) and sodium and calcium contents were determined by inductively coupled plasma optical emission spectrometry (ICP-OES) using a Varian Vista-MPX ICP-OES instrument (Varian, Inc., Palo Alto, California, USA). Details of the experimental setups can be found in Salomonsen et al.[24]

4.3. NMR spectroscopy

^{13}C CP-MAS NMR spectra of alginate powder were recorded on a Bruker Avance™ III 500 spectrometer (Bruker Biospin Gmbh, Rheinstetten, Germany) operating at 125.77 MHz for ^{13}C and 500.12 MHz for ^{1}H using a 4 mm CP-MAS probe head. Alginate powder (approximately 40 mg) was packed in a Zirconia rotor and spun at 15 kHz. The spectra were recorded with a sweep width of 62.5 kHz. The acquisition time, recycle delay and contact time were 10 ms, 2 s and 2 ms, respectively. 1024 scans were acquired and all spectra were recorded with the same receiver gain. The spectra were externally referenced to the carbonyl signal of glycine at 176.03 ppm. The raw data were zero filled to 4K data points prior to Fourier transformation. No line broadening was applied. The total measurement time was 35 min. The single pulse ^{13}C experiment was acquired with a 90° flip angle, a recycle delay of 120 s and 3328 scans, resulting in a total measurement time was 110.5 h. All spectra were acquired using high power ^{1}H decoupling.

The ^{1}H NMR spectra of alginate in solution were recorded on a Bruker Avance™ 400 spectrometer (Bruker Biospin Gmbh, Rheinstetten, Germany) operating at 400.13 MHz for ^{1}H using a 5 mm broad band inverse probe head. The samples were

hydrolysed and prepared for NMR analysis (1.0% (w/v) solutions), as previously described.[24] Sodium hexametaphosphate (chelating agent) was added to samples with calcium contents above 0.2% in order to prevent line-broadening leading to incorrect estimations of the M/G ratio.[24] The spectra were recorded with a single pulse with a 30° flip angle and a sweep width of 8278 Hz. The acquisition time and recycle delay were both 4 s. 32 scans were acquired and all spectra were recorded with the same receiver gain. During acquisition, the sample temperature was 90°C. 3-(trimethylsilyl)propionic acid-d_4 sodium salt (TSP-d4) was used as chemical shift reference compound (δ=0.0 ppm). The raw data were apodised by 1.0 Hz of exponential line broadening prior to Fourier transformation. No zero filling was applied. The total measurement time was 5 min (exclusive sample preparation).

4.4. Data analysis

The M/G ratios of the 42 seaweed alginates were calculated from the relative areas of the signals in the anomeric region in the solution-state ^{1}H NMR spectra as described by Salomonsen et al[24] and from the ^{13}C CP-MAS NMR spectra using two different approaches: (I) deconvolution using Gaussian and/or Lorentzian line shapes and (II) multivariate curve resolution (MCR) using constrained alternating least squares (ALS) regression.[25] The ^{13}C CP-MAS NMR spectra were normalised prior to data analysis by dividing each variable in the spectrum by the total area intensity of the anomeric and pyranose signals in order to eliminate intensity variations (e.g. due to different packing densities of the alginate powders).

(I) The deconvolution of the five signals in the pyranose region (60-90 ppm) of each ^{13}C CP-MAS spectrum was carried out using the Simplex algorithm[37] for the non-linear parameters (centre position and width) in the Gaussian and/or Lorentzian functions combined with a least squares fit of the linear scaling amplitude parameter (height) inside the function evaluation call. This simple approach proved to exhibit extremely robust convergence behaviour and to be relatively fast. No constraints with respect to centre position, width and height of the fitted functions were applied. The Gaussian and Lorentzian functions were fitted using Equation 1 and 2, respectively:

$$f(x) = a_0 \cdot \exp\left[-\ln(2) \cdot \left(\frac{x - a_1}{a_2} \right)^2 \right] \qquad \textbf{Equation 1}$$

$$f(x) = \frac{a_0}{1 + \left(\frac{x - a_1}{a_2} \right)} \qquad \textbf{Equation 2}$$

where a_0 is the height, a_1 is the centre position and a_2 is the width (full width at half maximum (FWHM) = $a_2 \cdot 2\sqrt{2\ln 2}$) of the fitted function.

(II) MCR-ALS was applied to the 60-110 ppm region in the ^{13}C CP-MAS NMR spectra of the 43 alginates under investigation in this study. MCR-ALS is a mathematical curve resolution method that decomposes a matrix X consisting of spectra of the relevant chemical components into three matrices: C that contains the estimated concentrations of the chemical components, S that contains the pure spectra of the chemical components and E that contains the residuals, i.e. what is not explained in C and S. The multivariate curve resolution model can be written as: $X = CS^T + E$, where T is transposed and the matrix dimensions are: X (n samples, m variables), C (n samples, p pure components), S (m variables, p pure components) and E (n samples, m variables). The model parameters are estimated using an ALS regression algorithm that iteratively fits the C and S^T matrices to the experimental data X. Modelling is completed when no further improvements are observed in the least squares sense. In its native form, ALS regression does not enforce any constraints on the latent variables. Therefore, the solution in a pure ALS regression approach is often sensitive to the initial guess of hidden profiles. A significant stabilisation of the ALS regression solutions can in practice often be dealt with by adding constraints. In this study we use the non-negativity constraint implemented in the least squares sense[38] with the sacrifice of a significant decrease in convergence speed. The model is fitted with a pre-defined number of components representing the number of chemical components causing variability in the data set. All models reported in this study were computed factorwise with two components reflecting mannuronate and guluronate, respectively, and initialised using the mean spectrum of the 43 alginates in the data set as the first estimate and randomly selected spectra in the following iterations.

All calculations were carried out in MatLab 7.5 (Mathworks, Natick, Massachusetts, USA) using in-house software. The routine for non-negativity constrained least squares regression are available at http://www.models.life.ku.dk

Acknowledgements

The authors wish to thank the Ministry of Science, Technology and Innovation for partly sponsoring the Industrial PhD project conducted by Tina Salomonsen in co-operation with Danisco A/S and Quality & Technology, Department of Food Science, Faculty of Life Sciences (LIFE) at the University of Copenhagen. Kurt I. Draget from Department of Biotechnology at the Norwegian University of Science and Technology in Trondheim is greatly acknowledged for donating the bacterial alginate of pure mannuronate. Gilda Kischinovsky, LIFE is acknowledged for proofreading the manuscript.

References

1. Hirst, E.; Rees, D. A., *J. Chem. Soc.* **1965,** 1182-1188.
2. Rees, D. A.; Samuel, J. W. B., *J. Chem. Soc.* **1967,** 2295-2299.
3. Haug, A.; Larsen, B.; Smidsrød, O., *Carbohydr. Res.* **1974,** *32*, 217-225.
4. Gorin, P. A. J.; Spencer, J. F. T., *Can. J. Chem.* **1966,** *44*, 993-998.
5. Linker, A.; Jones, R. S., *J. Biol. Chem.* **1966,** *241*, 3845-3851.
6. Onsøyen, E., *Carbohydrates in Europe.* **1996,** *14*, 26-31.
7. Fischer, F. G.; Dörfel, H., *Hoppe-Seylers Zeitschrift fur Physiologische Chemie.* **1955,** *301*, 224-234.
8. Haug, A.; Larsen, B., *Acta Chem. Scand.* **1962,** *16*, 1908-1918.
9. Larsen, B.; Haug, A., *Acta Chem. Scand.* **1961,** *15*, 1397-1398.
10. Knutson, C. A.; Jeanes, A., *Anal. Biochem.* **1968,** *24*, 482-490.
11. Siddiqui, I. R., *Carbohydr. Res.* **1978,** *67*, 289-293.
12. Annison, G.; Cheetham, N. W. H.; Couperwhite, I., *J. Chromatogr.* **1983,** *264*, 137-143.
13. Krull, L. H.; Cote, G. L., *Carbohydr. Polym.* **1992,** *17*, 205-207.
14. Vadas, L.; Prihar, H. S.; Pugashetti, B. K.; Feingold, D. S., *Anal. Biochem.* **1981,** *114*, 294-298.
15. Donati, I.; Gamini, A.; Skjåk-Bræk, G.; Vetere, A.; Campa, C.; Coslovi, A.; Paoletti, S., *Carbohydr. Res.* **2003,** *338*, 1139-1142.
16. Morris, E. R.; Rees, D. A.; Sanderson, G. R.; Thom, D., *J. Chem. Soc.* **1975,** 1418-1425.
17. Morris, E. R.; Rees, D. A.; Thom, D., *Carbohydr. Res.* **1980,** *81*, 305-314.
18. Salomonsen, T.; Jensen, H. M.; Stenbæk, D.; Engelsen, S. B., *Carbohydr. Polym.* **2008,** *72*, 730-739.
19. Grasdalen, H.; Larsen, B.; Smidsrød, O., *Carbohydr. Res.* **1979,** *68*, 23-31.
20. Grasdalen, H.; Larsen, B.; Smidsrød, O., *Carbohydr. Res.* **1981,** *89*, 179-191.
21. Grasdalen, H., *Carbohydr. Res.* **1983,** *118*, 255-260.
22. Grasdalen, H.; Larsen, B.; Smidsrød, O., *Carbohydr. Res.* **1977,** *56*, C11-C15.
23. Penman, A.; Sanderson, G. R., *Carbohydr. Res.* **1972,** *25*, 273-282.
24. Salomonsen, T.; Jensen, H. M.; Larsen, F. H.; Steuernagel, S.; Engelsen, S. B., *Food Hydrocolloids.* **2009,** *23*, 1579-1586.
25. Tauler, R., *Chemom. Intell. Lab. Syst.* **1995,** *30*, 133-146.
26. Draget, K. I.; Strand, B.; Hartmann, M.; Valla, S.; Smidsrød, O.; Skjåk-Bræk, G., *Int. J. Biol. Macromol.* **2000,** *27*, 117-122.
27. Grant, G. T.; Morris, E. R.; Rees, D. A.; Smith, P. J. C.; Thom, D., *FEBS Lett.* **1973,** *32*, 195-198.
28. Llanes, F.; Sauriol, F.; Morin, F. G.; Perlin, A. S., *Can. J. Chem.* **1997,** *75*, 585-590.
29. Jarvis, M. C.; Apperley, D. C., *Carbohydr. Res.* **1995,** *275*, 131-145.
30. Hoffmann, R. A.; Gidley, M. J.; Cooke, D.; Frith, W. J., *Food Hydrocolloids.* **1995,** *9*, 281-289.
31. Horii, F.; Hirai, A.; Kitamaru, R., *Macromolecules.* **1986,** *19*, 930-932.
32. Larsson, P. T.; Hult, E. L.; Wickholm, K.; Pettersson, E.; Iversen, T., *Solid State Nucl. Magn. Reson.* **1999,** *15*, 31-40.
33. Atkins, E. D. T.; Nieduszy, I. A.; Parker, K. D., *Biopolymers.* **1973,** *12*, 1865-1878.
34. Atkins, E. D. T.; Nieduszy, I. A.; Parker, K. D.; Smolko, E. E., *Biopolymers.* **1973,** *12*, 1879-1887.
35. Winning, H.; Larsen, F. H.; Bro, R.; Engelsen, S. B., *J. Magn. Reson.* **2008,** *190*, 26-32.
36. Gimmestad, M.; Sletta, H.; Ertesvåg, H.; Bakkevig, K.; Jain, S.; Suh, S.; Skjåk-Bræk, G.; Ellingsen, T. E.; Ohman, D. E.; Valla, S., *J. Bacteriol.* **2003,** *185*, 3515-3523.
37. Nelder, J. A.; Mead, R., *Computer Journal.* **1965,** *7*, 308-313.
38. Bro, R.; de Jong, S., *J. Chemom.* **1997,** *11*, 393-401.

Kemometri optimerer fødevareproduktionen

B. Pedersen & T. Salomonsen

Plus Proces, 10, (2007), 12-15

Det kemometriske rum. Kemometrisk kvalitetskontrol af alginat – et eksempel fra den virkelige verden

T. Salomonsen, S.B. Engelsen, L. Nørgaard & R. Bro

Dansk Kemi, 90(4), (2009), 28-29

SUPPLEMENT

PAT giver bedre fødevarer - og billigere produktion s. 12

Plus Proces

Nr. 10 - Oktober 2007 - 21. Årgang

Kæmpesektion med optakt til FoodPharmaTech s. 32-94

Øl og mælk smager af det samme s. 30

- Skab flere unikke produkter

Af Eva Kjer Hansen, fødevareminister

Kemometri optimerer fødevareproduktionen

ErhvervsPh.D-studerende Tina Salomonsen fra Det Biovidenskabelige Fakultet i København har i et samarbejde med Danisco A/S udviklet en ny hurtigmetode til kvalitetskontrol af alginat, som bl.a. anvendes i marmelade-geler i bake-off-produkter samt i kød og fiskeprodukter.

Af journalist, cand.scient. Birger Pedersen og Ph.d. studerende Tina Salomonsen

Kemometri har endnu engang vist sig at være et særdeles vigtigt redskab, når det gælder om at optimere produktionen fx inden for fødevareindustrien.
De første resultater fra et nystartet 3-årigt ErhvervsPhD-projekt, som udføres af Tina Salomonsen i et samarbejde mellem Danisco A/S (forsker Henrik Max Jensen) og forskningsgruppen Kvalitet og Teknologi ved Det Biovidenskabelige Fakultet (professor Søren Balling Engelsen) har nemlig vist, at spektroskopi i kombination med kemometri er særdeles velegnet som hurtigmetode til kvalitetskontrol af alginat – en fødevareingrediens, der blandt andet anvendes til dannelsen af varmestabile marmelade-geler i bake-off produkter samt til restrukturering af kød- og fiskeprodukter.
Med denne nye metode kan alginat-molekylets sammensætning bestemmes på nogle få minutter, hvilket er en væsentlig forskel fra den tidligere metode, som Danisco anvendte. Her tog det mindst to dage, før svaret lå klart. Dette betyder at Danisco i fremtiden vil være i stand til at lave 100% kvalitetskontrol på deres alginat-produkter frem for den nuværende stikprøvekontrol.
Alginater er lineære polysakkarider, der ekstraheres fra brunalger (*Phaeophyceae*) og anvendes som stabiliserings- og geleringsmidler inden for fødevare- og medicinalindustrien. Alginat er opbygget af mannuronsyre-(M) og guluronsyre-(G) enheder, som kan være fordelt i polymerkæden som blokke af ens og skiftende enheder (fx MMMMM, GGGGG og GMGMGMGM). Andelen af M og G afhænger af algeart, høsttidspunkt samt vækstbetingelser og har stor betydning for funktionaliteten i de produkter, hvori alginaten anvendes.
Det er derfor vigtigt for en virksomhed som Danisco, som er en af verdens førende virksomheder inden for produktion og salg af fødevareingredienser, heriblandt alginat, at kunne kontrollere alginatens molekylære sammensætning, inden det sendes ud til kunden.

PhD-studerende Tina Salomonsen har fundet en ny og billigere metode til kvalitetskontrol af alginaters (brunalger) molekylesammensætning.

Den traditionelle metode

Den traditionelle metode til dette formål er baseret på kernemagnetisk resonans (NMR), som er en af de mest nuancerede og informationsrige analyseteknikker der findes og således også kan give detaljeret information om alginatmolekylets sammensætning.
- Ulempen ved NMR i forbindelse med analysen af alginat er dog, at prøveforberedelsen til NMR-analysen er forholdsvis langvarig. For at opnå brugbare NMR-spektre er det nemlig nødvendigt at nedbryde polymerkæden – en proces der involverer en lang række trin og derfor er meget tidskrævende, fortæller 29-årige Tina Salomonsen og fortsætter:
- Det betyder, at det tager minimum to dage at analysere en alginatprøve, og der kan maksimalt igangsættes seks prøver om dagen. Andre ulemper ved NMR-metoden i ▶

forhold til kvalitetskontrol er, at metoden ikke er egnet til on-line kontrol på grund af det stærke magnetfelt samt at instrumentet er meget dyrt – 2-3 millioner kr. og opefter afhængigt af magnetstyrke samt tilhørende udstyr. Derudover kræver det stor ekspertise at betjene, hvorfor et NMR-instrument typisk vil være placeret centralt i virksomhedens udviklingsafdeling og ikke ude i produktionen.

PhD-studerende Tina Salomonsen anvender her den nye metode til kvalitetskontrol af alginaters molekylesammensætning.

Billigere metode

Med ovenstående problemstilling i baghovedet var det derfor oplagt at undersøge muligheden for at anvende forskellige vibrationsspektroskopiske teknikker, FT-IR, FT-Raman og NIR, som alternative metoder til at måle andelen af M og G i alginat, eftersom disse metoder er hurtige (et spektrum kan optages på sekunder), ikke kræver nogen prøveforberedelse og er væsentligt billigere end et NMR-instrument.

Det viste sig, at man ved hjælp af kemometri kunne finde en god korrelation mellem spektrene og alginatens molekylære sammensætning fundet ved NMR. De kemometriske kalibreringsmodeller baseret på FT-IR, FT-Raman og NIR-spektre af 100 forskellige alginater resulterede i en korrelation på 0.97 og en prædiktionsfejl, der er sammenlignelig med den fejl, der opnås fra NMR-metoden. Det vil sige at både IR-, Raman- og NIR-spektroskopi er særdeles velegnede metoder til kvalitetskontrol af alginat, da man på få minutter kan bestemme molekylets sammensætning, hvilket er en væsentlig forskel fra den traditionelle NMR-metode, hvor det tog mindst to dage, før svaret var klar.

Tidsbesparende

- Denne tidsbesparelse medfører, at Danisco hurtigere kan sende deres produkter på markedet samt langt mere effektivt kontrollere kvaliteten af produkterne og dermed opnå henholdsvis større produktflow samt bedre sikre, at produkterne rammer kundernes specifikke krav, siger Tina Salomonsen. Det igangværende projekt, som startede i maj 2006 og forventes afsluttet i april 2009, er et godt eksempel på et frugtbart samarbejde mellem erhvervslivet og den offentlige forskning. Projektet er et såkaldt ErhvervsPhD projekt, der delvist finansieres af Danisco og delvist af Ministeriet for Videnskab, Teknologi og Udvikling.

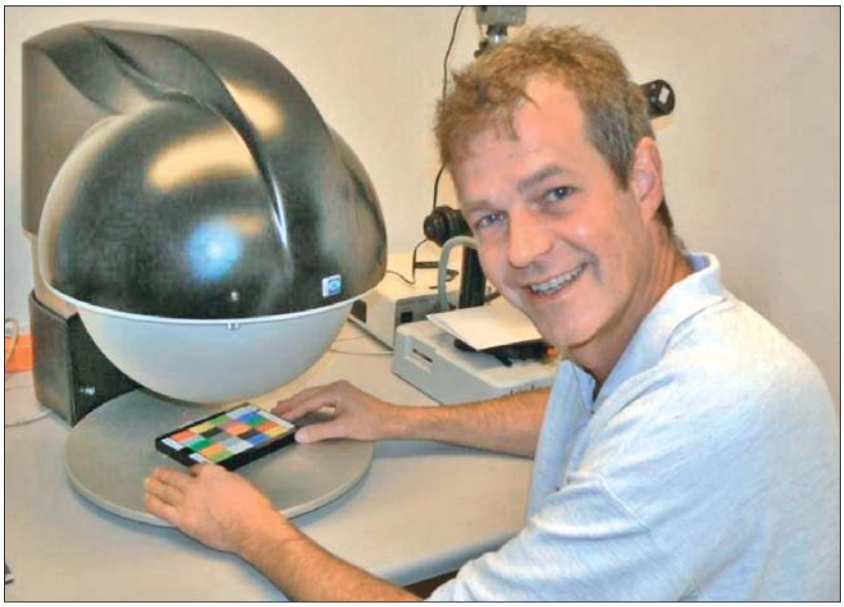

- I kraft af PAT og kemometri får man både bedre fødevarer og billigere produktion, siger Rasmus Bro, der er professor i kemometri.

Bliv Msc. i procesanalytisk teknologi (PAT)

På Det Biovidenskabelige Fakultet under Københavns Universitet er man netop gået i gang med en ny uddannelse – Master of Science (MSc), også kaldet kandidat, i procesanalytisk teknologi (PAT). Uddannelsen er to-årig, og gør dig i stand til at være i centrum for udvikling, overvågning og kontrol af produktion inden for en række forskellige områder som f.eks. fødevare- og medicinalproduktion.

Uddannelsen er et samarbejde mellem DTU og flere fakulteter på Københavns Universitet. På første år skal du have en række obligatoriske kurser, bl.a. i proceskendskab, produktion, kemometri og spektroskopi. Første år afslutter du med et temaprojekt, gerne i samarbejde med industrien. På andet år kan du vælge mellem mange forskellige valgfag, og du slutter af med et speciale, der skal laves i samarbejde med en dansk eller udenlandsk virksomhed. Læs mere på www.life.ku.dk/pat.

Hvad er kemometri?
Kemometri er en videnskabelig disciplin, der uddrager og visualiserer information fra komplicerede kemiske data. Kemometri er ofte baseret på avancerede målinger som f.eks. spektroskopiske data og meget ofte målt direkte på fx en bøf eller lignende.
Resultatet af sådanne en måling er tusindvis af tal, der reflekterer den komplicerede kemiske og fysiske tilstand af prøven – et såkaldt fingeraftryk.
I sig selv giver disse tal ikke meget mening, men de matematiske modeller, som kemometrien anvender, kan omdanne tallene til meningsfyldte parametre såsom koncentrationen af et stof, mørheden af kødet, forbrugerens præference osv.
Det betyder at man med én måling pludselig kan få mange informationer og at man kan få mere relevante informationer end med traditionelle metoder. Det betyder også at man pludselig kan få nye ideer om en problemstilling fra målingerne selv frem for udelukkende at basere sig på hypoteser postuleret på forhånd.

- Som jeg ser det, er et ErhvervsPhD-projekt en fordel for alle parter. Virksomheden får adgang til ny viden, som den kan bruge i sin udvikling. Samtidig får universitetet ny viden tilbage fra erhvervslivet, fordi ErhvervsPhD'en bygger bro mellem de to verdener, og for mig er det meget motiverende, at der er så stor interesse og opbakning fra virksomhedens side samt at mine resultater kan bruges til noget i den virkelige verden, siger Tina Salomonsen, der er MSc i Food Science and Technology – på dansk levnedsmiddelkandidat.

Ny uddannelse
- På Det Biovidenskabelige Fakultet tilbyder vi nu også bachelor-studerende en helt ny MSc i procesanalytisk teknologi (PAT), fortæller professor i kemometri, Rasmus Bro. Se mere om dette i faktaboksen på side 14.
Han er særdeles tilfreds med de foreløbige resultater af Tina Salomonsens arbejde, og glæder sig over, at kemometrien og spektroskopien atter har vist sin store værdi som særdeles effektive PAT-redskaber til forbedringer i fødevareproduktionen.
- Senest har post.doc. Christian Zachariassen i sit ErhvervsPhD-projekt vist, at han med nærinfrarød spektroskopi og PAT var i stand til at optimere pektinproduktionen på CPKelco, ligesom andre projekter – målinger på eksempelvis sildelage og ost – har afsløret, at man i kraft af PAT ikke blot kan få bedre fødevarer, men også en bedre kontrol af varer og billigere produktion, siger Rasmus Bro.

PAT – et nyt begreb
Proces-analytisk teknologi (PAT) er et nyt begreb som dækker over metoder, der har været anvendt i stigende grad gennem de sidste årtier. I bund og grund er PAT kombinationen af kemometri og spektroskopi. Når disse bringes i anvendelse i produktionsøjemed, så får man nye muligheder for at styre og optimere processer på et rationelt grundlag. Mange processer styres ud fra erfaring og tommelfingerfornemmelser og på baggrund af det forhåndenværendes søm princip. Ved hjælp af PAT kan man forstå og kontrollere fx produktionsprocesser i fødevareindustrien langt mere effektivt.

Kemometrisk kvalitetskontrol af alginat – et eksempel fra den virkelige verden

I samarbejde med Danisco A/S er udviklet en hurtigmetode baseret på kemometri og infrarød spektroskopi til analyse af fødevareingrediensen alginat. Metoden reducerer analysetiden og optimerer kvalitetskontrollen af alginat

Af Tina Salomonsen, Søren Balling Engelsen, Lars Nørgaard og Rasmus Bro, Københavns Universitet

Metoden, der beskrives her, er udarbejdet i forbindelse med et ErhvervsPh.d.-projekt, der udføres som et samarbejde mellem ErhvervsPh.d.-studerende Tina Salomonsen, Danisco A/S og forskningsgruppen Kvalitet og Teknologi ved Det Biovidenskabelige Fakultet, Københavns Universitet . Den nye metode kan på under et minut forudsige alginatets molekylære sammensætning [1], som har betydning for funktionaliteten i de produkter, hvor det anvendes.

Baggrund

Alginat er et lineært polysakkarid, som udvindes fra brunalger (*Phaeophyceae*), og primært anvendes i fødevareindustrien til dannelse af varmestabile marmelade-geler i bake-off-produkter samt til restrukturering af frugt, grøntsager, fisk og kød. Byggestenene i alginatmolekylet er α-L-guluronsyre (G) og β-D-mannuronsyre (M) og forholdet mellem dem er tæt forbundet med funktionaliteten i produkterne. Hvis man f.eks. ønsker en meget fast og hård gel, anvendes et alginat med meget G, hvorimod en blødere og mere elastisk gel dannes fra et alginat med meget M. M/G-forholdet varierer ift. arten af tang, høsttidspunkt og vækstbetingelser. Det er vigtigt for producenten at kende M/G-forholdet i de færdige produkter, for at sikre at funktionaliteten stemmer overens med kundernes specifikationer. M/G-forholdet måles traditionelt vha. kernemagnetisk resonans (NMR) spektroskopi. Ulempen ved denne metode er, at prøveforberedelsen er forholdsvis langvarig. For at opnå brugbare NMR-spektre er det nødvendigt at nedbryde polysakkariderne. De består typisk af omkring 1500 monomer-enheder, som skal nedbrydes til kæder med omkring 150 enheder. Denne proces involverer flere trin og er derfor tidskrævende. Derudover kræver det ekspertise at betjene et NMR-instrument, hvorfor det typisk vil være placeret centralt i virksomhedens udviklingsafdeling og ikke ude i produktionen. Det blev derfor undersøgt, om spektre opnået ved infrarød spektroskopi (hurtig måling) kunne korreleres med M/G-forholdet bestemt ved NMR (langsom måling) og dermed opbygge en prædiktiv model, som prædikterer M/G-forholdet i det kommercielle alginatpulver ud fra et spektrum af pulveret.

Prøverne

For at udvikle en prædiktiv model blev der sammensat et prøvesæt bestående af 100 prøver af den type alginat (natriumalginatpulver), som virksomheden ønsker at benytte modellen til. Prøverne blev udvalgt således, at de varierede mest muligt i deres M/G-forhold (0,5-2,1). M/G-forholdet af alle prøverne blev bestemt ved NMR-spektroskopi (referencemetoden). Prøverne blev opdelt i et kalibreringssæt og et testsæt bestående af hhv. 75 og 25 prøver. Figur 1 viser M/G-forholdet af de 75 kalibreringsprøver og 25 testprøver ordnet efter M/G-forholdet bestemt vha. referencemetoden. Der blev ligeledes målt Fourier transform infrarød (FT-IR) spektre af alle prøverne på et Perkin Elmer Spectrum One FT-IR spektrometer udstyret med en attenuated total reflectance (ATR)-enhed med en single-bounce diamant. Spektrene blev målt i området 650 til 4000 cm^{-1} med 1 cm^{-1} intervaller. Til dataanalysen blev kun området fra 650 cm^{-1} til 1800 cm^{-1} (1150 variable) anvendt. Hver prøve måltes tre gange og gennemsnitsspektret blev brugt i dataanalysen.

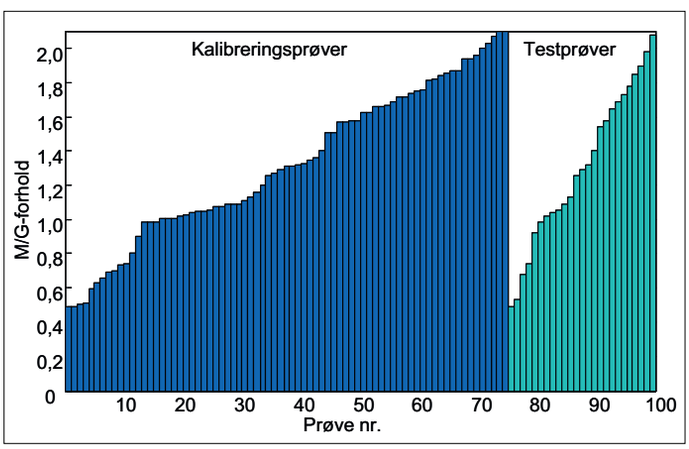

Figur 1. M/G-forholdene af de 75 kalibreringsprøver og de 25 testprøver.

Eksplorativ dataanalyse

I figur 2a ses de rå spektre af de 75 kalibreringsprøver. Spektrene er farvet efter M/G-forholdet, men ved visuel inspektion er det svært at få et overblik over, hvilke dele af spektret der er relateret til M/G-forholdet. For at få et overblik over variationen i data udføres først en *Principal Component Analysis* (PCA) af de rå spektre efter centrering (hver måling er fratrukket variablens middelværdi). PCA og centrering er tidligere beskrevet i denne klumme (Dansk Kemi 2, 2008). Scoreplottet fra PCA af de rå spektre er vist i figur 2b og viser at principal komponent et (PC1) og to (PC2) forklarer hhv. 92,5% og 4,3% af variationen i data. Det ses ligeledes, at

prøverne i scoreplottet, som ligeledes er farvet efter M/G-forholdet, er fordelt langs PC2. Der ses en gradient fra det laveste M/G-forhold øverst i plottet til højeste M/G-forhold nederst i plottet. Der kan altså konkluderes, at hovedparten af den spektrale variation (92,5%) er relateret til anden information end M/G-forholdet. Denne ukendte variation er sandsynligvis relateret til små forskelle i kontakten til diamanten på ATR-enheden. Det er altså sandsynligt, at den variation, der forklares i PC1, er ikke-kemisk og med fordel kan fjernes vha. *Multiplicative Scatter/Signal Correction* (MSC) (Dansk Kemi 1, 2009). Derved opnås en mere simpel model, der udelukkende fokuserer på den kemiske information. De MSC-behandlede spektre er vist i figur 2c, og der ses en tydelig effekt af forbehandlingen.

I scoreplottet fra en PCA af de MSC-behandlede spektre ses nu ligeledes en tydelig systematisk variation i forhold til M/G-forholdet (farvekode) langs PC1, som forklarer 59,0% af variationen i data. Den eksplorative analyse af data viser, at FT-IR-spektrene indeholder information om M/G-forholdet, og det kan derfor forventes, at det er muligt at opbygge en kalibreringsmodel mellem spektrene (hurtig måling) og M/G-forholdet bestemt vha. referencemetoden (langsom måling).

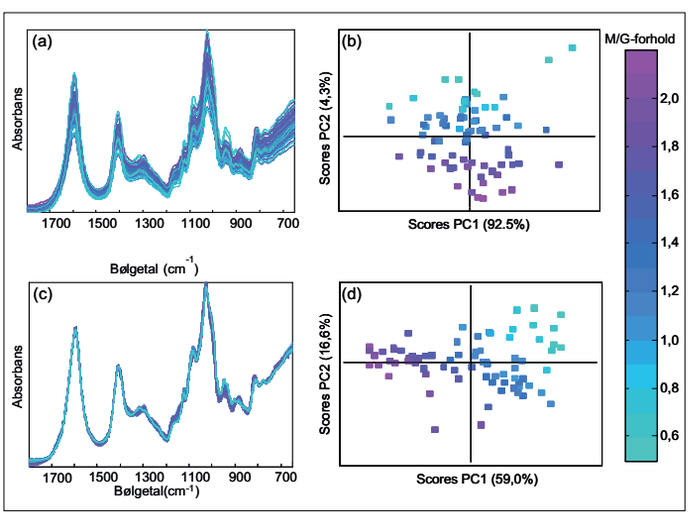

Figur 2. (a) Rå og (c) MSC-behandlede FT-IR-spektre af de 75 alginat kalibreringsprøver i det spektrale område 650-1800 samt PCA scoreplot på de (b) rå og (d) MSC-behandlede spektre. Spektre og scores er farvet efter prøvernes M/G-forhold.

Kalibreringsmodellen

Kalibreringsmodellen mellem de MSC-behandlede spektre (figur 2c) og referenceværdierne (figur 1) blev opbygget vha. *Partial Least Squares* (PLS) regression (Dansk Kemi 11, 2008). Spektrene og referenceværdierne blev centreret inden modellering for at fokusere på variationerne mellem de enkelte prøver i stedet for det overordnede signalniveau. De 75 kalibreringsprøver blev brugt til udviklingen af modellen, hvorefter de 25 testprøver blev brugt til at teste, hvor god modellen er til at prædiktere nye prøver. Det optimale antal PLS-komponenter for denne model blev bestemt til at være fire ved fuld krydsvalidering (Dansk Kemi 3, 2009). I figur 3a ses M/G-forholdene målt vha. referencemetoden plottet mod M/G-forholdene prædikteret ud fra FT-IR-spektrene for både kalibreringsprøverne og testprøverne. Både *Root Mean Square Error of Cross Validation* (RMSECV) og *Root Mean Square Error of Prediction* (RMSEP), som er hhv. den gennemsnitlige kalibreringsfejl og den gennemsnitlige prædiktionsfejl (Dansk Kemi 3, 2009), blev beregnet til 0,08, som er i samme størrelsesorden som standardafvigelsen på referencemetoden. Det betyder at fejlen i PLS-modellens prædiktioner er på niveau med referencemetoden, samt at det kan forventes, at modellen er lige så god til at prædiktere nye ukendte prøver, som den er til at prædiktere de prøver modellen bygger på. Med andre ord – modellen er robust. Figur 3b viser modellens regressionskoefficienter plottet sammen med et spektrum af to alginatprøver med hhv. et højt og et lavt M/G-forhold. Overordnet kan der konkluderes, at det meste af fingerprintområdet mellem 800 cm^{-1} til 1200 cm^{-1} har betydning for kalibreringen. De steder, hvor man visuelt kan se en forskel på de to spektre i figur 3b, vægtes højest.

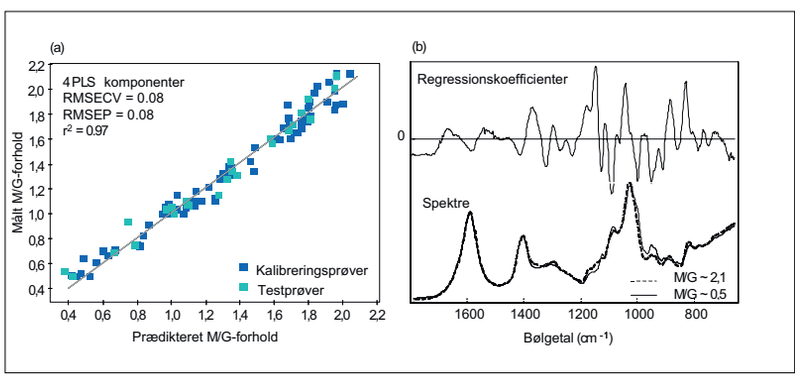

Figur 3. (a) M/G-forholdene målt vha. referencemetoden plottet mod M/G-forholdene prædikteret ud fra FT-IR-spektrene for både kalibrerings- og testprøverne. (b) Regressionskoefficienter for PLS-modellen baseret på fire PLS-komponenter plottet sammen med FT-IR-spektrene for to ekstreme prøver (lavest og højest M/G-forhold).

Outro

Udviklingen af kalibreringsmodellen til prædiktion af M/G-forholdet i alginat har haft stor betydning for Daniscos alginatfabrik, som ligger ud til Atlanterhavet i Bretagne, Frankrig. Fabrikken sendte førhen prøver til Danmark for at få dem analyseret på NMR-instrumentet i udviklingsafdelingen og måtte vente flere dage på resultatet pga. den tidskrævende prøveforberedelse. I dag ser verden anderledes ud. Nu måles M/G-forholdet af alginaterne på under et minut på fabrikkens eget FT-IR-instrument, hvori kalibreringsmodellen er indbygget.

E-mail-adresser
Tina Salomonsen: tisa@life.ku.dk
Søren Balling Engelsen: se@life.ku.dk
Lars Nørgaard: lan@life.ku.dk

Reference
1. T. Salomonsen, H.M. Jensen, D. Stenbæk & S.B. Engelsen. Chemometric prediction of alginate monomer composition: A comparative spectroscopic study using IR, Raman, NIR and NMR. Carbohydrate Polymers 72, 730-739, 2008.